The University of Nottingham

UNITED KINGDOM · CHINA · MALAYSIA

The impacts of bed rest and acute trauma on muscle metabolic health in humans.

Dr Natalie F Shur (2023)

The impacts of bed rest and acute trauma on muscle metabolic health in humans.

Natalie F Shur, MBChB, MRCP (UK), MFSEM

Thesis submitted to The University of Nottingham for the Degree of Doctor of Philosophy

July 2023

Abstract

Physical inactivity is a global public health problem and has significant detrimental health consequences. Periods of physical inactivity or immobilisation are common in clinical populations secondary to injury, illness, disease or advancing age. There are currently substantial gaps in our knowledge of the rate and magnitude of skeletal muscle and metabolic dysregulation during bed rest and trauma. Further insight into the processes underpinning these changes is required to develop effective future countermeasures.

The objective of this thesis was to further the understanding of the underlying mechanisms driving skeletal muscle atrophy, changes in muscle protein turnover and a reduction in whole-body and leg insulin sensitivity in immobilisation and trauma. Three human volunteer studies were conducted during the course of this thesis. The first study aimed to evaluate the change in insulin-stimulated whole-body glucose disposal, muscle glycogen content and fuel oxidation during acute (3 days) and chronic (56 days) bed rest in healthy male participants maintained in energy balance. The reduction in insulin-stimulated whole-body insulin sensitivity was rapid (manifested by 3 days), and a similar magnitude to that observed after chronic bed rest. However chronic bed rest was associated with a shift in fuel oxidation, which could not be explained by changes in intramyocellular lipid (IMCL) content but was reflected by the muscle transcriptional response to chronic bed rest, suggesting differences in underlying mechanisms from the acute to chronic state.

The second study assessed for concurrent changes in leg muscle volume, protein turnover and insulin-stimulated leg glucose uptake and muscle glycogen storage in acute bed rest and subsequent structured remobilisation of 3 days duration. Concurrent reductions in leg glucose uptake (explained by reductions in leg blood flow), and muscle glycogen storage as well as myofibrillar protein synthesis (MPS) and whole-body myofibrillar protein breakdown (MPB) after 3 days of bed rest were apparent. Structured remobilisation (but not ambulation alone) restored bed rest-associated reductions in leg muscle volume and MPS, but not insulin-stimulated leg glucose uptake or muscle glycogen storage after bed rest. This study highlighted divergences in muscle fuel and protein metabolism, as well as the importance of exercise rehabilitation following short duration bed rest.

The final study aimed to evaluate the individual and combined impact of immobilisation and trauma/inflammation on *medial gastrocnemius* muscle thickness and architecture, cumulative MPS and whole-body MPB in ankle fracture patients and matched healthy volunteers undergoing 2 weeks of unilateral cast immobilisation. Trauma plus immobilisation caused greater declines in *medial gastrocnemius* muscle thickness compared with immobilisation alone, but similar declines in cumulative MPS over 2 weeks and no difference in whole-body MPB measured at 2 weeks. Trauma was also associated with a profound systemic (pro-inflammatory cytokines) and muscle (mRNA) inflammatory response which was absent in immobilisation alone in the healthy volunteers. Furthermore, a reduction in chronic MPS and muscle

thickness was evident in the injured leg, but not the uninjured leg, suggesting a differential impact on muscle of local vs systemic inflammation.

Collectively, the work in this thesis presents novel mechanistic insight into the impact of immobilisation and trauma on skeletal muscle mass and immobilisation on whole-body and limb insulin sensitivity. Namely, that acute and chronic bed rest cause a similar magnitude in decline in whole-body insulin sensitivity, however the underlying mechanisms appear to differ. Secondly, that although acute bed rest causes rapid reductions in muscle mass, protein turnover and leg glucose uptake, there is a mismatch in their restoration after a short period of structured remobilisation. Finally, trauma plus inflammation causes greater declines in muscle thickness compared with immobilisation alone, with similar reductions in MPS, and local inflammation is implicated in muscle mass loss in acute limb trauma. These findings may provide the basis to the development of future potential countermeasures.

Declaration

The work carried out in this thesis was funded by Versus Arthritis, the Biotechnology and Biological Sciences Research Council (BBSRC), the Nottingham Biomedical Research Council (BRC) and the European Society for Clinical Nutrition and Metabolism (ESPEN).

The running of the Acute bed rest study (Chapter 3) and the Ankle fracture study (Chapter 5) was coordinated by myself and all participants in these studies were recruited by me. The hyperinsulinaemic euglycaemic clamps performed in Chapters 3 and 4 were performed by myself and Dr Liz Simpson. All muscle biopsy and femoral venous cannulation procedures in the acute bed rest and ankle fracture study were undertaken by myself. Statistical analysis where not stated below was performed by me. Where others contributed to the data presented in this thesis is declared below.

In Chapter 3, the Chronic bed rest study was run by the team in the Institute of Space Medicine and Physiology (MEDES), Toulouse, who also recruited the participants for this study. Doctors employed by MEDES undertook the muscle biopsies in the chronic bed rest participants. Operator scanning using magnetic resonance imaging for the quantification of skeletal muscle volume was performed by staff of the Sir Peter Mansfield Imaging Centre including Olivier Mougin and Christopher Bradley. Analysis was performed by myself. Dr Jo Mallinson undertook the ultrasound measurements of femoral artery blood flow in Chapter 4. Analysis of blood samples for plasma insulin, triacylglycerol and non-esterified fatty acids, was performed by Sally Corden. Pro-inflammatory

cytokine analysis was performed by Dr Jo Mallinson. Intramyocellular lipid content analysis was performed by Dr Prince Chivaka. Stable isotope tracer analysis including deuterium oxide and 3-methylhistidine was performed by Dr Matthew Brook and Dr Hannah Crossland. Muscle glycogen, lactate, acetylcarnitine, and long chain acylcarnitine content, and protein expression levels of pyruvate kinase 2 and 4 and pyruvate dehydrogenase phosphatase 1 were performed by Dr Hannah Crossland and Dr Tim Constantin. Muscle mRNA expression analyses for Chapter 3 and 4 were performed by Dr Despina Constantin and for Chapter 5 by Scott Cooper.

Except where assistance by colleagues in academic and technical roles at The University of Nottingham has been declared in the preceding statements, I attest to the fact that this thesis was composed by me and serves as an accurate record of the work I have performed. No part of this thesis has previously been submitted for the degree of Doctor of Philosophy or any other degree in higher education.

Natalie Shur, July 2023

Acknowledgements

Undertaking this PhD has been a truly challenging, humbling, surprising and rewarding experience.

I would like to sincerely thank both of my supervisors, Professor Paul Greenhaff and Professor Ian MacDonald. Paul has taught me several important lessons. Firstly, to trust the data and to question accepted “truths”. I have tried to develop, via his example, incredible attention to detail, succinct academic writing and the ability to present complex science with simplicity and clarity. I am incredibly grateful for his patience and trust in guiding a medic through the world of metabolic physiology and allowing me into the team. I would like to thank Ian Macdonald for his astute and precise guidance and calming influence. I am grateful for his timely feedback, direction and encouragement throughout the process.

There are several individuals who have been instrumental in the success of this thesis and the studies within it to whom I am indebted. Thank you to Dr Liz Simpson, the “clamp queen” who taught me the hyperinsulinaemic euglycaemic clamp technique, has been a most trusted colleague and an enjoyable companion to share French cheese with. I would like to thank Dr Jo Mallinson the “maestra of muscle” for training me in ultrasound measurement of muscle mass and architecture and generally being a wide fountain of knowledge regarding anything muscle-related.

Thank you to the staff at the Sir Peter Mansfield Imaging Centre, especially Olivier Mougin and Chris Bradley who helped to devise the full body magnetic

resonance imaging (MRI) scanning technique and spent hours scanning our participants. To the Derby team, particularly Matt Brook, Kenny Smith and Hannah Crossland whose expertise on stable isotope tracer techniques and analysis were integral to some of the important findings of this work.

To the staff in the David Greenfield Human Physiology Unit, including Sara Brown (the boss), Dr Tariq Taylor, Aline Nixon, Ben Rippon, Matt Westerman, Mel Marshall, and Mia Keeton who became like my second family. It was a team effort to pull off the acute bed rest study, in particular, and thank you for all your hard work, listening to my pregnancy ailments and providing hours of chats over muscle biopsies and insulin clamps together.

To the other PhD students in our team including Pardeep Pabla, Andrew Wilhelmsen, Jordon McGing and Prince Chivaka, thank you for being a listening ear when I needed it and for sharing the highs and the lows of the PhD experience.

Thank you to the participants who kindly gave up their time towards the studies in this thesis, none of which were straightforward as a volunteer. Getting to know each participant was a pleasure.

To my parents who have provided me with unrelenting support, not only in this, but in all that I do. I hope that I bring you great “nachas”.

To my husband Nick. Thank you for allowing me the space and time to fulfil my potential and never holding me back, but always lifting me up. Thank you for taking the reins with the girls when I have needed to dedicate more time to my work. Your selflessness, compassion and scientific curiosity has enabled me to get through this journey (relatively) unscathed.

To my daughters, Eva and Fran, who during the course of this PhD made me a mother. Being your mum has given me new purpose, pride and reward in my life. You remain my most amazing achievements to date.

Publication and Presentations

Peer-reviewed publications arising from the work in this thesis

- Shur NF, Simpson EJ, Crossland H, Chivaka PK, Constantin D, Cordon SM, Constantin-Teodosiu D, Stephens FB, Lobo DN, Szewczyk N, Narici M, Prats C, Macdonald IA, Greenhaff PL. Human adaptation to immobilization: Novel insights of impacts on glucose disposal and fuel utilization. J Cachexia Sarcopenia Muscle. 2022 Sep 4. doi: 10.1002/jcsm.13075. PMID: 36058634.
- Shur NF, Creedon L, Skirrow S, Atherton PJ, MacDonald IA, Lund J, Greenhaff PL. Age-related changes in muscle architecture and metabolism in humans: The likely contribution of physical inactivity to age-related functional decline. Ageing Res Rev. 2021 Jul;68:101344. doi: 10.1016/j.arr.2021.101344. Epub 2021 Apr 16. PMID: 33872778; PMCID: PMC8140403.
- Trim WV, Walhin JP, Koumanov F, Turner JE, Shur NF, Simpson EJ, Macdonald IA, Greenhaff PL, Thompson D. The impact of physical inactivity on glucose homeostasis when diet is adjusted to maintain energy balance in healthy, young males. Clin Nutr. 2023 Apr;42(4):532-540. doi: 10.1016/j.clnu.2023.02.006. Epub 2023 Feb 16. PMID: 36857962.

Published Abstracts

- Shur NF, Simpson EJ, Chivaka P, Crossland H, Constantin D, Constantin-Teodosiu T, Stephens FB, Lobo DN, Prats C, Macdonald IA, Greenhaff PL. Impaired insulin sensitivity and carbohydrate oxidation during bed rest in healthy participants. Clinical Nutrition, 2020; volume 40: 434-435. DOI: https://doi.org/10.1016/j.clnesp.2020.09.093

- Shur NF, Simpson EJ, Chivaka PK, Crossland H, Constantin D, Cordon SM, Constantin-Teodosiu D, Stephens FB, Lobo DN, Szewczyk N, et al.

O105 Human adaptation to immobilisation: novel insights of impacts on glucose disposal and fuel utilization. British Journal of Surgery 2022;109(Supplement_4):znac242.105. doi: 10.1093/bjs/znac242.105.

Conference presentations

Invited speaker

- April 2022: The Biomedical Basis of Elite Performance, Nottingham, UK
- March 2022: Surgical Research Society 2022, Nottingham, UK
- September 2020: ESPEN Congress, Fellows' Symposium, UK (online due to COVID)
- September 2020: Japanese Society of Physical Fitness and Sports Medicine Congress (cancelled due to COVID)

Oral presentations

- Bed rest and exercise remobilisation: concurrent adaptations in muscle glucose and protein metabolism. Postgraduate researcher (PGR) symposium, School of Life Sciences, University of Nottingham, 2023. **1st prize, oral presentation category.**
- Three days bed rest appreciably impairs whole-body glucose disposal (which is fully restored by exercise) but is not further accentuated after 56 days bed rest. European College of Sports Science Congress (ECSS), July 2019. **Young Investigator Award (YIA) winner, 3rd place**

Poster presentations

- Whole-body insulin mediated glucose disposal is dissociated from fuel oxidation during acute bed rest under conditions of controlled energy intake in healthy young volunteers, PGR symposium, School of Life Sciences, University of Nottingham, 2020.

Prizes and funding

- July 2023: 1st prize oral presentation, PGR Conference Life Sciences, University of Nottingham
- July 2019: Winner of the Young Investigator Award (top 3 out of 112 finalists), ECSS, Prague. 2,000 Euros prize and invited speaker to the Japanese Society of Physical Fitness and Sports Medicine Congress, Sept 2020.
- May 2017 €49,393 ESPEN Research Fellowship

Other academic activity arising during my PhD studies

- Shur NF, Johns DJ, Kluzek S, Peirce N. Physical Inactivity and Health Inequality During Coronavirus: a novel opportunity or total lockdown? *BMJ Open Sport and Exercise Medicine* 2020;0:e000903.

- Co-author of book chapter “Invasive Physiological Measures” in *BASES Physiological Exercise Testing Guidelines*. Routledge

Impact of COVID-19 Pandemic and Parental Leave

During the course of my PhD studies I have had two periods of parental leave, November 2018-June 2019 and December 2021-September 2022.

The number of participants recruited to the study in Chapter 5 was fewer than anticipated due to the effect of the COVID-19 pandemic. Closure of the university shortly after commencement of the study restricted recruitment for >8 months, and during this time I was seconded back to the National Health Service (NHS) to provide clinical care. Furthermore, the effect of lockdown after the university reopened, meant fewer people were undertaking normal activities of daily living including recreational sport and outside physical activity, which negatively impacted the number of people presenting with ankle fracture to Queen's Medical Centre (QMC) in Nottingham. Thus, the study may have been underpowered to detect changes in secondary outcome measures. I had a 6 month extension to my PhD studies prior to re-entering clinical training in the NHS in order to try to recruit more participants.

Table of Contents

List of Figures

List of Tables

List of Abbreviations

AMP	Adenosine monophosphate
AMPK	Adenosine monophosphate (AMP)-activated protein kinase
ANOVA	Analysis of variance
APE	Atom percent excess
AS160	TBC1 domain family member 2
ATP	Adenosine triphosphate
AV	Arterialised-venous
AV-V	Arterialised-venous-venous
BBSRC	Biotechnology and Biological Sciences Research Council
BMI	Body mass index
BMR	Basal metabolic rate
BR	Bed Rest
BRC	Biomedical Research Centre
CACT	Carnitine acylcarnitine translocase
CAT	Carnitine acyl transferase
CD36	Fatty acid translocase
CHO	Carbohydrate
CLIX-IR	Clamp-like index
CO_2	Carbon dioxide
COPD	Chronic obstructive pulmonary disease
CPT	Carnitine palmitoyltransferase
CRP	C-reactive protein
CSA	Cross sectional area
CT	Computed tomography
D_2O	Deuterium oxide
DEXA	Dual energy x-ray absorptiometry
DGHPU	David Greenfield human physiology unit
DI	Dry immersion
DNA	Deoxyribonucleic acid
DVT	Deep vein thrombosis
ECG	Electrocardiogram
EGTA	Ethylene glycol tetra acetic acid
ELISA	Enzyme-linked immunosorbent assay
EMCL	Extramyocellular lipid
EMG	Electromyographic
ESA	European Space Agency
ESPEN	European Society for Clinical Nutrition and Metabolism
ESR	Exercise-supplemented remobilisation
FAA	Femoral artery cross sectional area
FABP	Fatty acid binding proteins
FAD	Femoral artery diameter

FAT	Fatty acid translocase
FOXO	Forkhead box class 0-1
FSR	Fractional synthetic rate
G6P	Glucose-6-phosphate
GABA	Gamma-aminobutyric acid
GD	Glucose disposal
GEM	Gas Exchange Machine
GIR	Glucose infusion rate
GLUT	Glucose Transporter
GORD	Gastro-oesophageal reflux disease
GS	Glycogen synthase
GTP	Guanosine-5'-triphosphate
H_2O	Water
HDL	High density lipoprotein
HDT	Head-down tilt
HMBS	Hydroxymethylbilane synthase
HOMA-IR	Homeostasis model assessment insulin resistance
HRA	Health Research Authority
ICU	Intensive care unit
IGF	Insulin-like growth factor
IGFR	Insulin-like growth factor receptor
IL	Interleukin
IMAT	Intramuscular adipose tissue
IMCL	Intramyocellular lipid
IMTG	Intramyocellular triacylglycerol
IPA	Ingenuity pathway analysis
IRMS	Isotope ratio mass spectrometry
IRS	Insulin receptor substrate
IU	International units
LBM	Lean body mass
LD	Lipid droplet
LPS	Lipopolysaccharide
MAFBx	Muscle atrophy f-box-1
MBV	Mean blood velocity
MEDES	Institute of Space Medicine and Physiology
MHC	Myosin heavy chain
MPB	Myofibrillar protein breakdown
MPS	Myofibrillar protein synthesis
MRC	Medical Research Council
MRI	Magnetic Resonance Imaging
MRS	Magnetic Resonance Spectroscopy
MTOR	Mammalian target of rapamycin
MURF	Muscle ring finger protein 1
MVC	Maximal voluntary contraction

NADH	Nicotinamide adenine dinucleotide + hydrogen
NCAM	Neural cellular adhesion molecule
NEFA	Non-esterified fatty acid
NHS	National Health Service
NIDDM	Non insulin-dependent diabetes mellitus
NIHR	National Institute for Health and Care Research
NO	Nitric oxide
O_2	Oxygen
OGTT	Oral glucose tolerance test
ORO	Oil red O
PAL	Physical activity level
PBS	Phosphate buffered saline
PCA	Perchloric acid
PDC	Pyruvate dehydrogenase complex
PDK	Pyruvate dehydrogenase kinase
PDP	Pyruvate dehydrogenase phosphatase
PI3K	Phosphatidylinositol 3-kinase
PIL	Participant information leaflet
PIP2	Phosphatidylinositol-4,5-bisphosphate
PIP3	Phosphatidylinositol-3,4,5-triphosphate
PPAR	Peroxisome proliferator-activated receptor
QMC	Queen's Medical Centre
QUICKI	Quantitative insulin sensitivity check index
REC	Research Ethics Committee
RER	Respiratory Exchange Ratio
RMR	Resting Metabolic Rate
RNA	Ribonucleic acid
ROI	Region of interest
SEM	Standard error of the mean
SMAD	Vertebrate homolog of *Drosophila* protein MAD (mothers against decapentaplegic) and Caenorhabditis elegans protein SMA
SPMIC	Sir Peter Mansfield Imaging Centre
TAG	Triacylglycerol
TBC1D1	TBC1 domain family member 1
TBC1D4	TBC1 domain family member 4
TCA	Krebs/tricarboxylic acid cycle
TEE	Total energy expenditure
THL	Tetrahydrolipostatin
TNF-α	Tumour necrosis factor alpha
UK	United Kingdom
ULLS	Unilateral lower limb suspension
US	Ultrasound
USA	United States of America

VCO_2	Carbon dioxide production
VL	Vastus lateralis
VLDL	Very low density lipoprotein
V_{O2}	Oxygen production
WHO	World Health Organisation
YSI	Yellow Springs Instrument

Chapter 1 Introduction

1.1 The burden of physical inactivity

Physical inactivity has been identified as the fourth leading risk factor for global mortality (6% of deaths globally) (Lee et al. 2012). It is estimated that 500 million people will develop coronary heart disease, obesity, diabetes or other non-communicable diseases attributable to physical inactivity between 2020 and 2030, costing $27 billion annually (WHO 2022). The World Health Organisation (WHO) released global recommendations for physical activity, with adults aged 18-64 years recommended to do 150 minutes of moderate-intensity aerobic physical activity per week (WHO 2010). However, around a quarter of adults are insufficiently active and these figures have remained largely unchanged for several decades (Guthold et al. 2018) leading the WHO to publish the first Global Action Plan on Physical Activity in 2018 (WHO 2018). The WHO's progress report has shown that progress is slow with inequitable actions to address physical activity across world regions (WHO 2022). As well as low levels of habitual physical activity in the general population, periods of increased sedentariness are common following illness or injury. In 2021-2022 there were 16 million hospital admissions in the United Kingdom (UK)(NHS Digital 2022), with the average length of stay 6 days (OECD 2023). Individuals admitted to hospital, particularly older adults, spend significant periods of time (up to 23 hours) sitting or lying (Baldwin et al. 2017) and this is associated with

a poorer recovery, prolonged admission and mortality (Biswas et al. 2015). Common sequelae of periods of immobilisation as well as inflammation which is present during illness or trauma include a reduction in whole-body insulin sensitivity and muscle atrophy, which may predispose to the development of chronic metabolic disease such as type II diabetes and a loss of muscle mass and function, termed sarcopenia. The huge burden of global physical inactivity, increasing hospital admissions and non-communicable disease associated with these situations is a great obstacle to enabling good health and independent living with longer life expectancy.

Evidence on the relationship between health outcomes and sedentary behaviour has been extrapolated from the data on physical activity studies, as well as in research looking at sedentary behaviour and its relationship to non-communicable disease. A meta-analysis of 1 million people demonstrated that increased sedentary time is associated with increased all-cause mortality (Ekelund et al. 2016). Some meta-analyses have reported that moderate to vigorous physical activity can attenuate the hazardous association with prolonged sitting time and all-cause mortality (Chau et al. 2013; Ekelund et al. 2016). However, another meta-analysis has reported that sedentary time was associated with increased risk of deleterious health outcomes regardless of physical activity level (Biswas et al. 2015). Objectively measured increased sedentary time has been associated with higher plasma glucose, insulin and triacylglycerol (TAG) concentrations as well as lower concentrations of advantageous HDL-cholesterol and larger waist circumference (Powell et al. 2018). Whether a sedentary lifestyle accelerates skeletal muscle loss in older

adults is currently unresolved. Master athletes, physically-active older adults who have accrued a significant volume of physical activity across their lifespan, have a greater muscle strength and power than sedentary controls (Pearson et al. 2002). However age-related declines in their muscle peak power and force were similar compared with healthy controls. A loss of muscle mass and quality with age contribute to functional disability and may impair other physiological functions including glucose regulation and so understanding the relationship between physical inactivity and maintenance of muscle mass is important.

Epidemiological studies however can only provide information on association and therefore to investigate the precise mechanisms underpinning how physical inactivity leads to detrimental health outcomes, more prospective experimental models must be used. Models of partial (reduced step count) and complete (bed rest, unilateral limb immobilisation) physical inactivity have provided invaluable information regarding the effect of immobilisation on whole-body and muscle insulin sensitivity and muscle mass and their underlying mechanisms. A significant number of long-term bed rest studies, of several weeks' duration have demonstrated a reduction in whole-body insulin-stimulated glucose disposal and a reduction in muscle protein synthesis (Cree et al. 2010; Ferrando et al. 1996). However, time points in these studies have largely been confined to pre and post-bed rest, with little insight as to the rate or magnitude of change during these time frames. Furthermore, some studies have failed to control for dietary intake, meaning that it is inconclusive as to whether the end points measured were secondary to overfeeding or physical inactivity *per se*. Shorter duration limb immobilisation (<7 days) studies have

also demonstrated a rapid decline in glucose disposal (Burns et al. 2021). As evidence for an independent effect of sedentary behaviour emerges, further work is required to establish the dose-response relationship between sedentary behaviour and health outcomes, the underlying pathophysiological mechanisms and potential countermeasures.

1.2 Human models of immobilisation

Several models of immobilisation have been utilised to study the effect of muscle disuse in humans, and these are represented in Figure 1.1 and summarised in Table 1.1.

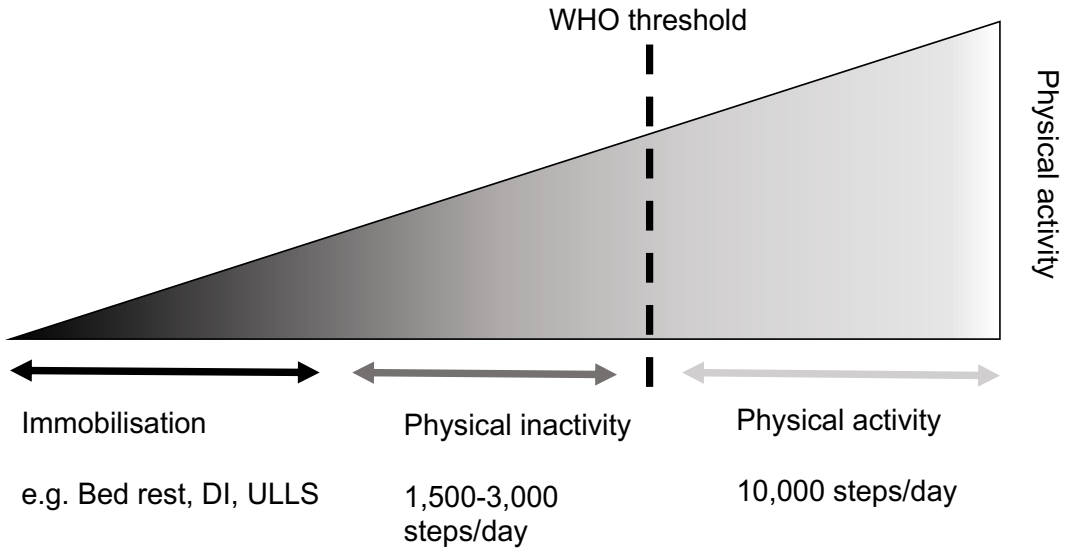

Figure 1.1. Models of immobilisation on the spectrum of physical activity and inactivity. DI, dry immersion, ULLS, unilateral lower limb suspension, WHO, World Health Organisation. Image taken from (Shur et al. 2021).

1.2.1 Reduced ambulatory activity

Reduced ambulatory activity, normally achieved through a reduction in step count (step reduction model), is the model most realistic to free-living scenarios. The model was originally designed to assess changes in insulin sensitivity and body composition in response to physical inactivity (Krogh-Madsen et al. 2010a; Olsen et al. 2008). Participants are normally given a pedometer or accelerometer to wear and advised to keep step count to below 1,500 steps which some have viewed as a benchmark for low levels of physical activity (Tudor-Locke and Bassett 2004). The physiological adaptations induced by a reduction in ambulatory activity often take longer to manifest compared to other models but are more relevant to free-living individuals. Limitations of reduced step count studies with a pedometer include the inability to capture subtle activities which may increase energy expenditure without an increase in steps e.g. various domestic activities. For this reason, accelerometers are generally preferred with some objective measure of intensity e.g. heart rate, with duration also captured. For a recent review of the step reduction model see Sarto (Sarto et al. 2023).

1.2.2 Limb casting

Limb immobilisation via limb casting is a commonly-used model to study disuse atrophy. In casting of the lower limb, participants are provided with crutches to ambulate and advised not to weight bear during the study period. In this model

the contralateral leg can be used as an internal control. Care must be taken to cast the leg in an anatomical position, for example in below-knee casting, avoiding the equinuus position to reduce the risk of Achilles tendon shortening and subsequent negative impact on gait. Limitations of this model include the impact on physical activity behaviour i.e. participants may inadvertently reduce step count due to the impracticality of crutches leading to overall reduced physical activity. Objective measures of step count must therefore be taken to carefully control for this confounder. In addition, there are likely to be changes in loading of the contralateral non-casted limb due to the use of crutches, different to normal ambulation. Upper limb casting using a forearm model has also been employed previously and has the benefit of being easier to undertake vascular measurements using ultrasonography e.g. brachial artery compared with the lower limb e.g. femoral artery due to the depth of the vessels. Upper body immobilisation is also generally more convenient and better tolerated by participants than lower limb immobilisation.

1.2.3 Limb suspension

Unilateral lower limb suspension (ULLS) is the unloading of one lower limb without movement restriction and is normally achieved via the use of crutches. Two methods exist to achieve the desired effect and have the advantage of using the other limb as a control. The first method is using a support strap to suspend one lower limb. In this method the knee is in flexion during ambulatory activity, therefore the muscle length may differ depending on the amount of time

in ambulatory activity. In the second method, a platform shoe is used on the contralateral limb to prevent weight bearing on the ipsilateral leg. The benefit of the platform shoe method is that the leg is in a neutral anatomical position. Muscle activity across the knee joint may differ between these methods and therefore may not induce the same changes seen in bed rest or spaceflight.

1.2.4 Bed rest

Bed rest is a commonly employed model of whole-body physical inactivity in physiological research. Head-down-tilt (HDT) bed rest studies have been used for decades in spaceflight research and provided unique insights into the physiology of unloading and deconditioning of the musculoskeletal and cardiovascular system associated with microgravity (Adams, Caiozzo, and Baldwin 2003). The -6^{o} position has been utilized as it better mimics the cephalic fluid shifts and tissue fluid accumulation encountered during microgravity conditions compared with horizontal bed rest (Hargens and Vico 2016). However, these fluid shifts may be a confounding factor when generalising the model to physical inactivity outwith spaceflight research. The benefits of bed rest experiments are the ability to investigate an intervention such as diet or exercise countermeasures whilst tightly controlling for confounding factors such as energy intake, circadian rhythm and physical activity levels. Limitations are largely financial and logistic as a team of clinicians and scientists are required on-site at all times, and specialist

equipment and facilities or infrastructure are required to deliver long duration bed rest experiments.

1.2.5 Dry immersion

An alternative model of whole-body physical inactivity is ‘dry’ water immersion (DI), which can be used as a model of weightlessness. It involves immersing the subject in thermoneutral water and subjects are protected from water contact with a thin elastic waterproof fabric. ‘Dry’ water immersion produces similar physiological effects to those observed during bed rest, but the effects may occur at a faster rate (Shenkman et al. 1997; Navasiolava et al. 2010). Due to the specialised equipment and inconvenience for participants, only short-term DI experiments have been carried out, and so are best utilised to study the early period of muscle deconditioning.

Table 1.1. Human models of immobilisation and their advantages and disadvantages. HDT, Head-down tilt.

Model of immobilisation		Advantages	Disadvantages
Reduced step count		• Easy and cheap • Minimal equipment required • More representative of "free living' conditions	• No internal control
Limb casting	Upper body	• More convenient and better tolerated than lower limb immobilisation • Easier to perform vascular measurements compared with lower limb • Contralateral limb can act as an internal control	• Not required for weight-bearing • Changes to immobilisation may be more modest compared with lower body
	Lower body	• Contralateral limb can act as an internal control	• Cumbersome for participants • Contralateral limb may experience different loading to 'free living' conditions due to crutches

			• Alteration in physical activity behaviour due to crutches
Limb suspension		• Contralateral limb can act as an internal control	• Cumbersome for participants • Contralateral limb may experience different loading to 'free living' conditions due to crutches
Bed rest		• Can carefully control temperature, circadian rhythm, diet and intervention	• Expensive and logistically challenging with several personnel required • HDT bed rest causes cephalic fluid shifts which may confound other variables.
Dry immersion		• Can carefully control temperature, circadian rhythm, diet and intervention	• Inconvenience means that not suitable for long duration immobilisation

1.3 Insulin sensitivity, glucose uptake and fuel oxidation

1.3.1 Definitions of insulin sensitivity

Insulin is a hormone produced by β cells in the islets of Langerhans of the pancreas in response to elevation of the intracellular Ca^{2+} concentration, in order to regulate circulating blood glucose concentrations (Bratanova-Tochkova et al. 2002). Insulin stimulates glucose uptake and glycolysis in muscle, whilst in the liver it decreases endogenous glucose production and stimulates glycogen synthesis. In adipose tissue, insulin suppresses lipolysis and release of non-esterified fatty acids (NEFA) and stimulates fatty acid (FA) re-esterification and TAG synthesis. Its secretion is tightly controlled to the availability of glucose, allowing a fine tuning of blood glucose concentration to maintain glucose homeostasis. Insulin resistance is said to be the decreased sensitivity or responsiveness to the metabolic actions of insulin to increase whole-body glucose uptake and utilisation (Lebovitz 2001). The underlying pathological mechanism is a reduction in peripheral tissues' (particularly skeletal muscle) ability to respond to circulating insulin, resulting in a compensatory increased production of insulin by the β cells of the pancreas to address increasing blood glucose concentration, which over time can fail. Hepatic insulin resistance also occurs, characterised by the inability of insulin to suppress hepatic glucose output (Santoleri and Titchenell 2019). Type II

diabetes is therefore characterised by relative insulin deficiency caused by pancreatic β-cell dysfunction and insulin resistance in target organs.

Whilst the terms ‘insulin sensitivity’, ‘insulin responsiveness’ and ‘insulin resistance’ are often used interchangeably to refer to insulin action on glucose metabolism, they are distinct entities with separate underlying mechanisms. Pathological states can be divided into those due to a decreased sensitivity to a hormone, causing a shift in the dose-response curve to the right, and those due to a decreased responsiveness, defined as a decrease in the maximal response to the hormone, or a combination of both (Kahn 1978) (Figure 1.2). Disorders associated with changes at the prereceptor and/or receptor level of insulin lead to decreased insulin sensitivity, whilst those disorders associated with changes at the postreceptor steps in insulin action are more likely to produce decreased responsiveness. This distinction is important to recognise as it may have implications on designing potential strategies to ameliorate these changes in different cohorts.

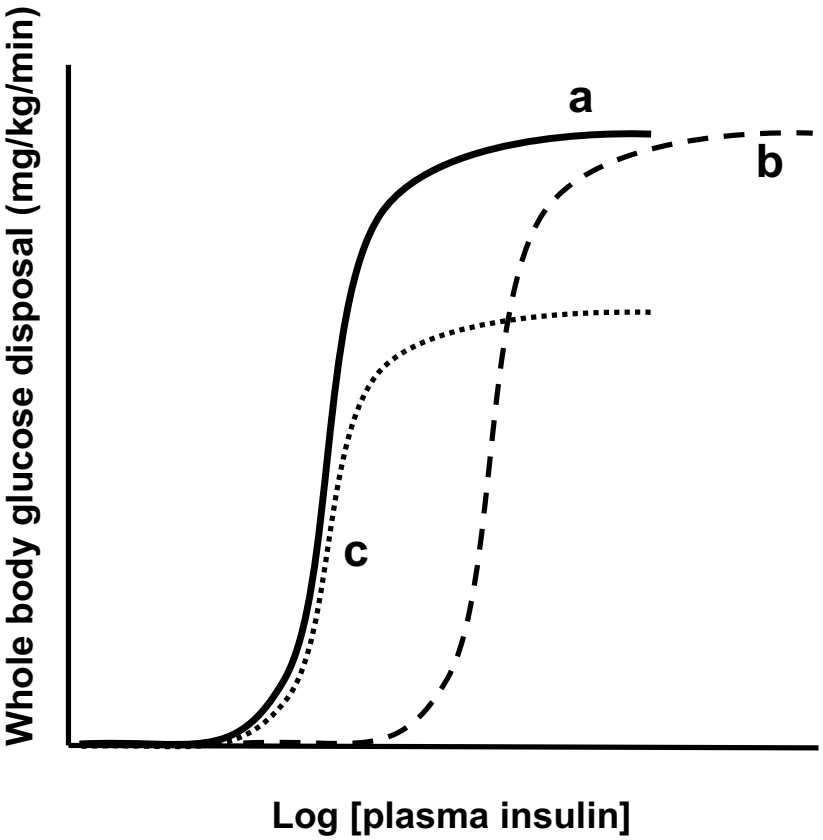

Figure 1.2. Dose response curve characterising insulin action on glucose utilisation. a) represents normal reference value, b) decreased sensitivity defined by a right shift in the curve c) decreased insulin responsiveness defined by a reduced maximal effect of insulin.

1.3.2 Techniques to measure whole-body insulin sensitivity

In vivo assessment of insulin sensitivity of glucose metabolism can be divided into those disrupting the feedback loop between plasma glucose concentration

and insulin secretion and those assessing the feedback loop. Under postabsorptive conditions glucose production is predominantly by the liver (95%) and to a lesser extent the kidneys (5%) and utilised by a variety of tissues (Roden 2007). In healthy volunteers, during insulin-stimulated conditions, endogenous glucose production is suppressed by hyperinsulinaemia and skeletal muscle accounts for 75-80% of whole-body glucose uptake (DeFronzo et al. 1981). Fasting plasma concentrations of glucose and insulin can be measured, and indices of fasting insulin sensitivity derived from the use of mathematical models e.g. homeostasis model assessment insulin resistance (HOMA-IR) and quantitative insulin sensitivity check index (QUICKI). The benefit of these methods is their relative ease and inexpense of carrying out, and as such have been utilised in large epidemiological studies (Katz et al. 2000; Mather et al. 2001; Matthews et al. 1985). However, as they are measured when fasted, they largely reflect hepatic insulin sensitivity and there are significant interlaboratory variations in insulin assay, meaning comparing absolute values across different studies is difficult (Isokuortti et al. 2017). Other methods which harness the normal feedback loop include the oral glucose tolerance test (OGTT) which measures glucose and insulin responses, normally for 2 hours after an oral glucose challenge. Whilst being technically straightforward, the technique does not differentiate between reduced sensitivity of peripheral tissues to insulin or pancreatic β cell dysfunction and it is also impacted by gastric emptying rate, absorption from the gut and gut blood flow (Thompson et al. 1982). Decreased glucose tolerance using the OGTT has

previously been demonstrated following bed rest relative to before bed rest (Yanagibori et al. 1994; Reidy et al. 2017).

Techniques which remove the negative feedback loop can be used to determine insulin sensitivity, and include the insulin tolerance test (Bonora et al. 1989) and the hyperinsulinaemic euglycaemic clamp technique (DeFronzo, Tobin, and Andres 1979). The hyperinsulinaemic euglycaemic (insulin) clamp technique originally developed by Andres and de Fronzo (de Fronzo 1975) is widely accepted as the gold standard for directly determining glucose uptake as a measure of insulin sensitivity in humans. In a hyperinsulinaemic euglycaemic clamp, in fasted participants, insulin is infused intravenously at a fixed rate determined by body surface area, that can typically range between 40-120 mU/m^2/min depending on the aims of the study. The fixed insulin infusion causes a new steady-state insulin level that is supraphysiological (hyperinsulinaemic). This stimulates skeletal muscle and adipose glucose uptake and suppresses hepatic gluconeogenesis. A 20% glucose infusion is also titrated at a variable rate to “clamp” blood glucose concentrations at physiological levels circa 4.5 mmol/L to achieve euglycaemia. Steady state conditions are normally achieved within 2-3 hours of a constant insulin infusion for plasma insulin, blood glucose and the glucose infusion rate. At this steady state point, assuming hepatic gluconeogenesis (HGP) is suppressed and there is no net change in blood glucose concentrations, glucose infusion rate (GIR) is equal to glucose disposal rate (M). M can then be normalised for lean/ fat-free mass in kilograms (kg) determined using dual energy x-ray absorptiometry (DEXA). In healthy controls, HGP is normally suppressed with an insulin

infusion rate in the range 40-60 mU/m^2/min, however considerations should be given to conditions in which there is resistance of insulin-induced suppression of endogenous glucose output including type II diabetes, obesity and increased availability of NEFA (Bonadonna et al. 1990; Conte et al. 2012). Campbell showed that in patients with type II diabetes, the half maximal effective plasma insulin concentration to supress endogenous glucose output is increased twofold compared with controls without diabetes (Campbell, Mandarino, and Gerich 1988). The ability to achieve steady state determines the validity of insulin sensitivity using the insulin clamp technique and ideally endogenous glucose output should be measured. An advantage of the hyperinsulinaemic euglycaemic clamp technique compared with the OGTT is it is a direct measure of insulin sensitivity under steady-state conditions and its high reproducibility (the repeated measures coefficient of variation for the whole-body hyperinsulinaemic euglycaemic clamp technique within our laboratory is 10%). However, it is resource intensive, burdensome for participants, requires clinical support, has associated risks including hypoglycaemia and hypokalaemia and involves multiple blood sampling.

1.3.3 Links between vascular and metabolic actions of insulin

Skeletal muscle glucose delivery is mediated by muscle blood flow and perfusion. Insulin has important actions on skeletal muscle vasculature including limb blood flow and capillary recruitment; it enhances its own delivery to the muscle by increasing total tissue blood flow and recruiting muscle

microvasculature. There is some debate as to the significance of insulin-mediated vasodilatation in glucose uptake. Early studies reported that insulin increases whole-limb blood flow in a dose-dependent manner in lean humans, and correlates with skeletal muscle glucose uptake, measured using a euglycaemic clamp and leg balance techniques across a range of serum insulin concentrations (Laakso et al. 1990; Baron et al. 1991). It is believed that insulin vasodilation of skeletal muscle vasculature occurs via endothelium-derived nitric oxide release (Steinberg et al. 1994). Other studies challenge the role of blood flow in skeletal muscle glucose uptake, as augmentation of limb blood flow via bradykinin infusion did not lead to increased insulin-stimulated skeletal muscle glucose uptake (Nuutila et al. 1996). Discrepancies in observed effects of insulin on blood flow may be explained by participant selection, due to a large interindividual response, likely due to differing levels of physical activity, musculature and capillarisation. In addition, there is criticism of the sequential insulin infusions which were maintained for several hours before an increase in flow was detected, therefore questioning how physiologically relevant they are (Laakso et al. 1990). Insulin also has effects on microvascular recruitment within skeletal muscle; Vincent showed that insulin modulates microvascular perfusion through capillary recruitment, and this occurs before changes in total limb blood flow that peak after 2 hours of insulin infusion (Vincent et al. 2004; Vincent et al. 2002). Treatment with a nitric oxide synthase inhibitor has been shown to attenuate insulin-enhanced capillary volume, suggesting these effects are in part nitric-oxide dependent (Vincent et al. 2003). Seven days of bed rest has previously been shown to cause a reduction in insulin-mediated leg blood

flow, but was not able to fully account for reductions in leg glucose uptake (Mikines et al. 1991). Therefore there is some evidence in the literature that a reduction in insulin-stimulated glucose uptake may in part be explained by alterations in glucose delivery to the muscle due to changes in insulin-stimulated bulk blood flow, but is unlikely to be the predominant factor. Whether any changes in insulin-mediated blood flow occur after only a few days of bed rest and whether they are reversible after a similar period of remobilisation is unknown.

1.3.4 Skeletal muscle glucose uptake and metabolism

Skeletal muscle glucose uptake is potently stimulated by both insulin and muscle contraction via distinct pathways and is summarised in Figure 1.3. Under normal physiological conditions in the resting state, skeletal muscle glucose transport is the rate limiting step in blood glucose disposal. Insulin-dependent and independent skeletal muscle glucose disposal requires 1) glucose delivery to the muscle (discussed in **Section 1.3.3**) 2) glucose transport to the cell membrane and uptake via glucose transporters and 3) glucose metabolism. Glucose is transported into cells via glucose transporters (GLUTs), of which GLUT4 is the primary transporter in skeletal muscle (Birnbaum 1989). In the insulin-stimulated glucose uptake pathway in skeletal muscle, after feeding, circulating insulin concentration increases and insulin binds to its skeletal muscle receptor. This causes rapid phosphorylation of the insulin receptor substrate (IRS)(Van Obberghen et al. 2001) on tyrosine residues and the activation of phosphatidylinositol 3-kinase (PI3K), which leads to the

activation of the Akt (protein kinase B) pathway (Figure 1.4). Activation of this pathway modulates Rab Guanosine-5'-triphosphate (GTP)ase protein activity, which triggers the translocation of GLUT4 from the cytosol into the cell surface membrane, facilitating glucose to move down its concentration gradient into the cell (Fukuda 2008). Insulin-directed recruitment of GLUT4 results in a 10-20 fold increase in glucose transport (Bryant, Govers, and James 2002).

During contraction of skeletal muscle, bulk blood flow increases up to 20-fold from rest (Andersen and Saltin 1985) and capillary recruitment increases, facilitating glucose delivery to the muscle. Contraction of skeletal muscle also signals GLUT4 translocation, however the exact mechanisms are less certain. Glucose uptake by contracting skeletal muscle occurs by facilitated diffusion, dependent on GLUT4 in the surface membrane and an inward diffusion gradient. One regulator believed to be critical in contraction-mediated glucose uptake is adenosine monophosphate (AMP)-activated protein kinase (AMPK). AMPK is a serine-threonine kinase which is sensitive to changes in the intracellular ratio of AMP:ATP and thus, to exercise (Richter and Ruderman 2009). Both moderate-intensity aerobic cycle exercise (Wojtaszewski et al. 2000), and high-intensity sprint exercise (Chen et al. 2000) can increase AMPK activity in skeletal muscle in humans. There is now evidence to suggest that other mechanisms are also involved in exercise regulation of muscle glucose transport such as calcium-activated proteins [for a review on the area see Jessen (Jessen and Goodyear 2005)]. Although insulin-mediated and muscle contraction-mediated glucose uptake occur via distinct pathways, at least distally, there are believed to be signalling molecules that are activated by both

insulin and muscle contraction, TBC1D1 and TBC1D4 (Bruss et al. 2005) which upregulate the activity of Rab GTPase activity. In chronic disease, an impairment of muscle glucose transport in association with decreased recruitment of GLUT4 to the muscle plasma membrane is found in both obesity and NIDDM (Kelley et al. 1996).

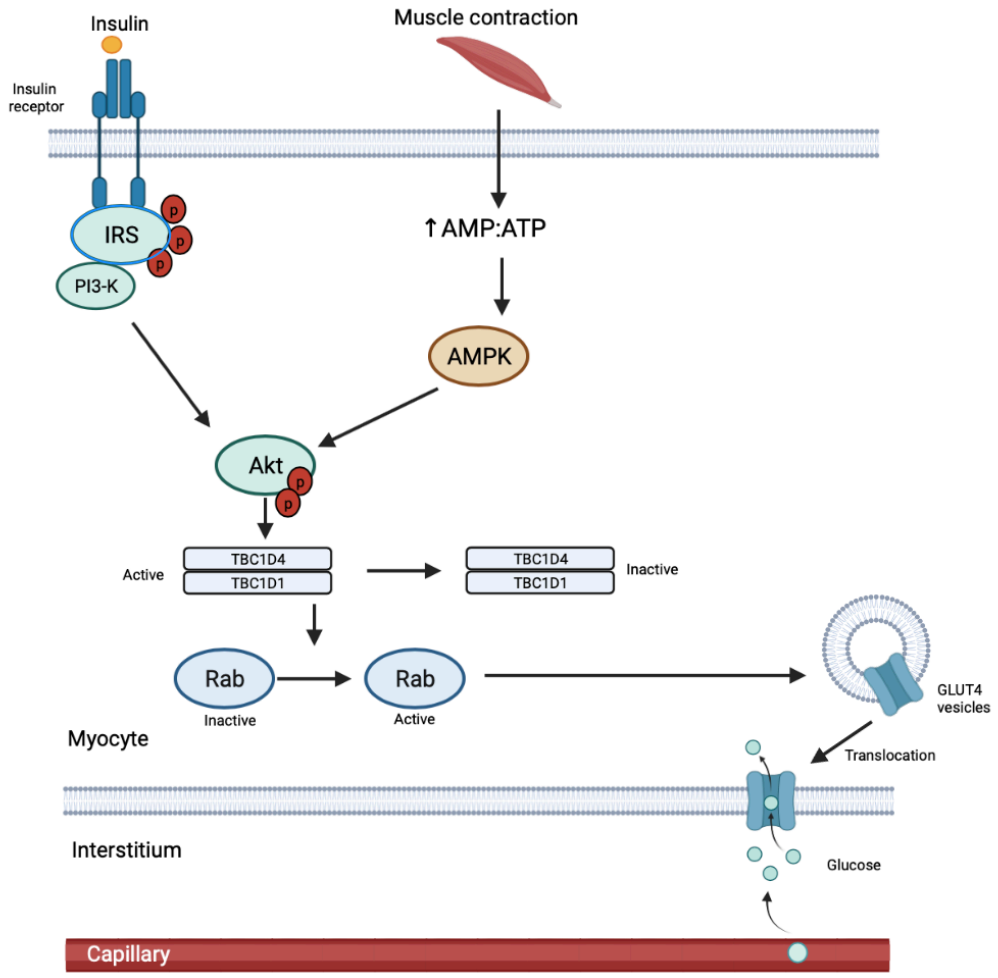

Figure 1.3. Simplified schematic of the regulation of skeletal muscle glucose uptake mediated by insulin and muscle contraction. AMPK: AMP-activated protein kinase, Akt: protein kinase B, GLUT4: Glucose transporter type 4, IRS: insulin receptor substrate, PI3-K: phosphatidylinositol-3-kinase, Rab: Ras-

associated binding, TBC1D1: TBC1 domain family member 1, TBC1D4: TBC1 domain family member 2.

Once glucose is taken up into skeletal muscle by GLUT4 via facilitated diffusion, it is then phosphorylated to glucose-6-phosphate (G6P) via an ATP-dependent reaction catalysed by hexokinase II (Roberts and Miyamoto 2015). This maintains the transmembrane glucose gradient for facilitated diffusion of glucose. G6P can then be converted to glycogen (through glycogenesis) for storage via glycogen synthase or metabolised (through glycolysis) to pyruvate (Fig 1.4). Pyruvate is either anaerobically reduced to lactate in the cytoplasm catalysed by lactate dehydrogenase or can enter the mitochondrial matrix and be oxidised to form acetyl-CoA, catalysed by the pyruvate dehydrogenase complex (PDC). The PDC is an inner mitochondrial multi-enzyme complex essential in the maintenance of normal glucose homeostasis and is key in determining muscle fuel selection. It is responsible for the irreversible conversion of pyruvate to acetyl-CoA for metabolism in the Kreb's/tricarboxylic acid (TCA) cycle and for FA synthesis. The PDC is regulated by reversible phosphorylation controlled by two regulatory enzymes, pyruvate dehydrogenase kinase (PDK) and pyruvate dehydrogenase phosphatase (PDP)(Wieland 1983), with the most abundant isoforms of PDK in muscle being PDK2 and 4 (Bowker-Kinley et al. 1998). Acetyl-CoA can then enter the TCA cycle to generate ATP (adenosine triphosphate). An overview of glucose and lipid metabolism is summarised in Figure 1.5.

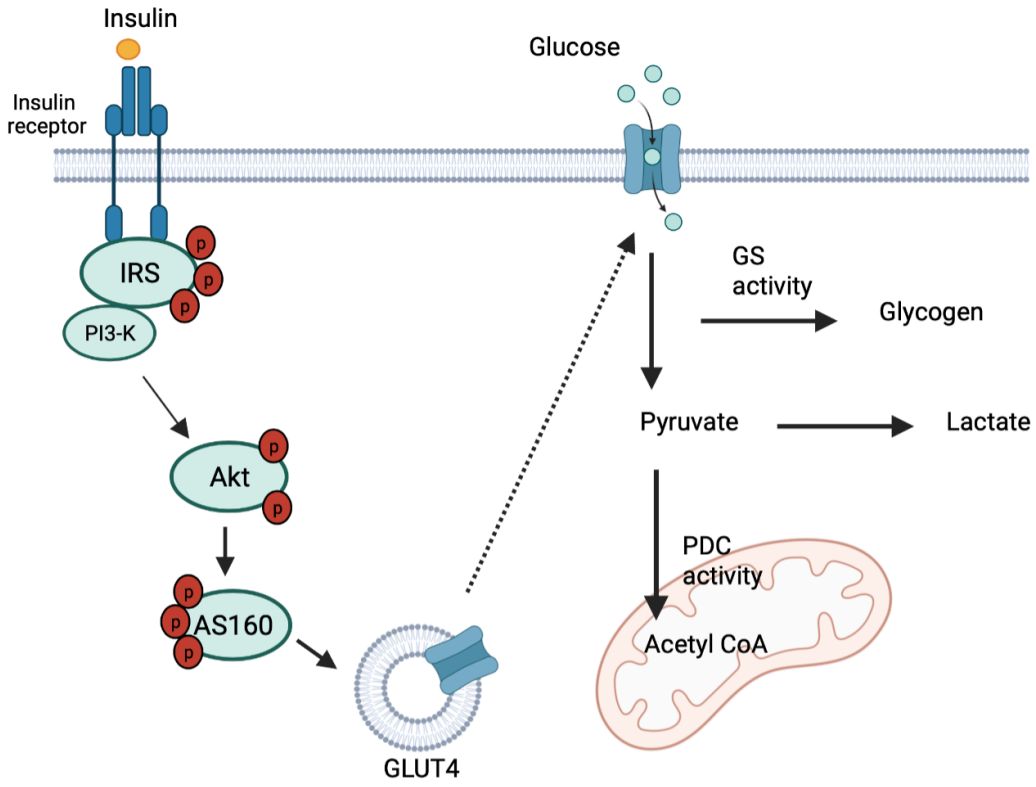

Figure 1.4. Overview of insulin-stimulated skeletal muscle glucose uptake in humans. Insulin binds to the insulin receptor and activates a signaling cascade resulting in the translocation of glucose transporter type 4 (GLUT4) to the plasma membrane. This facilitates glucose uptake into the muscle cell. The majority of glucose is then either stored as glycogen, oxidised in the mitochondria, or converted to lactate. Akt: protein kinase B, AS160/TBC1D4: TBC1 domain family member 2, GLUT4: Glucose transporter type 4, IRS: insulin receptor substrate, PI3-K: phosphatidylinositol-3-kinase, GS: glycogen synthase; PDC: pyruvate dehydrogenase complex.

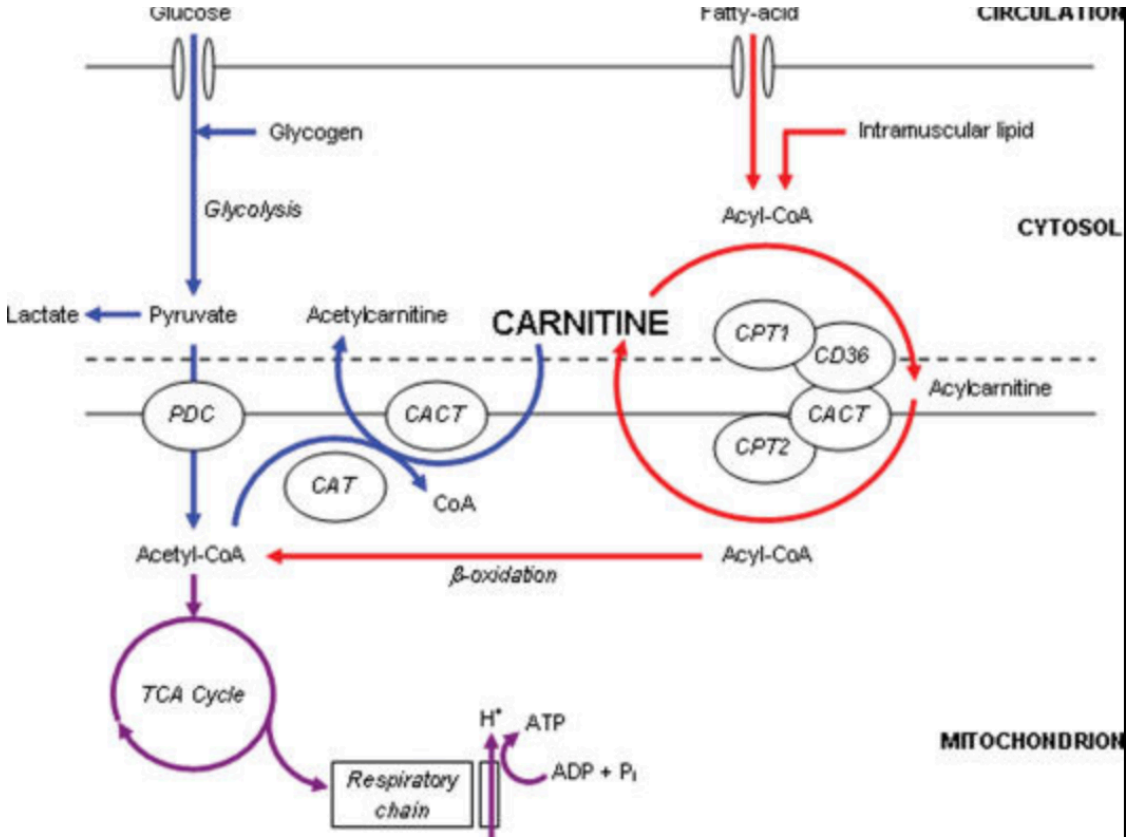

Figure 1.5. A schematic overview of skeletal muscle glucose and lipid metabolism, originally published in (Stephens, Constantin-Teodosiu, and Greenhaff 2007), also depicting the metabolic roles of carnitine. ATP, adenosine triphosphate; ADP, adenosine

diphosphate; Pi, inorganic phosphate; CACT, carnitine acylcarnitine translocase; CAT, carnitine acyl transferase; CPT, carnitine palmitoyltransferase; CD36, fatty acid translocate; GLUT4, glucose transporter 4; PDC, pyruvate dehydrogenase complex; TCA, tricarboxylic acid cycle.

1.3.5 Fatty acid uptake and metabolism

In order to fully understand the effects of immobilisation on insulin sensitivity, it is important to understand the regulation of FA metabolism, particularly within skeletal muscle, as FA are an important energy source. Whilst feeding, dietary fat is hydrolysed by gastrointestinal lipases to form NEFAs, which are absorbed by enterocytes within the intestine, and converted back to TAG before being absorbed into the lymphatic system and ultimately the blood. Lipid is primarily stored in adipose tissue under normal physiological conditions. The dietary TAG is hydrolysed within the capillaries of the adipose tissue and the NEFA are taken up by the adipocytes and re-esterified to TAG for storage. The stored TAG can be hydrolysed and the NEFA released into the circulation during periods of fasting or increased substrate demand e.g. exercise. The liver can also supply lipid after consumption of large amounts of carbohydrate, particularly sugars and refined starch, as it is able to convert excess glucose to FAs, a process termed *de novo* lipogenesis. The liver forms very low density lipoproteins (VLDL) from TAG formed from the newly formed NEFA, which can then be transported via the blood to peripheral tissues (adipose tissue and skeletal muscle), where the FAs are released from the TAG core by lipoprotein lipases. NEFAs cross the cell membrane via specific transport proteins e.g fatty acid translocase (FAT/CD36) and fatty acid binding proteins (FABP), as they are impermeable to cell membranes due to their negative charge. Plasma FAs can derive from three sources: dietary TAG, hepatic *de novo* lipogenesis from

dietary carbohydrate, and hydrolysis of TAG and phospholipids within peripheral tissues to release NEFA.

Once FAs enter the skeletal muscle, their fate depends on the metabolic status of the cell (Figure 1.5). NEFA can be re-esterified to form TAG which is incorporated into intramyocellular lipid (IMCL), or they can enter the mitochondria and undergo β-oxidation to produce acetyl-CoA. IMCL is mainly composed of intracellular lipid droplets localised between the sarcomeres and adjacent to mitochondria. Alternatively, lipid can be subcutaneous or intermuscular, extramyocellular lipid (EMCL). EMCL is located under the epimysium (between bundles of muscle fibres) and under the perimysium (between muscle fibres). Prior to undergoing β-oxidation, long-chain FAs are transferred across the impermeable inner mitochondrial membrane via the carnitine shuttle. Pioneering work by Fritz and McEwan established that carnitine and carnitine palmitoyltransferase (CPT) were essential for the translocation of long-chain FAs into skeletal muscle mitochondria (Fritz and McEwen 1959). CPT1 catalyses the esterification of carnitine with long-chain acyl-CoA forming long-chain acylcarnitine (Longo, Amat di San Filippo, and Pasquali 2006). Acylcarnitine in the cytosol is transported into the mitochondria via exchange with intramitochondrial free carnitine via carnitine acylcarnitine translocase (CACT). Acylcarnitine is converted back to acyl-CoA and free carnitine catalysed by CPT2 and the intramitochondrial acyl-CoA is oxidised by the β-oxidation pathway. It has been shown that muscle acetylcarnitine content is a marker of PDC flux. However this is during contraction when PDC is highly

activated and glycolytic flux is in excess of carbohydrate oxidation (Stephens, Constantin-Teodosiu, and Greenhaff 2007).

1.3.6 Fuel selection and metabolic flexibility

Skeletal muscle and adipose tissue play a key role in energy metabolism. In lean healthy individuals, skeletal muscle has substantial metabolic flexibility, namely the ability to modify fuel oxidation in response to changes in nutrient availability. Lipid oxidation predominates during fasting conditions, whilst the suppression of lipid oxidation and increased glucose uptake, oxidation and storage occurs in insulin-stimulated conditions (Kelley et al. 1990). The primary role of this substrate shift is to effectively store energy in skeletal muscle, adipose and liver tissue, of which insulin is a key regulator. Randle was the first to put forward in 1963 that there was flexibility in fuel selection between glucose and fatty acid for oxidation in skeletal muscle and adipose tissue (Randle et al. 1963). He proposed that, at rest, fatty acid oxidation caused a decline in glucose oxidation as well as an increase in the mitochondrial levels of acetyl-CoA and cytoplasmic NADH/NAD+ ratio, subsequently inhibiting PDC via end product inhibition (Randle 1998). Thus, an elevation of circulating free fatty acids seen in insulin resistant states may negatively influence insulin responsiveness and glucose uptake in skeletal muscle at rest. Kelley and colleagues later described metabolic inflexibility in patients with type 2 diabetes and obesity in a series of experiments, in which they demonstrated that during resting post-absorptive conditions, there is an elevated rate of whole-body

glucose oxidation and a lower rate of whole-body fatty acid oxidation compared with healthy controls (Kelley and Mandarino 1990; Kelley et al. 1993). Similarly, it was noted in individuals with obesity and type II diabetes that there is a reduced suppression of resting, whole-body lipid oxidation under insulin-stimulated conditions (Felber et al. 1987). Physical activity has a impact on metabolic flexibility, with 1 hour of daily aerobic exercise (70% V_{O2peak}) shown to increase the rate of fatty acid oxidation in response to a high fat diet in adults with obesity compared to lean individuals (Battaglia et al. 2012). Relatively less is known about metabolic flexibility in response to physical inactivity in comparison to exercise, in particular the impact of inactivity induced reduced glucose uptake and the temporal juxtaposition with changes in substrate oxidation in response to feeding in humans.

1.4 Immobilisation and insulin sensitivity, substrate oxidation and lipid content

1.4.1 The impact of immobilisation on insulin sensitivity and substrate oxidation

A reduction in whole-body insulin sensitivity has been identified as occurring as early as 3-5 days of bed rest (Yanagibori et al. 1994; Smorawinski et al. 2000; Reidy et al. 2017), but was not detectable after one day of bed rest (Dirks et al. 2018). Mikines was the first to demonstrate that reduced glucose uptake after 7 days of bed rest was predominantly at the level of the muscle measured using AV-V difference and blood flow across the leg, where it was found that leg

glucose uptake was blunted across a wide range of serum insulin concentrations (10-352 μU/ml)(Mikines et al. 1991). Furthermore, reduced muscle glucose uptake measured using the hyperinsulinaemic euglycaemic clamp and stable isotope-based techniques has been shown to develop after more modest reductions in physical activity such as 3-14 days of reduced step count (Krogh-Madsen et al. 2010b). Although these findings suggest that it is predominantly inactive muscle driving the metabolic dysregulation secondary to inactivity, the mechanisms underlying this are not completely understood.

A reduction in skeletal muscle glucose uptake has been suggested as a key outcome of immobilisation-induced insulin resistance via impaired glucose transport or adaptive changes in muscle glucose phosphorylation, glycogen synthesis or glucose oxidation. Previous studies have noted a reduction in key regulatory proteins in glucose transport, phosphorylation and storage including skeletal muscle GLUT4 and hexokinase II content and also insulin-stimulated glycogen synthase activity after 7 days of bed rest (Bienso et al. 2012; Ringholm et al. 2011). Bed rest studies have also demonstrated a blunted insulin-stimulated Akt phosphorylation in humans (Mortensen et al. 2014). However, it is unclear if these events were causative in the reduction in skeletal muscle glucose disposal observed during bed rest or in response to a reduction in muscle glucose uptake itself. One study (Burns et al. 2021) utilising a forearm immobilisation model showed a significant reduction in forearm glucose uptake after 24-hours of immobilisation which did not occur in the non-immobilised arm. This suggests that acutely, inactivity-induced declines in glucose uptake are secondary to a lack of muscular contraction *per se*. The precise temporal

changes in the reduction in whole-body glucose disposal and their magnitude in response to acute (<7 days) and longer duration bed rest and the relationship to underlying mechanistic processes is currently lacking.

The impact of immobilisation on fuel selection, and how soon metabolic inflexibility develops after a reduction in whole-body glucose uptake is also unclear. Bergouignon performed a retrospective analysis of longitudinal interventional studies across a range of physical activity levels (PAL), and found active individuals had higher variances in non-protein respiratory quotient (the ratio of carbohydrate to fat oxidation calculated from indirect calorimetry data) for lower variances in insulin than sedentary individuals (Bergouignan et al. 2013). In other words, a high shift in the fuel mix being oxidised at a low insulin signal, indicating a better metabolic flexibility. However, in many of these studies, energy intake was not controlled. Rudwill and colleagues studied healthy males in energy balance undergoing 21 days of bed rest and showed the onset of metabolic inflexibility (assessed via indirect calorimetry following a high-fat, high-energy test meal) manifested by 21 days (Rudwill et al. 2018). In a 3 day HDT bed rest study, Acheson showed an increased lipid oxidation in the fasted state but unchanged rates of glucose and fat oxidation (when cumulated over the course of the OGTT with respect to baseline values) after a glucose load (Acheson et al. 1995). Energy intake was also not carefully controlled in the run-up to the bed rest period potentially affecting results. Overall, the time course of onset of metabolic inflexibility during bed rest, and how this relates to changes in whole-body glucose disposal, is not clear.

1.4.2 The impact of immobilisation on muscle lipid content

Purported mechanisms for the immobilisation-mediated decline in insulin sensitivity include an increase in lipid content within the muscle, evidenced by studies demonstrating a strong negative relationship between IMCL content and insulin sensitivity (Pan et al. 1997). There have been several mechanisms proposed that may explain this association. Incomplete hydrolysis of TAG with elevated diacylglycerol (DAG) as well as alterations in lipid droplet (LD) coating, morphology and subcellular location (subsarcolemmal) have been shown to be determinants of insulin insensitivity (Gemmink et al. 2017; Nielsen et al. 2010), as well as the accumulation of toxic lipid intermediates such as ceramides which may interfere with insulin signalling (Cree et al. 2010). Another mechanism by which lipids may influence insulin sensitivity is via a chronic elevated inflammatory response characterised by altered cytokine production and activation of inflammatory signalling pathways. This is reported to be either from inflammatory intermediates directly inducing insulin resistance via serine phosphorylation of IRS-1 in muscle or liver, or from inflammatory cell infiltration e.g. TNF-α and IL-6 within adipose tissue, leading to altered adipocyte lipid metabolism (Wellen and Hotamisligil 2003). However, a study infusing TNF-α antibody failed to alter insulin sensitivity in obese NIDDM (Ofei et al. 1996), raising uncertainty of this particular pathway.

Several studies have reported changes in IMCL content in response to immobilisation. A 28-day bed rest model by Cree and colleagues demonstrated an almost two-fold increase in intramyocellular TAG in 6 healthy males measured using 1H MRS and a significant decrease in post bed rest insulin-

stimulated muscle glucose uptake during a hyperinsulinaemic euglycaemic clamp (Cree et al. 2010). However, this magnitude of IMCL change has not been reported in other studies in response to bed rest and was also conducted with concomitant hypercortisolaemia (to represent the increased production of cortisol during spaceflight) which may potentially drive changes in IMCL independent of immobilisation. Increases in intramuscular adipose tissue (IMAT) of a magnitude 14-20% measured using MRI in the lower limb have also been reported in a lower limb suspension model of disuse (Manini et al. 2007). However, in both these studies, dietary energy intake was not controlled for and thus results may have been a reflection of overfeeding, rather than physical inactivity *per se.* Further methodological considerations of the quantification of IMCL should also be considered. Limitations have been reported in previously used histochemical methods to quantify lipid droplets such as oil red O (ORO) and the associated air drying of sections which can cause precipitates, blocking the transmission of light through the stained sections (Prats et al. 2013). ORO is a fat soluble dye used for staining neutral lipids which can be visualised by fluorescence or bright field microscopy. One drawback is that it stains lipids as part of the intracellular membranes and thus these need to be accounted for so as to not overestimate lipid droplet content. Bodipy has therefore been suggested as the dye of choice to image IMTG as it does not affect light transmission (Prats et al. 2013).

Evidence supporting IMCL being a primary driver of immobilisation-induced reductions in insulin sensitivity in shorter duration bed rest is also equivocal. A study of bed rest of 1 week duration reported no significant IMCL

content changes, measured using ORO despite a reduction in whole-body insulin sensitivity (Dirks et al. 2016). Pagano reported that short term disuse via a 3-day dry immersion model caused an increased protein expression of two major markers of mature adipocytes, perilipin and fatty acid binding protein 4, but no change in IMAT adipocyte CSA, however the authors reported that the study was underpowered (Pagano et al. 2018). Another dry immersion study of 3 days duration reported no significant change in percentage intramuscular fat of the thigh as measured by MRI using a T1 Dixon water/fat method (Demangel et al. 2017). Taken together, at present it is equivocal whether IMCL accumulation is a primary driver of immobilisation-induced changes in insulin sensitivity, especially during short duration bed rest, due to differences in methods employed to measure IMCL, and a lack of dietary control in previous studies. The determination of IMCL content after acute bed rest, its relationship to whole-body insulin sensitivity and substrate oxidation and the impact of remobilisation remain unclear.

1.4.3 The impact of immobilisation on muscle vasculature

As explained earlier in **Section 1.3.3**, adaptations in muscle glucose uptake theoretically can be influenced by changes in its delivery to the muscle via alterations in limb blood flow or capillarisation. Five days of bed rest has been shown to induce reductions in reactive hyperaemia measured following cuff occlusion in the upper arm, and this was accompanied by increases in fasting insulin, glucose and HOMA-IR. (Hamburg et al. 2007). Reactive hyperaemia is the increase in blood flow following transient ischaemia and is thought to reflect

both endothelium-dependent and-independent dilation of resistance vessels (Loscalzo and Vita 1994). Insulin-mediated bulk limb blood flow has also been shown to be affected by immobilisation. Sonne showed that after 10 days of bed rest, insulin-stimulated forearm blood flow measured using venous occlusion plethysmography decreased 53% compared to before bed rest, indicating changes to vascular insulin action (Sonne et al. 2010). The effect in the lower limb is likely to be different to the upper limb, where a reduction in muscular contraction in bed rest is less apparent, and furthermore the HDT bed rest model can result in changes in plasma volume which may affect measures. Bed rest of duration 7 days or less has not consistently shown changes in capillary density measured using immunohistochemistry, with some reporting no change (Dirks et al. 2016; Ringholm et al. 2011; Mikines et al. 1991) and others reporting an increase (Montero et al. 2018). However, in the latter study, fasting glucose/insulin ratio was not correlated with capillary density, indicating that changes in skeletal muscle glucose uptake is unlikely to be secondary to changes in muscle capillarisation. Microvascular function, an important measure of nutrient delivery to muscle has also been reported to be altered by immobilisation. Two weeks of unilateral lower-limb casting reduced microvascular endothelial function, measured by the vasodilator response to an intra-arterial infusion of acetylcholine and sodium nitroprusside (Rytter et al. 2020). Overall therefore, immobilisation appears to cause adaptations in both bulk and microvascular blood flow, but not capillarisation.

1.5 Immobilisation, muscle atrophy and architecture

1.5.1 Skeletal muscle atrophy

Models of physical inactivity have demonstrated profound detriments in skeletal muscle mass, architecture and function secondary to immobilisation. Early studies involving bed rest immobilisation by Cuthbertson and Deitrick demonstrated skeletal muscle atophy via increased nitrogen excretion (Cuthbertson 1929; Deitrick, Whedon, and Shorr 1948). The extent of muscle atrophy and rapidity of muscle loss observed in studies has been variable depending on the muscle group studied, the model of physical inactivity used and the method of measurement i.e. magnetic resonance imaging (MRI)/ultrasound (US)/DEXA (Rudrappa et al. 2016). Changes in muscle volume of 1.7% measured using MRI have been noted in as short a time period as 2 days unilateral limb suspension (Kilroe, Fulford, Jackman, et al. 2020). Immobilisation of 5 days duration using unilateral below-knee leg casting has been shown to reduce quadriceps cross sectional area (CSA) by 3.5% measured using computed tomography (CT) (Wall et al. 2014) despite whole-body lean mass remaining unchanged, with similar reductions in *vastus lateralis* CSA reported after 7 days of bed rest, measured using MRI (Ferrando et al. 1995). Studies involving 2 weeks of unilateral lower limb immobilisation resulted in a reduction in quadriceps lean mass measured using DEXA, of 4.7% (Jones et al. 2004) and CSA, measured using MRI of 5.2% (de Boer et al. 2007). Longer duration (>2 weeks) bed rest studies have reported 30% atrophy in ankle extensors (gastrocnemius and soleus) and 21% loss in ankle flexors

(anterior tibialis) as well as 16-18% muscle atrophy in the quadriceps and hamstrings and 9% loss in the intrinsic lower back muscles after 17 weeks of bedrest measured using MRI (LeBlanc et al. 1992). Evidence also suggests atrophy to be accelerated in the initial stages of unloading, after which it reaches a plateau of muscle loss at a slower rate. One 90-day bed rest study reported slower rates of quadriceps atrophy during the final 2-months compared to the first month (Alkner and Tesch 2004). Similarly, Fitts reported that loss in muscle volume in a microgravity environment is exponential with the largest decline in the initial month and a new steady state reached by 120 days (Fitts et al. 2007). Furthermore, reduction in muscle volume and subsequent strength was not significantly worse at 237 days compared with 110 days. A potential problematic factor during HDT bed rest is the cephalic fluid shifts, particularly acutely during short duration bed rest, where there may be apparent change of muscle volume, when in fact net muscle protein loss may be unchanged (Conley et al. 1996). Most bed rest studies have focussed on muscle mass loss in the lower extremity only, with few studies taking measures of upper and lower body concurrently, and none that we are aware of after only 3 days of bed rest.

1.5.2 Muscle group

The degree of skeletal muscle atrophy during immobilisation varies between muscle groups. Increased muscle loss has been observed during bed rest in the antigravity, weight bearing muscles, which primarily consist of type I fibres (slow-twitch), especially of the lower limb such as *soleus*, and the postural back muscles compared to the type II (fast-twitch) muscles (LeBlanc et al. 1992). In

the lower limb, Alkner reported a greater degree of atrophy in the plantar flexor muscles (*soleus* and *gastrocnemius*) with a loss of CSA of 29% compared with an 18% reduction of the knee extensors (*vastus lateralis* and *rectus femoris*) during 90 days of HDT bed rest (Alkner and Tesch 2004). Similarly, Akima noted the most significant losses in *soleus* and *gastrocnemius* CSA (approximately 10%) using MRI after 20 days of bed rest compared to other muscles of the lower limb (Akima et al. 1997). Plantarflexion is required for adequate propulsion during the toe off phase of gait, and therefore even modest reductions in calf muscle volume may negatively impact walking. Most bed rest studies have focussed on muscle mass loss in the lower extremity only, with few studies taking measures of upper and lower body concurrently. Upper body muscles are not involved in weight bearing or postural control, and therefore have a relatively lower time under tension and protein turnover compared to lower limb muscles. Muscle mass loss is therefore relatively less than lower limb muscles during immobilisation such as bed rest. One study using DEXA to determine lean mass in the trunks, arms and legs in healthy men undergoing 17 weeks of bed rest reported no change in lean mass of the arms or trunk, whilst total body lean mass declined by 4% and legs by 12% (LeBlanc et al. 1992). To my knowledge, no studies have evaluated regional changes in muscle volume following short duration bed rest.

1.5.3 Muscle fibre type

In mammalian skeletal muscle, fibre type is determined according to myosin heavy chain composition. In humans, there are 3 types (isoforms) of myosin heavy chains (MHC) that are expressed in either slow or fast fibres, (type I, IIa

and IIx)(Schiaffino et al. 1989). Type I muscle fibres are necessary for long-lasting activity with greater time under tension compared with type II fibres, and rely on oxidative metabolic processes, resulting in lower fatigue resistance capacity. Studies of prolonged spaceflight (Fitts et al. 2010), bed rest (Brocca et al. 2012) and lower limb immobilisation (Gibson et al. 1987) in humans of more than 30 days have demonstrated a preferential effect of atrophy of type I fibres compared to type IIa or IIx fibres. Other studies in humans have however reported both type I and type II muscle fibre atrophy following 14 days of immobilisation (Hvid et al. 2010; Bamman et al. 1998), but not as early as 8 days of bed rest (Brocca et al. 2012). A preferential atrophy of type II fibres in older individuals undergoing bed rest has also been reported however (Hvid et al. 2010). Previous limb immobilisation models have suggested that certain muscle groups are “atrophy susceptible” e.g. *medial gastrocnemius* whilst others are “atrophy resistant” e.g. *tibialis anterior* (Bass et al. 2021). In the latter study, muscle volume using MRI and muscle thickness using US were evaluated in both muscles after 15 days of ULLS, and fibre type composition was comparable between the two muscles (predominantly type I in humans), indicating fibre type was unlikely to account for the differences in atrophy observed. Atrophy of type I muscle fibres is greater in rodent models compared to human studies (Thomason and Booth 1990). This has been partly attributed to the fact that rates of protein turnover are more homogenous between fibre types in humans than they are between fibre types in rodents, where the variations in protein turnover are as high as twofold between fast and slow fibres types (Phillips, Glover, and Rennie 2009).

1.5.4 Muscle strength

Reductions in muscular strength following immobilisation are disproportionately greater than the loss of muscle CSA, suggesting other mechanisms must be responsible in part for the loss of muscle strength. The greatest detriments appear to occur early in immobilisation, mimicking the temporal onset of muscle atrophy. Dirks reported a 3.5% reduction in quadriceps CSA and 9% reduction in strength in a study involving 5 days of leg cast immobilisation (Dirks et al. 2014). Another study reported a 10% reduction in myofibre area and 13% reduction in strength after just 4 days of immobilisation using whole leg casting (Suetta et al. 2012). Another study involving 14 days of leg immobilisation resulted in an 8% reduction in quadriceps CSA and a 23% reduction in strength (Wall, Dirks, and van Loon 2013). A purported mechanism contributing to reduction in strength following physical inactivity is a reduction in neuromuscular drive and motor unit recruitment. Duchateau noted 33% decrease in muscle activation indicated by a reduction in torque and electromyographic (EMG) activity, measured during maximal voluntary contraction (MVC) in the *triceps surae* after 5 weeks of bed rest (Duchateau 1995). This was hypothesised to be due to a reduction in both motor unit recruitment and maximal firing rate after bed rest. Similar central activation deficits have been reported to account for the strength loss in the quadriceps after total knee replacement (Thomas and Stevens-Lapsley 2012). In a 3 day dry immersion model in 12 healthy young participants, Demangel reported 11% maximal voluntary contraction loss with a 2.4% decrease in quadriceps CSA (Demangel et al. 2017). They attributed the discrepancy in magnitude of

strength loss compared to mass loss to fibre type denervation, evidenced by an increase in neural cellular adhesion molecule (NCAM)-positive myofibres. NCAM is classically used to identify muscle fibres undergoing regeneration or denervation processes. This suggests that motor denervation begins very early in the context of disuse and impacts motor recruitment patterns. Work from Piasecki's lab has described suppressed motor unit firing rate following 15 days of ULLS measured using intramuscular myography which was confined to the immobilised limb and was observed at multiple contraction levels (Inns et al. 2022). Thus, functional muscle deficits appear to be attributable to more than muscle mass loss in human disuse atrophy.

1.6 Mechanisms of muscle atrophy during physical inactivity

The primary drivers for maintenance of skeletal muscle mass in humans include the availability of amino acids, in particular leucine, and physical activity which both increase myofibrillar protein synthesis (MPS), as well as insulin responses to food, which inhibit muscle protein breakdown (MPB) (Kumar, Atherton, et al. 2009; Rennie 2005; Greenhaff et al. 2008). Any substantial losses of skeletal muscle mass must be underpinned by a net imbalance between MPS and MPB (Figure 1.6). This protein balance has a diurnal variation and MPS is predominantly stimulated by food intake (Wilkinson et al. 2015) and physical activity (Kumar, Selby, et al. 2009). However, the relative contribution to either a reduction in MPS, an increase in MPB, or a combination of both in disuse atrophy is much debated, particularly when attempting to translate evidence from rodent models to humans.

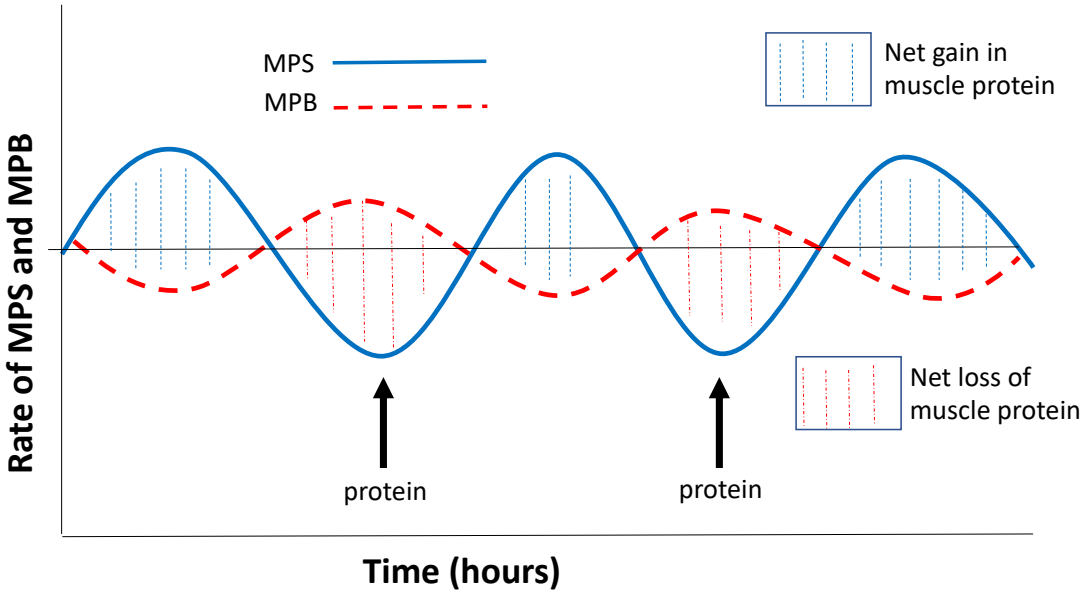

Figure 1.6. Equilibrium of myofibrillar protein synthesis and muscle protein breakdown related to feeding. MPS = myofibrillar protein synthesis, MPB = muscle protein breakdown

Much research has been conducted trying to determine the anabolic and catabolic signalling pathways that control skeletal muscle mass via the regulation of protein synthesis and degradation, so that effective countermeasures can be employed to prevent muscle wasting. Increases in MPS rates are regulated at various molecular levels within the translation initiation and elongation process in response to anabolic stimuli. The mammalian target of rapamycin (mTOR) pathway has been identified as the major hub for the integration of upstream signalling pathways which result in increased translational efficiency (Figure 1.7). This has been demonstrated in studies where blockade of the mTORC1 signalling pathway by rapamycin led to decreased rates of MPS, causing inhibition of muscle hypertrophy

(Drummond et al. 2009; Bodine, Stitt, et al. 2001). The mTOR pathway can be stimulated by insulin and IGF-1, amino acids, energy stress and mechanical stress. In this phosphorylation-regulated signalling pathway, IGF1 (or another anabolic signal) activates phosphatidylinositol 3 kinase (PI3K), which phosphorylates phosphatidylinositol-4,5-bisphosphate (PIP2) to phosphatidylinositol-3,4,5-triphosphate (PIP3) in the membrane, and this creates a binding site for protein kinase B (Akt). Activation of Akt phosphorylates and activates mTOR kinase which increases protein synthesis by phosphorylation and activation of p70S6kinase ($p70^{S6K}$) and eukaryotic translation initiation factor 4E binding protein 1 (4EBP-1)(Gingras et al. 1999). Increased phosphorylation of Akt leads to the inhibition of forkhead box class 0-1 (FOXO) and caspase-3 resulting in inhibition of protein breakdown via the ubiquitin ligases muscle ring finger-1 (MuRF-1) and muscle atrophy F-box (MAFbx/atrogin-1) (Bodine, Latres, et al. 2001). However, evidence has demonstrated a dissociation in mTOR pathway signalling protein phosphorylation and muscle protein synthesis when insulin has been infused in a stepwise fashion alongside amino acid infusion (Greenhaff et al. 2008).

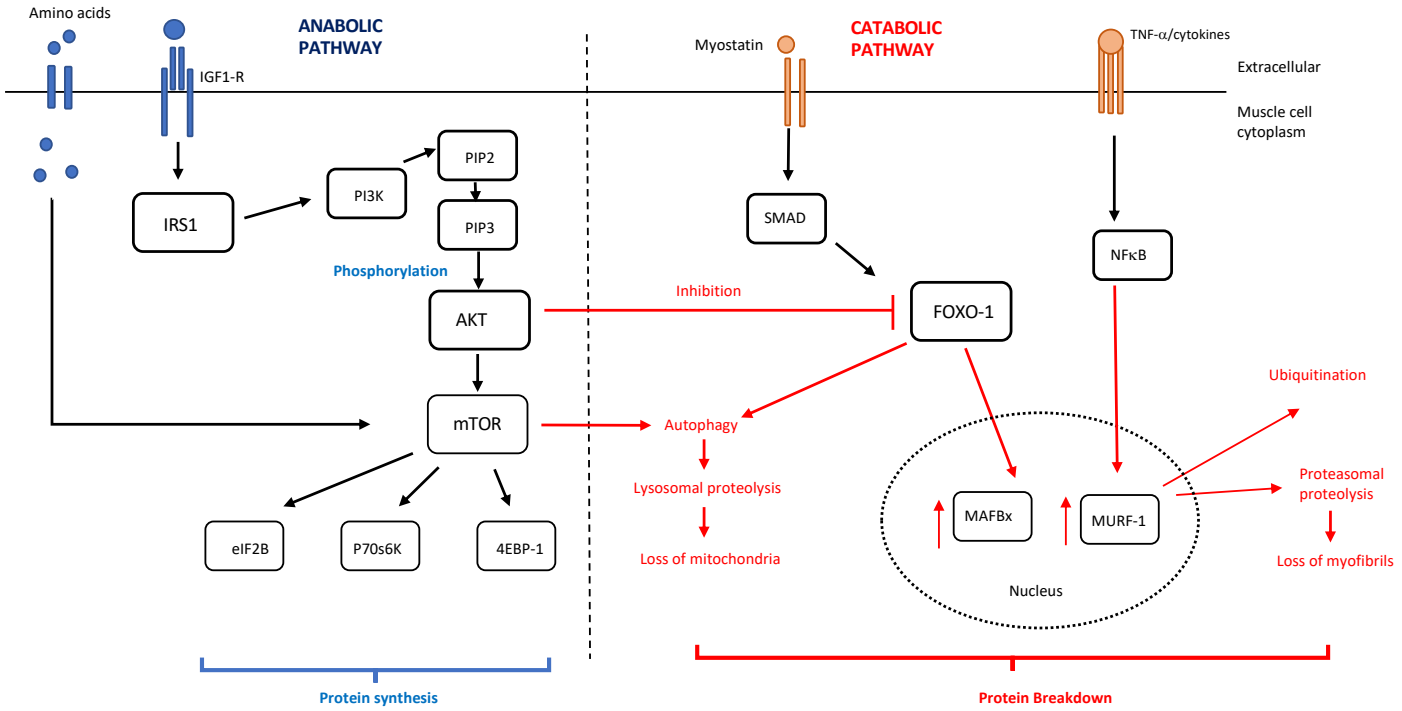

Figure 1.7. Simplified summary of the anabolic and catabolic pathways in skeletal muscle leading to protein synthesis (represented in blue) and protein breakdown (represented in red) respectively. Akt, protein kinase B; 4EBP-1, eukaryotic translation initiation factor 4E-binding protein; eEF2, eukaryotic elongation factor 2; eIF2B, eukaryotic initiation factor 2; eIF4E, eukaryotic initiation factor 4E;

FOXO-1, forkhead box class O-1; IGFR-1, insulin-like growth factor 1 receptor, IRS1, insulin receptor substrate 1, MAFBx, muscle atrophy f-box-1; mTOR, mammalian target of rapamycin; MURF-1, muscle ring finger protein 1; NFκB, nuclear factor κB; P70s6K, 70-kDa s6 protein kinase; PI3-K, phosphatidylinositol-3-kinase, PIP2, phosphatidylinositol 4,5-bisphosphate, phosphatidylinositol 3,4,5-trisphosphate; PIP3, phosphatidylinositol 3,4,5-trisphosphate; SMAD, vertebrate homolog of Drosophila protein MAD (mothers against decapentaplegic) and Caenorhabditis elegans protein SMA; TNF-α, tumour necrosis factor alpha.

1.6.1 Myofibrillar protein synthesis

Stable isotope tracers have allowed MPS and whole-body MPB to be investigated in humans *in vivo* in metabolic physiology experiments. The methodology involves the measurement of the dilution of the tracer into the metabolic pool of the tracee of interest. Isotopes are elements that occupy the same position in the periodic table but differ in mass due to the same number of protons but a differing number of neutrons within the nucleus. In metabolic physiology research, although they are chemically and functionally identical, they can be distinguished analytically, thus making them ideal for “tracing” metabolic processes. Stable isotopes are normally detected using mass spectrometry, which separates atoms or molecules based on their mass or charge as they pass through an electrical or magnetic field under vacuum. They are combined with chromatographic (gas chromatography or liquid chromatography) separation techniques prior to detection in the mass spectrometer (Wilkinson et al. 2017).

By combining arteriovenous tracer labelling techniques, protein synthesis and protein breakdown in limbs (which are predominantly skeletal muscle) can also be measured over short periods of time (minutes to hours). In early studies, measurements of leg protein synthesis during immobilisation were primarily made in the postabsorptive state. The decline in postabsorptive MPS is thought to account for the majority of muscle volume loss observed during 21 days of ULLS (de Boer et al. 2007) and 10 days of bed rest (Kortebein

et al. 2007), with the suggested rate of decline during disuse being approximately 0.5% per day (Phillips, Glover, and Rennie 2009). Glover et al. were the first to demonstrate the existence of muscle “anabolic resistance” in response to immobilisation (Glover et al. 2008), a phenomenon more commonly reported in older individuals (Cuthbertson et al. 2005). In Glover’s study, suppressed MPS in the postprandial state was observed following 14 days of lower limb immobilisation in healthy, young volunteers, which persisted even under conditions of high dose amino acid administration (Glover et al. 2008). Thus, disuse atrophy in humans is characterised by reductions in both the fasted and fed-state MPS, causing a global daily reduction of MPS. A shorter duration study of 5 days unilateral knee immobilisation using a full leg cast confirmed these observations as a reduction in rates of postabsorptive and postprandial MPS in young healthy men was reported, which was accompanied by a 4% loss of quadriceps CSA (Wall et al. 2016). Of note, the phosphorylation state of signalling proteins in the mammalian target of rapamycin (mTOR) pathway did not explain the reduction in MPS (Glover et al. 2008; de Boer et al. 2007) and, in another study, 2 weeks of limb immobilisation showed no increased phosphorylation of mTOR and $p70^{S6K}$ (Wall et al. 2013). These studies demonstrate at present our lack of understanding of the precise mechanisms underpinning disuse-induced muscle mass loss and questions whether protein phosphorylation is a robust proxy of Akt/mTOR activity.

The above studies utilised measures that were taken acutely using intravenous infusions of stable isotope tracers and represent a “snapshot” in time of MPS. However, traditional substrate-specific stable isotope tracer

methods have several limitations, namely measurements need to be performed over only short durations (<8-12 hours), they require venous and/or arterial cannulation, expensive sterile infusions and multiple biopsy collection periods within controlled laboratory conditions. Newer, orally ingested stable isotope tracers have more recently been employed to enable chronic estimation of these processes. Deuterium oxide (D_2O) is administered orally, and rapidly equilibrates with body water (1-2 hours in humans) which creates a homogenously labelled precursor pool, with a half-life of 9-11 days (Wilkinson et al. 2014). The slow turnover rate allows measurements over longer periods i.e. days to weeks compared to traditional stable isotope methods, which allows the scrutiny of chronic, cumulative metabolic flux, which are more relevant to clinical studies. Using mass spectrometry, the level of deuterium in water can be measured, distinguishing D_2O from H_2O; deuterium exchanges into the free amino acid alanine which is then incorporated into body proteins. The labelling of water in saliva, blood or urine is used as a surrogate precursor to follow the labelling of deuterium in the free alanine. By measuring the rate of incorporation of this deuterated alanine into protein over time the rate of synthesis of the protein can be determined (using the precursor-product approach; Figure 1.8). Chronic MPS derived using D_2O during a 6 week resistance exercise training study correlated with long term muscle hypertrophy, demonstrating the utility of D_2O in predicting chronic adaptations to exercise (Brook et al. 2015). The utility in estimating protein losses has also been demonstrated. Brook et al. found a reduction in muscle size and strength following 4 days of ULLS which was driven by declines in MPS measured chronically using D_2O, indicating a

sustained depression of MPS over short duration immobilisation (Brook et al. 2022). Thus far however, these techniques have been limited to healthy volunteer studies, with few studies able to employ them in clinical populations. This application would be valuable in helping to elucidate chronic changes in muscle protein turnover in clinical populations with chronic disease or acute illness in which muscle protein loss is elevated.

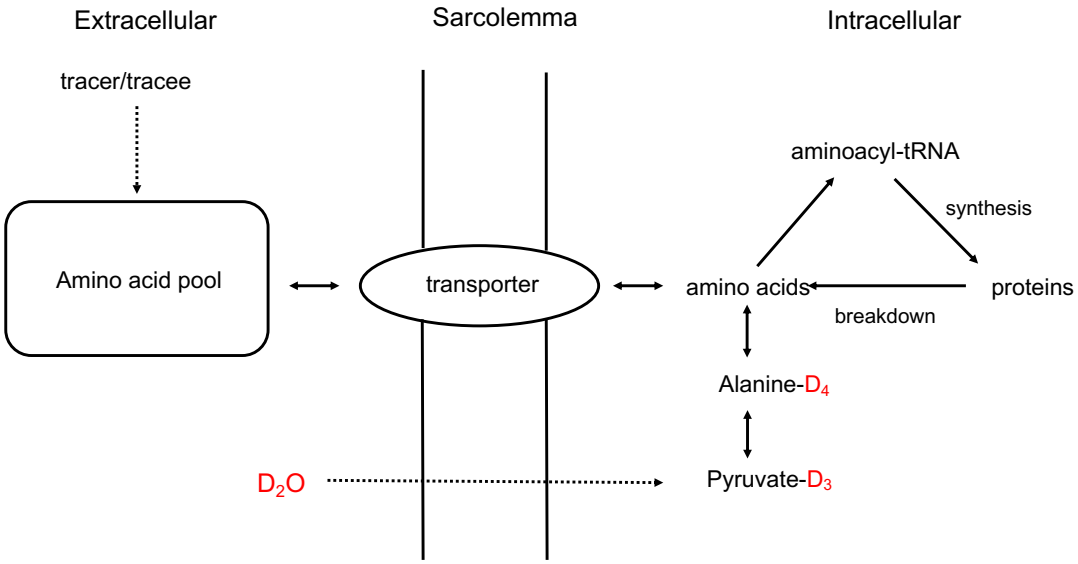

Figure 1.8. Precursor:product labelling method to determine myofibrillar protein synthesis. Here a labelled tracer, deuterium oxide (D_2O) equilibrates with body water and labels amino acids e.g. alanine intracellularly, which can then become incorporated into proteins.

1.6.2 Muscle protein breakdown

An increase in MPB has also been suggested as a mechanism driving disuse atrophy, largely based on evidence of increased markers of MPB in rodent

models during the early stages of immobilisation. The major regulators of MPB in skeletal muscle include the ubiquitin proteosome system, autophagy-lysosomal and calcium-activated calpain and caspase-dependent cleavage of actinomyosin complexes (Figure 1.7). Degradation of proteins by the ubiquitin-proteosome pathway is regulated in skeletal muscle by MAFbx and muscle RING finger-1 MURF-1. Lecker showed that both MAFbx and MURF-1 were the main “atrogenes” upregulated in a number of muscle wasting disease states in mice including cancer cachexia, uraemia and streptozotocin-induced diabetes (Lecker et al. 2004). MAFbx and MURF-1 are transcriptionally regulated by the forkhead box gene group O (FOXO) transcription factors. After phosphorylation by Akt of the FOXO transcription factors, they are rendered inactive. Akt is therefore a common point of convergence in the pathways of MPS and MPB.

There is less evidence available in the literature regarding the role of MPB in short-duration disuse atrophy, at least partly due to the technical challenges associated with directly measuring protein degradation *in vivo* in humans. Overall, although there is some evidence to suggest in rodents that MPB may be transiently elevated early in immobilisation (Krawiec et al. 2005; Taillandier et al. 2003), recent evidence in human studies has not supported this theory (Brook et al. 2022). There are significant differences in muscle protein turnover when comparing responses to immobilisation in rodents vs humans, making direct comparison difficult to interpret. Furthermore, previous human studies supporting an increase in MPB reported increase markers of MPB e.g. an increase in the ubiquitin proteosome and autophagy-lysosomal systems after 5

days of bed rest, rather than direct MPB rates (Tanner et al. 2015), again questioning whether MPB is truly raised under these conditions. This specific matter will be discussed further in **Chapter 4.**

1.7 Post-immobilisation physical activity intervention

Given the rapid declines in whole-body and limb glucose disposal and muscle mass in disuse, which, in the case of glucose disposal, are specific to the immobilised limb, and likely a consequence of a lack of muscle contraction *per se*, it seems reasonable to suggest these changes could be restored equally as rapidly by the resumption of muscular contraction. In a previous 21-day bed rest study in healthy, sedentary young males maintained in energy balance, 4 days of habitual free living was insufficient to restore whole-body glucose tolerance measured using an OGTT, and 5-14 days of normal ambulation was required to restore impaired glucose tolerance (Heer et al. 2014). This is supported by gene expression studies during bed rest which showed that over 4,500 genes predominantly related to insulin sensitivity, fatty acid metabolism and mitochondrial function were downregulated after 9 days of bed rest, which were only partially restored after 4 weeks of retraining (Alibegovic et al. 2010). Other studies have shown whole-body insulin sensitivity, measured using the CLIX-IR, an index of insulin sensitivity derived from an OGTT, was restored after 8 weeks of progressive lower limb eccentric exercise (knee and hip extensor training 3-times per week) following 5 days of bed rest (Reidy et al. 2017). However, it is likely that an improvement after this length of time may have been expected after the resumption of normal ambulation alone. Similarly,

4 weeks of aerobic exercise training (3 times per week) has been shown to restore deficits in limb microvascular function following 2 weeks of unilateral leg immobilisation (Rytter et al. 2020). Evidence shows that even a single bout of resistance exercise improves insulin-stimulated leg glucose uptake (Richter et al. 1989) and glucose tolerance in healthy volunteers (Gordon et al. 2012). There is currently a dearth of research investigating whether disuse-associated reductions in whole-body glucose disposal or leg glucose uptake over short durations of only a few days can be equally as rapidly restored using resistance exercise. Furthermore, it is unclear the type, intensity and duration of activity required to fully restore insulin sensitivity following bed rest, or whether this would restore with free living alone. This information would be important to establish to inform recovery and rehabilitation guidelines for those undergoing short periods of immobilisation such as during a hospital stay.

The time-course of change of muscle mass, MPS and MPB with immobilisation, and their rate of restoration, particularly over short periods in humans, is also currently unresolved. Resistance exercise is one of the most common countermeasures to be employed to mitigate against muscle mass and strength losses with disuse. Resistance exercise has been used both after disuse, as a period of rehabilitation, as well as during immobilisation, to lessen the muscle mass and strength losses. However the relative success has depended on the particular types of exercise performed and which muscles were targeted (Alkner and Tesch 2004; Akima et al. 1997; Akima et al. 2003). Overall, there are few, if any, studies specifically looking at the restoration of MPS and whole-body and leg insulin sensitivity after short duration (<3 days)

remobilisation. Rodent studies suggest that the restoration of MPS occurs rapidly e.g. in as short as 6 hours after recovery from immobilisation (Tucker, Seider, and Booth 1981). However, the limitations of the translatability of rodent models to humans has already been touched upon. In human studies, in the main, most remobilisation studies are several weeks long e.g., 8 weeks (Tanner et al. 2015) and it is unclear if restoration of MPS would have occurred anyway with this extended period of free living. This matter is discussed in more detail in **Chapter 4**, but currently, whether a short period of reloading can restore both whole-body and muscle insulin sensitivity and myofibrillar protein synthesis to the same extent is not known.

1.8 Inflammation and trauma

1.8.1 The metabolic response to inflammation and trauma

Similar to conditions of immobilisation, skeletal muscle mass loss and changes in muscle architecture as well as reductions in insulin sensitivity have been observed in conditions where inflammation is present, e.g. patients who sustain an injury or in postoperative surgical patients. Cuthbertson was the first to describe the metabolic response to trauma over 50-years ago and the posttraumatic changes of nitrogen loss, breakdown of lean tissue, fever and increased oxygen consumption (Campbell and Cuthbertson 1967). Inflammatory burden can be present in a spectrum of clinical states, such as following a systemic infection in sepsis or after an injury or trauma. Sepsis is an uncontrolled, systemic inflammatory response that occurs secondary to an infection (typically originating from the lungs, urinary tract or abdominal cavity).

Detrimental changes observed in muscle mass regulation or insulin sensitivity may be exacerbated by the inflammatory burden of surgery itself or iatrogenic interventions, as well as the initial injury or insult. At the most extreme end of the spectrum, patients with critical illness are anesthetised and ventilated in intensive care units (ICU). Not only are these patients immobilised but they are also sedated and although sedation remains an unknown factor in immobilisation-related muscle remodelling, it is believed to compound muscle wasting to a greater extent than just “conscious immobility” in the absence of sedation (Parry and Puthucheary 2015). Furthermore, following major abdominal surgery for example, a systemic postoperative proinflammatory response is seen and is accompanied by muscle inflammation and metabolic dysregulation both locally and remote to the site of the surgery (Varadhan et al. 2018).

The metabolic response to trauma is complex and fundamentally driven by the primary events of tissue ischaemia and reperfusion and tissue disruption. It has been defined in three phases.

1) Ebb phase (decreased metabolic rate)
2) Flow phase (catabolic phase)
3) Anabolic phase

The ‘ebb’ phase is an early (24-48 hours) hypometabolic state of catabolism which is initiated in response to the initial trauma and where there is reduced energy expenditure, hypovolaemia and an increased sympatho-adrenal activity associated with counter-regulatory hormones after injury (Frayn et al. 1985).

Post traumatic “stress hyperglycaemia” which is present during the ebb phase is believed to be initially the result of increased hepatic glycogenolysis and subsequently secondary to increased glucose production and reduced peripheral utilisation (Wolfe, Allsop, and Burke 1977). This is stimulated by an increase in stress hormones such as glucagon and catecholamines and suppression of insulin levels (Allison, Hinton, and Chamberlain 1968; Halter, Pflug, and Porte 1977). The ‘flow’ phase is characterised by a high metabolic rate with an increased energy expenditure, breakdown of protein and fat, activation of the innate immune system and induction of the hepatic acute-phase response, as well rising insulin levels with subsequently increased glucose production (Frayn 1986). In order to meet the increased metabolic need of the elevated energy expenditure, wound healing and acute phase protein production, during this phase there can be excessive loss of skeletal muscle mass and increased turnover of fatty acids with increased lactate production (Frayn et al. 1985). The transition from the catabolic state to the anabolic state depends on injury severity and magnitude of surgical trauma. It occurs approximately 3-8 days after uncomplicated elective surgery but may take weeks to months after severe trauma and sepsis.

The metabolic response can be further aggravated by secondary events such as blood transfusions, delayed operative procedures and infection, which promote initiation of the cellular immune system (monocytes, macrophages and neutrophils), and activation of complement and coagulation cascades (Stahel, Smith, and Moore 2007). This results in the release of mediators including cytokines (e.g. TNF-α, IL1, IL2, IL3, IL4, and IL6), nitric oxide and chemokines

which are thought to lead to mitochondrial dysfunction, microvascular thrombosis and apoptosis. However, treatment strategies aimed at controlling the extent of posttraumatic inflammation have been conflicting. Corticosteroids e.g. prednisolone are anti-inflammatory agents that inhibit transcription factors that control synthesis of pro-inflammatory mediators and inhibit the production of tissue-destructive enzymes (e.g. collagenase) and have been investigated in the setting of acute trauma. Randomised controlled trials using high dose methylprednisolone have shown an increased mortality in patients with head injury (Roberts et al. 2004) and acute respiratory distress syndrome (Steinberg et al. 2006). The molecular targets for modulating the inflammatory cascade after trauma are therefore complex, and evidence suggests the global immune depression by the administration of corticosteroids does not work in the setting of complex trauma.

1.8.2 Models of acute and chronic inflammatory insult

There are various models to examine the effect of an acute and chronic inflammatory insult on muscle mass and metabolism. These include an endotoxin model via the intravenous administration of lipopolysaccharide (LPS), a compound derived from the cell membrane of Gram-negative bacteria. This causes a reproducible systemic effect of fever, myalgia and an increased level of plasma cytokines such as IL6 and IL10 (Bahador and Cross 2007). Findings are however limited in their generalisability due to the acute nature of the measures and time period. In addition, because no infection is present, it can only really represent a model of systemic inflammation, rather than sepsis.

Acute clinical models include patients with critical illness, limb trauma or undergoing surgical trauma, however there can be difficulties in deriving baseline data. Mechanistic studies in ICU patients are challenging due to the heterogeneity of the critical illness syndromes, treatment and underlying primary aetiology. Limb trauma models are able to provide insight into the effect of local injury and inflammation, as well as systemic inflammation using the contralateral leg as an internal control. Surgery itself is a potent stimulus for inflammation, however considerations in this setting which may impact outcome measures include perioperative fasting, general anaesthesia, local anaesthesia and sedation, as well as local tissue perfusion changes during surgery, pain response, medication use and anticoagulation. Systemic chronic inflammation has been associated with several chronic diseases (including type 2 diabetes, cardiovascular disease, cancer, chronic kidney disease and non-alcoholic fatty liver disease). Chronic inflammation is thought to ultimately cause collateral damage to organs and tissues over longer periods of time than acute inflammation via mechanisms such as oxidative stress, and has been associated with increasing age (Ferrucci and Fabbri 2018). Finally, previous researchers have drawn attention to the association between increased sedentary time and chronic low-grade inflammation (CRP and IL6) measured in cross sectional studies (Yates et al. 2012; Howard et al. 2015; Mora et al. 2006). However, these results are often attenuated when adjusting for BMI, and sedentary time has tended to be captured using self-report. Whilst some mechanistic studies have shown an increase in pro-inflammatory cytokines with immobilisation, often these remained within the standard “healthy” reference

range, questioning the clinical significance despite a statistical increase (Bosutti et al. 2008; Drummond et al. 2013).

1.8.3 Muscle mass loss in inflammation and trauma

Skeletal muscle mass loss and changes in muscle architecture are known sequelae of trauma and have been observed in patients who sustain an injury or illness, often to a greater extent than immobilisation alone. Studies of lower limb casting following fracture of the fifth *metatarsal* or *fibula* have reported a reduction in thigh CSA of 10% after 4 weeks of casting, with no change in IMCL content (Yoshiko et al. 2018). Other authors have reported a 17% loss of total calf muscle volume measured using MRI after 29 days of immobilisation following ankle fracture, with a 6.6% decrease in the contralateral (uninjured) side (Psatha et al. 2012) with losses most pronounced early (a ~5% reduction in muscle volume in the injured side occurring by day 8). This degree of muscle atrophy is significant given the role of the calf musculature in plantarflexion and therefore the role in maintenance of posture and propulsion in gait. A limitation of the study of Psatha et al. (2012) was the lack of physical activity and/or step count data, and it is therefore difficult to determine if muscle mass loss on the uninjured side was driven by the reduction in step count, systemic inflammation associated with the injury itself, or a combination of both. In addition to a loss of calf muscle volume in this study, there was a significant decrease in muscle pennation angle in the calf of the casted leg. Pennation angle is a measure of muscle architecture and has been suggested by some to be a proxy measure

for the amount of muscle activation, as during muscle contraction, muscle fibres shorten and pennation angle increases (Hodges et al. 2003).

Perhaps most striking is the muscle mass loss observed in patients with sepsis. Patients with critical illness admitted to ICU had a ~18% loss of *rectus femoris* CSA measured using US by day 10 of admission (Puthucheary et al. 2013). In the same study, muscle wasting occurred early and rapidly during the first week of admission and was accentuated in those with multiorgan failure, indicating a positive correlation between degree of inflammation and muscle atrophy. The degree of muscle mass loss is directly implicated in subsequent physical disability in those who survive critical illness (Herridge et al. 2003) and is therefore an important public health issue. *Vastus lateralis* muscle biopsies from patients with critical illness-induced muscle atrophy have shown a reduction in myofiber CSA in all fibre types, but particularly type II (Bierbrauer et al. 2012). There is also a greater magnitude of loss of myosin which is associated with a change in force generation-associated calcium sensitivity, negatively affecting force generation (Ochala and Larsson 2008). There are multiple potential risk factors for muscle mass loss associated with an ICU admission including malnutrition, immobilisation, and the high use of corticosteroids, neuromuscular blockers and certain antimicrobials e.g. aminoglycosides and colistin.

Sarcopenia is also a feature of many chronic non-communicable diseases including diabetes mellitus, cancer, chronic lung disease, heart failure, human immunodeficiency virus and obesity. Whilst it is outside the scope of this thesis to discuss the individual mechanisms of muscle atrophy in

each disease, mechanisms associated with muscle loss include physical inactivity, insulin resistance, insulin deficiency, inflammation, testosterone deficiency and oxidative stress (Raoul et al. 2017).

1.8.4 Mechanisms of muscle mass loss in inflammation

Pro-inflammatory cytokines such as CRP, IL1, IL6 and TNF-α have been implicated as key mediators of skeletal muscle atrophy in a variety of chronic diseases. In humans, C-reactive protein (CRP), an acute-phase protein of hepatic origin that increases following IL-6 secretion by macrophages and T cells has been directly associated with reduced muscle mass in the elderly via a CRP-mediated reduction in muscle protein fractional synthetic rate (Wahlin-Larsson et al. 2017). There is a limited number of mechanistic, experimental patient volunteer studies focussed on muscle mass loss and protein turnover in inflammation due to the inherent difficulty in acquiring baseline data. Short duration endotoxin administration in healthy volunteers under post-absorptive conditions has demonstrated acute decreases in both muscle protein synthesis and breakdown to an equal extent, thereby resulting in an unaffected protein balance (Vesali et al. 2009). However, the generalisability of these findings to clinical populations and patients with inflammation is debatable. Patient studies have revealed an early loss of muscle CSA of the magnitude -12.5% by day 7, measured via ultrasound of the *rectus femoris* in critically ill patients (Puthucheary et al. 2013). The relative contribution of myofibrillar protein synthesis and breakdown to muscle mass loss however was difficult to interpret in this study due to confounding factors of insulin infusion, parenteral nutrition

and acute measures of protein turnover using stable isotope tracers. One study investigating key genes and proteins involved in muscle protein synthesis and breakdown in critically ill patients within 6-8 hours of ICU admission demonstrated widespread dephosphorylation of proteins regulating translation initiation factor activation and protein synthesis (Akt/mTOR/p70S6K) in tandem with increased muscle specific E3-ligases (MAFbx and MuRF1) relative to controls (Constantin et al. 2011). This appears to be mediated by dampened Akt phosphorylation which activates FOXO transcription factors leading to expression of downstream FOXO gene targets such as MAFbx and MuRF1 (Crossland et al. 2008). Therefore, there may be distinct processes governing loss of muscle mass in simple unloading-mediated disuse atrophy in non-diseased states compared with disease states where there is a pronounced hypercortisolaemia, hypercytokinaemia and markedly elevated oxidative stress, which are pro-catabolic triggers. The current understanding of the chronic changes in MPS and MPB in the weeks following trauma and the underlying molecular mechanisms are unknown. This may be partly due to the difficulty in measuring these processes chronically *in vivo* in patient studies and the logistical difficulty and heterogenous nature of many critically ill clinical populations together with the confounding factors related to nutritional and other metabolic support required in this setting.

A meta-analysis of stable isotope techniques revealed that elective abdominal surgery reduced skeletal MPS with equivocal change in whole-body MPB (Jaconelli et al. 2022). Previous studies have looked at the impact of major surgery on blood glucose concentrations and examined the effect of local

trauma at the site of the incision (e.g., abdominal muscles in abdominal surgery) and at tissues remote to the site of surgery (e.g., quadriceps on muscle mRNA measurements) related to inflammation, to allow interrogation of the differential effect of local and systemic inflammation (Varadhan et al. 2018). A rodent model which investigated the direct effect of IL-6 on muscle atrophy showed that in the absence of elevated systemic effects, IL6 was able to directly induce skeletal muscle atrophy via its effect on the myofibrillar protein compartment (Haddad et al. 2005). This model has important considerations, particularly when examining insulin sensitivity and MPS; namely the effect of general or regional anaesthesia and perioperative fasting. Both preoperative fasting, traditionally for periods between 12-18 hours whilst awaiting surgery, and surgery-induced catabolism can accelerate skeletal MPB in order to supply amino acid precursors for wound healing, gluconeogenesis and immune function (Pozefsky et al. 1976). Furthermore, general anaesthesia or sedation using Propofol and benzodiazepines may positively modulate the inhibitory function of the inhibitory neurotransmitter gamma-aminobutyric acid (GABA).

An impairment in mitochondrial function has also been demonstrated in the context of surgical trauma. In one study, muscle maximal mitochondrial ATP production rates from muscle biopsies of the thigh in patients undergoing major abdominal surgery reduced ~40%, accompanied by a >50% reduction in muscle PDC activity, without any change in mitochondrial content (Atkins et al. 2021). However, this was in the absence of convincing evidence of muscle inflammation compared with that local to the site of surgery. General anaesthesia has also been shown in this context to profoundly impair

mitochondrial function in patients undergoing hip replacement or femoral fracture repair compared to the same procedure performed under regional anaesthesia (Miró et al. 1999). It is unclear to what extent however mitochondrial function is altered due to surgical trauma or general anaesthesia, or both.

1.9 Specific aims of the thesis

The present thesis examined the effect of immobilisation and inflammation on muscle metabolic health and the underlying mechanisms driving changes in muscle volume, protein turnover and insulin sensitivity. The overarching research questions were as follows:

Chapter 3, The temporal relationship between the onset of reductions in insulin-stimulated whole-body glucose disposal, insulin-stimulated glycogen storage and metabolic inflexibility during bed rest is not clear, particularly as previous research has been confounded by energy oversupply. This chapter aimed to determine the impact of acute (3 days) bed rest vs chronic (56 days) bed rest on insulin-stimulated whole-body glucose disposal, glycogen storage and substrate oxidation in healthy men maintained in energy balance. A second aim was to determine whether any differences observed could be explained by associated changes in leg IMCL content and/or targeted muscle mRNA expression.

Chapter 4, Research to date has focussed on the impact of bed rest on insulin-stimulated leg and whole-body insulin sensitivity. Additionally, muscle protein turnover and atrophy during bed rest has received significant research attention. However, perhaps surprisingly, few studies have investigated these central physiological events concurrently in the same individuals during bed rest, which was the first aim of this chapter. Given decrements in insulin-stimulated whole-body glucose uptake and MPS in response to bed rest appear to happen relatively quickly, it would not be unreasonable to suggest that post-bed rest muscle loading would restore these deficits rapidly. The second aim of this chapter therefore was to investigate whether an acute period of structured resistance exercise remobilisation (3 days) could fully restore any decrements in whole-body glucose disposal, leg glucose uptake, muscle glycogen storage and MPS after 3 days of bed rest.

Chapter 5, Both immobilisation and inflammation result in skeletal muscle mass loss, however the contribution of MPS and MPB in driving muscle mass loss in these two conditions is much debated. Whilst immobilisation appears to be driven predominantly by a reduction in MPS, in conditions of inflammation, an increase in MPB has been proposed to also occur. However, demonstrating this mechanistically has been challenging, particularly because *in vivo* measures of MPB are difficult to ascertain. The first aim of this chapter was to investigate the impact of immobilisation and trauma-related inflammation on *medial gastrocnemius* muscle architecture, chronic MPS and whole-body MPB in acute unilateral ankle fracture patients vs matched healthy control volunteers

undergoing 2 weeks of unilateral cast immobilisation. By investigating both limbs of each volunteer, a second research question could be addressed, which was to determine whether there was a differential impact of systemic versus local inflammation in ankle fracture patients on end-point measures.

Chapter 2 General Methods

2.1 Ethical approval

All studies described in this thesis were granted ethical approval and were in accordance with the Declaration of Helsinki. The chronic bed rest study in Chapter 3 was approved by the French Ethics Committee (CPP Sud Uoest et Outre Mer I) and French Drug Agency (ANSM) (Ethics Reference 14-981) and was conducted in the MEDES facility in Toulouse, France. The acute bed rest study in Chapter 4 was granted ethical approval by the University of Nottingham ethics committee (reference: 6-1704). The protocols for both these studies were registered at **http://www.clinicaltrials.gov/** (NCT03495128 and NCT03594799). The study in Chapter 5 was granted ethical approval by the NHS Health Research Authority (HRA) Research Ethics Committee (REC reference: 18/EM/0404). All corresponding documentation can be found in Appendix 1 (**Sections 7.1, 7.2 and 7.3**).

2.2 Recruitment

Details of recruitment for the Chronic bed rest study (Chapter 3) the Acute bed rest study (Chapters 3 and 4) and the Ankle fracture study (Chapter 5) are presented in their respective chapters.

Healthy volunteers recruited in the Acute bed rest study and the Ankle fracture study were recruited from the general population via posters and advertisements placed around the University of Nottingham, as well as on appropriate popular social media platforms (Gumtree, Facebook). After expressing initial interest in the study, participants were sent a detailed participant information leaflet (PIL) and a dual energy x-ray absorptiometry (DEXA) leaflet (Appendix 1, **Section 7.4**) and then they were invited to attend the David Greenfield Human Physiology Unit for an initial meeting prior to screening. Chronic bed rest participants were recruited by the Institute of Space Medicine and Physiology (MEDES) team in Toulouse, France. Ankle fracture patients were recruited from the acute trauma list presenting to Queen's Medical Centre in Nottingham and healthy controls were recruited from the general population as above.

2.1 Inclusion and exclusion criteria

Inclusion criteria for the acute and chronic bed rest participants recruited in Chapters 3 and 4 are shown below. Inclusion and exclusion criteria for the ankle fracture study in Chapter 5 is described in the individual chapter.

Inclusion Criteria:

. Physically and mentally healthy participants

. Males

. Age range 20 – 45 years

. Body mass index 20 - 26 kg/m^2

. Height 158 - 190 cm (62 – 75 inches),

. Participants that are able to consent to participation in the entire study

. Signed informed consent

Exclusion criteria:

. Medication required that may interfere with the interpretation of the results

. Family history of thrombosis or abnormal clotting on screening bloods

. History of: thyroid dysfunction, renal function disorder including renal stones, diabetes, cardiac arrhythmias and cardiovascular disorders, hypertension, hyperlipidaemia, hiatus hernia, and gastro-oesophageal reflux

. History of a mental health disorder

. Smoker within six months prior to the start of the study

. Dependence on drugs, medicine or alcohol

. History of orthostatic intolerance, vestibular disorders or claustrophobia

. Special food diet, vegetarian or vegan, history of intolerance to lactose or food allergy,

. Osteosynthesis material, presence of metallic implants, history of knee problems or joint surgery/broken leg,

. Orthopaedic or musculoskeletal disorders

. Not participating in any other studies within the last 3 months

2.3 Medical screening

Participants in the Acute bed rest study (Chapters 3 and 4) and the healthy volunteers in the Ankle fracture study (Chapter 5) undertook their medical screening at the David Greenfield Human Physiology Unit (DGHPU) at the University of Nottingham. Participants were only medically screened if they had read the PIL and had been given a detailed verbal explanation of the study in person more than 24-hours prior. A repeat detailed verbal explanation was given for the study during medical screening, with written information for all invasive procedures, ensuring each participant understood the protocol and that they had the right to withdraw from the study at any time. Written informed consent was obtained from each participant. Thereafter participants completed a general health questionnaire (Appendix 1, **Section 7.5**), and the participant's height and weight were recorded to calculate body mass index (BMI). Participants' heart rate and a lying, sitting and standing blood pressure were recorded to rule out hypertension or postural hypotension. A significant postural drop was considered as a drop ≥ 20 mmHG in systolic blood pressure. A blood sample was collected from an antecubital vein and analysed for full blood count, urea and electrolytes, liver function tests and coagulation by the Departments

of Haematology and Clinical Chemistry, Queen's Medical Centre, Nottingham, UK. An electrocardiograph (ECG; Schiller, Altgasse, Switzerland) was performed. Participants were screened for a history of cardiovascular disease, metabolic and/or respiratory disease, musculoskeletal or vestibular disorders. Participants were not included if they had a family history of clotting abnormalities or thrombosis including deep vein thrombosis or pulmonary embolus. For the Acute bed rest study (Chapters 3 and 4) food preferences or allergies were recorded during the medical screening and were taken into account when designing their diet.

2.4 Hyperinsulinaemic euglycaemic clamp

Overview

The hyperinsulinaemic euglycaemic clamp ("insulin clamp") technique was used in Chapters 3 and 4 in this thesis to measure whole-body insulin-stimulated glucose uptake during the Acute and Chronic bed rest studies. It is an *in vivo* technique for the assessment of insulin sensitivity of whole-body glucose metabolism under insulin-stimulated conditions, first developed by Andres and later de Fronzo (DeFronzo, Tobin, and Andres 1979). In the fasted state, participants receive a fixed-rate exogenous insulin infusion to create a hyperinsulinaemic state, whilst plasma glucose concentration is maintained ("clamped") at a fixed, predefined target level via a variable exogenous glucose infusion. The rate of endogenous glucose infusion required to maintain euglycaemia during the period of the insulin clamp, provided endogenous glucose output is suppressed, provides a measure of the net effect of insulin on

whole-body glucose metabolism (M value; (DeFronzo, Tobin, and Andres 1979)). This provides a measure of insulin sensitivity in the peripheral tissues, on particular skeletal muscle. The M value calculation is shown in Appendix 2 (**Section 7.8**).

The advantage of the insulin clamp in estimating insulin sensitivity is that it directly measures whole-body glucose disposal at a given level of insulinaemia under steady state conditions, with an intraindividual coefficient of variation of 10% (Mather et al. 2001). The disadvantages of the hyperinsulinaemic euglycaemic clamp is that it is labour intensive, requiring trained clinicians, a number of intravenous cannulae and can involve prolonged protocols. It is therefore practically unsuitable for large epidemiological studies, and studies where insulin resistance is not a primary outcome measure. Some argue that the technique utilises steady-state conditions that are supraphysiological, and therefore do not accurately reflect insulin and glucose dynamics in real world situations (Muniyappa et al. 2008). It also has the risk of associated hypoglycaemic or cardiac arrhythmias due to hypokalaemia induced by infusing insulin. Trained individuals are required to be present at all times to deal with these potential risks.

Protocol

An example of the hyperinsulinaemic euglycaemic data collection form is shown in Appendix 1 (**Section 7.6**). Participants arrived at the laboratory at 8am fasted since midnight the night before on the morning of the hyperinsulinaemic euglycaemic clamp. A cannula was inserted retrograde into a superficial vein

on the dorsal surface of the non-dominant hand and a second inserted anterograde into an antecubital vein in the same arm. The cannulated hand was kept in a hand-warming unit (air temperature 50-55°C) to arterialise the venous drainage of the hand, and a 0.9% slow saline drip was attached to keep the cannula patent for repeated blood sampling (Gallen and Macdonald 1990). For the Acute bed rest study in this thesis, an anterograde femoral venous catheter was also inserted (using the Seldinger technique under ultrasound guidance), to enable venous blood draining from the leg to be analysed for glucose concentration. A 3-lead electrocardiogram was attached to the participants for the duration of the clamp to assess for arrythmias associated with hypokalaemia, which is a potential risk when infusing insulin. Thereafter the hyperinsulinaemic euglycaemic clamp was performed, with insulin (human Actrapid, Novo Nordisk) infused into the non-dominant arm at a rate of 60 mU/m^2/min for 180 minutes. Arterialised-venous blood glucose concentration was measured in <1ml blood every 5-min and maintained at 4.5 mmol/l by a variable rate infusion of 20% glucose (Baxter Healthcare). Arterialised-venous blood samples (2.5 ml) were taken at baseline and every 30 minutes for the final hour during the clamp for the measurement of insulin, TAG, and NEFA. The insulin clamps were started immediately after baseline measures were made and in the Acute bed rest study a femoral venous blood sample (2ml) was collected at 0, 150, 160, 170 and 180 mins for measurement of venous glucose concentration as well. At the same time as the femoral venous blood sample was taken, a femoral artery blood flow assessment (mmol/min) was made using ultrasonography to calculate leg glucose uptake.

Values at time points 135, 150 and 165 minutes were used for calculation of "steady state" whole-body glucose uptake, which were normalised to lean body mass (kg) using DEXA values. Insulin infusions were stopped after the final muscle biopsy was taken, and participants provided with a high carbohydrate meal. The glucose infusion was gradually reduced as glucose from the gut appeared in the blood. Once the participants' blood glucose had been stable for 30 minutes without the infusion, all lines were removed. Each femoral venous catheterisation and hyperinsulinaemic euglycaemic clamp was performed in the horizontal, supine position, to reduce the risk of air embolism. For the purpose of this thesis an insulin infusion rate of 60 mU/m^2/min has been used, as this level has been shown to suppress hepatic gluconeogenesis (Chokkalingam et al. 2007). A clamp duration of 180-minutes was used as Morris has demonstrated that clamps of 120 minutes duration have acceptable reproducibility but may underestimate glucose disposal by up to 10% when compared with measurements derived after 180 minutes (Morris et al. 1997). The hyperinsulinaemic euglycaemic clamp technique was chosen as whole-body glucose uptake was a primary outcome measure, the technique is considered the "gold standard" for measuring *in vivo* insulin sensitivity and a relatively small number of participants were studied, therefore, for these studies the technique was feasible in terms of labour and cost.

2.5 Indirect calorimetry

Indirect calorimetry was used in Chapters 3 and 4 of this thesis to calculate whole-body substrate oxidation in the Acute and Chronic bed rest studies prior to and during the last 15-minutes of the hyperinsulinaemic euglycaemic clamp performed in both studies. The estimation of whole-body substrate oxidation *in vivo* lends important insights into an individual's metabolic flexibility in the fasted and insulin-stimulated state before and after an intervention. Indirect calorimetry is a method for measuring whole-body substrate oxidation and energy expenditure and is defined by oxygen consumption and/or carbon dioxide being measured and converted to energy expenditure using formulae. This differs from direct calorimetry, where the rate of heat loss from the participant to the calorimeter is measured.

In indirect calorimetry, the measurement of oxygen consumption (VO_2) and CO_2 production (VCO_2) can be used to quantify the rate of carbohydrate and fat oxidation. The stoichiometry for the oxidation of glucose is:

$C_6H_{12}O_6$	+	6 O_2	→	6 H_2O	+	6 CO_2
Glucose		Oxygen		Water		Carbon dioxide

Thus, for each mole of glucose that is oxidised, 6 moles of O_2 are consumed and 6 moles of CO_2 are produced. The Respiratory Exchange Ratio (RER = VCO_2/VO_2) of glucose is therefore equal to 1.

The stoichiometry of an average fat is:

$C_{55}H_{104}O_6$	+	78 O_2	→	55 CO_2	+	52 H_2O
Triacylglycerol		Oxygen		Carbon dioxide		Water

For each mole of TAG oxidised, 78 moles of O_2 are consumed and 55 moles of CO_2 are produced. The respiratory quotient of fat is therefore equal to 0.7.

In the indirect calorimetry method used in this thesis, a ventilated open circuit method was used. A plastic hood was placed over the participant and the air drawn through this canopy via a pump was used to measure its composition and flow rate (Figure 2.1). Continuous sampling of expired gases takes place via O_2 and CO_2 analysers , with results adjusted for inspired air concentration. For the Chronic bed rest study (Chapter 3) presented in this thesis a Gas Exchange Machine (GEM) online gas analysis system was used (GEM machine GEMNutrition Ltd, Cheshire, UK). For the Acute bed rest study (Chapters 3 and 4) a Quark RMR system was used (COSMED, Rome, Italy). The gas analysers were serviced annually during the period of study, and calibration was carried out prior to each measurement. Known amounts of ethanol were combusted in the ventilated hood systems at regular intervals to monitor the accuracy and reproducibility of the overall measurements. Steady state measurements for glucose disposal and fuel oxidation taken in the final 15-minutes of the insulin clamp in this thesis were taken prior to muscle biopsies being performed.

Urine was not routinely collected for measurement of nitrogen excretion in this

thesis and it was assumed that protein oxidation did not vary throughout the clamp experiment. Equations from Peronnet and Massicotte 1991 (Peronnet and Massicotte 1991) were used to calculate substrate oxidation.

Carbohydrate oxidation: 4.585 * VCO2 – 3.226 * VO2

Fat oxidation: 1.695 * VO2 – 1.701 * VCO2

There are some limitations to the method of indirect calorimetry. There are challenges of achieving perfect and consistent conditions during measurements. Conditions that contribute to errors or variability in measurements include operator expertise, participant compliance and respiratory rate and environmental stimulation.

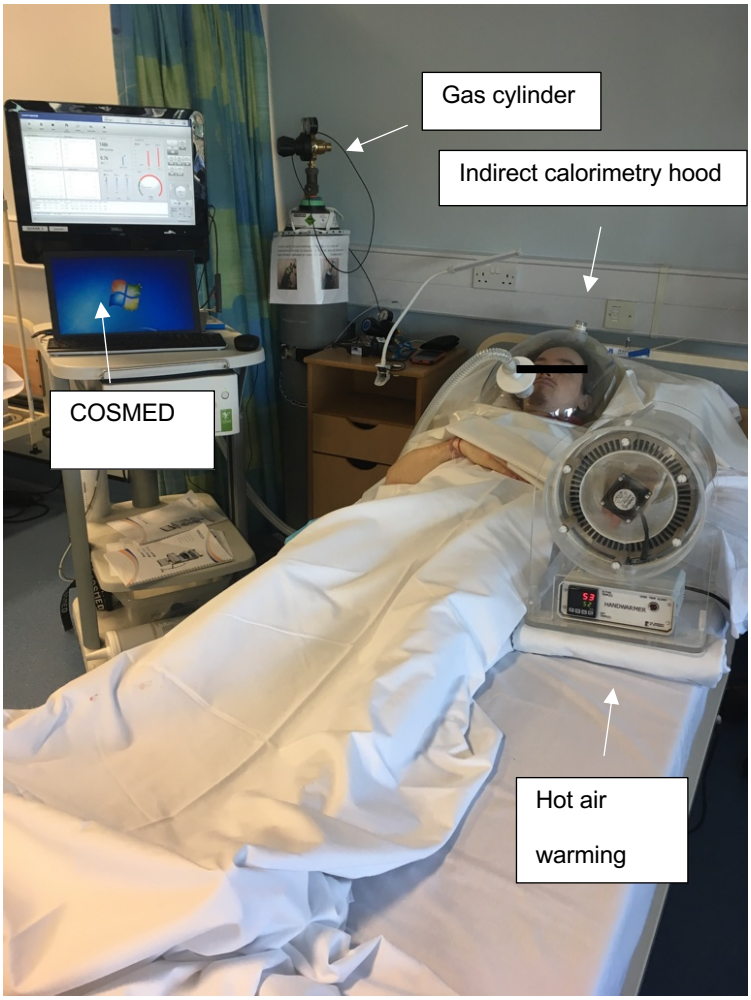

Figure 2.1. Indirect calorimetry setup.

2.6 Dual energy x-ray absorptiometry (DEXA)

DEXA scans were used in the Chronic bed rest study (Chapter 3) and the Acute bed rest study (Chapters 3 and 4) to measure body composition. Scans (Hologic, QDR4500C, Massachusetts, USA) were performed on days -14 and -2 before bed rest and days 4, 25, 39 and 58 of the Chronic bed rest study to detect changes in body fat mass and allow small adjustments in energy intake in order to achieve energy balance. In the Acute bed rest study, a one-off DEXA

scan (Lunar Prodigy, GE Healthcare, UK) only was performed prior to the period of bed rest to establish baseline body compositional information. A repeat bed rest scan could not be justified within the UK X-ray regulations due to any changes after 3 days of bed rest being too small to be detectable using DEXA, and so from an ethical viewpoint it did not warrant exposing participants to ionising radiation twice.

Initially designed to estimate whole-body and regional bone mineral density (Peppler and Mazess 1981), DEXA is a widely employed method to determine body compositional data, including fat and lean masses. During a DEXA scan, low-radiation x-rays of two different photon energy levels pass through the body and are identified by a photon detector. This measures the amount of energy that is absorbed (attenuated) by soft tissue and bone at each pixel. It is therefore based on the principle that an object's composition can be determined by the attenuation of two distinct low and high-energy beams, with the ratio between them termed the R value. One energy level is well absorbed by soft tissue, e.g., adipose, the other is better absorbed by denser tissue, e.g., bone. The x-ray attenuation of each pixel is compared to the known attenuation of reference materials. Estimates of fat and fat-free mass are then determined based on proprietary equations. Generally, DEXA scans are composed of a flat table where the participant lies supine with an x-ray generator below the table and a movable x-ray detector above. The x-ray source underneath emits a pencil or fan beam of x-rays at two energy levels, allowing algorithms for quantification of the two different tissue types. Accuracy of the DEXA is monitored by carrying out a daily quality assurance scan using a phantom block

of known attenuation coefficient value (CV of these measurements <2%). extreme age, DEXA may be inaccurate (Thomsen, Jensen, and Henriksen 1998). The advantages of DEXA are that it is fairly well available, has a short scanning time of 10-20 minutes, it is better for claustrophobic patients, the radiation dose is small (5-7μSv) compared to computed tomography (CT) (2.7-10 mSv) and it is of lower cost compared with CT and MRI.

2.7 Muscle biopsies

Muscle biopsies were obtained of the *vastus* lateralis in the Acute and Chronic bed rest study (Chapters 3 and 4) and of the *medial gastrocnemius* in Chapter 5 of this thesis. Participants in the Chronic bed rest study had muscle biopsies (2 passes) performed using a 5mm Bergström needle prior to the insulin clamp and in the final 15-minutes of the insulin clamp before and after bed rest. Participants in the Acute bed rest study had muscle biopsies using both a Bergström needle (as per the chronic bed rest study before and after bed rest and after remobilisation) and a Bard® 12G microbiopsy needle (Bard Ltd, UK) on day 0 and 2 of bed rest and on the non-rehabilitated leg prior to the insulin clamp on day 7 to measure myofibrillar protein synthesis).

Muscle biopsy of the *Vastus Lateralis*

Each participant gave written informed consent for the procedure. The location of the sample to be taken was marked on the leg; the position was located 10-15cm proximal to the superior pole of the patella and 4-5cm lateral with the participant supine. The area was aseptically cleaned approximately 5-10cm

around the marked point using betadine (or equivalent) solution. After this 1ml of 1% lidocaine was infiltrated subcutaneously as a small bleb. Following this, a further 5-8mls of lidocaine was infiltrated down to the muscle, aspirating before each infiltrate to ensure a blood vessel was not being directly injected into. Once the local anaesthetic had taken effect (2-5 minutes), a 4-5mm horizontal incision was made through the skin and continued through the superficial fascia then pressure applied using a gauze to reduce bleeding. After this a 5mm Bergström needle was introduced through the incision, applying firm pressure in order to advance the needle approximately 1-2cm beyond the fascia. Obtaining a muscle biopsy using a Bergström needle is a relatively quick and well tolerated method for obtaining muscle samples where significant volumes of tissue are required for analysis (Bergstrom 1975). Once through the fascia, the inner trochar was pulled back enough to open the cutting aperture whilst suction was applied using a 50ml syringe and tubing attached to the other end of the needle. Using suction has been shown to significantly increase the yield of the muscle sample during biopsies (Hennessey et al. 1997). The needle is then firmly closed and with suction being maintained two or three further samples are taken in which the needle may be rotated between each sample. After the final biopsy, the needle is removed and firm pressure was applied with a sterile gauze for a further 5 minutes, or longer if there was persistently oozing. The incision was closed using sterile Steristrips™ (3M, UK) ensuring opposition of the wound edges. A Tegaderm™ (3M, UK) was applied over the top for further protection and a self-adherent wrap e.g., Coban™ (3M, UK) used for 12 hours to provide compression thereafter. The first pass muscle biopsy was

immediately snap-frozen in liquid nitrogen and stored at -80°C for subsequent analysis. A portion of muscle from the second pass being orientated and embedded in OCT mounting medium (361603E, VWR Chemical) and frozen in cooled isopentane (Thermo Fisher Scientific Ltd., Loughborough, UK) for histochemical analysis. The remaining muscle from the second pass was frozen in liquid nitrogen. These muscle samples were subsequently analysed to determine muscle substrates, IMCL content, and gene transcripts, respectively.

Where a muscle biopsy was taken with a Bard® microbiopsy needle during the Acute bed rest study, the same preparatory steps were followed as with the Bergström needle as above initially, however a smaller incision which does not include the fascia is required and a Bard® 12G needle was introduced into the muscle belly instead. Following this, the device is triggered and a sample taken (Figure 2.2a and b). Multiple passes (up to 6) were taken whereby the needle angle was adjusted slightly each time to ensure fresh muscle is sampled. Semi-open biopsy techniques such as the Bergström and conchotome techniques require larger incisions increasing the risk of complications such as bleeding, infection and pain. Microbiopsy techniques have the advantage of being practical for resting studies where multiple samples can be obtained. The microbiopsy device consists of a disposable core biopsy needle and it is a variant of a spring loaded one-handed automated biopsy device.

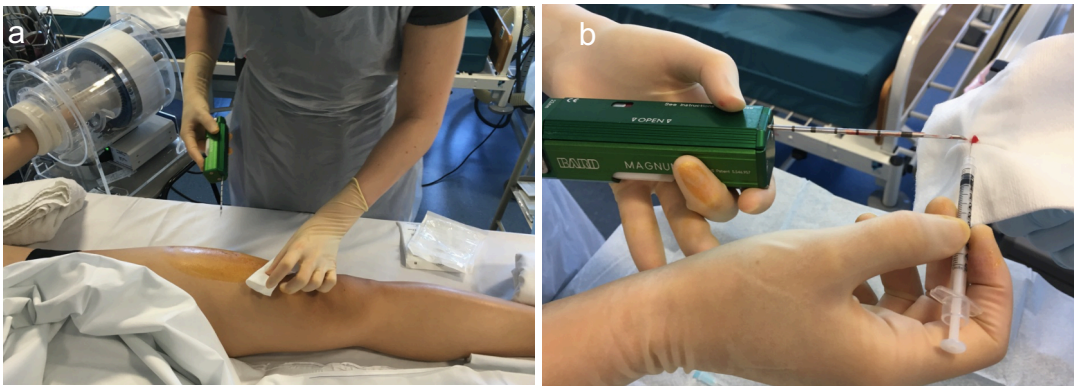

Figure 2.2. Muscle microbiopsy. a) Positioning of participant for Bard microbiopsy sample of vastus lateralis. b) Bard microbiopsy needle with muscle sample being placed onto gauze.

2.8. Blood sampling and analyses

Blood sampling

In the Acute bed rest study (Chapters 3 and 4) and the Chronic bed rest study (Chapter 3), arterialised-venous samples were collected from a cannula (Venflon™; Sweden) which had been inserted retrograde into a dorsal hand vein. This was subsequently placed into a hand warmer and heated to 55ºC (The David Greenfield Physiology Unit, The University of Nottingham) and kept patent using a slow running infusion of 0.9% NaCl (Baxter Healthcare, Norfolk, UK). The heated hand technique is a safe and less invasive method for accurate blood sampling compared to sampling blood from arteries requiring arterial cannulation (Gallen and Macdonald 1990). Furthermore, Liu demonstrated that the difference in blood glucose between arterial and arterialised-venous blood was 0.1mmol/l (95% CI -0.19 to 0.41 mmol/l) (Liu et al. 1992).

During the hyperinsulinaemic euglycaemic clamps performed in Chapters 3 and 4, blood samples were drawn into syringes from a 3-way tap with the first 2 ml discarded to avoid saline contamination. For the measurement of blood glucose concentration 0.3 ml was immediately analysed using the Yellow Springs Analyser 2300 STAT Plus Glucose and Lactate Analyzer (YSI) at 5-minute intervals. Before the insulin clamp, and in every 15-minutes in the final hour of the insulin clamp, a 5ml sample of whole blood was collected for analysis of serum insulin, serum TAG and plasma NEFA. Blood for determination of serum variables was collected into a microtube with coagulation activator (Sarstedt, Nümbrecht, Germany) and left to clot for at least 15-minutes before being centrifuged (15G for 2 minutes). Serum was aliquoted into 2 cryovials and frozen at -80°C. For plasma measures, lithium heparin microtubes (Sarstedt, Nümbrecht, Germany) used to collect blood were pre-filled with 7.5ul per ml plasma of ethylene glycol tetraacetic acid (EGTA)-Gluthathione, a preservative to prevent degradation of NEFAs during storage and 10uL of Tetrahydrolipostatin (THL) to inhibit in vitro lipolysis and prevent falsely high plasma NEFA readings before the addition of 1.3 ml whole blood. This was immediately centrifuged after gentle inversion, with plasma removed from the cell pellet and frozen at -80°C until analysis.

2.8.1. Blood glucose concentration

The YSI is a Class II in-vitro diagnostics (IVD) medical device, which is widely accepted as a method for reference measurements and system calibration by most manufacturers of blood glucose monitoring systems. The YSI was

calibrated using glucose standards of known concentration before and during every study. Where paired samples were required for arterio-venous difference (Chapter 4), approximately 0.3ml of blood from each cannula (retrograde dorsal hand cannula and femoral vein cannula) was dispensed into a fluoride/oxalate tube and placed on a roller for 3-minutes before being analysed using the YSI. The YSI STAT analyser probe is fitted with a three-layer membrane with immobilised enzyme in the middle layer. When the injected sample contacts this layer, it is rapidly oxidised, producing hydrogen peroxide. The hydrogen peroxide is then oxidised at a platinum anode, producing electrons. A dynamic equilibrium is achieved when the rate of hydrogen peroxide production and the rate at which it leaves the enzyme later are constant, resulting in a steady state response. The electron flow is proportional to the steady state hydrogen peroxide concentration and therefore the concentration of the substrate (YSI 2009). The benefits of the YSI are that it only requires small samples (0.025ml for analysis) and it is quick (takes around 1 minute to obtain the result), which is necessary when performing a hyperinsulinaemic euglycaemic clamp. Inter-assay and intra-assay coefficient of variation (CV) of this measure is 1%.

2.8.2. Serum Insulin Concentration

Serum insulin concentration was measured using a solid-phase ^{125}I radioimmunoassay using standard insulin kits (Millipore Insulin, Linco Research, USA). The Millipore Human Insulin assay utilises ^{125}I-labeled human insulin and a human insulin antiserum to determine the level of insulin in serum by the double antibody technique. Standard calibrators were prepared from

assay buffer and human insulin standards of a known concentration. Assay buffer was added to a glass tube alongside either serum samples or standard calibrators. This was followed by the addition of hydrated ^{125}I radio labelled insulin and human insulin antibody, the insulin in the serum samples or the insulin in the standard calibrators competes with the exogenous radioactive insulin for sites on an insulin specific antibody. Tubes were vortexed before being incubated at room temperature for 24-hours. Cold precipitating reagent was added to all tubes before being vortexed and incubated and centrifuged. Competitive binding was terminated by decanting the supernatant, leaving the bound insulin which had formed a solid pellet. The tubes were dried before a gamma counter measured the radioactivity of the precipitated pellets. A standard binding curve was plotted from the radioactivity levels in which the standard calibrators were added. The unknown concentrations of the serum samples were determined using the standard curve.

2.8.3 Serum Triacylglycerols

Serum TAGs were measured using enzymic photometric methods with an automated analyser (ABX Pentra 400, Horiba Medical, Montpellier, France) with the intra-assay CV being 2.16%, and inter-assay CV being 3.27%. TAGs are broken down to glycerol and fatty acids via lipoprotein lipase. Glycerol is then converted to glycerol-3-phosphate and ADP, catalyzed by glycerokinase. Glycerol-3-phosphate is converted to hydrogen peroxide and dihydroxyacetone phosphate (DHAP) via an oxidase enzyme. Peroxidase catalyses the coupling of hydrogen peroxide with 4-aminoantipyrine and p-chlorophenol to produce a

quinoneimine dye. The increase in absorbance is proportional to the amount of TAGs concentration in the sample.

2.8.4 Plasma non-esterified fatty acid concentration

Plasma non-esterified fatty acid (NEFA) was analysed by the Metabolic Physiology Analytical Laboratory, University of Nottingham. NEFA were measured using an automated immunoassay analyser (ABX Pentra, Montpellier, France) and commercially available kit (WAKO Chemicals GmbH, Richmond, VA, USA; intra-assay CV of 0.65%, an inter-assay CV of 2.95%). Plasma NEFA concentration is determined via the acylation of coenzyme A (CoA) by the fatty acids in the presence of added acyl-CoA synthetase (ACS). The acyl-CoA produced is then oxidised by added acyl-CoA oxidase (ACOD) with the generation of hydrogen peroxide. This produces a purple pigment which can be measured colorimetrically at 550nm.

$$\text{RCOOH (NEFA)} + \text{ATP} + \text{CoA-SH} \xrightarrow{\text{ACS}} \text{Acyl-CoA} + \text{AMP} + \text{PPi}$$

$$\text{Acyl-CoA} + 0_2 \xrightarrow{\text{ACOD}} \text{2,3-trans-Enoyl-CoA} + H_2O_2$$

$$2\ H_2O_2 + \text{4-Aminophenazone} + \text{MEHA} \xrightarrow{\text{POD}} \text{Quinoneimine-color} + 4H_2O$$

2.8.5. Whole-body muscle protein breakdown (MPB)

The stable isotope tracer 3-methylhistidine (3-MeH) was used in the Acute bed rest study (Chapter 4) and the ankle fracture study (Chapter 5) of this thesis to estimate the rate of whole-body MPB. In the acute bed rest study, 10mg 3-MeH was ingested (dissolved in 50ml distilled water) on day -1 prior to the bed rest period and day 1 at 09:00am. Following this, an anterograde venous cannula was inserted 24 hours later into the arm at the antecubital fossa for sampling of venous blood every hour for a total of 7 hours for the measurement of D_3-MeH enrichment. In the ankle fracture study, for participants in the treatment group 10mg was ingested (dissolved in 50ml distilled water) on the morning of the 2 week follow-up appointment, with blood samples taken as above 24 hours later. For participants in the control group 10mg was ingested (dissolved in 50mg distilled water) at 09:00am on visit 3 (2 weeks after lower leg immobilisation with below-knee casting), with blood sampling as above occurring 24-hours later.

2.9. Skeletal muscle analysis

2.9.1. Fractional myofibrillar protein synthesis (MPS)

Heavy water was used in the Acute bed rest study (Chapter 4) and the Ankle fracture study (Chapter 5) in this thesis to quantify cumulative MPS rates. In the Acute bed rest study (Chapter 4), an initial oral bolus of 3mg/kg was administered at 09:00am (divided into 3 equal doses 30-minutes apart to reduce the risk of side effects) on day -4 prior to bedrest, with individualised

top-ups on day 0, day 3 and day 7. Top ups were calculated based upon the rate of decay of water and total body water of 60% in men, e.g. in a 75kg man, initial loading bolus was 225ml followed by a top up of 77ml on day 7. This was with the aim to label and maintain the body water pool to ~0.2% atom percent excess (APE). Saliva samples (1ml) were collected prior to and two hours after each D_2O ingestion (to determine precursor labelling), as well as additional samples at 09:00 on day 0, day 1 and day 7 of the protocol for analysis of D_2O enrichment. They were advised not to drink fluids 30 minutes prior to each saliva sample. In the ankle fracture study (Chapter 5), an initial oral bolus of 3mg/kg was administered postoperatively (or at visit 1 if a healthy volunteer) at 09:00am divided into 3 equal doses, 30-minutes apart. Individualised top-ups (calculated as described above) were provided to take one week following discharge, with saliva samples (1ml) collected prior to and two hours after each D_2O ingestion, for analysis of D_2O enrichment as detailed above. When samples were obtained at home, participants collected these in sterile plastic tubes and kept them refrigerated until they either brought them to the next visit or they were collected by NFS at their home. Upon receipt of saliva samples in the laboratory, they were immediately cold centrifuged to remove any debris that might have been present and then aliquoted into 2ml vials and frozen at -20^{o}C until analysis.

Body water and muscle protein enrichment were measured as previously described (Wilkinson et al. 2014). Pure fractions of body water were extracted by heating 100 µl of saliva in an inverted 2 ml autosampler vial for 4 h at 100°C. Vials were then placed upright on ice to condense extracted body

water and transferred to a clean autosampler vial ready for injection. Body water (0.1 µl) was injected into a high-temperature conversion elemental analyser (TCEA, Thermo Scientific, Hemel Hempstead, UK) connected to an isotope ratio mass spectrometer (Delta V Advantage, Thermo Scientific). For isolation of myofibrillar protein, 30–50 mg of muscle was homogenized in ice-cold homogenization buffer (Wilkinson et al. 2014), rotated for 10 min, and the supernatant was collected after centrifugation at 13,000 *g* for 5 min at 4°C. The myofibrillar pellet was solubilized in 0.3 M NaOH and separated from the insoluble collagen by centrifugation, and the myofibrillar protein was precipitated using 1 M perchloric acid (PCA). Myofibrillar proteins were precipitated from the sample homogenate with 1 M PCA and separated by centrifugation. Protein-bound amino acids were released using acid hydrolysis by incubating at 110°C in 0.1 M HCl in Dowex H^+ resin slurry overnight before being eluted from the resin with 2 M NH_4OH and evaporated to dryness; amino acids were then derivatized as their *n*-methoxycarbonyl methyl esters (MCME). Dried samples were suspended in 60 µl distilled water and 32 µl methanol, and following vortex, 10 µl of pyridine and 8 µl of methylchloroformate were added. Samples were vortexed for 30 s and left to react at room temperature for 5 min. The newly formed *n*-methoxycarbonyl methyl esters of amino acids were then extracted into 100 µl of chloroform. A molecular sieve was added to each sample for ~20 s before being transferred to a clean glass Gas Chromatography insert, removing any remaining water by size exclusion absorption. Incorporation of deuterium into protein bound alanine was determined by gas chromatography–pyrolysis–isotope ratio mass spectrometry

(GC-pyrolysis-IRMS, Thermo Scientific, Hemel Hempstead, UK) alongside a standard curve of known L-alanine-2,3,3,3-d4 enrichment to validate measurement accuracy of the instrument.

Calculation of fractional synthetic rate (FSR)

The FSR of myofibrillar proteins (MPS) was determined as described by Wilkinson (Wilkinson et al. 2015) using the precursor-product approach. This involved the incorporation of deuterium labelled alanine into protein, using the enrichment of body water (corrected for the mean number of deuterium moieties incorporated per alanine, i.e., 3.7, and the total number of hydrogen within the MCME derivative, [11]) as the surrogate precursor labelling between subsequent biopsies. In brief, the standard equation is:

$FSR\ (\%.h^{-1}) = [(\delta Ala)] / [(\ \delta p) \times t] \times 100$

where, δAla = deuterium enrichment (in delta per mil) of protein-bound alanine between subsequent biopsies, δP = precursor enrichment (i.e. saliva D_2O, corrected for 3.7 deuterium in Alanine, in delta per mil) and t, time between biopsies.

2.9.2. Glycogen and lactate

Muscle glycogen and lactate was quantified in the Acute and Chronic bed rest study (Chapters 3 and 4) of this thesis. Muscle tissue from *vastus lateralis* muscle biopsies was freeze-dried for 24-hours, visible blood and connective tissue were removed, and the remaining biopsy was powdered in a mortar. A portion of powdered tissue was extracted using 0.1 $mol \cdot l^{-1}$ NaOH for

determination of glycogen content, using a modification of a spectrophotometric method by (Harris, Hultman, and Nordesjo 1974).

2.9.3. Acetyl carnitine and long-chain acylcarnitine

Metabolites were extracted using 0.5 $mmol \cdot l^{-1}$ perchloric acid and neutralised using $KHCO_3$ following centrifugation. Tissue acetyl carnitine was measured in the neutralised extract using radioisotope enzymatic assays (Cederblad et al. 1990), along with long-chain acylcarnitine's, which were extracted from the acid-insoluble tissue pellets.

2.9.4. IMCL quantification

Immunohistochemical Staining of VL Sections

The method used in the for the immunohistochemical staining of IMCL with the fluorescent dye Bodipy-493/503 (D3922, ThermoFisher) has been described previously (Prats et al. 2013). In brief, frozen *vastus lateralis* samples were embedded in OCT mounting medium (361603E, VWR Chemical) before being secured to the object holder of a Leica CM3050 S Research Cryostat. Transverse sections of 15 µm thickness were trimmed and collected from each muscle block. These sections were mounted on SuperFrost Plus adhesion microscope slides (631-0108P, VWR Chemical). Sections were immersed in 50 mL of Zamboni fixative, supplemented with 2.5 ml of 2% glyceraldehyde in 0.05M phosphate buffer (pH 7.4), for 60 minutes. After a 20-minute wash in phosphate buffered saline (PBS), the sections were incubated for 60 minutes

in PBS containing 20 µg/mL Bodipy-493/503 followed by a final wash in PBS for 20 minutes.

Image Acquisition

A Zeiss LSM700, Axio Imager 2 confocal microscope was used to image stained sections at 20x magnification through a 20x/0.8 M27 Plan-Apochromat objective. A 488 nm argon laser, optimal for the excitation of Bodipy 493/503 and Alexa Fluor 488, was used. Pinhole size was maintained at 0.96 AU. Z-stacks, imaged from the top to the bottom of each section and consisting of 5 segments of total thickness 3.642 µm, 910.54 nm between segments, were obtained for each muscle sample. From each image, a maximum projection was generated using the processing function in ZEN software. Maximum projections were then exported as Tiff Format (64 bit) (Big Tiff) images. These images were analysed using the FIJI software package (Schindelin et al. 2012).

Image Analysis

A *"Gaussian Blur"* of radius 1.00 was applied to each imported maximum projection. Thresholding was performed using the Bernsen Algorithm (radius=50). Regions of interest (ROIs) were manually drawn and the *"Analyse Particles"* function was used to measure the value of several variables within these regions from which lipid droplet (LD) count, LD size and % IMCL were calculated. The circularity filter was set to 0.50-1.00 to exclude sarcolemmal lipid and accurately calculate LD size and LD count. This filter was not applied

in the calculation of the ratio of lipid area to whole tissue area (% IMCL). LD count was calculated as total LD count/ total tissue area and is presented here as droplets per micrometre of muscle. LD size was calculated as a mean of the size of every droplet within an ROI. Here LD size is presented as the mean number of pixels composing a LD -a single pixel having an area of 0.0244 μm^2. Pixel aspect ratio for all maximal projections was 1 µm = 6.3983 pixels.

2.9.5. Muscle mRNA expression

Total RNA extraction and targeted muscle mRNA expression measurements

Total RNA was extracted from frozen muscle biopsies according to a method previously described (Constantin et al. 2013). The RNAs were extracted using TRI Reagent (Ambion, Huntingdon, UK), according to the manufacturers protocol. First strand cDNA was then synthesised from 1 µg RNA using random primers (Promega) and Superscript III (InVitrogen) and stored at −80°C until analysis. TaqMan low-density arrays were performed using an ABI PRISM 7900HT sequence detection system, and data analysed using SDS 2.1 software (Applied Biosystems). Data were further analysed using RQ Manager software (Applied Biosystems), where the threshold level was normalized across all plates before Ct values were calculated for each gene target and sample. Relative quantification of mRNAs of interest was measured using the $2^{-\Delta\Delta Ct}$ method with hydroxymethylbilane synthase (HMBS) as the endogenous control, with the mean of the baseline sample used as the calibrator. Multiple mRNA expression measurements (191 targets) were made

according to the manufacturer's instructions. The mRNAs investigated were deemed to be representative of insulin sensitivity, carbohydrate and fat metabolism, inflammation, and protein turnover according to research findings in muscle from human volunteer studies that included unbiased gene analysis (Murton et al. 2014; Murton et al. 2015; Stephens et al. 2013; Porter et al. 2017), and from an *in vivo* animal study (Murton et al. 2015). These studies from the laboratory in Nottingham involved interventions that altered physical activity levels, adiposity and fuel oxidation rates, all of which are metabolic and physiological traits highly relevant to the bed rest condition. The validation approach also included detailed literature searches, and SA Biosciences and IPA databases interrogation to confirm the targets. Targets also included confirmed calcium activated/sarcoplasmic reticulum genes. (https://analysis.ingenuity.com/). Data were further analysed using Applied Biosystems RQ Manager software (Thermo Fisher Scientific Ltd., Loughborough, UK) where the threshold level was normalised across all plates before Ct values were calculated for each gene target and sample. Relative quantification of mRNAs of interest was measured using the $2^{-\Delta\Delta Ct}$ method with hydroxymethylbilane synthase (HMBS) as the endogenous control, with the mean of the baseline sample used as the calibrator. To associate a biological function to the identified probe sets, Ct values were uploaded to IPA software (Redwood City, CA, USA) for pathway analysis of gene expression data. A full list of genes is shown in Table 2.1.

Table 2.1. List of genes selected for mRNA expression measurements using TaqMan low-density array gene card.

Gene symbol	Function
18S	Eukaryotic 18S rRNA
ACO1	aconitase 1
ACTA1	actin, alpha 1, skeletal muscle
ADIPOQ	adiponectin, C1Q and collagen domain containing
AKT1	v-akt murine thymoma viral oncogene homolog 1
ALDH2	aldehyde dehydrogenase 2 family (mitochondrial)
AMPD1	adenosine monophosphate deaminase 1
ATF4	activating transcription factor 4
ATF6	activating transcription factor 6
ATG12	autophagy related 12
ATG9A	autophagy related 9A
ATP2A1	ATPase sarcoplasmic/endoplasmic reticulum Ca2+ transporting 1
ATP2A2	ATPase sarcoplasmic/endoplasmic reticulum Ca2+ transporting 2
ATP2B2	ATPase plasma membrane Ca2+ transporting 2
ATP2B4	ATPase plasma membrane Ca2+ transporting 4
ATP5B	ATP synthase, H+ transporting, mitochondrial F1 complex, beta polypeptide
ATP5I	ATP synthase, H+ transporting, mitochondrial Fo complex, subunit E
ATP6AP2	ATPase H+ transporting accessory protein 2

B2M	beta-2-microglobulin
BECN1	beclin 1, autophagy related
BRD4	bromodomain containing 4
CALM1	calmodulin 1
CALR	calreticulin
CAMK2A	calcium/calmodulin dependent protein kinase II alpha
CAMK4	calcium/calmodulin dependent protein kinase IV
CANX	calnexin
CAPN1	calpain 1, (mu/I) large subunit
CAPN2	calpain 2, (m/II) large subunit
CARM1	coactivator associated arginine methyltransferase 1
CAS3	caspase 3
CASP8	caspase 8, apoptosis-related cysteine peptidase
CASQ1	calsequestrin 1
casq2	calsequestrin 2
CAT	catalase
CCL19	chemokine (C-C motif) ligand 19
COL1A1	collagen, type I, alpha 1
COL2A1	collagen, type II, alpha 1
COl4A1	collagen type IV alpha 1 chain
COL6A3	collagen type VI alpha 3 chain
COX5A	cytochrome c oxidase subunit 5A
COX5B	cytochrome c oxidase subunit Vb
COX6B1	cytochrome c oxidase subunit 6B1

CPT1A	carnitine palmitoyltransferase 1A (liver)
CPT1B;CHKB-CPT1B	carnitine palmitoyltransferase 1B (muscle),CHKB-CPT1B readthrough (NMD candidate)
CRTC1	CREB regulated transcription coactivator 1
CS	citrate synthase
CTSL	cathepsin L
CUL4A	cullin 4A
CYCS	cytochrome c, somatic
DLAT	dihydrolipoamide S-acetyltransferase
DLD	dihydrolipoamide dehydrogenase
EIF2S1	eukaryotic translation initiation factor 2, subunit 1 alpha, 35kDa
EIF4B	eukaryotic translation initiation factor 4B
EIF4E	eukaryotic translation initiation factor 4E
EIF4EBP1	eukaryotic translation initiation factor 4E binding protein 1
eno3	fibronectin 1
ERK1	mitogen-activated protein kinase 3
FABP3	fatty acid binding protein 3, muscle and heart (mammary-derived growth inhibitor)
FBXO32	F-box protein 32
FGF21	fibroblast growth factor 21
FOXO1	forkhead box O1
FOXO3B;FOXO3	forkhead box O3B pseudogene,forkhead box O3
FST	follistatin
GAPDH	glyceraldehyde-3-phosphate dehydrogenase

Glud1	glutamate dehydrogenase 1
GPD2	glycerol-3-phosphate dehydrogenase 2 (mitochondrial)
GSK3B	glycogen synthase kinase 3 beta
HADH	hydroxyacyl-CoA dehydrogenase
HIF1A	hypoxia inducible factor 1, alpha subunit (basic helix-loop-helix transcription factor)
HK2	hexokinase 2
HMBS	hydroxymethylbilane synthase
HSPA8	heat shock 70kDa protein 8
IDH2	isocitrate dehydrogenase (NADP(+)) 2, mitochondrial
IER2	immediate early response 2
IFI30	IFI30, lysosomal thiol reductase
IGBP1	immunoglobulin (CD79A) binding protein 1
IGF1	insulin-like growth factor 1 (somatomedin C)
IGFBP1	insulin like growth factor binding protein 1
IKBKB	inhibitor of kappa light polypeptide gene enhancer in B-cells, kinase beta
IL6	interleukin 6 (interferon, beta 2)
IL6R	interleukin 6 receptor
INSR	insulin receptor
IRS1	insulin receptor substrate 1
ITPR1	inositol 1,4,5-trisphosphate receptor type 1
ITPR3	inositol 1,4,5-trisphosphate receptor type 3
JKAMP	JNK1/MAPK8-associated membrane protein
JPH1	junctophilin 1

KCNT1	potassium sodium-activated channel subfamily T member 1
LDHA	lactate dehydrogenase A
M6PRBP1	perilipin 3
MAP1LC3A	microtubule-associated protein 1 light chain 3 alpha
MAPK9	mitogen-activated protein kinase 9
MCUR1	mitochondrial calcium uniporter regulator 1
MDH2	malate dehydrogenase 2
MNF1	mitochondrial nucleoid factor 1
MPC2	mitochondrial pyruvate carrier 2
MPST	mercaptopyruvate sulfurtransferase
MRF4	myogenic factor 6
MSTN	myostatin
MT1A	metallothionein 1A
MTFR1	mitochondrial fission regulator 1
MTOR	mechanistic target of rapamycin (serine/threonine kinase)
MYBPC1	myosin binding protein C, slow type
Myf5	myogenic factor 5
MYH1	myosin heavy chain 1
MYH2	myosin heavy chain 2
MYH3	myosin, heavy chain 3, skeletal muscle, embryonic
MYH4	myosin, heavy chain 4, skeletal muscle
MYL1	myosin, light chain 1, alkali; skeletal, fast

MYL6	myosin, light chain 6, alkali, smooth muscle and non-muscle
MYLK2	myosin light chain kinase 2
MYLPF	myosin light chain, phosphorylatable, fast skeletal muscle
MYO5C	myosin VC
MYOG	myogenin (myogenic factor 4)
NAT1	N-acetyltransferase 1
NAT2	N-acetyltransferase 2
NDUFB3	NADH:ubiquinone oxidoreductase subunit B3
NDUFB5	NADH:ubiquinone oxidoreductase subunit B5
NFE2L2	nuclear factor, erythroid 2-like 2
NFKB1	nuclear factor of kappa light polypeptide gene enhancer in B-cells 1
NRF1	nuclear respiratory factor 1
OGDH	oxoglutarate dehydrogenase
OPTN	optineurin
OSTN	osteocrin
OTOP1	otopetrin 1
PARKIN	parkin RBR E3 ubiquitin protein ligase
PAX3	paired box 3
PAX7	paired box 7
PDHA1	pyruvate dehydrogenase (lipoamide) alpha 1
PDIA2	protein disulfide isomerase family A member 2
PDK2	pyruvate dehydrogenase kinase, isozyme 2

PDK4	pyruvate dehydrogenase kinase, isozyme 4
PFKM	phosphofructokinase, muscle
PKM	pyruvate kinase, muscle
POLRMT	polymerase (RNA) mitochondrial (DNA directed)
PPARA	peroxisome proliferator-activated receptor alpha
PPARG	peroxisome proliferator-activated receptor gamma
PPARGC1A	peroxisome proliferator-activated receptor gamma, coactivator 1 alpha
PPP3CA	protein phosphatase 3 catalytic subunit alpha
PRKAA1	protein kinase, AMP-activated, alpha 1 catalytic subunit
PRKAA2	protein kinase, AMP-activated, alpha 2 catalytic subunit
PRKAB1	protein kinase AMP-activated non-catalytic subunit beta 1
PSMA1	proteasome (prosome, macropain) subunit, alpha type, 1
PSMC1	proteasome (prosome, macropain) 26S subunit, ATPase, 1
PSMC4	proteasome 26S subunit, ATPase 4
PTEN	phosphatase and tensin homolog
PYGM	phosphorylase, glycogen, muscle
RELA	RELA proto-oncogene, NF-kB subunit
RHOA	ras homolog family member A
RICTOR	RPTOR independent companion of MTOR, complex 2
RPS6KB1	ribosomal protein S6 kinase B1
RPS6KB2	ribosomal protein S6 kinase, 70kDa, polypeptide 2
RPTOR	regulatory associated protein of MTOR, complex 1

RYR1	ryanodine receptor 1
SDHA	succinate dehydrogenase complex, subunit A, flavoprotein (Fp)
SIX1	SIX homeobox 1
SLC39A6	solute carrier family 39 member 6
SMAD	SMAD family member 2
SOCS3	suppressor of cytokine signaling 3
SOD2	superoxide dismutase 2, mitochondrial
SREBF1	sterol regulatory element binding transcription factor 1
SREBP	sterol regulatory element binding transcription factor 1
SRF	serum response factor
STAT1	signal transducer and activator of transcription 1, 91kDa
STAT3	signal transducer and activator of transcription 3 (acute-phase response factor)
STIM1	stromal interaction molecule 1
TFAM	transcription factor A, mitochondrial
TFB2M	transcription factor B2, mitochondrial
TGFB1	transforming growth factor, beta 1
TJP2	tight junction protein 2
TLR4	toll-like receptor 4
TNC	tenascin C
TNFR1	TNF receptor superfamily member 1A
TNNC2	troponin C2, fast skeletal type
TNNT1	troponin T1, slow skeletal type
TRAF3	TNF receptor-associated factor 3

TRIM63	tripartite motif containing 63, E3 ubiquitin protein ligase
TRPM1	transient receptor potential cation channel subfamily M member 1
TRPM7	transient receptor potential cation channel subfamily M member 7
TTN	titin
TUFM	Tu translation elongation factor, mitochondrial
UCP1	uncoupling protein 1 (mitochondrial, proton carrier)
UCP3	uncoupling protein 3 (mitochondrial, proton carrier)
YWHAZ	tyrosine 3-monooxygenase/tryptophan 5-monooxygenase activation
ZFAND5	zinc finger AN1-type containing 5
NDUFS6	NADH:ubiquinone oxidoreductase subunit S6
SCNN1A	sodium channel epithelial 1 alpha subunit
CTNNAL1	alpha catenin
PDPK1	3-phosphoinositide-dependent protein kinase 1
PIK3R5	phosphoinositide-3-kinase regulatory subunit 5
SLC2A4	solute carrier family 2 member 4/Glut4 transporter

Ingenuity Pathway Analysis (IPA)

Analysis of mRNA abundance by IPA was performed as follows:

1) First, fold change from mean baseline was calculated from the Ct values to determine differential expression of mRNAs.
2) Subsequently, statistical significance (p-values) were determined from the fold change data using a paired sample t-test.

3) Data filtering was set with a fold change cut-off of 1.5 and p-value cut-off of $p<0.05$ to select for the most significantly changed genes. These genes were then used as the input for the subsequent core IPA analysis.
4) The overall outcome of IPA (e.g. upstream regular analysis, cellular function, activation status) was predicted by calculating a regulation Z-score and an overlap p-value, which were based on: (1) the number of regulated target genes' function; (2) the magnitude of expression change; (3) the direction of expression change; and (4) their concordance with the IPA database, which is constructed from a curated literature database.
5) A second p-value called the "p-value of overlap" was calculated by IPA to identify significantly enriched function pathways from the submitted list of significantly changed genes. These p-values were generated from the right-tailed Fisher's Exact Test, and a significance threshold of 0.05 was used to assess the statistical significance of the function pathways

In order to control for any enrichment of false positive results when undertaking multiple comparisons (type II errors) IPA utilises Bonferroni's corrected p-value set at < 0.05. For muscle mRNA cellular function analysis, the Benjamini-Hochberg method for multiple hypothesis correction was employed to account for the possibility of false-positive results (type I errors). This is a default function within the IPA platform.

2.10. Statistical Analysis

The statistics, calculations and graphs presented in this thesis were completed using SPSS software (version 24; SPSS, Chicago, IL) or GraphPad Prism (version 7; Graphpad Software Inc, USA). Data were assessed for normality using the Shapiro-Wilks test, with criteria for normality met if $p<0.05$. Statistical analysis for each chapter is described in the individual chapter. All data are presented as mean ± SEM. Statistical significance was declared at $p<0.05$.

Chapter 3

The effect of acute (3 days) and chronic (56 days of) bed rest on insulin-mediated whole-body glucose disposal and fuel metabolism in healthy male participants in energy balance.

3.1 Introduction

Periods of physical inactivity of short duration (<7 days) such as bed rest are common during hospitalisation after illness or injury, with the average length of hospital stay in the United Kingdom 5.9 days (NHS Digital 2019). Chronic physical inactivity is a significant independent predictor of all-cause mortality (Ekelund et al. 2019) and the development of metabolic diseases such as type II diabetes (Aune et al. 2015). A defining feature of immobilisation-induced impairment of metabolic health after both short and long duration (>7 days) bed rest is a reduction in whole-body glucose disposal (GD) (insulin sensitivity) which has been observed over a range of insulin concentrations using the hyperinsulinaemic euglycaemic clamp technique (Stuart et al. 1988a, Mikines et al. 1991) or by oral glucose tolerance test (Yanagibori et al. 1994; Stuart et al. 1988b; Heer et al. 2014). This reduction in whole-body glucose disposal has been observed as early as after 3-5 days of bed rest (Yanagibori et al. 1994; Smorawinski et al. 2000; Reidy et al. 2017), but not detectable after one day of bed rest (Dirks et al. 2018). However, the precise metabolic and physiological

mechanisms and their temporal relationship underpinning the reduction in whole-body glucose disposal during bed rest is currently unclear.

Mechanistically, 7 days of bed rest has been reported to cause a reduction in insulin-stimulated whole-body glucose disposal, which predominantly occurs at the level of the muscle (Mikines et al. 1991; Stuart et al. 1988b). Biensø noted a reduction in quantity and activation status of key proteins regulating glucose transport, phosphorylation and storage, including skeletal muscle GLUT4 and hexokinase II content and insulin-stimulated glycogen synthase activity after 7 days of bed rest (Bienso et al. 2012). However, it is unclear if these events were causative in the reduction in skeletal muscle glucose disposal observed during bed rest or an adaptive response to a reduction in muscle glucose uptake itself. A recent study utilising a forearm immobilisation model showed a significant reduction in forearm glucose uptake after 24 hours of immobilisation which did not occur in the contralateral non-immobilised arm (Burns et al. 2021), which suggests that acutely, inactivity-induced declines in glucose uptake are secondary to a lack of muscular contraction *per se*. The pattern and magnitude of temporal changes in the reduction in whole-body glucose disposal during acute and longer duration bed rest is currently unknown, as is insight of any parallel muscle level responses.

Bed rest has also been shown to alter whole-body fuel selection when transitioning from a fasted to fed state. A 21-day bed rest experiment led to a significant reduction in post-prandial carbohydrate oxidation (standardised to fat-free mass) measured using indirect calorimetry after a standardised challenge test meal (Rudwill et al. 2018). It has been suggested that this shift

in fuel oxidation may be linked to muscle fibre type changes, with a larger reduction in oxidative muscle fibres relative to a reduction in glycolytic muscle fibres (Trappe et al. 2004). However, it is unclear if these changes happen before substrate oxidation changes manifest. The impact of acute and chronic bed rest on muscle fuel selection, especially in prolonged bed rest where skeletal muscle deconditioning and potential changes in body composition may occur, is unknown.

A purported mechanism for the immobilisation-mediated decline in glucose disposal is an increase in intramyocellular lipid (IMCL) content (Cree et al. 2010; Bergouignan et al. 2011; Manini et al. 2007). It is feasible from studies involving obese, insulin resistant volunteers that alterations in lipid droplet coating composition, morphology and subcellular location may also play a regulatory role, (Gemmink et al. 2017; Kristensen et al. 2018). This proposed link is largely extrapolated from studies demonstrating a strong negative relationship between IMCL content and insulin sensitivity primarily in people with obesity or diabetes (Goodpaster et al. 2000; Aguer et al. 2010). However, these observations may reflect chronic pathophysiological states, and whether IMCL accumulation is a primary driver of a reduction in insulin-mediated whole-body glucose disposal in immobilisation remains contested (Dirks, Wall, and Stephens 2020). Increased IMCL content in response to short duration bed rest seems unlikely, unless participants are overfed, and indeed 7 days of bed rest has previously been shown to result in a reduction in whole-body glucose disposal with no measurable change in IMCL content when participants were in energy balance (Dirks et al. 2016). Longer duration bed rest studies have

been confounded by the fact that dietary energy intake was not controlled (Cree et al. 2010) and so it is therefore inconclusive whether the outcomes were secondary to energy excess or physical inactivity *per se*. The impact of acute versus chronic bed rest on IMCL content, and how any differential responses associate with changes in whole-body glucose disposal and substrate oxidation, is unknown.

The work presented in this chapter aimed to determine the magnitude of decline in whole-body GD and substrate oxidation under euglycaemic hyperinsulinaemic clamp conditions following acute (3 days) and chronic (56 days) bed rest in young, healthy-weight volunteers maintained in energy balance. Secondary aims were to generate novel mechanistic insight of cellular and molecular events underpinning any observations.

3.2 Research Questions and Aims

3.2.1 Primary Aim

To determine the impact of separate acute (3 days) and chronic (56 days) periods of bed rest on insulin-stimulated whole-body glucose disposal in healthy men maintained in energy balance, to control for the likely confounding effect of a change in energy balance on glucose uptake.

3.2.2 Secondary Aims

To determine whole-body substrate oxidation, leg IMCL content, muscle cellular metabolism and associated mRNA expression responses to acute and

chronic bed rest that may bring mechanistic insight of any changes observed in whole-body insulin-stimulated glucose disposal under these conditions.

3.3 Methods

Study protocol

3.3.1 Acute bed rest study

3.3.1.1 Recruitment

Ten healthy physically active males (who were BMI-matched to the chronic bed rest participants) were recruited from the general population via posters and advertisements placed around the University of Nottingham, as well as on appropriate popular social media platforms (Gumtree, Facebook). Participants were enrolled if they met inclusion criteria and passed medical screening to undertake the study at the David Greenfield Human Physiology Unit (DGHPU) at the University of Nottingham, United Kingdom. Participants were excluded if they had a history of diabetes, cardiovascular disease, thrombosis or were taking any regular medication (see General methods on page 66 for full inclusion and exclusion criteria). Participants were given a minimum of 24-hours to consider the study.

3.3.1.2 Screening

After written consent to the study, participants had a medical screening which included a completion of a health questionnaire (Appendix 1, **Section 7.5**), a

12-lead electrocardiogram (ECG), height, weight and blood pressure measurement, and a blood sample taken for full blood count, blood clotting screen, liver function tests, thyroid function tests, random blood glucose, urea and electrolytes. Personal food preferences were noted during the medical screening to individually tailor their diet during the study. One participant who was recruited dropped out before beginning the study due to personal reasons and was replaced by a different individual. Two participants underwent medical screening but did not fulfil criteria for recruitment, and a total of ten participants completed the study. The acute bed rest study was conducted between January and May 2018 and was approved by the University of Nottingham Medical School Ethics Committee.

3.3.1.3 Protocol

The acute bed rest protocol is outlined in Figure 3.1 and consisted of:

- A 7-day 'run-in' phase
- A 3-day -6^{o} head-down tilt (HDT) bed rest phase

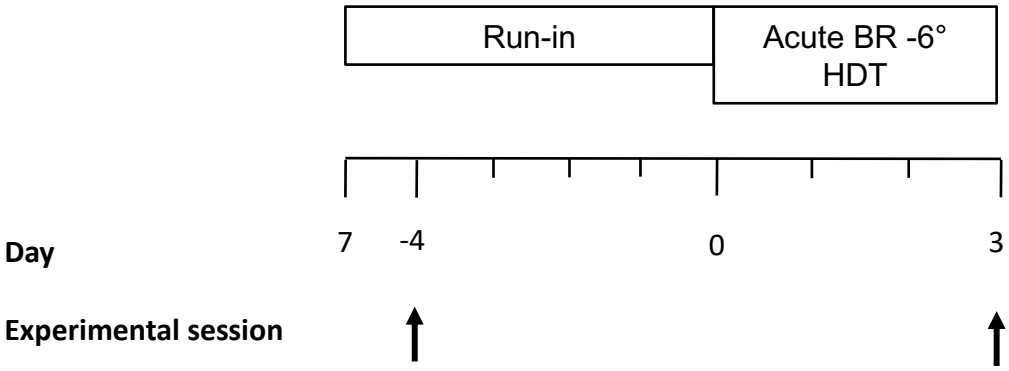

Figure 3.1. Acute bed rest schema. BR, bed rest, HDT, Head down tilt,

Experimental visits were performed 4 days prior to starting bed rest and on day 3 of bed rest (after completing 3 full days/72 hours of HDT bed rest; corresponding with day 3 on the schema). During the run-in phase, participants were provided with an accelerometer (Actiheart™, CamNtech Ltd., UK) for one week to obtain information of their pre-bed rest physical activity levels (PAL). Participants were asked to maintain normal levels of daily activity but not to engage in formal exercise during the 3 days leading up to the first experimental visit. The participants received an individually tailored, strictly controlled and standardised diet throughout all phases of the bed rest study. Individualised energy requirements were estimated using the modified Harris–Benedict resting metabolic rate equation, revised by Mifflin:

Males BMR = 10x weight (kg) + 6.25 x height (cm) – 5x age (years) + 5

This was subsequently multiplied by a physical activity level factor (PAL) of 1.4 for the run-in and of 1.2 for the bed rest phase (Roza and Shizgal 1984). Macronutrient composition (expressed as a percentage of total dietary energy

intake) was set at 55% carbohydrates, 30% fat and 15% protein. The intake of sodium was targeted to be <3,500 mg per day. During the study, participants were not allowed to eat any foods outside of the provided menu and alcohol and caffeine-containing beverages were disallowed but water was provided *ad libitum*. Adherence to the diet during the run-in phase was recorded in a food diary completed by each participant. The pre bed rest experimental visit was performed on day -4 prior to bed rest and a DEXA scan (GE Healthcare, Buckinghamshire, UK) was performed on the morning of day -4. After completing 3 full days (72-hours) of HDT bed rest (corresponding with day 3 on the schema), after an overnight fast, participants underwent the second experimental visit. After this, gradual, supervised return to 'upright' in the bed was carried out, with continuous cardiovascular monitoring to avoid postural hypotension. Participants remained in bed but were allowed to sit in the upright position until the morning of day 4 (after 96 hours). A D-dimer blood test was taken at the end of the study as a safety precaution to rule out a deep vein thrombosis (DVT) formation during bed rest.

3.3.2 Chronic bed rest study

3.3.2.1 Recruitment

Twenty healthy male participants underwent 60 days of 6^{o} HDT bed rest as part of a long-term bed rest study at the Institute of Space Medicine and Physiology (MEDES) facility in Toulouse, France. Inclusion and exclusion criteria were standardised by the European Space Agency for bed rest studies and were the same as for the acute bed rest study (see General Methods). The participants

were recruited by the MEDES team in France via the MEDES website in addition to direct mail and via media advertisements. Interested participants could get further information on conditions for application by calling MEDES through a dedicated line, through a local server and on the MEDES website. An initial screening to ensure they met inclusion/exclusion criteria was performed via telephone, and if deemed eligible a further telephone interview was conducted by a trained physician. Participants were given a minimum of one week to consider their participation.

3.3.2.2 Screening

Participants were then asked to attend a medical and psychological screening involving questionnaires and interviews. At the end of this selection process, the participants who passed the medical screening successfully and who were deemed to be able to cope with the study conditions were enrolled into the study. Participants were divided into two “campaigns”, ten participants undertaking bed rest between September and October 2017 and ten participants undertaking bed rest between November and December 2017. For each campaign, more than 300 people applied. For the first campaign, 35 were medically screened; 18 participated in the psychological interview and 14 participants passed the screening process successfully, of which 10 were enrolled into the first campaign of the study and 4 were backups. For the second campaign, 29 were medically screened; 19 participated in the psychological interview and 15 participants passed the screening process successfully of which 10 were enrolled into the second campaign of the study and 5 were backups. The chronic bed rest study was approved by the Toulouse ethics

committee of the Rangueil University Hospital (Comite´ de Protection des Personnes Sud-Ouest outre-Mer I, France) in accordance with the *Declaration of Helsinki* and the French Health Authorities.

3.3.2.3 Protocol

The chronic bed rest study protocol is shown in Figure 3.2 and consisted of:

- A 2-week run-in phase where baseline data (BDC) were collected within the MEDES facility,
- A 60-day -6° HDT bed rest phase.

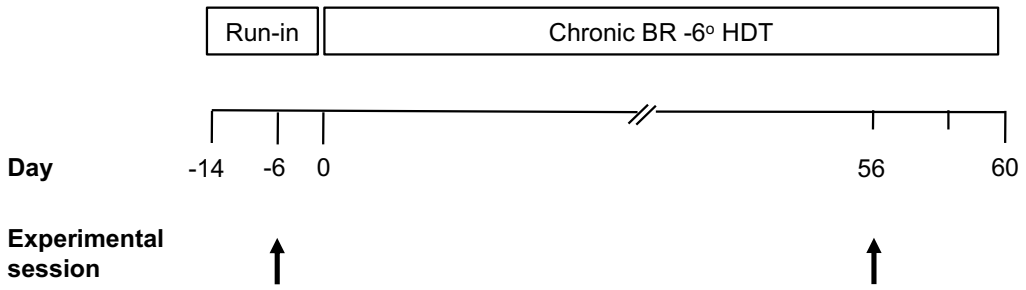

Figure 3.2. Chronic bed rest study schema. BR = bed rest HDT = head down tilt.

Experimental visits were performed 6 days prior to starting bed rest and on day 56 of bed rest. The habitual activity of enrolled participants was objectively measured at home prior to the run-in phase over a period of 10 consecutive days using an accelerometer (Actigraph 3GTX, Pensacola, USA) worn on the hip throughout the day. From the accelerometry-derived physical activity energy expenditure, an individualised activity programme during the 2 week

run-in phase at the MEDES facility was designed for each participant to prevent deconditioning over this time, with approximately 30% of activity energy expenditure being expended during structured exercise sessions (treadmill running or cycling on an ergometer cycle) and the remaining 70% reached by walking at least 8,000 steps in the MEDES facility, measured by an activity monitor worn on the wrist (Polar Loop, Kempele, Finland). One person was responsible for periodically checking the values and indicating to each volunteer if they should continue, increase or decrease his walking time.

Diet was strictly monitored and controlled throughout the entire investigation period during all phases. PAL, defined as the ratio between daily total energy expenditure (TEE) and resting metabolic rate (RMR) was estimated from accelerometry data for each participant collected prior to the run-in phase. RMR was measured for each participant on BDC -14. From the habitual PAL value and the measured RMR physical activity energy expenditure was estimated for each subject. Participants received three principal meals (breakfast, lunch and dinner) and 1 snack per day. Meals were prepared by in-house kitchen staff trained in preparing meals of set nutritional requirements to achieve energy intake with 55% carbohydrate, 30% fat and 15% protein, supervised by a dietician. Dietary intakes were quantified by measuring the weight of each dish before and after each meal and by calculating the intakes for each nutrient. Participants had to finish their tray of food; if they did not, the leftovers were weighed to record the ingested quantity. DEXA scans (Hologic, QDR 4500 C, Massachusetts, USA) were performed throughout the study on days -14 and -2 before bed rest and days 4, 25, 39 and 58 of bed rest to detect

changes in body fat mass and allow small adjustments in their diet in order to achieve energy balance. Fluid balance was strictly monitored, with each participant assigned their own water bottle and urine bottle. This longer-term bed rest study was a European Space Agency initiative designed as a double-blind, randomised, controlled trial where half of the participants received a daily oral antioxidant/anti-inflammatory supplement (741 mg of polyphenols, 138 mg of vitamin E, 80 µg of selenium, and 2.1 g of omega-3 fatty acids) and the other half received a placebo (constituents of the cocktail are shown in Appendix 2, **Section 7.9**). There were no differences between intervention groups in any of the physiological phenotype end-point measurements reported in this study, nor when comparing muscle metabolites and protein expression levels. Previous publications have also demonstrated no effect of the cocktail on muscle deconditioning (Arc-Chagnaud et al. 2020). Data showing whole-body glucose disposal in the placebo group alone, demonstrating no difference in findings is presented in Appendix 3 (**Section 7.10**). Therefore, the groups were combined given the lack of impact on end-point measurements.

Bed rest phase

During both bed rest studies, for simulation of the physiological effects of microgravity, the bed was maintained in a -6° head down tilt position. During bed rest, participants remained in bed for 24-hours a day. All activities of daily living such as hygienic procedures, eating, reading and toileting (using bedpans and urine bottles) took place whilst maintaining the head down position for the duration of the study. Participants were allowed to move from side to side (from

supine to ventral or lateral positions) but were not allowed to sit up or stand at any time. The use of one small size flat pillow was allowed as long as the shoulders were still touching the mattress. Entertainment (books, newspaper, magazines, radio, television, DVD, etc.) and social engagement with staff were provided to participants during the bed rest period. Participants kept a strict day-night cycle; they were woken at 07:00 and lights were switched off at 23:00. In the acute bed rest study, qualified nurses and healthcare technicians were present in the DGHPU, and available throughout the day and night, to attend to the participants in order to support their daily living requirements and also to ensure adherence to the study rules. During daytime hours (08:00 – 17:00), doctor cover was on site. Out of hours, a doctor was available over the telephone and able to be at the laboratory within thirty minutes. Emergency care resources were available in the bed rest facility. In the chronic bed rest study medical and nursing staff were on site 24 hours per day.

3.3.3 Experimental visits

The protocol for the experimental visits is outlined in Figure 3.3. On each experimental day, participants were given a standardised meal the evening before and then fasted from midnight. Participants in the chronic bed rest study underwent the experimental visit on the same day as another participant (their room partner) staggered by an interval of approximately one hour. On the morning of each experimental visit, with participants in the fasted state, a muscle biopsy sample was obtained from the *vastus lateralis* with a second biopsy taken at 180 minutes of the hyperinsulinaemic euglycaemic clamp (with the insulin infusion maintained until after the biopsy had been taken). Muscle

biopsies were obtained using a Bergström needle under sterile conditions, after prior injection of local anaesthetic (Bergstrom 1975). Two passes through the same entry point were made on each occasion, at a right angle to the belly of the *vastus lateralis* muscle, to harvest 100-300 mg of muscle tissue. The first pass was immediately snap frozen in liquid nitrogen, with a portion of muscle from the second pass processed for histochemical analysis. In short, this latter sample was orientated and embedded in OCT mounting medium (361603E, VWR Chemical), then frozen in cooled isopentane (Fisher Scientific, Loughborough, UK) to prevent the formation of ice crystals. The remainder of the wet muscle tissue from the second pass was frozen in liquid nitrogen. These muscle samples were subsequently analysed to determine muscle metabolites, IMCL content, and proteins and gene transcripts.

Following this, and after a period of quiet rest (approximately 45 minutes), ventilated-hood indirect calorimetry was performed to estimate whole-body substrate oxidation using a Quark RMR system (COSMED, Bicester, UK) for the acute bed rest study and a GEM calorimeter (GEMNutrition Ltd., Cheshire, UK) for the chronic bed rest study. Oxygen consumption and carbon dioxide production was measured over approximately 15 minutes before and during the steady-state period of each insulin clamp, with collection period adjusted to ensure at least 10 minutes of stable readings. Values were subsequently standardised to DEXA-determined lean body mass from pre bed rest (for both studies) and day 58 (for chronic bed rest study) measurements and non-protein substrate oxidation rates derived using the equations of Peronnet and Massicotte (Peronnet and Massicotte 1991). After

calorimetry measures had been completed, participants had an anterograde cannula inserted into an antecubital fossa vein under local anaesthesia for simultaneous infusion of insulin (Actrapid; Novo Nordisk, Bagsvaerd, Denmark) and 20% glucose (Baxter Healthcare, Norfolk, UK). Another cannula was inserted retrograde into a superficial vein on the dorsal surface of the non-dominant hand. The cannulated hand was placed into a hand-warming unit (air temperature 50-55°C) to arterialise the venous drainage of the hand (Gallen and Macdonald 1990), and a slow-running 0.9% saline drip (Baxter Healthcare, Norfolk, UK) was used to keep the cannula patent for repeated blood sampling. Thereafter, a 3 hour hyperinsulinaemic euglycaemic clamp was performed (DeFronzo, Tobin, and Andres 1979), with insulin infused into the antecubital vein at a rate of 60 mU/m^2/min. Arterialised-venous whole blood glucose concentration was measured every 5 min and maintained at 4.5 mmol/l by a variable rate infusion of 20% glucose (Baxter Healthcare, Norfolk, UK). Arterialised-venous blood samples were taken at baseline and every 15 minutes during the final hour of the insulin clamp for the measurement of insulin, TAGs, and NEFAs. Once the second biopsy was completed, the insulin infusion was stopped, and participants provided with a high carbohydrate meal. The glucose infusion was gradually reduced as glucose from the gut appeared in the blood. Once the participants' blood glucose had been stable for 30 minutes without the infusion, all lines were removed.

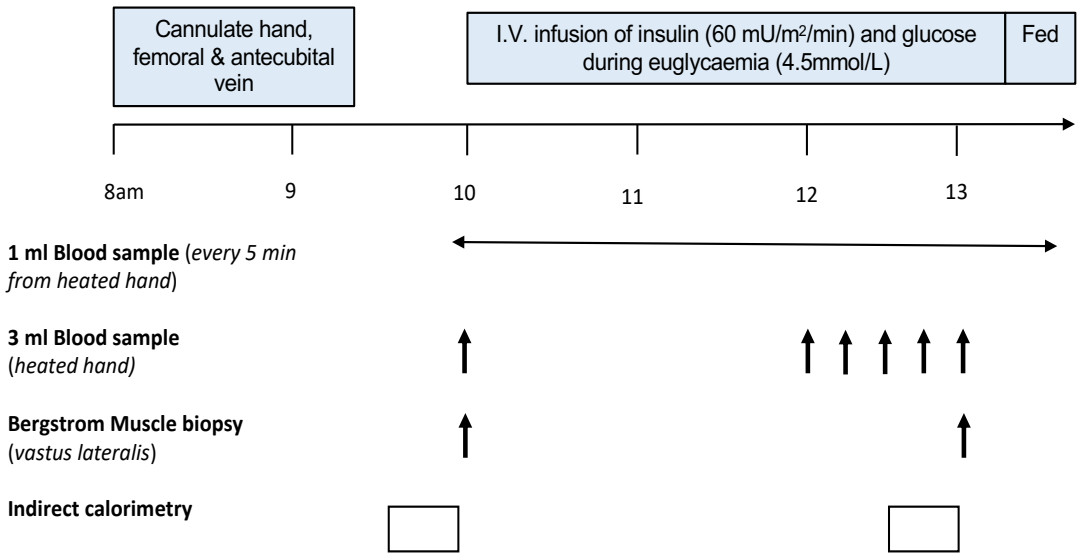

Figure 3.3. Experimental day schema. I.V. = intravenous.

3.3.4 Sample analyses

3.3.4.1 Whole-body glucose disposal

Whole blood collected during the insulin clamp was immediately analysed for glucose concentration using the glucose oxidase method (YSI 2300; Yellow Springs Inc, Ohio, USA). Whole-body glucose disposal was subsequently calculated according to standard methods (DeFronzo, Tobin, and Andres 1979) and standardised to pre bed rest DEXA-determined lean body mass. 'Steady state' glucose disposal was determined between minutes 135-165 of the clamp (DeFronzo, Tobin, and Andres 1979). Results have been expressed standardised to lean body mass using DEXA, as whole-body muscle volume on MRI did not change during the acute bed rest study, and a repeat DEXA scan after bed rest could not be justified within the UK X-ray regulations due to any changes after 3 days BR being too small to be detectable using DEXA.

Results did not change when glucose disposal was expressed standardised to body mass.

3.3.4.2 Blood analyses

Blood sample analysis is described in detail in Chapter 2, **Section 2.8**. Whole blood was collected for analysis of serum TAGs, serum insulin and plasma NEFA. Blood for determination of serum variables was collected into a microtube with coagulation activator (Sarstedt, Nümbrecht, Germany) and left to clot for at least 15 minutes before being centrifuged (15,000 G for 2 minutes). Serum was aliquoted into 2 cryovials and frozen at -80°C. To a lithium heparin microtube (Sarstedt, Nümbrecht, Germany) was added 7.5µl of ethylene glycol tetraacetic acid (EGTA)-Glutathione and 10 µl of Tetrahydrolipostatin (THL) before the addition of 1.3 ml whole blood. This was immediately centrifuged after gentle inversion, with plasma removed from the cell pellet and frozen at -80°C until analysis. Serum insulin concentration was measured using a solid-phase ^{125}I human-specific radioimmunoassay (Merck Millipore, Billerica, MA, USA). Plasma NEFA was analysed by the ACS-ACOD Method (Wako Diagnostics, Richmond, VA, USA) and serum TAGs were analysed using enzymic photometric methods (ABX Pentra 400, Horiba Medical, Montpellier, France).

3.3.4.3 IMCL quantification

Cross-sectional 14 µm thick vastus lateralis cryosections were cut consecutively at -20°C, transferred to SuperFrost Plus adhesion microscope

slides (Fisher Scientific, Loughborough, UK) and fixed by immersion into cold 2% Zamboni fixative (Newcomer Supply, Middleton, WI, USA), supplemented with 0.1% glutaraldehyde, for 1 hour. Sections were then washed with PBS and incubated for 30 minutes with 20 µg/mL Bodipy-493/503 (Fisher Scientific, Paisley, UK). Sections were washed again in PBS and coverslips were mounted with Vectashield mounting medium (H-100; Fisher Scientific, Loughborough, UK). Stained sections were imaged right after mounting with a Zeiss LSM 700 confocal microscope (Zeiss International, Jena, Germany), through a 20×/0.8 M27 Plan-Apochromat objective lens. The 488 nm argon laser line was used to excite Bodipy-493/503 and pinhole was maintained at 0.96 AU. The acquired images comprised z-stack tiles stitched together, with five z-planes 910.54 nm apart in z from the centre of the sections. These images were used to generate maximum projections for the quantification of LD count, LD size and IMCL content using the Fiji software package(Schindelin et al. 2012). In brief, ROI manager, combined with particle analysis, was used to quantify the IMCL threshold in all maximal projections.

3.3.4.4 Muscle metabolites

An aliquot of snap frozen muscle biopsy tissue was freeze dried and used to determine muscle substrates and metabolites: glycogen, lactate, acetylcarnitine and long chain acylcarnitine which were measured using methods previously described (Constantin-Teodosiu et al. 2019; Cederblad et al. 1990). In short, muscle tissue was freeze-dried for 24 hours, removed of visible blood and connective tissue and powdered. Metabolites were extracted

using 0.5 mmol/l perchloric acid and neutralised using $KHCO_3$ following centrifugation. Tissue lactate and acetylcarnitine were measured in the neutralised extract using spectrophotometric and radioisotopic enzymatic assays. Additionally, long-chain acylcarnitines were extracted from the acid-insoluble tissue pellet and determined as previously described (Stephens et al. 2006). A separate aliquot of freeze-dried muscle powder was extracted using 0.1 mol/l NaOH for determination of glycogen content (Harris, Hultman, and Nordesjo 1974).

3.3.4.5 Total RNA extraction and targeted muscle mRNA expression measurements

Total RNA was extracted from frozen muscle biopsies according to a method previously described (Constantin et al. 2013). Multiple mRNA expression measurements [191 targets, (Chapter 2, **Section 2.9.5**, Table 2.1) were made according to the manufacturer's instructions using 100 ng of cDNA obtained from total mRNA isolated from *vastus lateralis* muscle from all subjects in each group using Applied Biosystems 384-well microfluidics TaqMan array cards (Thermo Fisher Scientific Ltd, Loughborough, UK). Data were further analysed using Applied Biosystems RQ Manager software (Thermo Fisher Scientific Ltd., Loughborough, UK) where the threshold level was normalised across all plates before Ct values were calculated for each gene target and sample. Relative quantification of mRNAs of interest was measured using the $2^{-\Delta\Delta Ct}$ method with hydroxymethylbilane synthase (HMBS) as the endogenous control, with the mean of the baseline sample used as the calibrator. To associate a biological

function to the identified probe sets, Ct values were uploaded to IPA software (Redwood City, CA, USA) for pathway analysis of gene expression data.

3.3.4.6 Protein Expression levels of pyruvate kinase 2 and 4 and pyruvate dehydrogenase phosphatase 1.

The protein content of PDK4, PDK2 and PDP1 was analysed in the total muscle protein homogenates by Western blotting (Constantin et al. 2007).

3.3.5 Statistical analysis

All data were coded and analysed using SPSS version 24.0 (Statistical Package for the Social Sciences, Chicago, IL) or GraphPad Prism (version 7; Graphpad Software Inc, USA). Two-tailed paired t-tests were used to analyse differences in steady state whole-body glucose disposal between pre and post bed rest. A two-way analysis of variance (ANOVA) for repeated measures was performed to detect any main effects of visit (Pre BR and Post BR) and time (Pre clamp and During clamp) on outcome measures including substrate oxidation. Post-hoc analysis was performed using Bonferroni post-hoc test. Student's t test (or Willcoxin tests where data was nonparametric) was used to compare variables measured at one time point, between visits e.g., fasting blood glucose. Analysis of mRNA abundance by IPA is shown in Chapter 2, **Section 2.9.5** .

All data were initially checked for normality of distribution (using Shapiro-Wilks test). Mauchly's sphericity test was used to assess whether the variance

in the differences in between the pairs being compared were equal. Where Mauchly's W was <0.05, the Geisser-Greenhouse correction was used to calculate individual variance between the pairs being compared. All data are presented as mean ± SEM. Statistical significance was assumed where $p<0.05$.

Sample size

The repeat assessment coefficient of variation for the hyperinsulinaemic euglycaemic clamp technique within the DGHPU is 10%. Pilot studies by my research group have demonstrated a 30% reduction in GD over 72 hours of forearm immobilisation. Thus, it was calculated such an effect would be measurable in 8 subjects with a power of 80% at 5% significance level on a paired t-test basis.

3.4 Results

3.4.1 Participant demographics

Participant demographics for both bed rest experiments are displayed in Table 3.1. Participants in the acute and chronic bed rest studies were matched for BMI and were all in the healthy range (18.5 - 24.9 kg/m^2). Chronic bed rest participants were on average 10 years older than acute bed rest participants and had a greater fat mass (19.2 ± 0.9 vs 10.9 ± 3.8 kg, $p<0.001$) but there were no differences in lean mass (53.1 ± 1.3 vs 56.6 ± 2.1 kg) determined using DEXA. Age and fat mass were different between participants in the acute and chronic bed rest studies. Age was not correlated with glucose disposal at baseline ($R=0.05$, $p=0.40$), and as expected given they were young healthy volunteers, did not add to the predictive power of the multiple regression model,

so was discarded by the SPSS model. Fat mass was negatively associated with glucose disposal in the insulin clamp performed at baseline when data from both studies were combined ($R= -0.537$; $p<0.01$). Importantly however, the change in fat mass across the chronic bed rest period contributed <0.01% of the variability in the change in glucose disposal. Additionally, when study group (chronic or acute bedrest) was added into the regression model, it was not a predictor of the glucose disposal pre bed-rest. Finally, regression analysis revealed there was no association between any of the above variables and rates of carbohydrate or fat oxidation. There is therefore no robust evidence to support the view that demographic difference between the volunteer cohorts were responsible for the changes in glucose disposal and fuel utilisation observed in acute and chronic bed-rest. Indeed, the groups were well matched for lean body mass; a key determinant of glucose disposal (baseline steady state whole-body glucose disposal for the acute study [10.2 $\pm$ 0.4 mg/kg LBM/min] vs chronic study [11.5 $\pm$ 0.7 mg/kg LBM/min].

All but one (Ecuadorian national) participant in the chronic bed rest experiment were French nationals, whilst the acute bed rest experiment included individuals of 4 different nationalities (British, Belgian, Swedish and Malaysian). Participants in both studies were habitually physically active. Prior to the bed rest intervention the acute bed rest participants had an average daily physical activity level measured using an Actiheart as 1.5 ± 0.06 which approximately equates to between 9,000 and 10,000 steps per day (Ohkawara et al. 2011). Chronic bed rest participants accrued an average of 9562 ± 2469

steps/day in the two weeks prior to bed rest. Significant muscle mass losses were noted after bed rest in the chronic bed rest participants (Figure 3.4).

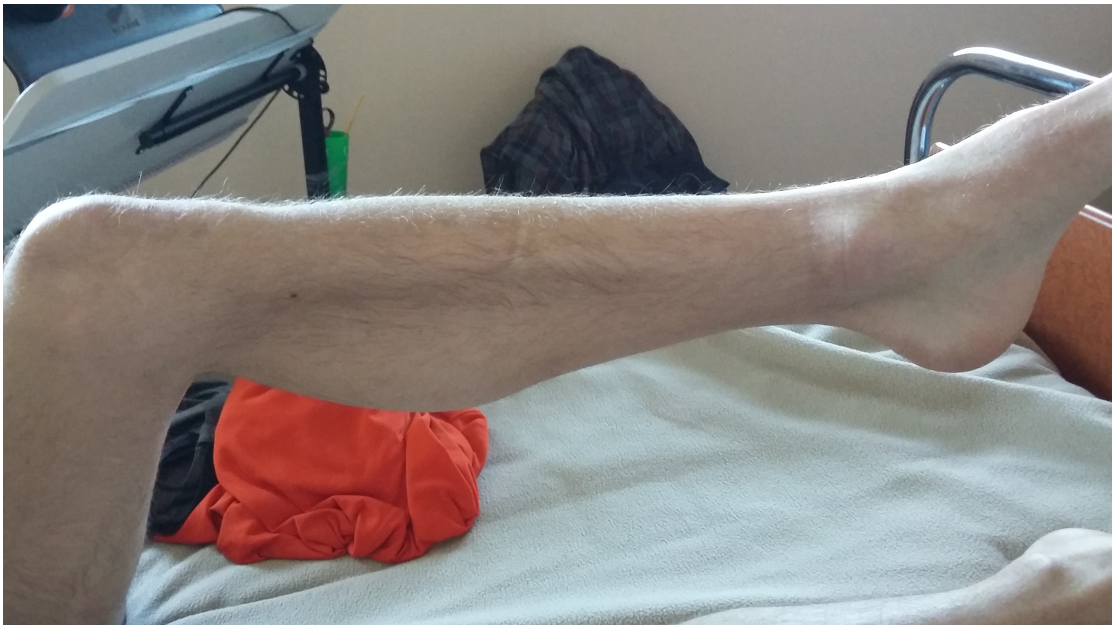

Figure 3.4. Lower leg of one of the chronic bed rest participants after 56 days of bed rest, demonstrating significant muscle atrophy of the calf.

*Table 3.1. Baseline characteristics of participants. ** p<0.01, p<0.001 compared with Acute bed rest, †† p<0.01 compared with pre clamp, $ p<0.05 compared with corresponding time-point pre bed rest. BMI = body mass index, DEXA = dual energy x-ray absorptiometry. Data are mean ± SEM.*

Parameter	**Acute Bed Rest (n = 10)**		**Chronic Bed Rest (n = 20)**	
	Pre bed rest	Post bed rest	Pre bed rest	Post bed rest
Age (years)	24 ± 1		34 ± 8**	
BMI (kg/m^2)	22.7 ± 0.6	22.7 ± 0.6	23.7 ± 1.5	23.4 ± 0.4
Body mass (kg)	70.7 ± 3.2	70.6 ± 3.2	73.5 ± 6.1	72.6 ± 1.6
Lean mass (DEXA) (kg and % body mass)	56.6 ± 2.1 (80%)	Not recorded	53.1 ± 1.3 (72%)	50.2 ± 1.2 (69%)
Fat mass (DEXA) (kg and % body mass)	10.9 ± 3.8 (15%)	Not recorded	19.2 ± 0.9*** (26%)	20.4 ± 0.9 (28%)
Resting energy expenditure (kJ/day) (Pre clamp)	7428 ± 396	7345 ± 261	5721 ± 143	5255 ± 121
Whole-body muscle volume (cm^3)	29370 ± 1613	29116 ± 1616	Not recorded	Not recorded

3.4.2 Energy Intake

Participants in both the acute and chronic bed rest study met the prescribed energy intake targets before and during bed rest. Prescribed and actual energy intake data per day during both bed rest experiments is shown in Table 3.2.

Table 3.2. Energy intake and macronutrient content in the acute and chronic bed rest studies. Energy Intake in kilojoules (kJ/day) and macronutrient content (g/day) prescribed and actual during acute and chronic bed rest. BR, bed rest. Data are mean ± SEM.

Parameter	**Acute bed rest**	**Chronic bed rest**
Average energy intake prescribed (kJ/day) pre bed rest	11041 ± 338	12496 ± 165
Average energy intake actual (kJ/day) pre bed rest	10960 ± 319	12300 ± 198
Difference prescribed vs actual (kJ/day) pre bed rest	-287 ± 88	-196 ± 53
Carbohydrate (g/day) pre bed rest	291 ± 14	392 ± 6
Protein (g/day) pre bed rest	83 ± 4	88 ± 2
Fat (g/day) pre bed rest	79 ± 4	104 ± 2

Average energy intake prescribed (kJ/day) during bed rest	8792 ± 275	9908 ± 146
Average energy intake actual (kJ/day) during bed rest	8950 ± 244	9793 ± 146
Difference prescribed vs actual (kJ/day) during bed rest	158 ± 23	-114 ± 19
Carbohydrate (g/day) during bed rest	250 ± 26	292 ± 4
Protein (g/day) during bed rest	73 ± 8	88 ± 2
Fat (g/day) during bed rest	68 ± 5	83 ± 1

3.4.3 Impact of Acute and Chronic bed rest on whole-body glucose uptake

Figure 3.5 shows whole-body GD standardised to kg lean-body mass (kg LBM) using DEXA in the acute and chronic bed rest studies. Using steady-state values in the period between 135-165 min of the clamp (whole blood glucose 4.49 ± 0.16 mmol/l), acute bed rest resulted in a 17% reduction in insulin-stimulated whole-body GD (11.5 ± 0.7 vs 9.6 ± 0.6 mg/kg LBM/min, $p<0.01$, $d=1.9$; Figure 3.5a), whilst chronic bed rest (whole blood glucose 4.47 ± 0.17 mmol/l), resulted in a 22% reduction in insulin-stimulated whole-body GD (10.2 ± 0.4 vs 7.9 ± 0.3 mg/kg LBM/min, $p<0.001$, $d=1.7$; Figure 3.5b). There was no

difference in the magnitude of change of glucose disposal between the acute or chronic study (p=0.83), however equivalence testing for group differences revealed a confidence interval of -0.58 to 0.70 which was out with pre-set boundaries of -0.5 to 0.5, suggesting the change in M value with bed rest was not equivalent between acute and chronic bed rest conditions.

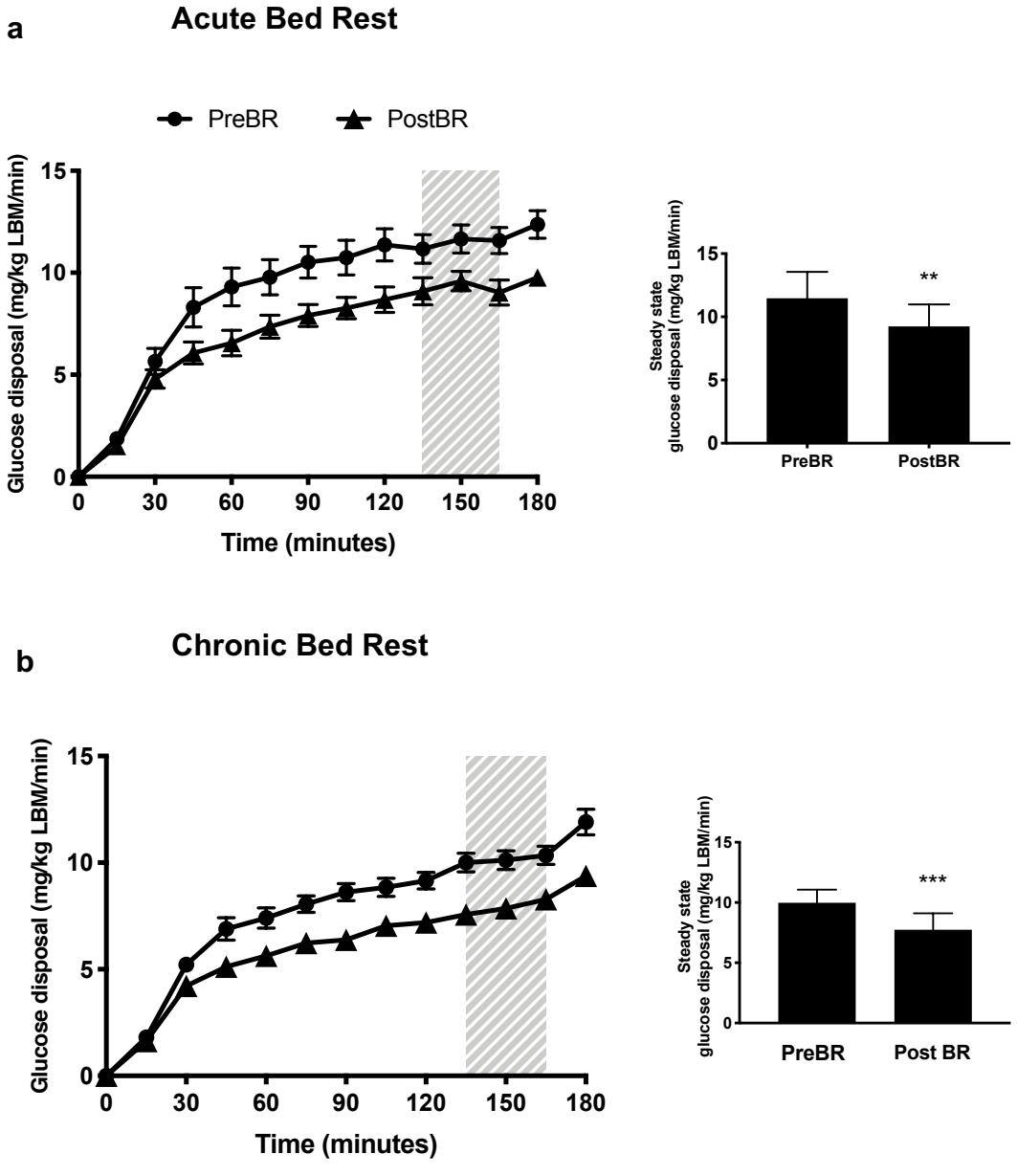

Figure 3.5. Whole-body glucose disposal during the hyperinsulinaemic euglycaemic clamp. Whole-body glucose disposal standardised to lean body mass (LBM) before bed rest (Pre BR) and after bed rest (Post BR) in a) acute bed rest (n=10), b) chronic bed rest (n=20). Hatched shading shows steady-state period with histogram depicting steady-state whole-body glucose disposal values. Data are mean ± SEM.

3.4.4 Impact of Acute and Chronic bed rest on whole-body substrate oxidation

Carbohydrate oxidation

Figure 3.6 shows the carbohydrate (a,b) and fat (c,d) oxidation rates standardised to kg LBM in acute and chronic bed rest. In acute bed rest, there was an increase in carbohydrate oxidation in response to the insulin clamp before ($p \leq 0.001$) and after bed rest ($p \leq 0.001$; Figure 3.6a), with no difference in the magnitude of response between these 2 time points. In chronic bed rest, there was also an increase in carbohydrate oxidation in response to the insulin clamp both before ($p < 0.05$) and after bed rest ($p < 0.05$; Figure 3.6b). However, compared with before bed rest, chronic bed rest resulted in a 19% blunting of the increase in insulin-stimulated carbohydrate oxidation ($p < 0.05$).

Lipid oxidation

In acute bed rest, there was a suppression in the rate of fat oxidation standardised to LBM in response to the insulin clamp before ($p \leq 0.001$) and after

bed rest (p≤0.001; Figure 3.6c), with no difference in the magnitude of response between pre and post-bed rest. In chronic bed rest, there was also a suppression of fat oxidation in response to the insulin clamp both before ($p<0.05$) and after bed rest ($p<0.05$; Figure 3.6d). However, compared with before bed rest, the insulin-mediated suppression of fat oxidation was 43% less ($p<0.05$) following chronic bed rest.

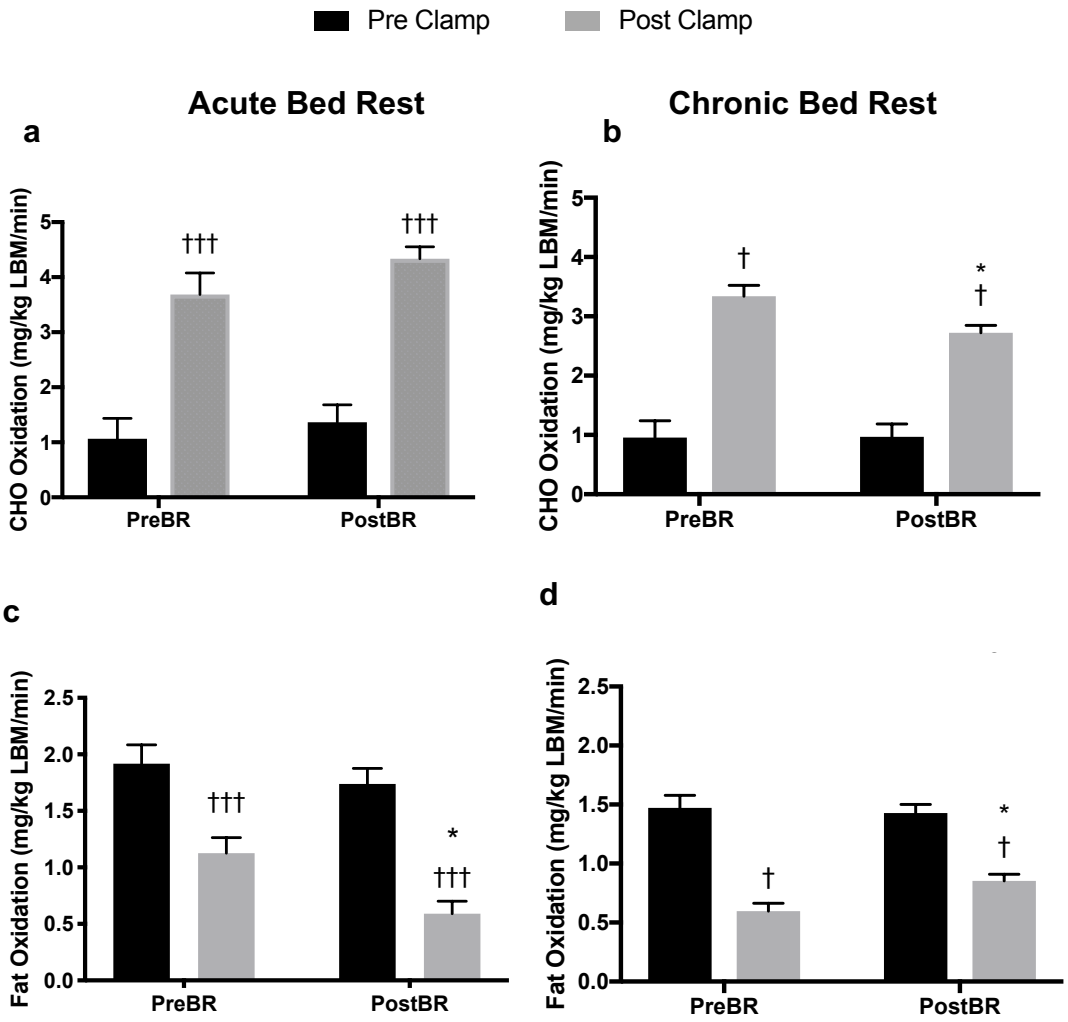

Figure 3.6. Substrate oxidation. Carbohydrate (CHO) oxidation during a) acute bed rest and b) chronic bed rest and fat oxidation during c) acute bed rest and d) chronic bed rest measured using indirect calorimetry, standardised to lean

*body mass (LBM) before (Pre BR) and after (Post BR) bed rest and before (Pre Clamp) and in the final 30 minutes (Post Clamp) of the hyperinsulinaemic euglycaemic clamp. Grey bars correspond to pre clamp values and solid colour bars correspond to post clamp values. * p<0.05 compared with corresponding time point Pre BR; † p<0.05, ††† p<0.001 compared with Pre clamp. (n=20) Values and mean ± SEM.*

3.4.5 Serum Insulin, TAGs and plasma NEFA

Table 3.3 shows the serum insulin, TAGs and plasma NEFA in the acute and chronic bed rest studies.

Serum insulin

In acute bed rest, compared with before bed rest, there were no differences in fasted insulin values after bed rest (p=0.44). There was no change in steady-state insulin after bed rest and no change over time during the clamp (p=0.35). Chronic bed rest resulted in a 25% increase in fasted insulin after bed rest (p≤0.01). There was an increase in steady-state insulin after chronic bed rest (120-180 minutes; p<0.05) but no change over time during the clamp (p=0.22).

Plasma NEFA

In acute bed rest, compared with before bed rest, there was a greater fasted NEFA concentration after bed rest (p<0.05). During the insulin clamp, there was a decrease in steady-state NEFA concentration over time (p≤0.001) but no

difference after bed rest (p=0.2). In chronic bed rest, there was no differences in fasted plasma NEFA concentration between before or after bed rest (p=0.8). There was a decrease in steady-state NEFA over time ($p<0.05$) but no differences in steady state NEFA values after bed rest compared with before bed rest (p=0.3).

Serum TAGs

In acute bed rest, compared with before bed rest, there was no difference in fasted (p=0.58) or steady-state (p=0.35) TAG after bed rest but there was a decrease in steady state TAG over time ($p<0.01$). In chronic bed rest there were no differences in fasted (p=0.51) or steady state TAG (p=0.43) after bed rest, but there was a decrease in TAG over time ($p<0.01$) and there was an effect of visit and time (p=0.045).

*Table 3.3. Serum insulin, TAG and plasma NEFA. Fasted and steady state insulin, NEFA and TAG concentrations in acute and chronic bed rest before (Pre BR) and after (Post BR) bed rest. * p<0.05, ** p<0.01 vs pre-bed rest. Values are mean +SEM.*

			Fasted	Steady state (average 120-180 minutes)
Serum insulin (mIU/L)	Acute BR	Pre BR	6.4 ± 1.7	107.4 ± 3.2
		Post BR	8.8 ± 1.6	105.8 ± 2.6
	Chronic BR	Pre BR	17.8 ± 1.7	137.8 ± 4.9
		Post BR	22.3 ± 1.5**	146.4 ± 6.2*
Plasma NEFA (mmol/L)	Acute BR	Pre BR	530 ± 40	10 ± 2
		Post BR	570 ± 60*	10 ± 1
	Chronic BR	Pre BR	430 ± 30	30 ± 2
		Post BR	440 ± 40	30 ± 3
Serum TAG (mmol/L)	Acute BR	Pre BR	0.69 ± 0.05	0.40 ± 0.04
		Post BR	0.76 ± 0.06	0.48 ± 0.03
	Chronic BR	Pre BR	0.66 ± 0.07	0.50 ± 0.06
		Post BR	0.61 ± 0.07	0.46 ± 0.06

3.4.6 Impact of acute and chronic bed rest on IMCL content

IMCL content was determined in pre clamp muscle biopsy samples. Figure 3.7 shows the LD density (a,d), LD size (b,e) and the fractional lipid area, or % IMCL (c,f) before and after acute and chronic bed rest. Acute bed rest participants had a lower mean LD size ($p<0.001$) and % IMCL ($p<0.01$) compared with chronic bed rest participants at baseline, in keeping with the greater whole-body fat mass in the chronic bed rest participants. Acute bed rest did not alter LD count ($p=0.72$), LD size ($p=0.121$) or % IMCL ($p=0.22$). Similarly, chronic bed rest, did not impact on LD count ($p=0.13$), LD size ($p=0.38$) or %IMCL ($p=0.60$). There was no impact of acute or chronic bed rest on fibre-specific IMCL parameters, although a decrease in LD count was observed after chronic bed rest ($p<0.05$; Appendix 3).

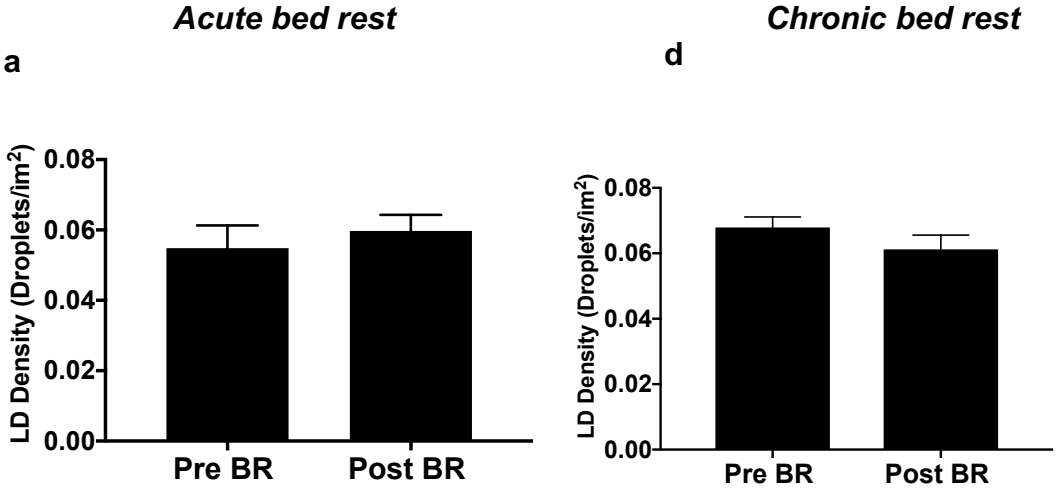

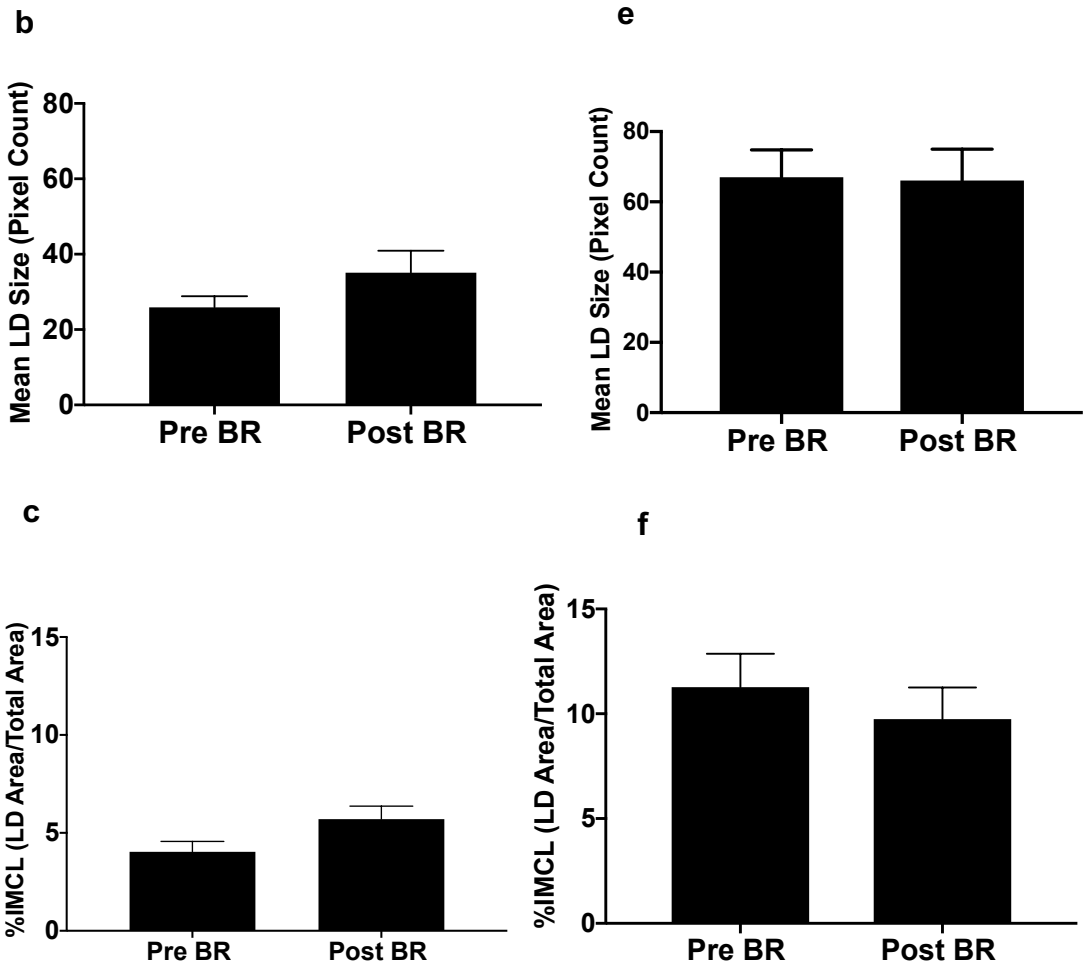

Figure 3.7. Intramyocellular lipid content. a) Lipid droplet (LD) density, b) LD size and c) the fractional lipid area, or % IMCL content of the vastus lateralis muscle tissue as a percentage of total tissue area before (Pre BR) and after (Post BR) acute bed rest and d) LD density, e) LD size and f) the % IMCL content of the muscle tissue as a percentage of total tissue area before and after chronic bed rest. All data are generated from pre clamp samples for each participant, at each time point. Values are mean ± SEM. For acute bed rest measures, n=6 pre bed rest (Pre BR) and n=7 post bed rest (Post BR) and for chronic bed rest measures n=19 for all time points.

3.4.7 Muscle substrates and metabolites

Table 3.4 shows muscle substrate and metabolite concentrations. Before acute bed rest, there was an 36% increase in muscle glycogen content during the insulin clamp ($p=0.056$, $d= -0.85$). There was no change in muscle glycogen content during the insulin clamp after bed rest ($p=0.69$). In the chronic bed rest study before bed rest, there was a 35% increase in muscle glycogen content during the insulin clamp ($p<0.01$, $d=-0.71$), which was not evident after bed rest ($p=0.42$). In the acute bed rest study, there was no change in muscle lactate content in response to the insulin clamp either before or after bed rest. In the chronic bed rest study, there was a 35% decrease in muscle lactate content in response to the insulin clamp before bed rest ($p<0.01$) and a 14% decrease after bed rest ($p<0.05$). In the acute bed rest study, there was no impact of the insulin clamp on muscle acetylcarnitine content either before or after bed rest. However, after bed rest, pre clamp muscle acetylcarnitine content was 33% lower compared with the corresponding value before bed rest ($p<0.01$). In the chronic bed rest study, the insulin clamp reduced muscle acetylcarnitine content by 67% before bed rest ($p<0.001$) and by 47% after bed rest ($p<0.05$). Furthermore, after bed rest, pre clamp muscle acetylcarnitine content was 42% lower compared with the corresponding value before bed rest ($p<0.001$). In the acute bed rest study, there was no impact of the insulin clamp on muscle long chain acyl carnitine content either before or after bed rest. In the chronic bed rest study, before bed rest, there was a 33% increase in long chain acyl carnitine content in response to the insulin clamp ($p<0.05$) which was not evident after bed rest ($p=0.20$).

*Table 3.4. Muscle substrates and metabolites. Muscle glycogen, muscle lactate, muscle acetylcarnitine and muscle long chain acylcarnitine measured before bed rest (Pre BR) and after bed rest (Post BR) and before (Pre Clamp) and in the final 30 minutes (Post Clamp) of the hyperinsulinaemic euglycaemic clamp. * p<0.05, ** p<0.01, *** p<0.001 compared with corresponding time-point Pre-BR, † p<0.05, ††p<0.01, †††p<0.001 compared with Pre-Clamp, #, p=0.056 compared with Pre-Clamp. Values are mean ± SEM.*

			Pre clamp	Post clamp
Muscle glycogen (mmol/kg dry mass)	Acute bed rest	Pre BR	428 ± 33	585 ± 72#
		Post BR	411 ± 53	387 ± 35*
	Chronic bed rest	Pre BR	314 ± 24	423 ± 29 ††
		Post BR	382 ± 22	396 ± 33
Muscle lactate (mmol/kg dry mass)	Acute bed rest	Pre BR	4.7 ± 1.1	5.5 ± 0.6
		Post BR	3.1 ± 0.5	5.1 ± 1.0
	Chronic bed rest	Pre BR	6.6 ± 0.8	3.3 ± 0.9††
		Post BR	7.3 ± 0.6	4.4 ± 0.7†
Muscle acetylcarnitine (mmol/kg dry mass)	Acute bed rest	Pre BR	3.0 ± 0.4	2.5 ± 0.2
		Post BR	2.0 ± 0.2**	2.3 ± 0.2
	Chronic bed rest	Pre BR	3.3 ± 0.4	1.1 ± 0.1†††
		Post BR	1.9 ± 0.2***	1.0 ± 0.1†
Muscle long chain	Acute bed rest	Pre BR	1042 ± 127	1042 ± 108
		Post BR	1169 ± 157	1191 ± 133

acylcarnitine (μmol/kg dry mass)	Chronic bed rest	Pre BR	543 ± 49	720 ± 67†
		Post BR	532 ± 56	644 ± 55

3.4.8 Muscle mRNA expression

Muscle mRNA expression was quantified in the pre-insulin clamp biopsies before and after bed rest. Cellular functions identified by Ingenuity Pathway Analysis (IPA) as being altered as a result of acute and chronic bed rest study are depicted in Figure 3.8. After 3 days' bed rest, 12 functions were identified as altered, the most notably affected being 'cell death and survival', 'cell morphology and cellular development', 'cellular growth and proliferation', and 'organismal injury and abnormalities' [-log (P value) ≥20] (Figure 3.8a). After 56 days' bed rest, 9 functions were identified by IPA as being significantly altered, of which 'skeletal and muscular system development and function', and 'organ morphology' had the greatest magnitude of change [-log (P value) ≥20] (Figure 3.8b).

Acute Bed Rest

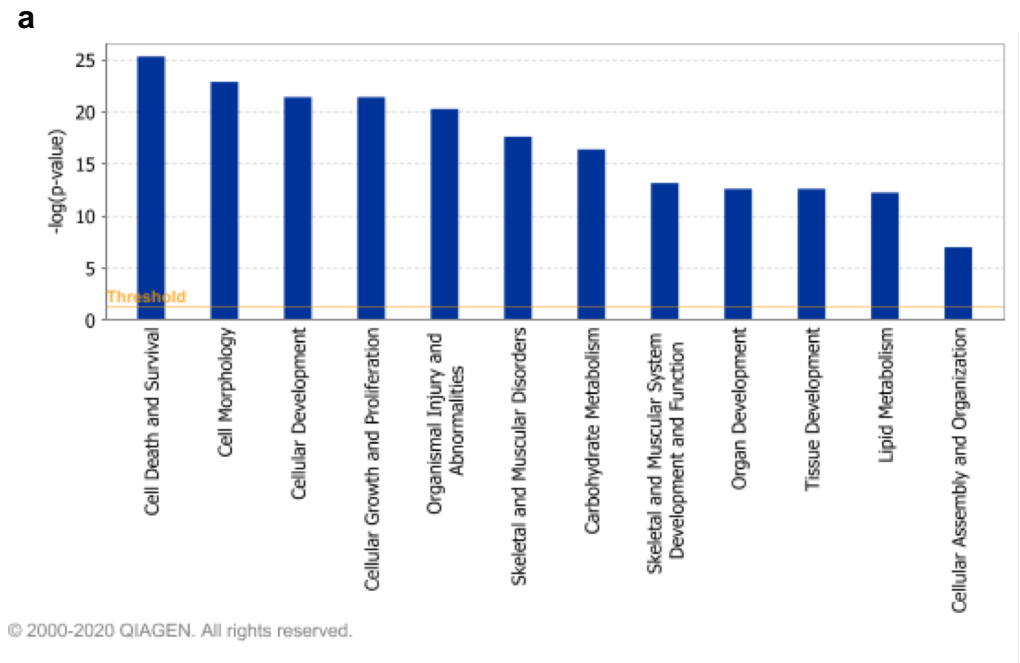

Chronic Bed Rest

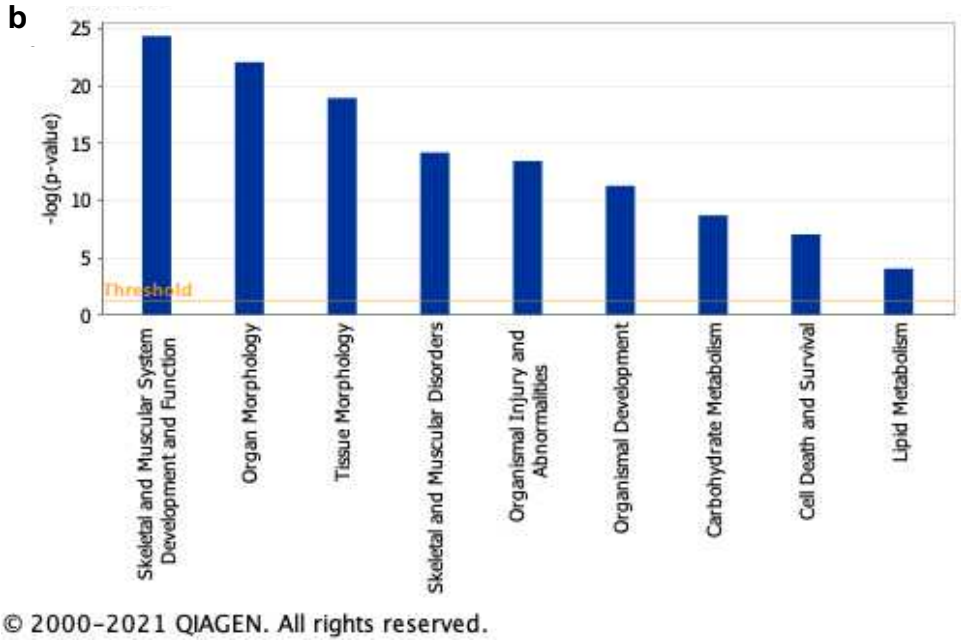

Figure 3.8. Muscle cellular functions in acute and chronic bed rest. Cellular functions identified by IPA as being altered in muscle from before to after bed rest in a) the acute bed rest study and in b) the chronic bed rest study based

on mRNA expression data generated using the low-density micro-array cards. The x-axis displays cellular functions most affected by bed rest and the y-axis displays -log of the p value. The threshold line corresponds to a p value of 0.05.

There were 7 cellular functions altered in both acute and chronic bed rest, namely 'cell death and survival', 'organismal injury and abnormalities', 'skeletal and muscular disorders', 'carbohydrate metabolism', 'skeletal and muscular system development and function', 'organ development' and 'lipid metabolism'. However, the size of the gene networks comprising these 7 altered common cellular functions was markedly greater in acute bed rest than in chronic bed rest, reflecting a more wide-ranging muscle transcriptional response in response to acute bed rest. Furthermore, several of the predicted cellular events generated by IPA based upon these mRNA responses to bed rest were distinct between acute and chronic bed rest, and often in divergent directions. For example, in the case of 'cell death and survival', 82 transcripts were either up or down regulated in response to acute bed rest and based on these collective transcriptional responses IPA predicted 'activation of cell survival' and 'cell viability' (Figure 3.9a). This is in contrast to chronic bed rest study where 7 transcripts were differentially regulated and IPA predicted an inhibition of 'necrosis', 'necrosis of muscle' and 'cell death of muscle' (Figure 3.9b).

Cell death and survival

a Acute bed rest

b Chronic bed rest

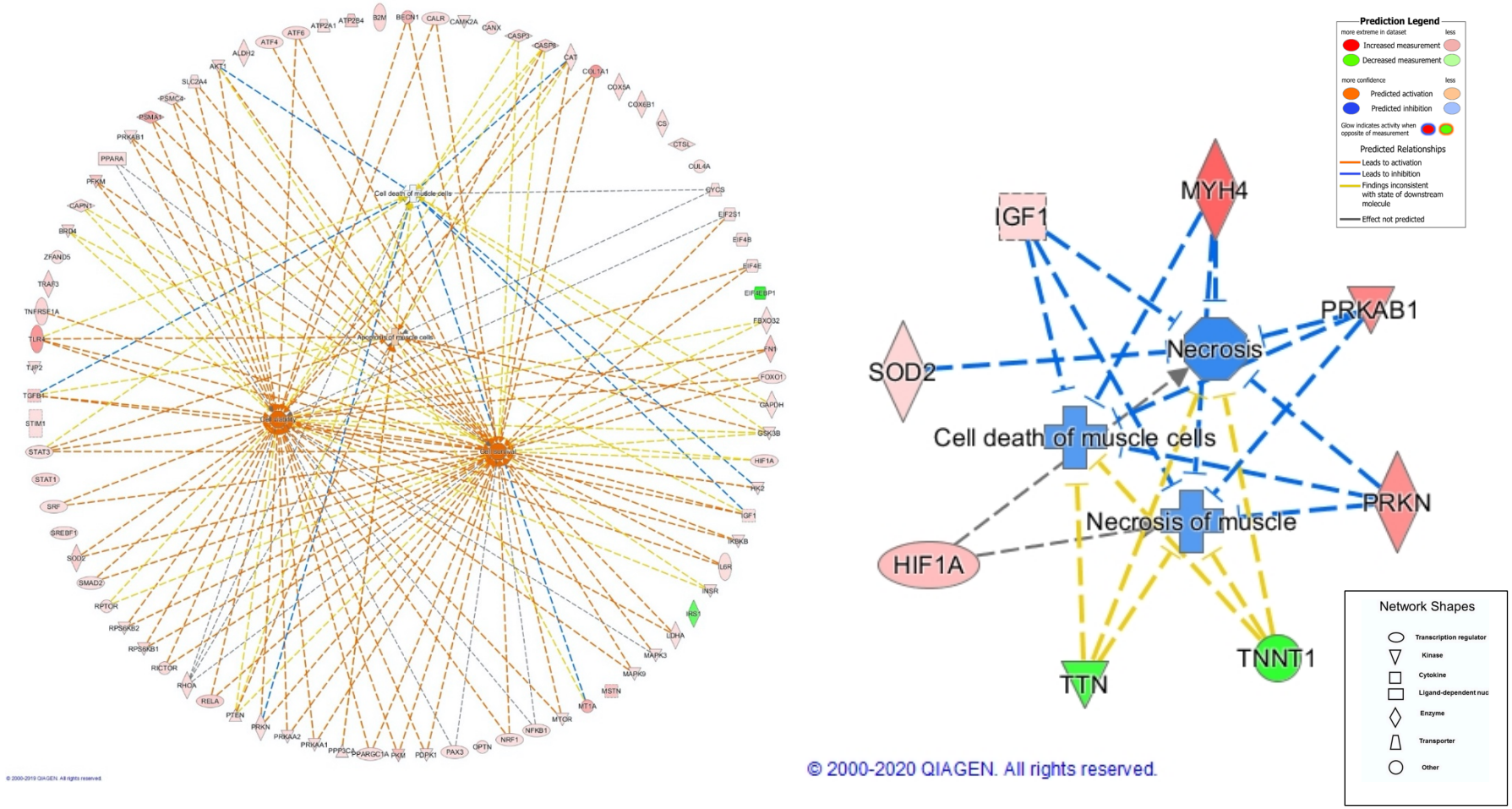

Figure 3.9. Pathway analysis for cell death and survival. Schematic highlighting the most differentially regulated muscle gene

expression (outer ring) and the cellular events predicted by Ingenuity Pathway Analysis to result from the collective changes in mRNA abundance (inner circles) associated with cell death and survival after bed rest compared with pre bed rest in a) acute bed rest and b) chronic bed rest. The associated prediction legend indicates the degree of confidence which is depicted by colour intensity.

The gene networks representing the altered cellular functions of carbohydrate and lipid metabolism are shown in Figures 3.10 and 3.11 because they are of direct relevance to the aims of the current study. In the case of carbohydrate metabolism, the size of the differentially regulated gene network was substantially greater for acute bed rest than chronic bed rest (Fig. 3.10). In acute bed rest 40 transcripts were identified as being altered in abundance relative to pre bed rest (Figure 3.10a), compared with 13 transcripts in chronic bed rest (Figure 3.10b). In acute bed rest, 39 of these transcripts were upregulated and one, Insulin Receptor Substrate 1 (IRS-1), was downregulated. Based on these collective differences, IPA predicted a comprehensive activation of a number of cellular processes including 'glycolysis', 'metabolism of carbohydrate', 'metabolism of polysaccharide', and 'synthesis of glycogen'. In chronic bed rest, of the 13 transcripts identified as being altered in abundance relative to pre bed rest, 11 were upregulated and 2 transcripts were downregulated, with a predicted activation of 'uptake of monosaccharide' and a comprehensive inhibition of 'quantity of glycogen' and 'quantity of carbohydrate'.

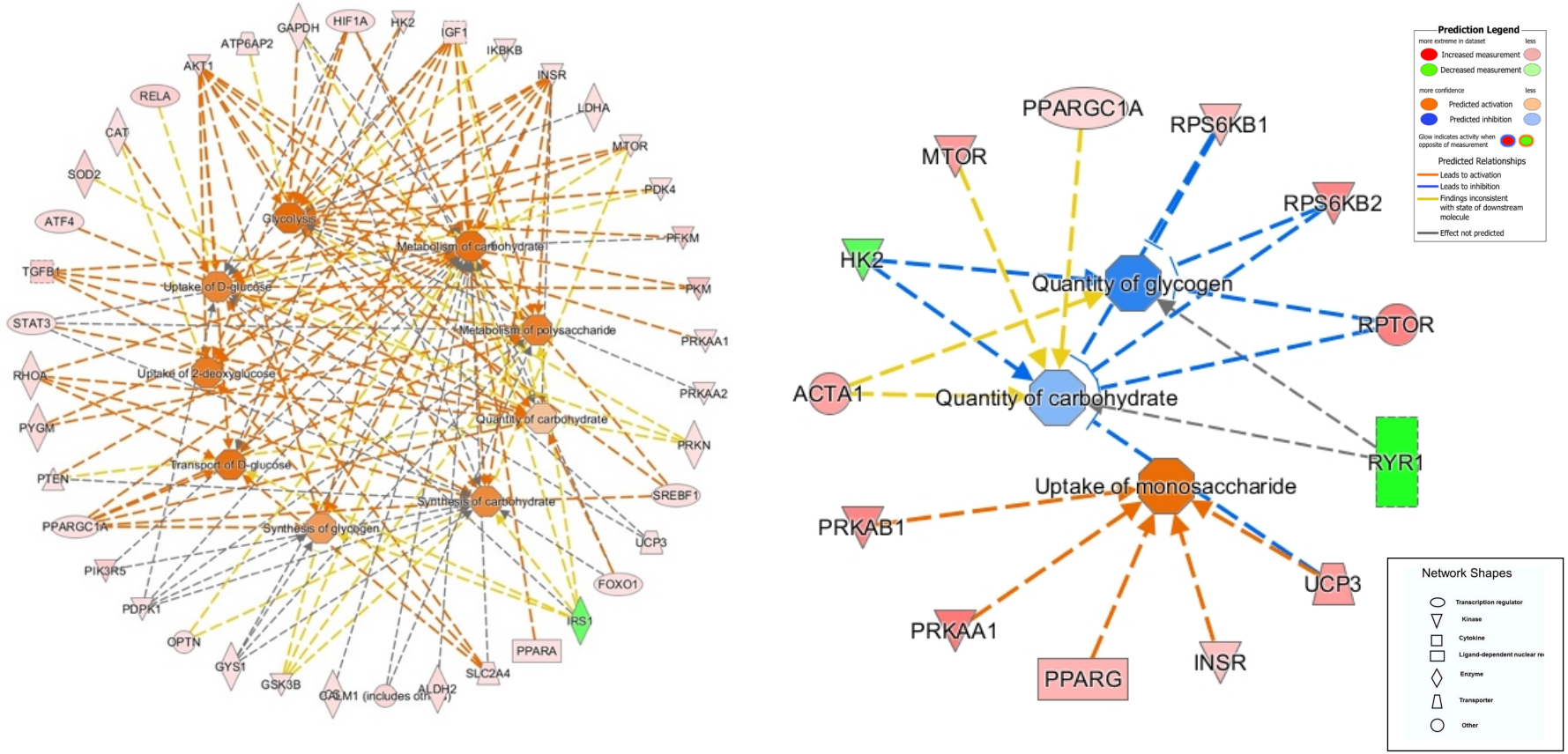

Figure 3.10. Pathway analysis for carbohydrate metabolism. Differentially regulated muscle gene expression (outer ring) and the cellular events predicted by Ingenuity Pathway Analysis to result from the collective changes in mRNA abundance (inner circles) associated with carbohydrate metabolism after bed rest compared with pre bed rest in a) acute and b) chronic bed rest.

Similarly, in the case of lipid metabolism, the size of the differentially regulated gene network was substantially greater for acute bed rest than chronic bed rest. During acute bed rest (Figure 3.11a), 44 transcripts were altered in abundance compared with 6 transcripts during chronic bed rest (Fig. 3.11b). In acute bed rest, there were 42 transcripts upregulated and 2 transcripts, IRS-1 and fatty-acid-binding protein 3 (FABP3), downregulated compared with before bed rest. Based on these collective differences, IPA predicted activation of 'fatty acid metabolism', 'synthesis of lipid', 'oxidation of lipid', 'oxidation of fatty acid', 'synthesis of fatty acid' and to a lesser extent 'concentration of lipid'. In chronic bed rest, 6 transcripts were upregulated with a predicted activation of 'oxidation of fatty acid' and to a lesser extent 'concentration of triacylglycerol'. Figures depicting the 4 remaining networks common to both acute and chronic bed rest are shown in Appendix 3 (Supplementary Figure 7.2 – 7.5).

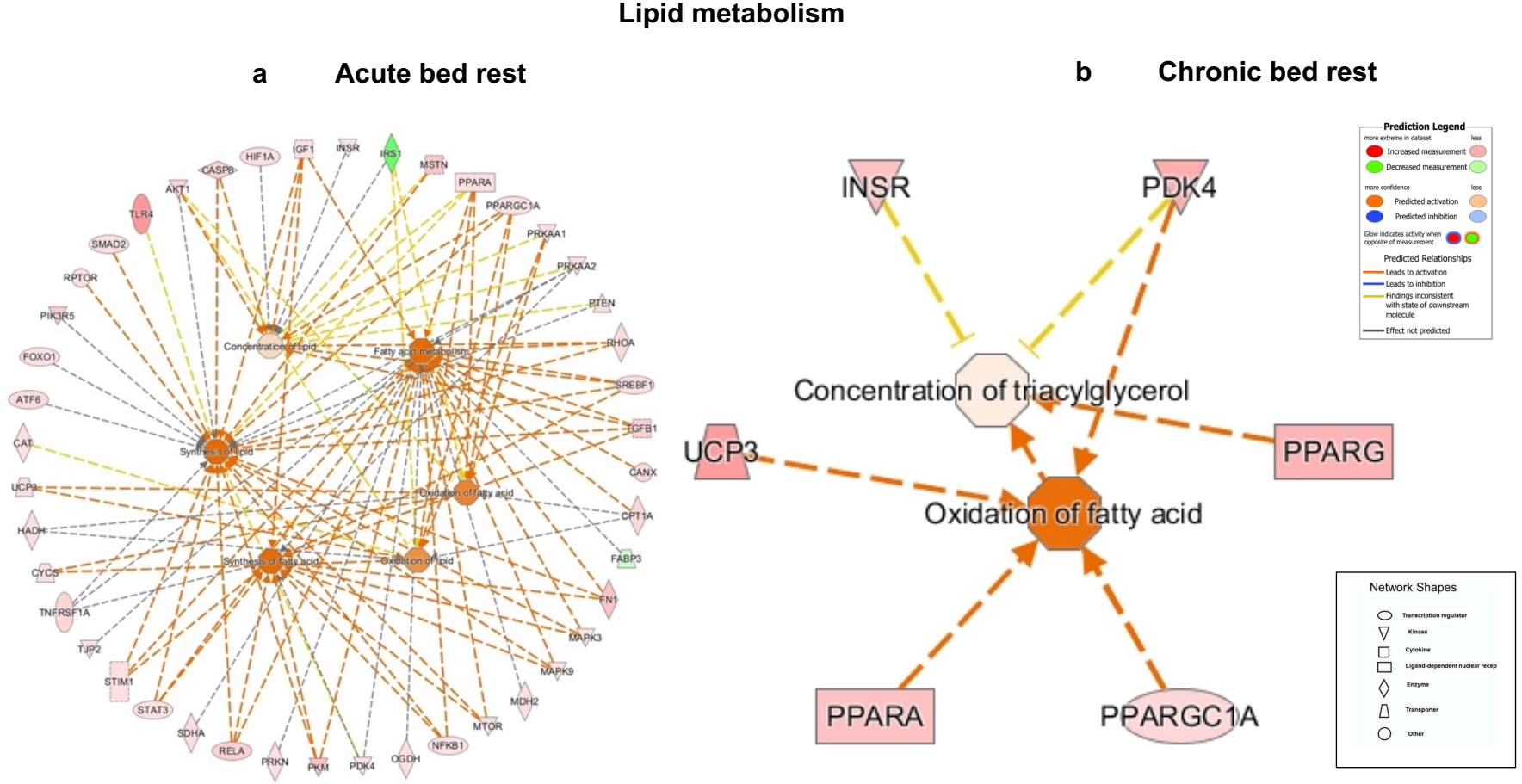

Figure 3.11. *Pathway analysis for lipid metabolism. Differentially regulated muscle gene expression (outer ring) and the cellular events predicted by Ingenuity Pathway Analysis to result from the collective changes in mRNA abundance (inner circles) associated with lipid metabolism after bed rest compared with pre bed rest in a) acute bed rest and b) chronic bed rest.*

3.4.9 Calcium activated genes

mRNA expression of targeted calcium activated genes, namely protein phosphatase 3 catalytic subunit alpha (PPP3CA), calcium/calmodulin-dependent protein kinase 2A (CAMK2A), calmodulin-1 (CALM1), calsequestrin (CASQ1), ATPase sarcoplasmic/endoplasmic reticulum Ca2+ transporting 2 (ATP2A2), ATPase sarcoplasmic/endoplasmic reticulum Ca2+ transporting (ATP2A1), calcium/calmodulin-dependent protein kinase 4 (CAMK4) and inositol 1,4,5-triphosphate receptor type 3 (ITPR3) is shown in Figure 3.12. Although a numerical increase in the expression of these calcium activated genes was seen after 3 days bed rest, relative to pre bed rest, this did not reach statistical significance. However, chronic bed rest increased mRNA expression significantly for all but one of these gene targets.

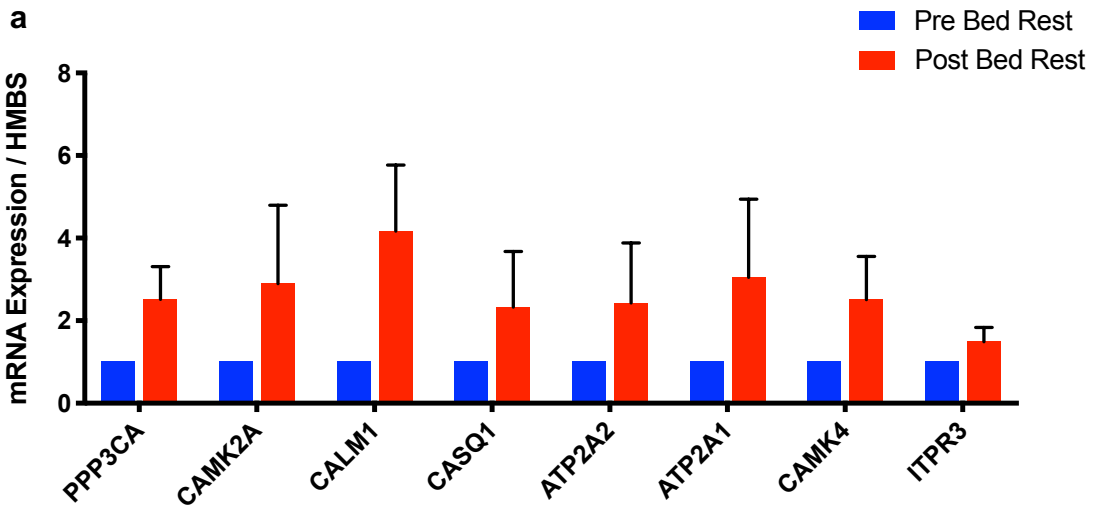

b

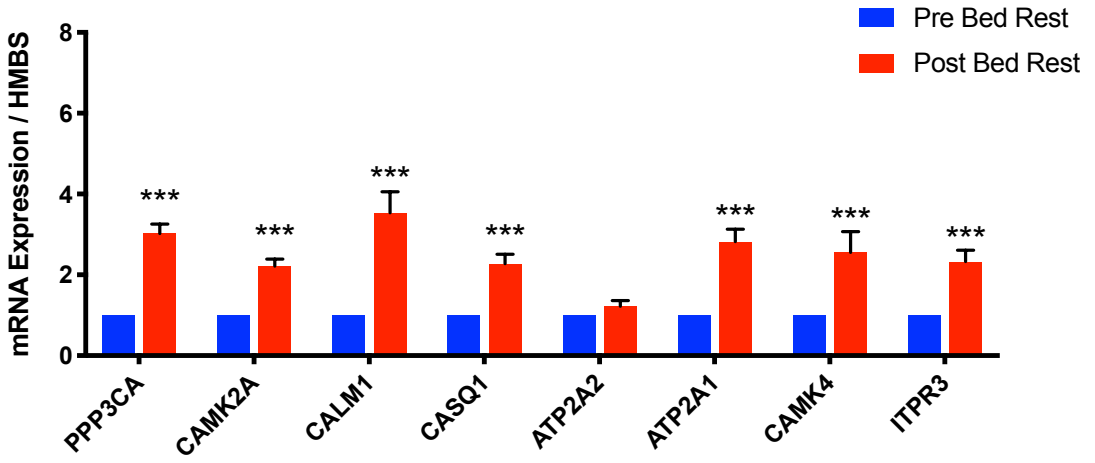

*Figure 3.12. Calcium targeted genes in muscle. Muscle PPP3CA, CAMK2A, CALM1, CASQ1, APT2A2, ATP2A1, CAMK4 and ITPR3 mRNA expression normalized to a mean of 1.0 after bed rest (Post BR) compared to before bed rest (Pre BR) in a) acute and (b) chronic bed rest in post clamp samples. *p<0.05, **p<0.01, ***p<0.001 vs Pre BR. Values are mean +SEM and represent fold change from pre bed rest which has been set at 1.*

3.4.10 Protein Expression levels of pyruvate kinase 2 and 4 and pyruvate dehydrogenase phosphatase 1.

There was no impact of acute bed rest on the pre-clamp expression levels of the target proteins pyruvate kinase 2 (PDK2) and 4 (PDK4), and pyruvate dehydrogenase phosphatase 1 (PDP1; Table 3.5). Furthermore, the insulin clamp had no impact on expression levels either before or after bed rest. Due to a limited availability of pre clamp muscle tissue in the chronic bed rest study, PDK2, PDK4 and PDP1 protein were only measured in post insulin clamp

samples. Compared with before bed rest, there was a significant increase in post clamp PDK4/Actin protein expression after bed rest ($p<0.01$). However, there was no impact of bed rest on post insulin clamp PDK2 or PDP1. Example western blots of PDK2, PDK4 and PDP1 in a) acute and b) chronic bed rest are shown in Figure 3.13.

*Table 3.5. PDK2, PDK4 and PDP1 data. Regulatory enzymes PDK4/Actin relative arbitrary units (RAU), PDK2/Actin (RAU) and PDP1/Actin (RAU) in acute and chronic bed rest measured on pre and post clamp samples before (Pre BR) and after (Post BR) bed rest. Due to a lack of pre clamp muscle tissue in the chronic bed rest study analyses were only performed on post clamp samples. Na, not measured. **p<0.01 compared with Pre BR. Values are mean ± SEM.*

			Pre clamp	Post clamp
PDK2/Actin (RAU)	Acute bed rest	Pre BR	1.0 ± 0.1	0.93 ± 0.04
		Post BR	0.8 ± 0.05	0.87 ± 0.05
	Chronic bed rest	Pre BR	na	1.0 ± 0.1
		Post BR	na	0.89 ± 0.1
PDK4/Actin (RAU)	Acute bed rest	Pre BR	1.0 ± 0.08	1.0 ± 0.1
		Post BR	1.3 ± 0.1	1.1 ± 0.2
	Chronic bed rest	Pre BR	na	1.0 ± 0.1
		Post BR	na	1.4 ± 0.1**
		Pre BR	1.03 ± 0.09	0.96 ± 0.1

PDP1/Actin (RAU)	Acute bed rest	Post BR	0.79 ± 0.06	0.91 ± 0.1
	Chronic bed rest	Pre BR	na	1.0 ± 0.1
		Post BR	na	1.1 ± 0.2

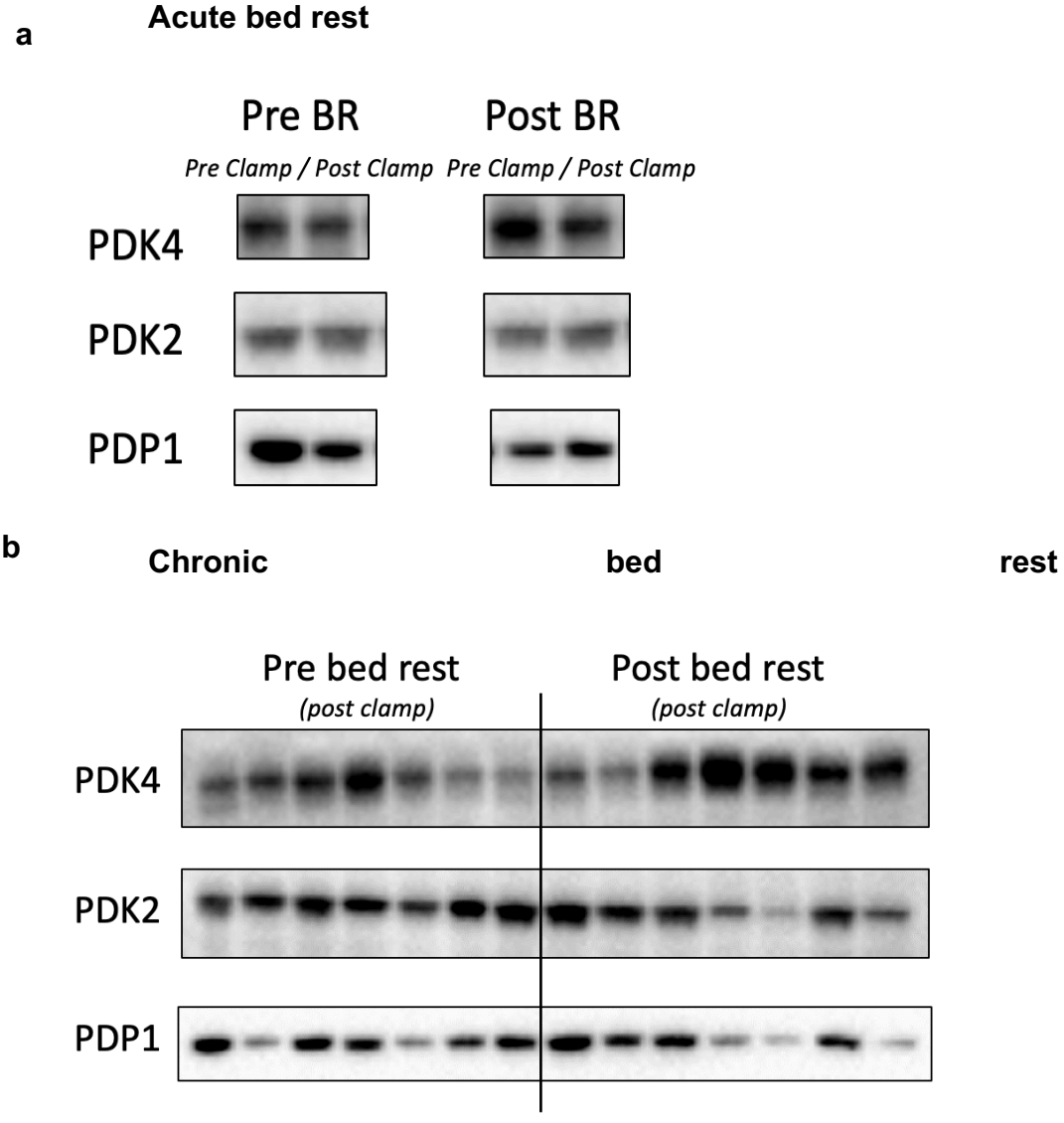

Figure 3.13. Example western blots of PDK2, PDK4 and PDP1 in a) acute and b) chronic bed rest.

3.5 Discussion

The main aim of this chapter was to identify any differences in whole-body insulin-stimulated glucose disposal following 3 days (acute) and 56 days (chronic) bed rest in healthy men maintained in energy balance. Secondary aims were to quantify whole-body substrate oxidation, and muscle mRNA expression, cellular metabolism and IMCL content in tandem to provide mechanistic insight of the metabolic responses to acute and chronic bed rest. A novel and unexpected observation was that the decrease in whole-body insulin-stimulated glucose disposal after 3 days bed rest was of a similar magnitude to that observed after 56 days of bed rest, indicating a rapid and substantial change in GD after the onset of bed rest, after which there is little further change. Furthermore, this blunting of GD was paralleled by reduced muscle glycogen storage under insulin clamp conditions following both acute and chronic bed rest. This clearly confirms that immobilisation rapidly supresses insulin-stimulated GD and glycogen storage, but remarkably this suppression remains relatively unchanged even after 56 days bed rest when volunteers are maintained in energy balance. However, despite this similarity in whole-body glucose disposal, the inhibition of fat oxidation under insulin clamp conditions after 56 days bed rest was less than after 3 days bed rest and was paralleled by a decrease in insulin-stimulated carbohydrate oxidation, which was not seen after 3 days bed rest. This demonstrates a dissociation of the regulation of glucose uptake from the regulation of substrate oxidation in

the transition from acute to chronic bed rest. Of note, the substantial mRNA abundance changes detected at 3 days across multiple cellular functions, including those controlling carbohydrate and lipid metabolism, preceded changes observed in fuel oxidation at a whole-body level. Moreover, after 56 days bed rest, when this shift in the pattern of substrate oxidation was evident, these mRNA abundance changes had waned substantially to reflect the changes observed in muscle glycogen and whole-body fuel oxidation during the hyperinsulinaemic euglycaemic clamp. Collectively these observations point to widespread transcriptional events occurring early in bed rest being causative in the shift in fuel metabolism seen after chronic bed rest. Importantly, this shift could not be explained by increased circulating lipids or muscle IMCL accumulation in this experimental design given volunteers were maintained in energy balance and IMCL was unchanged from the acute to chronic bed rest state, pointing to the lack of muscle contraction *per se* being the primary signal for the adaptation in fuel selection.

Several previous studies have reported declines in whole-body glucose uptake after bed rest of between 3 and 28 days duration measured under euglycaemic hyperinsulinaemic clamp conditions (Mikines et al. 1991; Kenny et al. 2017; Cree et al. 2010; Stettler et al. 2005). One commonly purported mechanism for bed rest associated impairment in glucose disposal, particularly in longer duration bed rest, is an alteration in body composition and a subsequent increase in IMCL (Gemmink et al. 2017). An acute bed rest study of 2 days duration in healthy men who were fed either an isocaloric high-saturated fat, or high-carbohydrate diet found a 17-32% increase in IMCL

measured using MRS, but only a reduction in glucose disposal measured by the hyperinsulinaemic euglycaemic clamp by 24% in the high-fat diet group, with no correlation found between GIR and IMCL overall (Stettler et al. 2005). One chronic bed rest study reported a 75% increase in IMCL measured using MRS after 4 weeks of bed rest (Cree et al. 2010). However participants were not maintained in energy balance and there was concomitant hypercortisolaemia, which has been shown to drive increases in IMCL content independently of immobilisation(Cree et al. 2007). Another study using a 28-day unilateral limb suspension model reported a 20% increase in calf IMCL. However this study failed to control dietary energy intake and physical activity levels were not measured prior to immobilisation (Manini et al. 2007), so it seems unlikely these participants were in energy balance. This study does not support an increase in IMCL content in healthy participants in either acute or chronic bed rest. Crucially, the present participants were maintained in energy balance throughout both experiments, removing the large confounding factor of energy oversupply. In addition to seeing no change in total IMCL content in response to acute and chronic bed rest, there was no change in fibre type specific IMCL content (Appendix 3), further supporting these results. These findings are consistent with the proposal that when in conditions of energy balance, IMCL accumulation is not the primary driver for a reduction in whole-body glucose disposal in either acute or chronic bed rest, and previous results may have been confounded by simultaneous positive energy balance.

An important finding from this study is the widespread extensive alteration in mRNA abundance across multiple cellular functions, including

carbohydrate and lipid metabolism at 3 days which precede subsequent changes in whole-body fuel oxidation at 56 days. In addition, although the gene network size had markedly decreased by 56 days, the genes contributing to these networks were more robustly altered in expression and remarkably reflected the changes observed in fuel oxidation at a whole-body level. Specifically, in the case of carbohydrate oxidation the 13 mRNAs identified as being altered in expression from pre bed rest collectively predicted the inhibition of the quantity of glycogen and quantity of carbohydrate with high confidence, which corresponded with the reduction in insulin-stimulated muscle glycogen storage and carbohydrate oxidation observed under insulin clamp conditions. Similarly in the case of lipid oxidation there was an increase in expression of 6 genes after 56 days bed rest, which collectively predict the activation of fatty acid oxidation with high confidence and tallied with the reduced suppression of whole-body fat oxidation observed under insulin clamp conditions at this time point. Previous research has shown that transcriptional responses associated with impairment in insulin signalling are not present after a single day of bed rest(Dirks et al. 2018), but expression is markedly changed after 9 days bed rest in association with insulin resistance in healthy men(Alibegovic et al. 2010). In the latter study by Alibegovic, in total over 4,500 genes were altered in expression after 9 days of bed rest, representing about 11% of all the gene transcripts present on the microarray, in particular genes involved in mitochondrial function such as oxidative phosphorylation, ubiquinone biosynthesis and fatty acid metabolism which were significantly downregulated. This study provides additional insight by demonstrating that a widespread

change in mRNA abundance occurs early in bed rest but then wanes as bed rest is sustained, and ultimately reflects the changes seen in fuel metabolism, under insulin clamp conditions, seen after chronic bed rest.

Disrupted calcium handling has been linked to muscle atrophy and metabolic dysregulation in muscle disorders(Agrawal, Suryakumar, and Rathor 2018) and may be a potential candidate responsible for the observed changes in fuel oxidation from the acute to chronic bed rest. Calcium is known to play a central role in muscle carbohydrate utilisation via control of the activity of glycogen phosphorylase, phosphofructokinase and the pyruvate dehydrogenase complex (Spriet 2014). Furthermore studies have noted alterations in muscle calcium homeostasis during immobilisation (Stettler et al. 2005, Kenny et al. 2007), it is plausible that it played a regulatory role in the shift in insulin-stimulated fuel oxidation observed from acute to chronic bed rest in the present study. In support of this, a clear increase in mRNA expression of calcium-activated genes was seen after 56 days' bed rest, which was accompanied by robust downregulation of genes regulating sarcoplasmic reticulum function (TTN and MYLPF) and calcium handling (RYR1), collectively suggesting an increase in intramyocellular free calcium occurred after chronic bed rest. In a 10-day bed rest study, caffeine-induced calcium release in isolated single muscle fibres was estimated via tension development (Monti et al. 2021). The authors pointed to reduced sarcoplasmic reticulum calcium release occurring after 10 days' bed rest, and attributed this to a reduction in the rate of sarcoplasmic reticulum calcium reuptake, which is in keeping with findings reported after 10 days' lower limb cast immobilisation(Thom et al.

2001). Another study involving 23 days' unilateral lower limb suspension found reduced sarcoplasmic reticulum calcium content, which was postulated to be due to increased calcium leakage(Lamboley et al. 2016). Along with an increase in muscle PDK4 protein expression, the present results point to disrupted calcium handling as a potential mechanism to explain the changes in insulin-stimulated substrate oxidation observed at 56 days' bed rest, particularly in the absence of changes in muscle IMCL content.

The findings from this chapter have important clinical implications. Periods of inactivity of short duration (<7 days) such as bed rest are common during hospitalisation after illness or injury, with the average length of hospital stay in the United Kingdom 5.9 days (NHS Digital, 2019). Clinical populations have the additional burden of inflammation which also causes rapid muscle mass loss (Puthucheary et al. 2013; Constantin et al. 2011) and reductions in whole-body glucose disposal (Chambrier et al. 2000) via mechanisms distinct to immobilisation alone. The results from this chapter indicate changes related to immobilisation alone are rapid and profound and it is unclear if the effect of immobilisation and inflammation may be summative (which will be addressed in Chapter 5). Without early interventions or countermeasures to reduce sedentary time during hospitalisations or periods of reduced physical activity, patients are likely to leave hospital more deconditioned and insulin resistant than when they entered. It is currently unclear whether changes in whole-body glucose disposal and underlying transcriptional changes seen early with immobilisation are fully reversed with a period of free living or a more extensive

period of exercise rehabilitation is needed, and what dose and duration would be required (which will be addressed in Chapter 4).

In summary, this study is the first to show that the reduction of muscle glycogen storage and decline in whole-body GD after acute bed rest were rapid, and then remain largely unchanged after chronic bed rest in healthy men maintained in energy balance. Furthermore, there was a clear dissociation of these events from the shift in insulin-stimulated whole-body substrate oxidation between acute to chronic bed rest. This temporal shift in fuel selection could not be rationalised by changes in blood lipid concentrations or IMCL content but was reflected by the muscle transcriptional response to chronic bed rest.

Chapter 4

The effect of 3 days bed rest and structured remobilisation on whole-body and leg glucose uptake, muscle protein turnover and muscle volume in healthy male participants.

4.1 Introduction

Both skeletal muscle atrophy and reductions in insulin-stimulated whole-body glucose disposal are manifestations of bed rest. The study in Chapter 3 demonstrated that as little as 3 days of bed rest reduced insulin-stimulated whole-body glucose disposal and muscle glycogen storage in volunteers maintained in energy balance but had no impact on fuel oxidation rates under insulin clamp conditions compared to the pre bed rest state. This relatively short duration bed rest also resulted in extensive changes in muscle mRNA expression representing multiple cellular functions. Studies of similar periods of bed rest (3-5 days duration) have also reported reductions in whole-body insulin sensitivity (Yanagibori et al. 1994; Smorawinski et al. 2000). Moreover, upper limb immobilisation of as short as 24-hours duration has been reported to reduce insulin-stimulated forearm glucose disposal, which was specific to the immobilised limb (Burns et al. 2021). In keeping with this, 7 days bed rest also reduced insulin-stimulated leg glucose uptake, which was of a greater magnitude than that seen at the whole-body level (Mikines et al. 1991). Collectively these observations highlight that immobilisation-induced reductions

in limb glucose uptake are rapid and most likely reside at a muscle level because of a lack of muscle contraction *per se*. This being the case, it is not unreasonable to suggest that exercise intervention following bed rest could rapidly restore limb glucose disposal to the pre immobilised state. A single bout of exercise acutely increases local insulin sensitivity (Richter et al. 1989), however the effect is diminished within 48-72 hours of exercise (King et al. 1995). In a previous study involving 21 days bed rest in healthy, sedentary young males maintained in energy balance, 4 days of normal ambulation was insufficient to restore whole-body glucose tolerance in response to an oral glucose challenge. However, 5-14 days of normal ambulation was able to restore glucose tolerance (Heer et al. 2014). Furthermore, in a study involving young and older participants maintained in energy balance, 5 days of bed rest resulted in a decline in whole-body insulin sensitivity in both groups (measured using the Clamp-Like Index (CLIX-IR), a measure of insulin sensitivity calculated from an OGTT), was fully restored following an 8 week lower limb eccentric exercise training programme, consisting of progressive resistance exercise of the knee and hip extensor muscles in a recumbent stepper-ergometer three times per week (Reidy et al. 2017). However, it is possible that this duration of free living alone could have restored insulin sensitivity without exercise intervention, and the absence of a control intervention in the study meant this was not tested. It is therefore currently unclear whether insulin sensitivity following 3 days of bed rest can be restored by 3 days of routine ambulatory behaviour, and furthermore whether prescribed exercise

intervention during this period can augment any restoration of glucose disposal observed.

Both bed rest and single limb immobilisation result in muscle mass loss. Disuse muscle atrophy is underpinned by a net imbalance between muscle protein synthesis (MPS) and muscle protein breakdown (MPB). Under conditions of 21 days lower limb immobilisation in healthy men it has been reported that the magnitude of decline in postabsorptive MPS can account for the majority of muscle volume loss observed (de Boer et al. 2007), however since then it has been questioned whether immobilisation is also accompanied by increased MPB and denervation, at least initially (Demangel et al. 2017). Adding to this, a 16% reduction in the rate of MPS in as short as 2 days of unilateral leg immobilisation has been reported, which was accompanied by a 1.7% decline in quadriceps volume (Kilroe, Fulford, Holwerda, et al. 2020). Glover et al. were the first to demonstrate the existence of muscle anabolic resistance in response to immobilisation, i.e., suppressed MPS in the postprandial state following 14 days lower limb immobilisation in healthy, young volunteers, which persisted even under conditions of high dose amino acid administration (Glover et al. 2008). A shorter duration study of 5 days unilateral knee immobilisation using a full leg cast confirmed these collective observations by reporting reductions in rates of postabsorptive and postprandial MPS in young healthy men, which was accompanied by a 4% loss of quadriceps CSA (Wall et al. 2016).

There is less evidence available in the literature regarding the role of MPB in short-duration disuse atrophy, partly due to the technical challenges

associated with directly measuring protein degradation *in vivo* in humans. Tesch showed an increase in muscle protein breakdown after 72 hours of unilateral leg immobilisation demonstrated by a 44% increase in interstitial 3-methylhistidine measured using microdialysis within the *vastus lateralis* (Tesch et al. 2008), however the validity of this technique has been previously questioned (Rennie, Phillips, and Smith 2008). Another study estimating MPB via urinary 3-MeH excretion during a 17 day bed rest experiment showed no change in MPB, however this was a much longer period of immobilisation (Stein and Schluter 1997). Other studies utilising stable isotope tracer infusions have reported no change in MPB in young participants after 14 days (Ferrando et al. 1996) and 21 days (Symons et al. 2009) bed rest, however these only allow estimates of MPB over a few hours. There is some limited evidence showing elevated expression of proteolytic genes and proteins during immobilisation, lending support to the theory that proteolysis is elevated with disuse. For example, the first few days of disuse has been shown to be associated with activation of the ubiquitin-proteasome degradation of proteins in rodents (Taillandier et al. 2003), but there are significant differences in muscle protein turnover when comparing responses to immobilisation in rodents vs humans. This incongruence between animal and human studies may be explained by the translatability of the rodent model, with immature rodents often used, the high metabolic rate compared with humans and the potential stress effect of the hindlimb immobilisation mode (Rennie et al. 2010). In a study by Brook and colleagues, healthy men undergoing 4 days unilateral leg immobilisation showed declines in MPS but no change in MPB when measured *in vivo* using

an acute pulse-chase tracer decay rate technique (Brook et al. 2022). In longer duration immobilisation, a comprehensive increase in mRNA expression for genes linked to the regulation of muscle atrophy in humans (MAFbx, MuRF1, p94 calpain) was found after 2 weeks ULLS (de Boer et al. 2007; Jones et al. 2004). A study in humans undergoing 3 days of dry immersion reported a 6-fold increase in neural cellular adhesion molecule (NCAM+) muscle fibres, a marker for muscle fibres undergoing regeneration or denervation, indicating early denervation (Demangel et al. 2017). One study of 5 days bed rest in young and older participants found a blunted MPS in the older individuals, as well as increased markers associated with the ubiquitin proteasome and autophagy-lysosomal systems (Tanner et al. 2015). However, these are molecular markers and direct measures of MPB were not performed. Currently, blunted MPS is considered the predominant mechanism for disuse atrophy in the short term in humans, and although animal hindlimb immobilisation studies have suggested an increase in MPB being at least partly responsible for a decrease in muscle mass (Krawiec et al. 2005), this has not been consistently established in human immobilisation studies (Rudrappa et al. 2016). Newer oral stable isotope techniques combining simultaneous measurements of MPS and MPB *in vivo* now allow the potential to directly measure these processes in acute models of disuse (Cegielski et al. 2021).

The time-course of change of MPS and MPB, and their rate of restoration, particularly over short periods in humans, is also unresolved. One study which assessed changes in muscle protein turnover after 5 days of bed rest and their restoration after 8 weeks of high intensity eccentric resistance

exercise found a restoration in blunted MPS and expression of mRNA MuRF-1 in the older participants (Tanner et al. 2015). However, similar to studies examining insulin sensitivity restoration after bed rest, it is unclear if restoration of muscle protein turnover would have occurred anyway with this extended period of free living. Whilst the reduction in muscle mass over the first few days of unloading appear to be predominantly attributable to declines in MPS in humans, it is unclear whether this rapidity of change is mirrored after reloading, particularly as *in vivo* measures of both MPS and MPB during short duration reloading in humans have not been performed. Rodent studies investigating the effects of reloading after hindlimb immobilisation (albeit in durations longer than 3 days immobilisation) have shown that increases in MPS occur as early as 6 hours after recovery (Tucker, Seider, and Booth 1981), and persist after 18 hours (Taillandier et al. 2003) and 72 hours (Baehr et al. 2016) of reloading up to 7 days (Taillandier et al. 2003; Baehr et al. 2016). There is currently a lack of data on whether short duration (<5 days) reloading can restore changes in direct measures of MPS associated with only a few days of bed rest in humans. A major novelty of the present study is that it explored *in vivo* measures of MPS and MPB as well as insulin sensitivity concurrently in the same individuals under the same experimental conditions.

Molecular regulators that have shown to be altered in short duration immobilisation include increased myostatin mRNA and protein after 3 days of unilateral leg immobilisation (Gustafsson, Osterlund, Flanagan, von Walden, et al. 2010), and genes related to protein ubiquitination and oxidative stress after 2 days of unilateral leg immobilisation, which were not restored by 24 hours of

reloading (Tesch et al. 2008). However, in both these studies direct measures of muscle protein turnover were not performed, not least because of difficulties on measuring MPB *in vivo* in humans. Glover et al. noted a reduction in the phosphorylation of the tension-sensing protein FAK associated with reduced MPS rates after 2 weeks of lower limb immobilisation, but interestingly no change in signalling of the akt-mTOR-p70S6 pathway (Glover et al. 2008). One study which utilised an untargeted approach to explore muscle transcriptomic changes in response to 4 days of unilateral lower leg immobilisation, and quantified MPS and thigh lean muscle mass using DEXA concurrently, found mRNA networks altered related to DEPTOR, a potent inhibitor of mTOR (Willis et al. 2021). However, De Boer et al (de Boer et al. 2007) found no impact of 10 days immobilisation on the phosphorylation status of proteins in the mTOR anabolic signalling pathway in fasted state volunteers. Similarly, Glover et al. found that whilst immobilisation induced a blunting in the MPS response to protein feeding in human volunteers, this anabolic resistance could not be explained by reduced phosphorylation of proteins in the mTOR signalling axis (Glover 2008). In addition, in the study of Willis (Willis et al. 2021) there was greater mRNA expression of proteolytic-related pathways, suggesting a link between proteolytic marker expression (and presumably MPB) and declines in MPS during short term disuse. Further studies to advance the mechanistic understanding of short-term disuse atrophy and insulin resistance and the rapidity of their restoration following remobilisation are still required, particularly where gold standard direct physiological measures are employed concurrently in the same individuals alongside molecular measurements. This chapter

describes novel changes in whole-body and limb insulin sensitivity and measures of muscle volume, MPS and MPB and muscle targeted mRNA expression (low density array cards) in healthy men following 3 days of bed rest and the restoration of whole-body and limb insulin sensitivity, muscle volume, MPS and muscle targeted mRNA expression after 3 days of remobilisation.

4.2 Research Question

Is the magnitude of restoration of whole-body glucose disposal, leg glucose uptake and muscle protein turnover after 3 days of structured remobilisation equivalent to their reduction after 3 days of bed rest?

Research Aims

i) To determine the impact of 3 days of bed rest on insulin-stimulated whole-body glucose disposal, leg glucose uptake, muscle glycogen storage, muscle volume and MPS and MPB concurrently in the same individuals.

ii) To determine the impact of 3 days of structured remobilisation following bed rest on insulin-stimulated whole-body glucose disposal, leg glucose uptake, muscle glycogen storage, muscle volume and MPS concurrently in the same individuals.

iii) Using a micro-fluidic gene card approach identify changes in targeted mRNA responses to 3 days of bed rest and structured remobilisation that may underpin any observations.

4.3 Methods

4.3.1 Plan of investigation

Ten healthy male participants were recruited from the general population and underwent 3 days of bed rest in the David Greenfield Human Physiology Unit at the University of Nottingham, as per the protocol described in full in Chapter 3 (see 3.3.1). The protocol consisted of a 7-day run-in period, a 3-day (72 hour) -6^{o} HDT bed rest period, followed by 3 days of exercise-supplemented remobilisation (ESR), during which the participants were otherwise free living (Figure 4.1). Experimental visits were carried out on day -4 (pre bed rest), day 3 (post bed rest) and day 7 (post remob) of the protocol. Diet was standardised and strictly controlled throughout as described in the previous chapter.

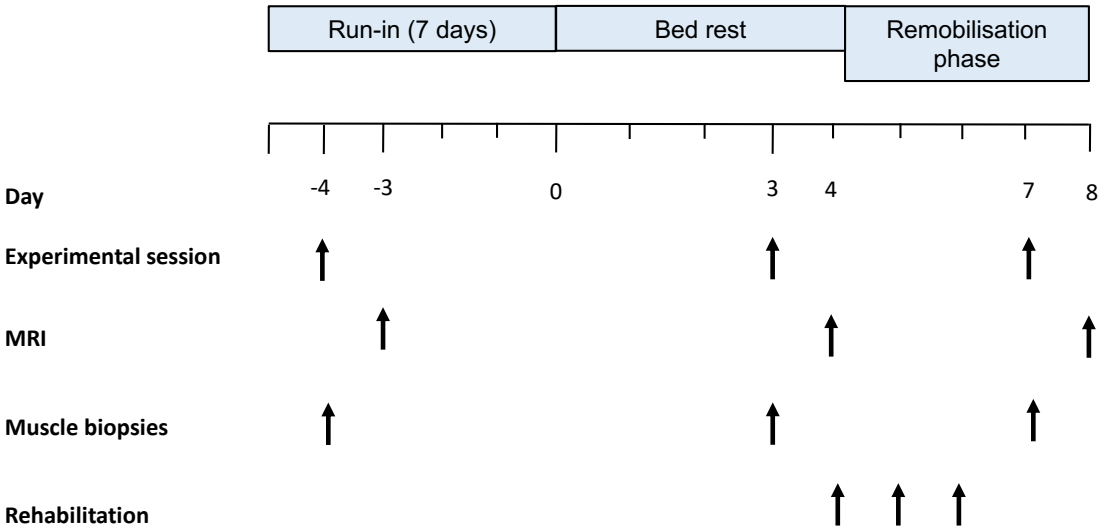

Figure 4.1. Acute bed rest and remobilisation schema. MRI, magnetic resonance imaging.

Run-in phase

During the run-in phase participants were free-living for 7 days and were provided with a standardised diet. Participants were advised to continue their usual activities of daily living, but to refrain from strenuous physical activity in the 3 days leading up to the first experimental visit on day -4. Participants received the oral stable isotope tracer deuterium oxide (D_2O/ heavy water) to quantify cumulative MPS rates. An initial oral bolus of 3mg/kg D_2O was administered at 09:00am (divided into 3 equal doses 30 minutes apart to reduce the risk of side effects) on day -4 prior to bedrest, with individualised top-ups on day 0 and day 3 calculated based upon the rate of decay of water and total body water of 60% in men (as described in **Chapter 2)**. To monitor the body water enrichment throughout the study, saliva samples (1ml) were collected prior to and two hours after each D_2O ingestion, as well as additional saliva

samples at 09:00 on day 0, day 1 and day 7 of the protocol. Samples were cold centrifuged at 16,000 g to remove any debris that may have been present and then aliquoted into 2 ml vials and frozen at -80^{o}C until analysis.

Bed rest phase

Participants underwent 3 days and 4 nights of -6^{o} HDT bed rest in the DGHPU. Full details of staffing, diet and personal hygiene is outlined in the previous chapter. During the bed rest phase, the stable isotope tracer 3-methylhistidine (3-MeH) was used to determine the rate of MPB over a 7 hour period on day 0 and day 2 of the protocol. Ten mg was ingested (dissolved in 50ml distilled water) on day -1 prior to the bed rest period and day 1 at 09:00am. Following this, an anterograde venous cannula was inserted 24 hours later (day 0 and day 2 of bed rest) into the arm at the antecubital fossa for sampling of venous blood every hour for a total of 7 hours for the measurement of D_3-MH enrichment. On the morning of day 3 (72 hours of bed rest) of the best rest phase, after an overnight fast, participants underwent the second experimental visit. After this, gradual, supervised return to 'upright' in the bed was carried out, with continuous cardiovascular monitoring to avoid postural hypotension. Participants remained in bed but were allowed to sit in the upright position until the morning of day 4 (after 96 hours of bed rest).

Remobilisation phase

On the morning of day 4, after an overnight fast, participants were transferred (without standing) to a wheelchair, then transported by taxi to a 3T Philips

Ingenia MR (Best, Netherlands) scanner at the Sir Peter Mansfield Imaging Centre, University of Nottingham (SPMIC) for their post bed rest MRI scans. Following this, participants were fed and allowed to return to standing in a controlled environment. They then underwent supervised rehabilitation in the DGHPU comprising of 5 sets of 30 repetitions of maximal isokinetic knee extensions (90^{o} per second) on an isokinetic dynamometer (Cybex, HUMAC Norm, CSMi Solutions, town, country) on their dominant leg, as this protocol been shown to provide an anabolic stimulus (Brook et al. 2016; Jones et al. 2004), and then they were allowed to return home. They returned on days 5 and 6 of the non-bed rest period to undergo repeat supervised rehabilitation sessions as above. At 08:00am on the morning of day 7 they presented to the DGHPU to undergo their final experimental visit. A D-dimer blood test was taken as a safety precaution to rule out a deep vein thrombosis (DVT) formation during bed rest. The participants completed the study after the final MRI scan was performed on day 8.

Experimental visits

Experimental visits were carried out on day -4 (pre bed rest), day 3 (post bed rest) and day 7 (post remobilisation) of the protocol. After fasting from midnight, on the morning of each visit, muscle biopsy samples were obtained using a Bergström needle (Bergstrom 1975) from the *vastus lateralis* of their right leg and in the final 10 minutes of the hyperinsulinaemic euglycaemic clamp in the opposite leg. Two passes through the same incision were made on each occasion at a right angle to the belly of the *vastus lateralis* and muscle tissue

was immediately snap frozen in liquid nitrogen-cooled isopentane (Fisher Scientific, Loughborough, UK) to prevent the formation of ice crystals and stored wet in liquid nitrogen until analysed.

Cannulae were inserted retrograde into a superficial vein on the dorsal surface of the non-dominant hand and anterograde into one arm. The cannulated hand with the dorsal surface cannula was kept in a hand-warming unit (55°C) to arterialise the venous drainage of the hand (Gallen and Macdonald 1990), and a 0.9% slow saline drip was attached to keep the cannula patent for repeated blood sampling. Following this, an anterograde femoral venous catheter was inserted (using the Seldinger technique under ultrasound guidance [Toshiba Diagnostic Ultrasound System, Model SSA-77OA]), to enable venous blood draining from the leg to be analysed for glucose concentration (Figure 4.2.). In brief, the point of insertion, which generally lies 1cm distal and medial to the mid inguinal point was marked with permanent marker. The skin was prepared with iodine and a surgical drape with an aperture was placed over the top and the ultrasound probe covered in a sterile plastic cover. A small amount (<1ml) of 1% lidocaine was injected subcutaneously to the marked point to form a bleb and under ultrasound guidance more was infiltrated along the tract to the vein. Once the skin was adequately anaesthetised, using ultrasound visualisation, a needle with a syringe loaded with 3ml 0.9% saline was advanced at 45^{o} towards the femoral vein, until entrance of the needle into the vessel was visualised. At this point the syringe was removed, and the guidewire was passed over the needle (Figure 4.2a). Once the guidewire was positioned in the vein, the needle was

removed, and a small incision made at the entry point to the skin with a scalpel. A dilator was fed over the guidewire to dilate the skin and subcutaneous tissues and inserted to a depth of approximately 2-3cm. Thereafter the femoral venous cannula was passed over the guidewire and the guidewire removed (Figure 4.2b). Care was taken to occlude the end of the cannula to avoid air entry into the lumen and possible risk of air embolism and a small sample of blood aspirated to ensure adequate aspiration. An infusion of 0.9% saline was connected with a slow infusion rate to maintain patency of the cannula and a sterile drape placed around the port (Figure 4.2c).

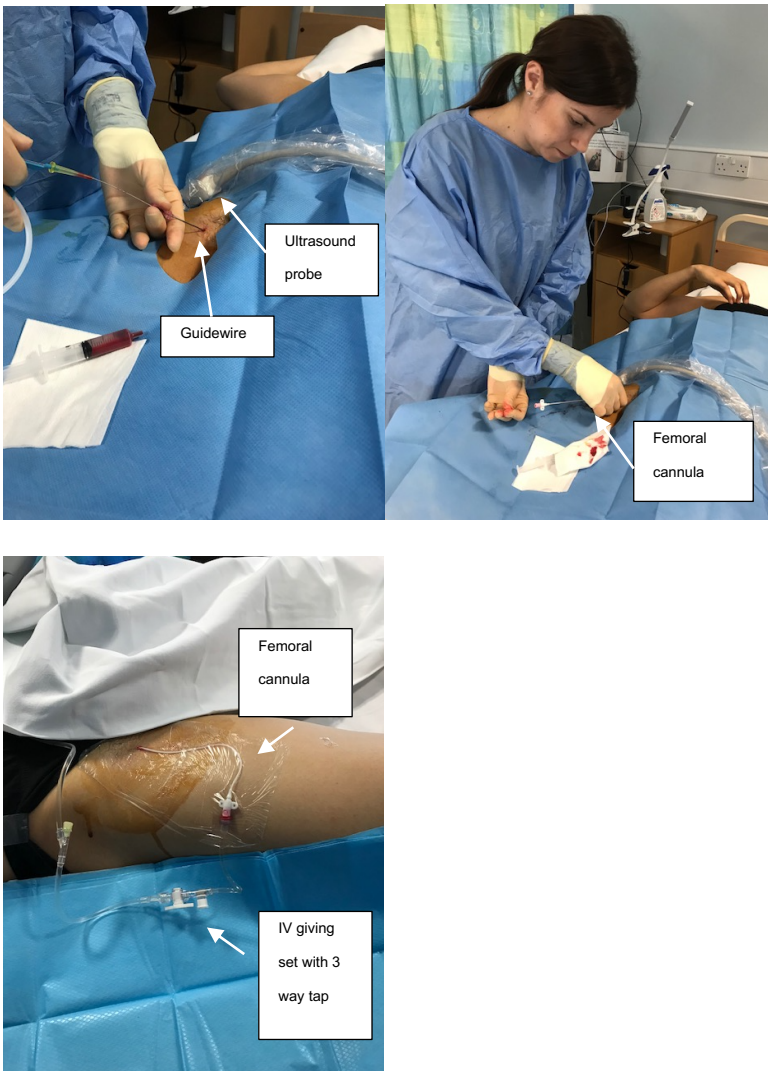

Figure 4.2. Femoral venous cannulation. a) Dilator passed over guidewire b) Femoral cannula being passed over guidewire c) Femoral venous cannula set up during experimental visits.

Simultaneous blood samples (1ml) were taken from the arterialised-venous heated hand cannula and the femoral venous line at baseline and 120, 135, 150, 165 and 180 minutes of the insulin clamp to calculate arterialised-venous vs venous (AV-V) difference. Femoral artery blood flow in the

contralateral limb was obtained at these same time points using Doppler ultrasonography to calculate leg glucose uptake (Figure 4.3).

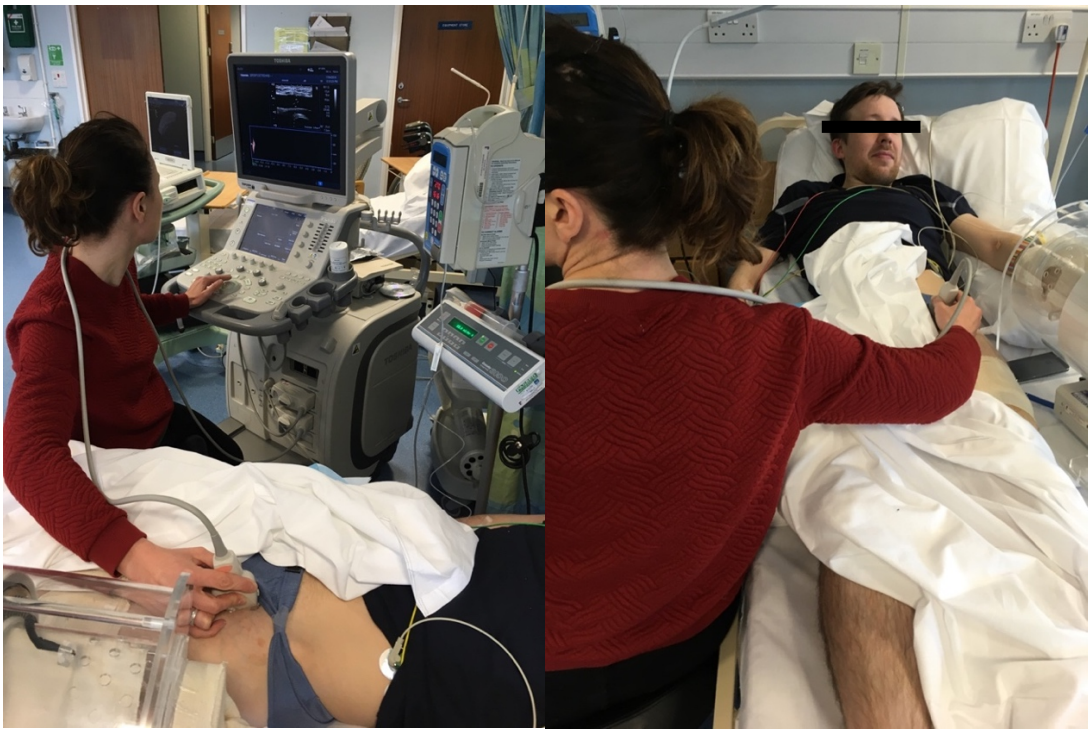

Figure 4.3. Femoral arterial blood flow measurement using US Doppler.

To measure femoral artery blood flow, participants lay supine on a bed with a 3-lead ECG attached to their chest. The femoral artery was located at the level of the inguinal crease (below the inguinal ligament) using the ultrasound scanning probe (Toshiba Diagnostic Ultrasound System, Model SSA-77OA) on the contralateral leg to the femoral venous catheter to reduce the risk of infection. Once a clear longitudinal image was obtained, pulse wave function was selected, and the Doppler window positioned so that it lay within the vessel. The Doppler angle was maintained at <60^{o} to maximise accuracy. Three mean blood velocity (MBV) in cm/sec and femoral artery images were recorded and

stored, with artery diameter measured from intima to intima, ensuring the diameter was placed perpendicular to the vessel edge.

Thereafter, a euglycaemic hyperinsulinaemic clamp was performed, with insulin (human Actrapid, Novo Nordisk) infused into the non-dominant arm at a rate of 60 mU/m^2/min for 3 hours. Arterialised-venous blood glucose concentration was measured in <1ml blood every 5 min and maintained at 4.5 mmol/l by a variable rate infusion of 20% glucose (Baxter Healthcare, Norfolk, UK). Arterialised-venous blood samples (3 ml) were taken at baseline and every 30 minutes during the final 60 minutes of the clamp for the measurement of insulin, triacylglycerol, and NEFA. Once the final muscle biopsy was completed, the insulin infusion was stopped, and participants provided with a high carbohydrate meal. During the remobilisation experimental visit (Day 7), an additional pre clamp muscle biopsy was performed on the control leg using a microbiopsy needle to quantify MPS compared with the rehabilitated leg. Femoral venous cannulation was placed in the rehabilitated side rather than the control leg side to determine the effect of resistance exercise on leg glucose uptake. The morning after each experimental visit, an MRI was performed to quantify whole-body muscle and leg muscle volume at the Sir Peter Mansfield Imaging Centre at the University of Nottingham.

4.3.2 Analytical methods

Blood sample analysis is described in detail in the General Methods. A portion of snap frozen muscle biopsy tissue was freeze dried and used to determine muscle glycogen content using methods previously described (Constantin-Teodosiu et al. 2019).

Whole-body insulin-stimulated glucose disposal

Whole blood was immediately analysed for glucose concentration (YSI 2300; Yellow Springs Inc,). Whole-body insulin-stimulated glucose disposal was calculated during the final hour of the clamp in steady-state (135-165 minutes). Whole-body glucose disposal was standardised to whole-body muscle volume (litres) measured using MRI in order to allow direct comparison of whole-body glucose disposal versus leg glucose uptake.

Femoral artery blood flow, AV-V difference and leg glucose uptake

Femoral artery diameter (FAD) was calculated using the mean of the 3 diameter measurements at diastole and the mean of the 3 diameter measurements at systole, with the diastolic (D) reading contributing 2/3 and systolic (S) contributing 1/3 to the mean femoral artery diameter value. Femoral artery cross sectional area (FAA) was then calculated from FAD and π (3.14159).

$$FAD = \left(\frac{2 \times D}{3}\right) + \left(\frac{1 \times S}{3}\right) \qquad FAA = \left(\frac{FAD}{2}\right)^2 \times \pi$$

Femoral artery blood flow was calculated from mean blood velocity (MBV: cm/sec) and FAA (cm^2) x 60 to express flow as cm^3/min. However, as cm^3 equates to ml, flow is usually expressed as ml/min.

Femoral artery blood flow (cm^3/min) = MBV x FAA x 60

AV-V difference was calculated by subtraction of venous blood glucose (mmol/L) obtained from femoral vein cannulation from the arterialised-venous blood glucose (mmol/L) obtained from retrograde hand cannula in heated hand box.

Leg glucose uptake (mmol/min) was calculated as:
Leg glucose uptake (mmol/min) = AV-V difference (mmol/L) x blood flow (cm^3/min).

Leg glucose uptake was then standardised to leg volume (litres) and expressed as mg/litre/minute. Insulin-stimulated leg glucose uptake was defined as during the 'steady state' of the insulin clamp which was determined between min 135-165 of the clamp.

Body water D_2O *enrichment*

Body water and muscle protein D_2O enrichment were measured as previously described (Wilkinson et al. 2014). Full description of the method is detailed in the General Methods chapter.

Calculation of Myofibrillar Protein Fractional Synthetic Rate (FSR)

The FSR of myofibrillar proteins using the D_2O tracer was determined as described by Wilkinson (Wilkinson et al. 2015). This was achieved using the precursor-product approach, from the incorporation of deuterium labelled alanine into protein, using the enrichment of body water (corrected for the mean number of deuterium moieties incorporated per alanine, 3.7, and the total number of hydrogens within the alanine derivative, 11) as the surrogate precursor labelling between subsequent biopsies. This is described further in Chapter 2, **Section 2.9.1**. In brief, the standard equation is:

FSR (%.h-1) = [(δAla)]/[(δp) x t] x 100

where, δAla = deuterium enrichment (in delta excess) of protein-bound alanine between subsequent biopsies, δP = precursor enrichment (in delta excess) and t, time between biopsies.

Muscle protein breakdown

A validated, stable-isotopic methodology was used to quantify the rate of MPB using D_3-MH (Sheffield-Moore et al. 2014) in response to bed rest (time points were day 0 and day 2), using the same method as described by Gharahdaghi (Gharahdaghi et al. 2019). Enrichment decay (k) of 3-MeH over the 7 hours of sampling in plasma was calculated within the first 48 hours of bed rest (from day 0 to day 2).

4.3.3 Muscle volume quantification using MRI

MRI was performed the morning after each experimental visit at the SPMIC to quantify whole-body muscle and leg (all muscle of the gluteal muscles, quadriceps, adductors and hamstrings) muscle volume. Prior to entering the MRI scanner, participants completed an MRI safety form to assess their suitability (Appendix 1, **Section 7.7**). Contraindications to taking part were having any metal within the body, e.g. pacemaker, cochlear implant, certain metal implants, being unable to lie flat for prolonged periods of time or claustrophobia. Participants removed all metal objects on their body and were given ear plugs to wear and an alarm bell to press should any problems arise during the scan. Participants lay supine head-first on the moveable MRI bed with their head resting on a pillow and their hands by their side. Their arms were secured into a fixed position using foam blocks to maintain the palms facing towards their body and a Velcro binder was placed across their body just proximal to their elbows to prevent their arms from falling outside the coil area. Two anterior dStream body coils and a posterior dStream bed coil (Philips, Best, Netherlands) were placed on the participants covering their clavicles to below their ankles (Figure 4.4).

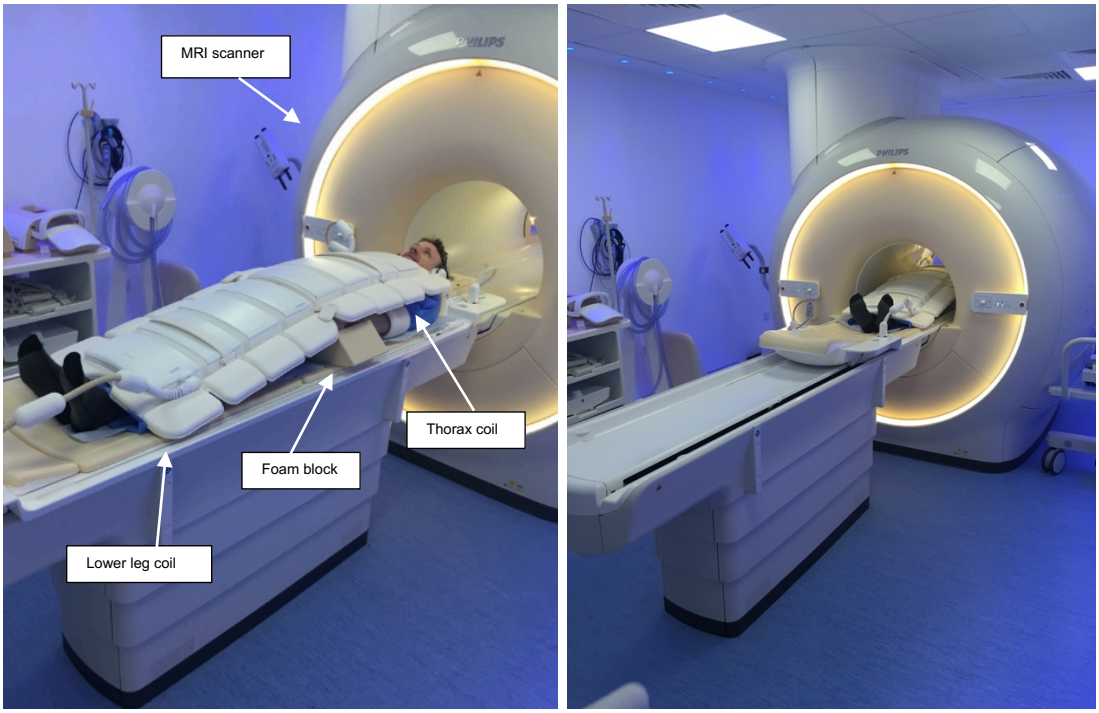

Figure 4.4 Magnetic Resonance Imaging setup. MRI scanner setup with coils placed on participant prior to entering magnet (left) and whilst inside the magnet (right).

4.3.3.1 Whole-body imaging protocol

Participants were scanned supine on a 3T Philips Ingenia Scanner in a fasted state (Philips, Best, Netherlands). Imaging of the whole-body was carried out using a T2-TSE sequence acquired over 6 different slabs and merged together online using Philips scanner parameters (Figure 4.5a). Each slab was acquired in a single breath-hold (particularly for the chest area), and consisted of a field of view of 448 x 560 x 300 mm, with a reconstruction voxel size of 1 x 1 x 1.5 mm. A total of 200 slices was acquired in 20 seconds, acquiring the whole-body images in around 6 minutes (taking into account bed motion and preparation

steps for each slab). Slice thickness was 1.5 mm. Water images were reconstructed online at the scanner using a Philips in-built product (mDIXON Quant package, Philips, Best, Netherlands) with scanner computer water images to measure muscle volume.

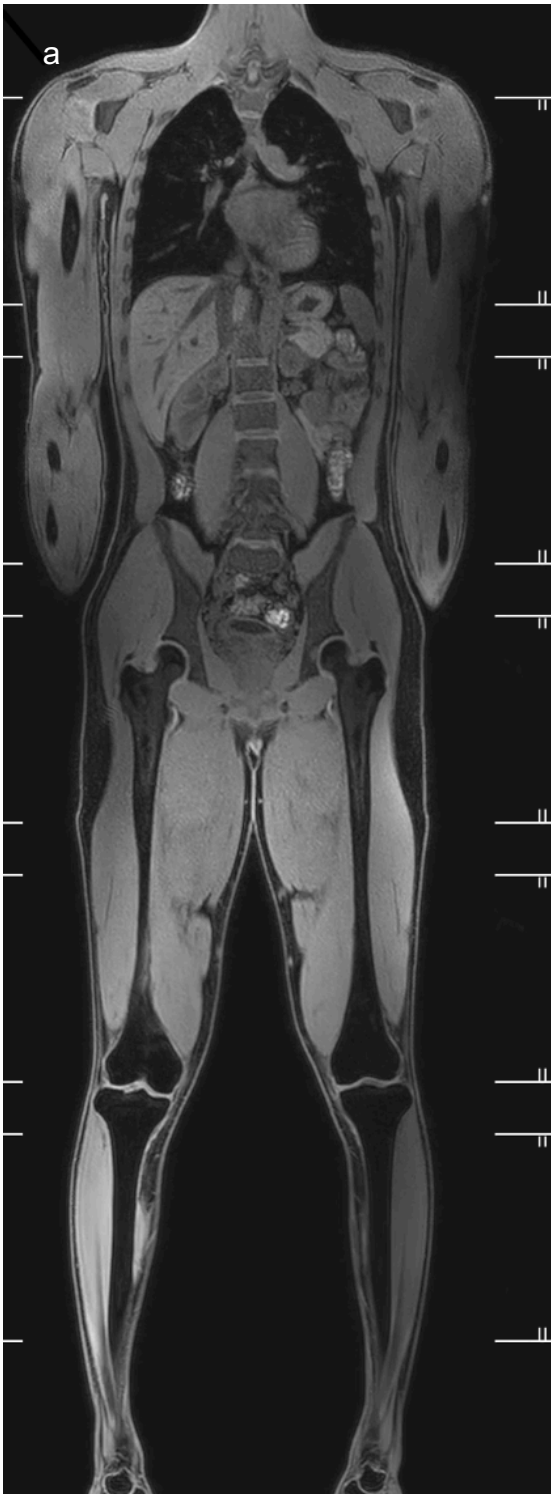

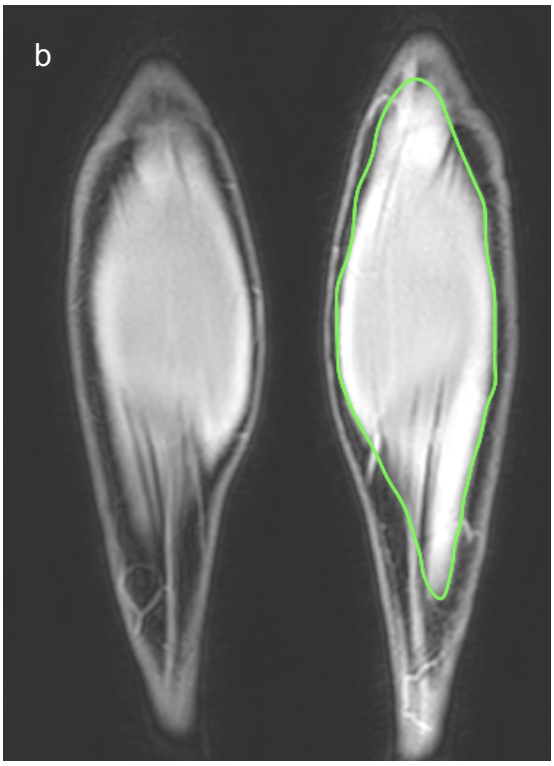

Figure 4.5. Magnetic Resonance Imaging whole-body example scans. a) MRI whole-body in coronal plane acquired during the acute bed rest study demonstrating a water only image and b) Leg calf muscle volume quantification with region of interest drawn around left calf in one slice in one scan.

4.3.3.2 Manual muscle volume quantification

Whole-body and leg muscle volume (cm^3) were quantified manually using Horos™ DICOM medical imaging software Version 3 (GPL-3.0, Annapolis, MD USA). Whole-body MRI scans were acquired in the coronal (longitudinal) plane and slices were analysed in this orientation as the resolution was best in this plane. The whole-body image was analysed in individual anatomical regions which were defined as; left calf, right calf, left upper leg and gluteal muscles (leg), right upper leg and gluteal muscles (leg), torso, left arm and right arm. Intrinsic muscles of the hands and feet and muscles of the face were not quantified due to the small volumes and difficulty in delineating muscle from connective tissue and tendons. Anatomical boundaries were defined as follows;

Torso – All muscle between shoulder joint and sacroiliac joint including abdominals but excluding thoracic and abdominal viscera

Arm – All muscle between wrist joint and shoulder joint

Leg – All muscle of the gluteal muscles, quadriceps, adductors and hamstrings.

Calf – All muscle between ankle joint and knee joint

Whole-body – All of the above combined

Muscle CSA (cm^2) was quantified every 10 slices. A region of interest (ROI) was drawn around the outer perimeter of the muscle (Figure 4.5b). Where there were several large muscle groups making up the anatomical region, several ROIs were drawn and added together. The CSA was then calculated for the slices not manually measured for each anatomical region using the formula:

CSA a + CSA b / 2 *10

Area was then multiplied by 0.15 (slice thickness) to get volume in cm^3.

The coefficient of variation for each region was calculated by taking the average of ten manually-measured repeated CSA measurements for each region of the baseline pre bed rest scan of participant BR02. They were as follows; torso 2.2%, right arm 2.0%, left arm 2.6%, right leg 1.3%, left leg 1.7%, right calf 1.5% and left calf 1.6%.

Validation of manual MRI muscle volume quantification

An automated muscle volume quantification method was used to validate the manual muscle volume quantification method above. Muscle leg volume (all muscle of the gluteal muscles, quadriceps, adductors and hamstrings) was calculated using automated quantification in using 3D slicer software (version 4.9, Boston, USA; https://www.slicer.org) (Fedorov et al. 2012). The leg region was cropped from the whole-body image, defined from the greater trochanter to the knee (tibiofemoral) joint space to ensure the whole leg muscle was taken into account. Within each slice being analysed, fiducial points were positioned within the muscle tissue at five different points randomly selected. Care was

taken to not place the fiducial points within a vessel, bone or other tissue. Simple region growing segmentation function was applied which automatically highlighted all of the tissue of interest selected (algorithm based on intensity statistics). The multiplier could be reduced if the area was over segmented, or more iterations used if it was under segmented. The parameters were set for all of the following slices in that region. The volume was quantified using the quantification, label statistics function in cm^3. This technique was developed in-house within the Nottingham NIHR Biomedical Research Centre. Raw automated values of MRI leg muscle volume before and after bed rest and after remobilisation were plotted against the raw manual muscle volume values and a Pearson correlation was run. This is presented in Figure 4.6a. A Bland-Altman plot of the differences between the automated and manual methods of muscle volume MRI quantification against the average values is shown in Figure 4.6b, indicating that the automated method tended to overestimate values compared with the manual method, but this was consistent.

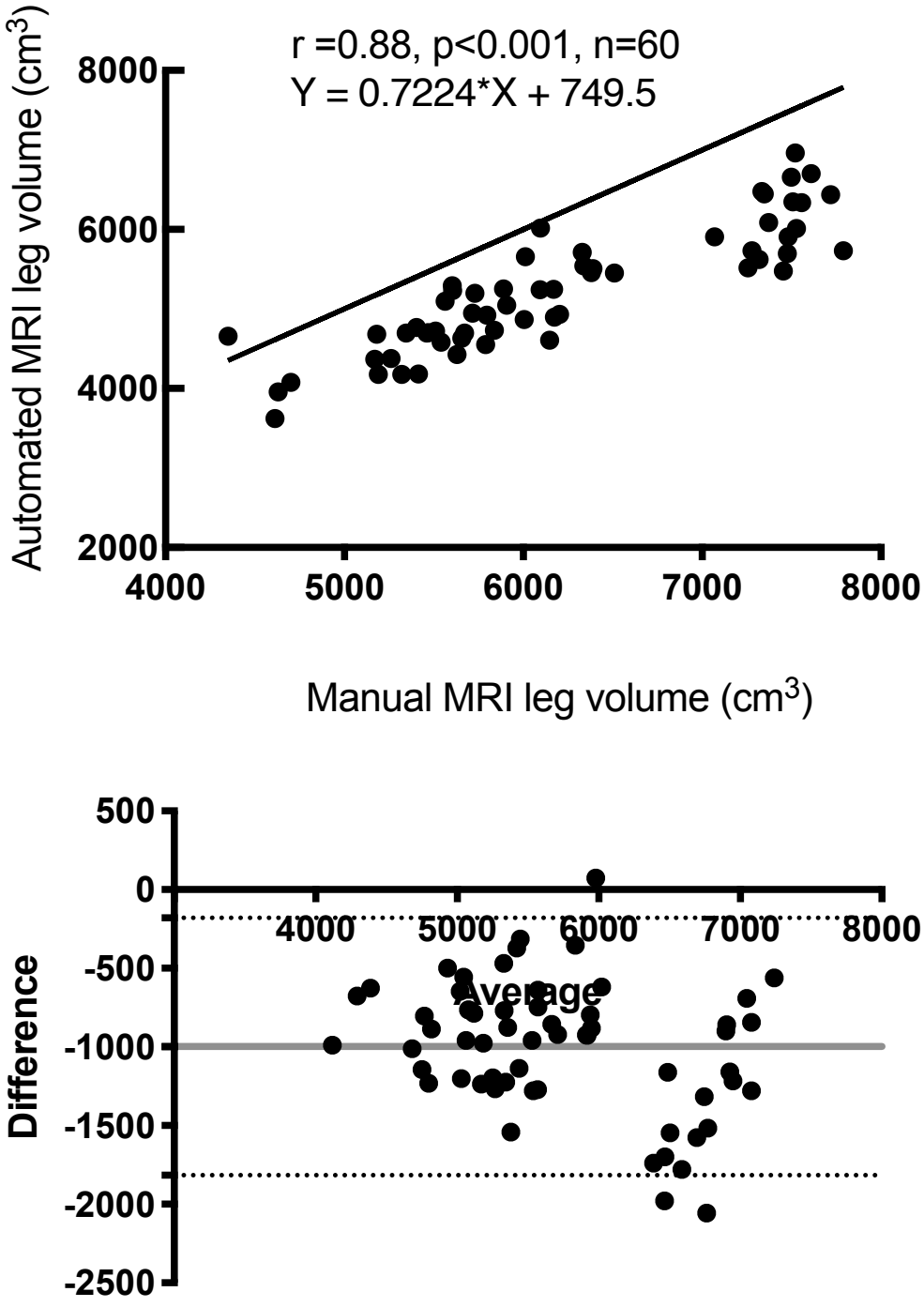

Figure 4.6. a) Correlation of automated vs manual muscle volume quantification using MRI. Pearson correlation for automated versus manual leg muscle volume (cm^3) measured before bed rest in the acute bed rest study. Line

indicates the line of identity where x=y. b) Bland-Altman plot of the difference between the automated and manual muscle volume quantification methods against the average leg volume in the 10 participants before bed rest. Grey line indicates the average of the differences and the dotted lines indicate the 95% limits of agreement.

Total RNA extraction and targeted muscle mRNA expression measurements

Procedures for total RNA extraction and muscle mRNA expression measurements using a microfluidic gene card approach (191 targets) are described in **Chapter 3**.

Statistical Analysis

The statistics, calculations and graphs presented were completed using SPSS software (version 24; SPSS, Chicago, IL) or GraphPad Prism (version 7; Graphpad Software Inc, USA). Data were first assessed for their suitability for parametric statistical testing using Shapiro-Wilks to assess the distribution of data. A two-way analysis of variance (ANOVA) for repeated measures was performed to detect any main effects of visit (pre-bed rest vs post-bed rest vs post remobilisation) and time (pre vs post clamp) on outcome measures. Post-hoc analysis was performed using Bonferroni post-hoc test. One-way repeated measures ANOVA was used to measure single variables over time and Student's t test was used when an ANOVA was not appropriate. All data are presented as mean ± SEM. Statistical significance was declared at $p<0.05$.

4.4 Results

4.4.1 Demographics

Participants had an average age of 24 ± 1 years, with a BMI of 22.7 ± 0.6 kg/m^2 and a lean mass of 56.6 ± 2.1kg. Full baseline characteristics are shown in Chapter 3 (Table 3.1). Compared with before bed rest there was no significant change in body weight after bed rest (70.7 ± 3.2 kg vs 70.6 ± 3.2 kg, $p<0.05$). Participants met the prescribed energy intake targets before, during and after bed rest (Table 4.1).

Table 4.1. Energy intake and macronutrient content in the acute bed rest study. Energy Intake in kilojoules (kJ/day) and macronutrient content (g/day) prescribed and actual pre bed rest, during bed rest and during remobilisation. Data are mean ± SEM.

Parameter	**Acute bed rest**
Average energy intake prescribed (kJ/day) pre bed rest	11041 ± 338
Average energy intake actual (kJ/day) pre bed rest	10960 ± 319
Difference prescribed vs actual (kJ/day) pre bed rest	-287 ± 88
Carbohydrate (g/day) pre bed rest	291 ± 14
Protein (g/day) pre bed rest	83 ± 4

Fat (g/day) pre bed rest	79 ± 4
Average energy intake prescribed (kJ/day) during bed rest	8792 ± 275
Average energy intake actual (kJ/day) during bed rest	8950 ± 244
Difference prescribed vs actual (kJ/day) during bed rest	158 ± 23
Carbohydrate (g/day) during bed rest	250 ± 26
Protein (g/day) during bed rest	73 ± 8
Fat (g/day) during bed rest	68 ± 5
Average energy intake prescribed (kJ/day) remobilisation	11041 ± 338
Average energy intake actual (kJ/day) remobilisation	10915 ± 276
Difference prescribed vs actual (kJ/day) remobilisation	126 ± 45
Carbohydrate (g/day) remobilisation	287 ± 12
Protein (g/day) remobilisation	80 ± 3
Fat (g/day) remobilisation	74 ± 2

4.4.2 Impact of 3 days bed rest and structured remobilisation on whole-body glucose disposal

Figure 4.7 shows whole-body glucose disposal standardised to whole-body muscle volume (litres). Acute bed rest resulted in a 17% reduction in insulin-stimulated whole-body glucose disposal ($p<0.01$), which was fully restored by structured remobilisation.

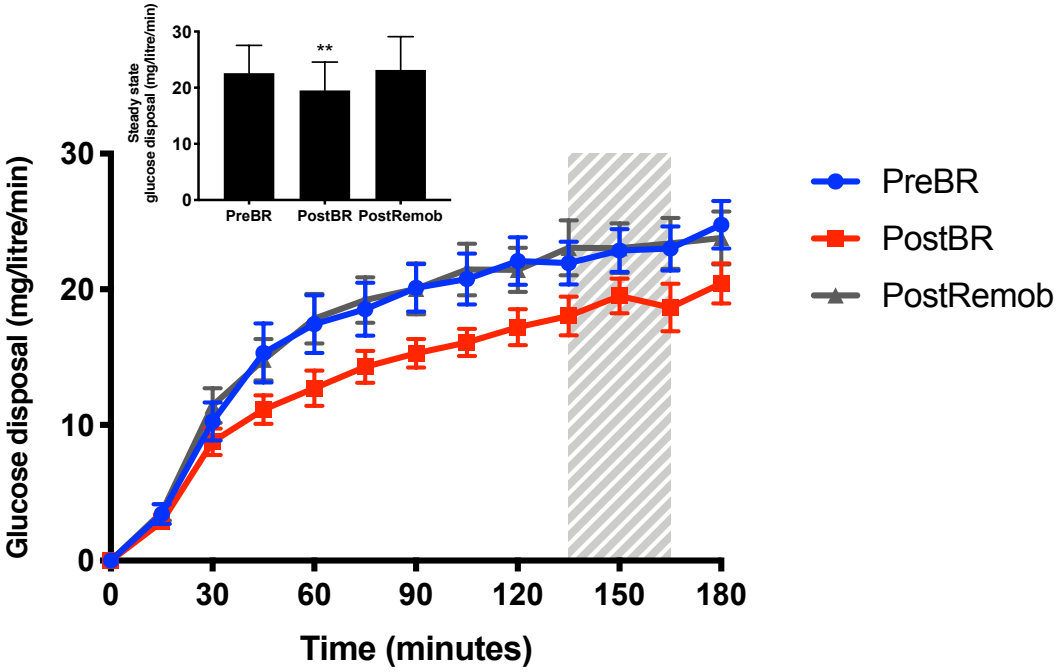

Figure 4.7. Whole-body glucose disposal during the hyperinsulinaemic euglycaemic clamp in acute bed rest. Whole-body glucose disposal in the acute bed rest experiment standardised to whole-body muscle volume (litres) at each time point (measured using MRI) with steady state values highlighted by the grey shaded area and separate histogram. Values are mean ± SEM. (n=10)

4.4.3 Impact of 3 days bed rest and structured remobilisation on leg glucose uptake

Table 4.2 summarises the leg arterialised-venous-venous (AV-V) difference, femoral arterial blood flow and leg glucose uptake standardised to leg muscle volume (litres) calculated at each time point (before bed rest, after bed rest and after remobilisation). Compared with before bed rest, there was a 45% reduction in resting steady-state leg glucose uptake, standardised to leg muscle volume (measured using MRI), after bed rest ($p<0.01$). In addition, leg glucose uptake was not fully restored after 3 days' exercise-supplemented remobilisation of the limb, being 30% lower than before bed rest ($p<0.05$). The reduction in insulin-stimulated leg glucose uptake after bed rest was paralleled by a 38% reduction in leg blood flow compared to before bed rest ($p<0.01$). Resting leg blood flow after the period of exercise-supplemented remobilisation was no different from before bed rest ($p=0.29$). Compared with before bed rest, there were no differences in the steady-state AV-V balance during the clamp after bed rest ($p=1.00$) or after remobilisation ($p=0.99$). Compared with before bed rest, there were no significant differences in baseline (0 minutes) leg AV-V difference, blood flow or glucose uptake after bed rest ($p>0.05$) (data not shown).

*Table 4.2. Arterialised-venous-venous difference, blood flow and leg glucose uptake. Steady state leg arterialised-venous-venous (AV-V) difference (mmol/l), blood flow (cm^3/min) and leg glucose uptake (mg/litre leg muscle volume /min) measured before bed rest (Pre BR), after bed rest (Post BR) and after ESR (Post ESR) *, p<0.05, **, p<0.01 compared with Pre bed rest. BR, bed rest. Values are mean ± SEM.*

	Time point	Steady-state (Average 135-165 minutes)
AV-V difference (mmol/L)	Pre BR	1.44 ± 0.2
	Post BR	1.23 ± 0.11
	Post ESR	1.24 ± 0.1
Blood Flow (cm^3/min)	Pre BR	424 ± 47.5
	Post BR	262 ± 24.2**
	Post ESR	331 ± 36.7 (p=0.052 compared with Post BR)
Leg Glucose Uptake (mg/litre /min)	Pre BR	17.6 ± 2.4
	Post BR	9.6 ± 1.2**
	Post ESR	12.4 ± 2.5*

4.4.4 Muscle glycogen

Figure 4.8 shows the change in muscle glycogen in response to bed rest and remobilisation and before and during the insulin clamp. Before bed rest there was a 36% increase in muscle glycogen content as a result of the insulin clamp (p=0.056). However, a corresponding increase in muscle glycogen content was not observed after bed rest (0.69) or ESR (p=0.57) in response to insulin.

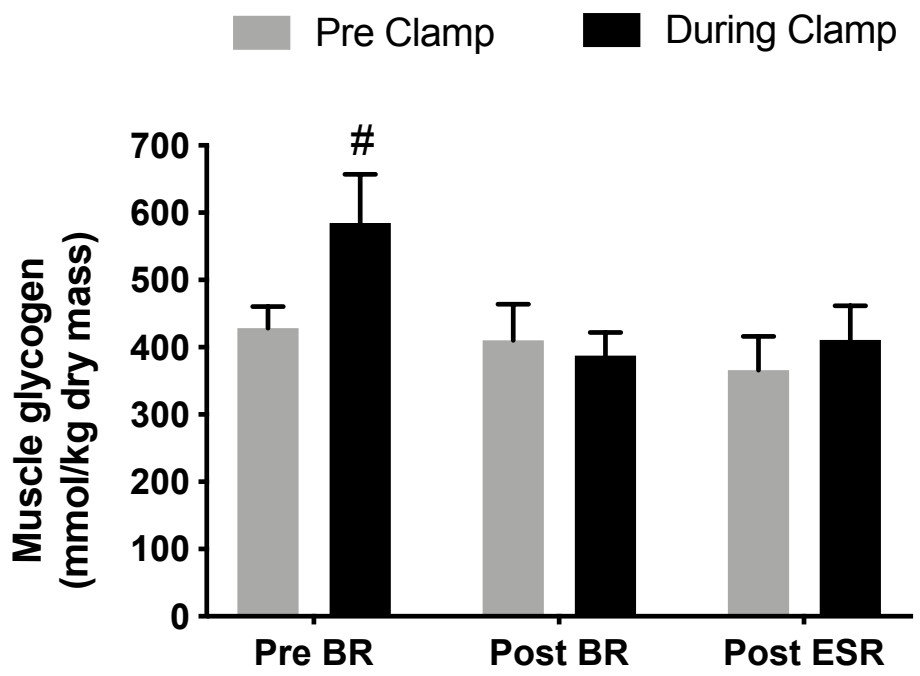

Figure 4.8. Muscle glycogen content. Muscle glycogen (mmol/kg dry mass), before bed rest (Pre BR) and after bed rest (Post BR) and after rehabilitation (Post Remob) and before (grey bars) and in the final 30 minutes (black bars) of the hyperinsulinaemic euglycaemic clamp. # p=0.056 vs pre clamp before bed rest, Values are mean ± SEM.

4.4.5 The impact of 3 days bed rest and structured remobilisation on muscle protein turnover

4.4.5.1 Myofibrillar fractional synthetic rate

Compared to before bed rest, myofibrillar FSR was unchanged over the first day of bed rest but had declined by 43% by day 3 ($p<0.05$, Fig 4.9a). Myofibrillar FSR was fully restored by exercise-supplemented remobilisation, but FSR in the non-exercised leg was 35% less compared to the exercised leg ($p<0.1$; Figure 4.9b).

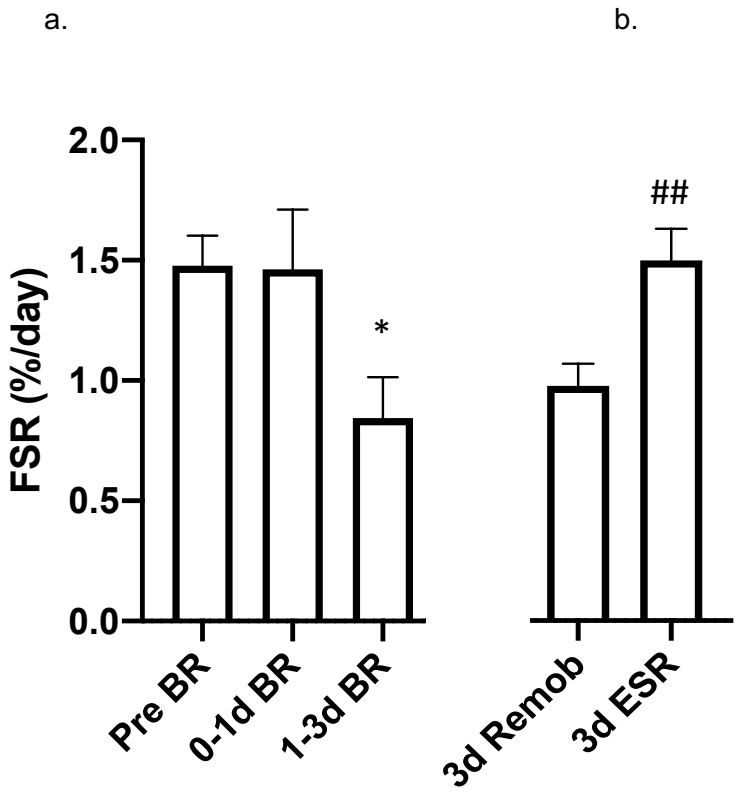

Figure 4.9. Myofibrillar protein synthesis. a) Myofibrillar fractional synthetic rate (FSR) in %/day a) before bed rest (Pre BR), after 24-hours of bed rest (0-1d

*BR), and between day 1 and 3 of bed rest (1-3d BR), *, p<0.05 vs Pre BR on Student's t-test. b) FSR (%/day) after remobilisation in the exercised leg (3d exercise supplemented remobilisation [ESR]) and the non-exercised leg (3d Remob). ##, p<0.1 vs non-remobilised leg on Student's t-test. Values are mean ± SEM (n=10)*

4.4.5.2 Muscle Protein breakdown

Isotopic enrichment of 3-MeH in plasma on day 0 and day 2 is shown in Figure 4.10a, and from this enrichment decay rate constants (k) were calculated, shown in Figure 4.10b. Over the 7 hours of sampling, plasma 3-MeH k decreased 30% within the first 48 hours (from day 0 to day 2) of bed rest indicating a decrease in the rate of whole-body MPB (p<0.05).

a

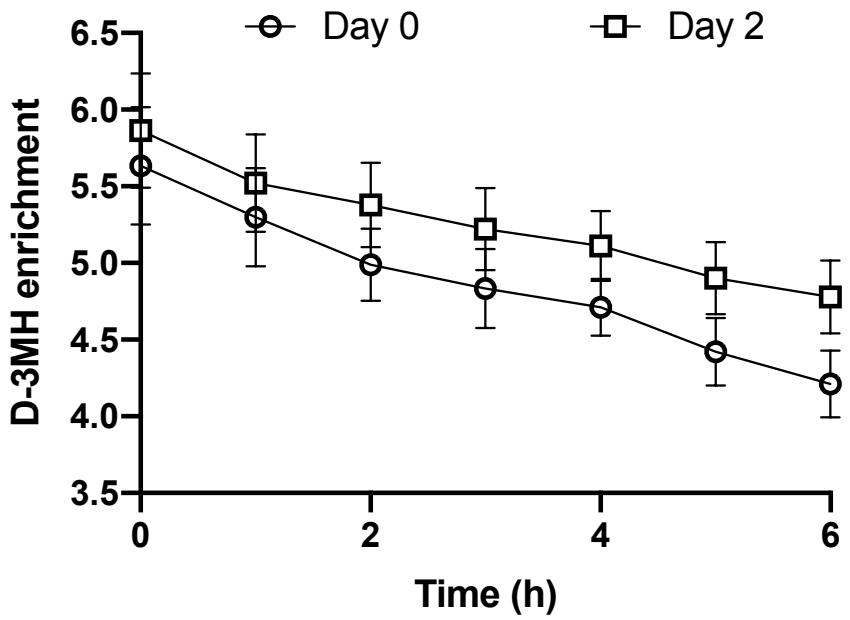

b.

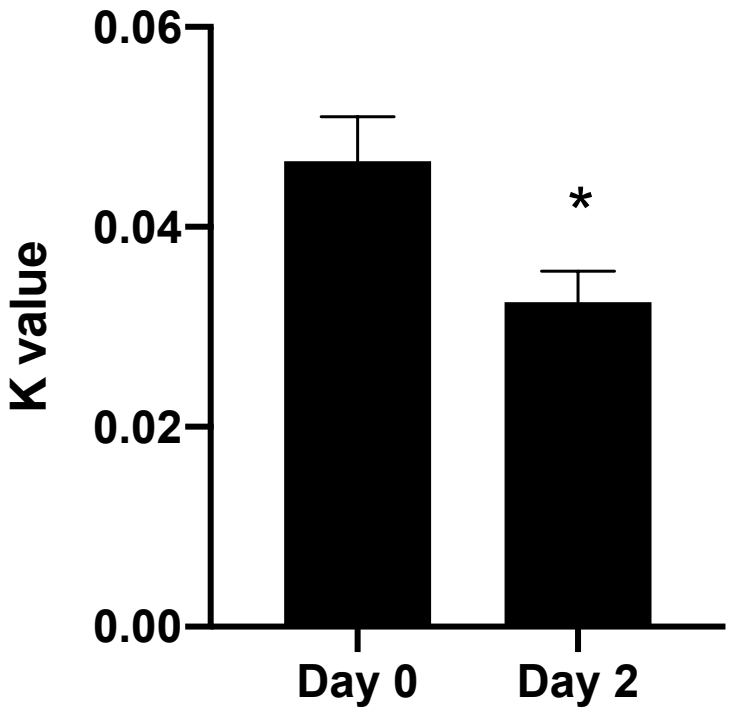

*Figure 4.10. Whole-body muscle protein breakdown. a) Isotopic enrichment of 3-MeH in plasma the day following oral stable isotope tracer administration on day 0 and day 2 of bed rest in units per hour and b) corresponding enrichment decay constants (k). *, p<0.05 vs Day 0 on Student's t-test. Values are mean ± SEM. n=9.*

4.4.6 The impact of 3 days bed rest and structured remobilisation on whole-body and leg muscle volume

The changes in muscle volume (for the whole-body and leg) are shown in Table 4.3. Data for the torso, arm and calf are included in Appendix 3 (**Section 7.12**). Compared with before bed rest, there was no change in whole-body muscle volume after bed rest (p=0.12) or after exercise-supplemented remobilisation (p=0.64). However, bed rest resulted in a -2.6% (p<0.01) and -2.5% (p<0.01)

reduction in the right and left leg muscle volume (MRI-derived), respectively, which was restored in the exercise-supplemented remobilised leg, but not the leg exposed to ambulation alone ($p<0.01$).

*Table 4.3. Muscle volume changes measured using MRI. Remob, Remobilisation leg. *, $p<0.05$, **, $p<0.01$ vs Pre bed rest. Values are mean ± SEM.*

	Time point	ESR Leg	Remobilised Leg
Whole-body % change	Post Bed rest	-0.7 ± 0.3%	n/a
	Post Remob	-0.5 ± 0.3%	n/a
Leg % change	Post Bed rest	-2.6 ± 0.54%**	-2.5 ± 0.6%**
	Post Remob	-0.7 ± 0.3%	-2.3 ± 0.3%**

4.4.7 Ingenuity Pathway Analysis (IPA)

Muscle mRNA expression was quantified using low-density array cards in the pre insulin clamp biopsies before and after bed rest and after ESR (in the leg that underwent 3 days of resistance exercise). Cellular functions identified by IPA as being altered as a result of bed rest and structured remobilisation relative to pre bed rest are depicted in Figure 4.11 (note this does not depict the direction of change). There were 12 cellular functions altered, the most notably affected [-log (*p* value) ≥ 20] being 'cell death and survival', 'cell morphology' and 'cellular development', 'cellular growth and proliferation' and 'organismal injury and abnormalities'.

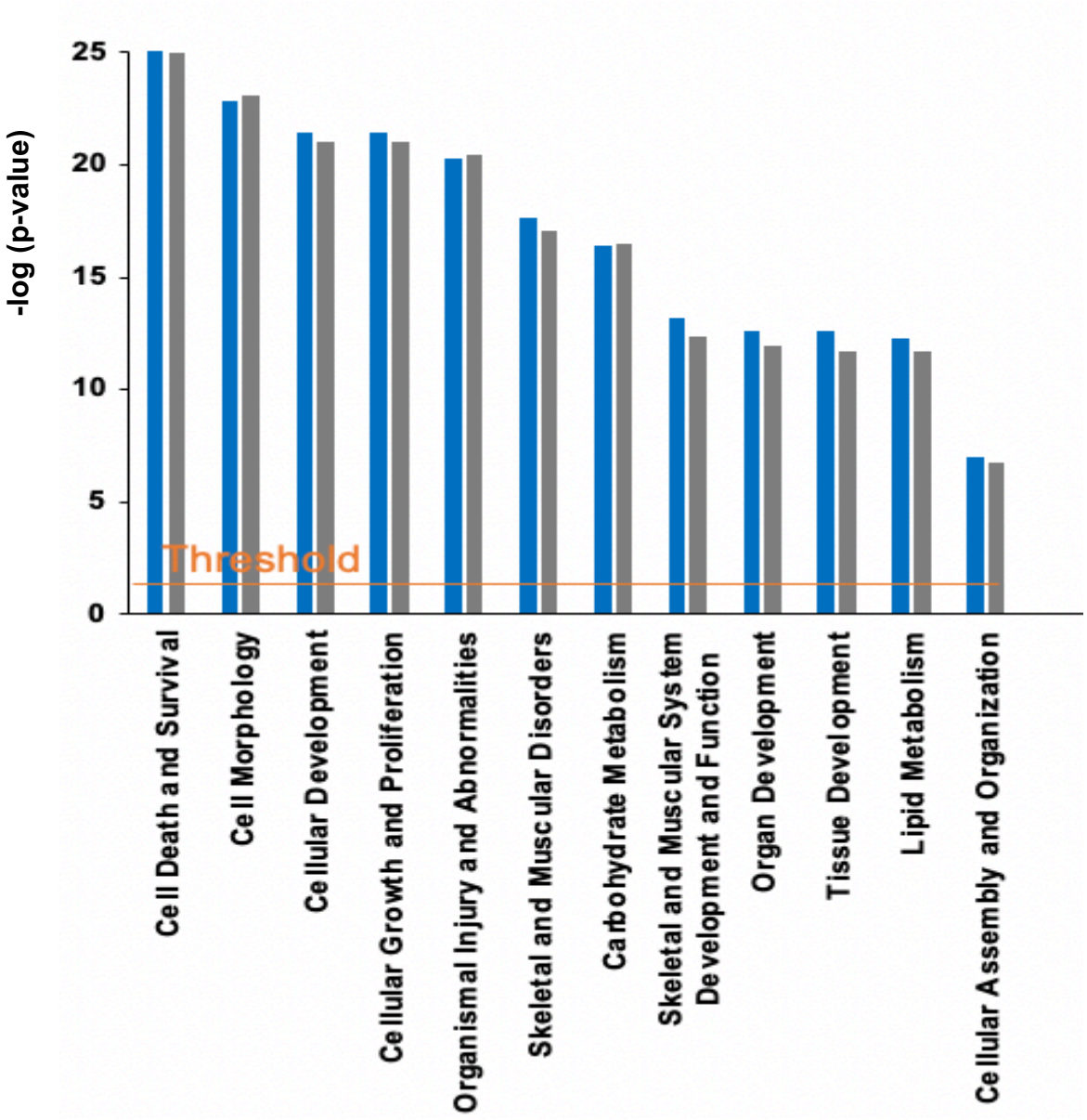

Figure 4.11. Muscle cellular functions in acute bed rest. Cellular functions identified by IPA as being most altered in muscle as a result of bed rest (blue bars) and remobilisation (grey bars) relative to pre bed rest based on muscle mRNA expression data generated using the low-density micro-array cards. The x-axis displays cellular functions and the y-axis displays -log of the p value. The threshold line corresponds to a p value of 0.05.

Those most relevant to the study aims will be discussed below and the remaining functions and predicted cellular events are included in Appendix 3 (Supplementary Figure 7.6 and 7.7). In the case of carbohydrate metabolism (Figure 4.12), after bed rest 40 transcripts were altered in abundance compared with before bed rest (39 upregulated and one, IRS1, downregulated), and based on these collective responses IPA strongly predicted the activation of 'glycolysis', 'quantity and synthesis of carbohydrate' and 'synthesis of glycogen'. After remobilisation there were 36 transcripts altered compared with pre bed rest (29 upregulated and 7 downregulated), with the activation of quantity and synthesis of carbohydrate being predicted. In the case of cell morphology, 34 transcripts were altered in abundance following bed rest (33 upregulated and one downregulated) and based on these collective differences IPA strongly predicted the activation of 'autophagy' and 'autophagy of cells'. After remobilisation 34 transcripts were altered (29 upregulated and 5 downregulated), and conversely to best rest, IPA predicted the inhibition of 'depolarisation of mitochondria' and 'macroautophagy of cells'. Activation of 'autophagy of cells 'was also predicted, but with less confidence compared with after bed rest (Figure 4.13).

For the functions cellular development and cellular growth and proliferation, the predicted cellular events generated by IPA relative to before bed rest were the same after bed rest and remobilisation. In the case of the function cellular development both after bed rest and after remobilisation there were 28 transcripts altered with a predicted activation of 'differentiation of muscle cells', 'differentiation of muscle', 'proliferation of muscle cells',

‘proliferation of myoblasts’ and inhibition of ‘differentiation of myoblasts’, which were all predicted with high confidence (Figure 4.14). Similarly, in the case of cellular growth and proliferation after bed rest there were 27 transcripts altered (26 upregulated and one, IRS, downregulated) with a predicted activation of ‘proliferation of connective cell tissues’ and ‘proliferation of muscle cells’ with high confidence. After remobilisation there were 26 transcripts altered (23 upregulated and 3 transcripts downregulated) with a predicted activation of ‘proliferation of connective tissue cells’ and ‘proliferation of muscle cells’ with high confidence (Figure 4.15). The gene predictions of networks relevant to the aims of this chapter have been summarised in Table 4.3. ‘

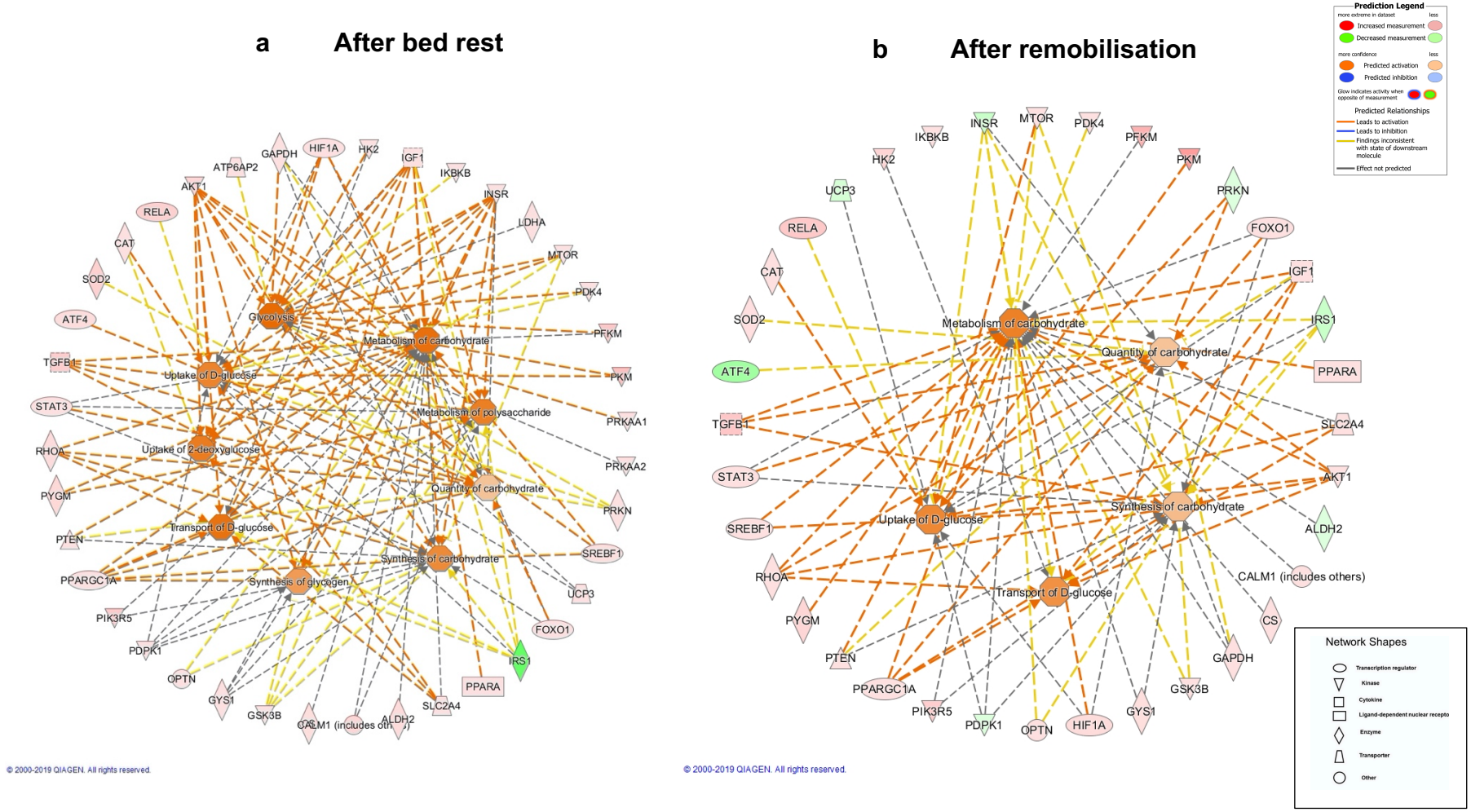

Figure 4.12. Pathway analysis for carbohydrate metabolism. Ingenuity Pathway Analysis schematic highlighting mRNAs differentially regulated from baseline in the carbohydrate metabolism network (outer ring) and the predicted cellular events (inner octagons) associated with these collective changes a) after bed rest and b) after remobilisation compared with pre bed rest.

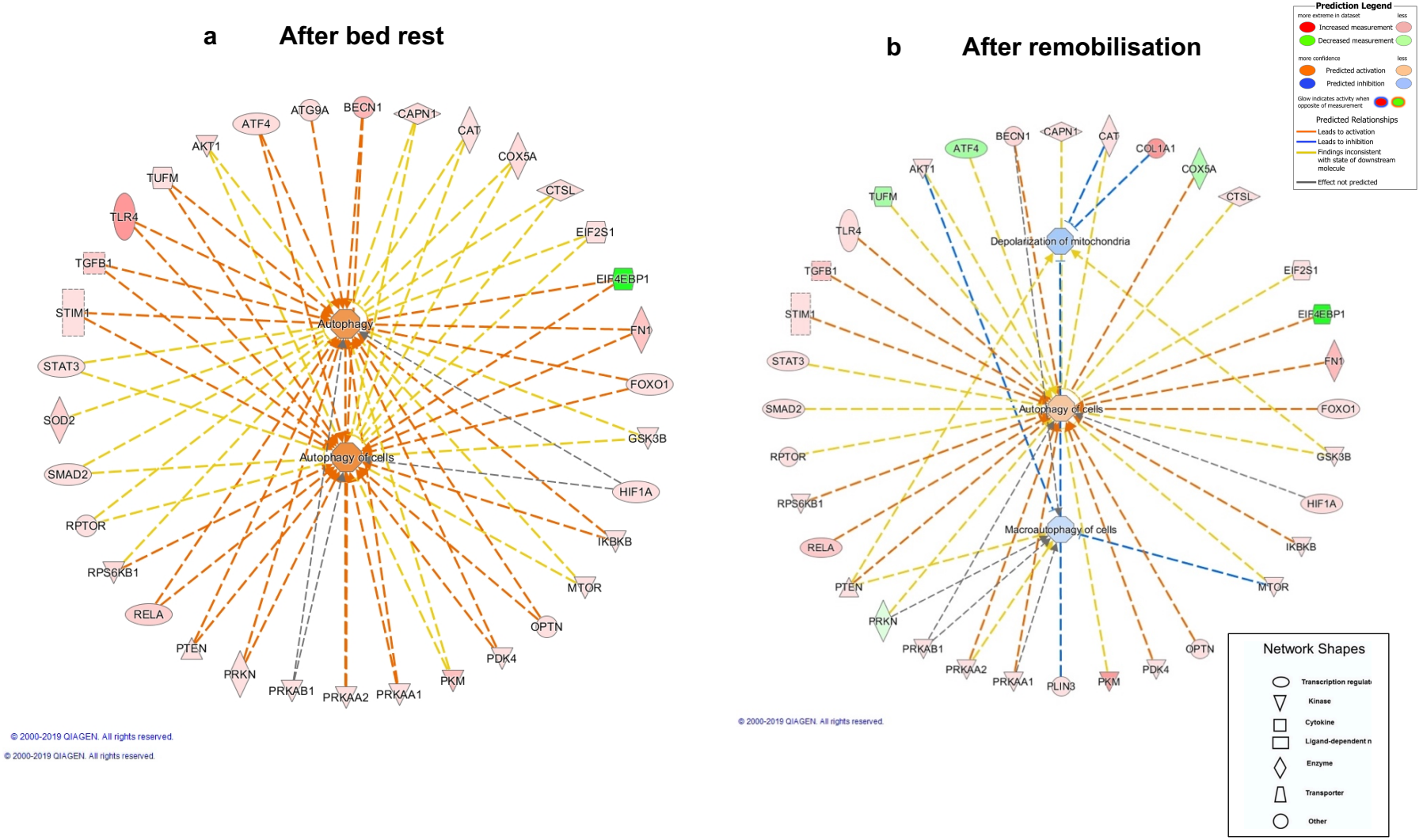

Figure 4.13. Pathway analysis for cell morphology. Ingenuity Pathway Analysis schematic highlighting mRNAs differentially regulated from baseline in the cell morphology network (outer ring) and the predicted cellular events (inner octagons) associated with these collective changes a) after bed rest and b) after remobilisation compared with pre bed rest.

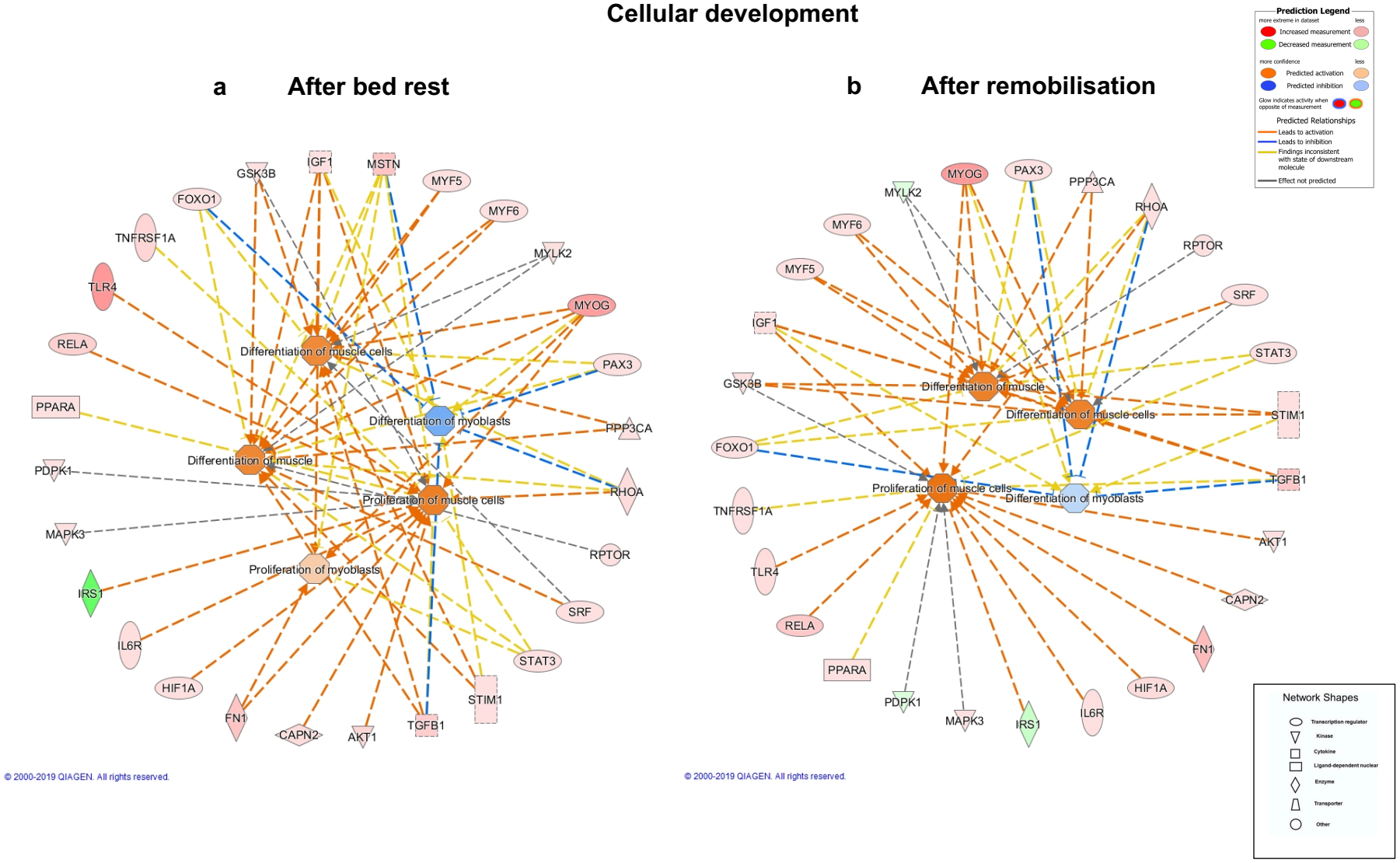

Figure 4.14. Pathway analysis for cellular development. Ingenuity Pathway Analysis schematic highlighting mRNAs differentially regulated from baseline in the cellular development network (outer ring) and the predicted cellular events (inner octagons) associated with these collective changes a) after bed rest and b) after remobilisation compared with pre bed rest.

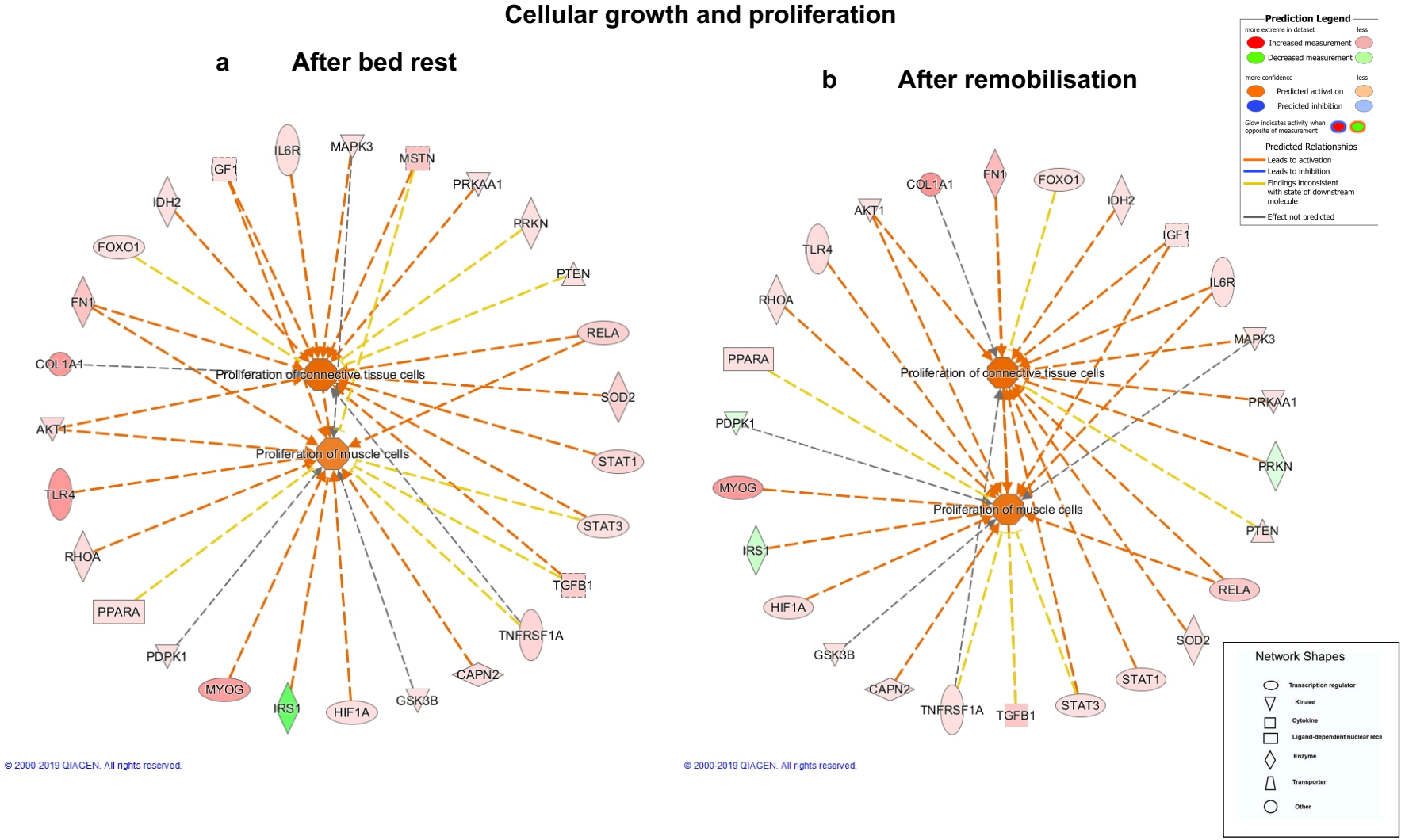

Figure 4.15. Pathway analysis for cellular growth and proliferation. Ingenuity Pathway Analysis schematic highlighting mRNAs differentially regulated from baseline in the cellular growth and proliferation network (outer ring) and the predicted cellular events (inner octagons) associated with these collective changes a) after bed rest and b) after remobilisation compared with pre bed rest.

Table 4.3. Summary of key muscle cellular functions after bed rest and remobilisation. Summary of the cellular functions relevant to the study and their number of differentially regulated mRNAs after bed rest and after remobilisation relative to before bed rest, and their associated predicted cellular events by IPA.

	After Bed Rest		After Remobilisation	
Cellular Function	**Number of differentially regulated mRNAs**	**IPA prediction of cellular events**	**Number of differentially regulated mRNAs**	**IPA prediction of cellular events**
Carbohydrate metabolism	40 transcripts (39 upregulated, 1 downregulated)	Activation of glycolysis, quantity, synthesis of carbohydrate and synthesis of glycogen	36 transcripts (29 upregulated and 7 downregulated)	Activation of quantity and synthesis of carbohydrate
Cell Morphology	34 transcripts (33 upregulated and one downregulated)	Activation of autophagy and autophagy of cells	34 transcripts (29 upregulated and 5 downregulated)	Inhibition of depolarisation of mitochondria and macroautophagy of cells
Cellular development	28 transcripts (27 upregulated and 1 downregulated)	Activation of differentiation of muscle cells, differentiation of muscle, proliferation of muscle cells, proliferation of myoblasts and inhibition of differentiation of myoblasts	28 transcripts (25 upregulated and 3 downregulated)	Activation of differentiation of muscle cells, differentiation of muscle, proliferation of muscle cells and inhibition of differentiation of myoblasts
Cellular growth and proliferation	27 transcripts (26 upregulated and 1 downregulated)	Activation of proliferation of connective cell tissues and proliferation of muscle cells	26 transcripts (23 upregulated and 3 downregulated)	Activation of proliferation of connective tissue cells and proliferation of muscle cells

4.4.8 Serum Insulin, TAGs and plasma NEFA

There was no difference in fasted serum insulin concentration after bed rest or remobilisation compared with before bed rest but was a significant decrease in the steady-state serum insulin concentration during the clamp after remobilisation ($p<0.05$; Table 4.4). There was a reduction in fasted plasma NEFA after remobilisation compared with before bed rest ($p<0.05$) but there was no significant difference in steady-state NEFA after bed rest or after remobilisation. There were no changes in fasted or steady-state serum TAGs after bed rest but there was a decrease in fasted ($p<0.05$) and steady-state ($p<0.001$) TAGs after remobilisation.

*Table 4.4. Serum insulin, TAG and NEFA in acute bed rest. Fasted and steady state serum insulin (mIU/L), plasma NEFA (mmol/L) and serum TAGs (mmol/L) measured before bed rest (Pre BR), after bed rest (Post BR) and after remobilisation (Post Remob). * p<0.05 compared with Pre BR. Values are mean ± SEM.*

		0 (fasted)	Steady-state
Serum insulin (mIU/L)	Pre BR	6.44 ± 1.67	106.7 ± 3.2
	Post BR	8.81 ± 1.6	107.1 ± 3.4
	Post Remob	7.19 ± 1.1	95.6 ± 2.9*
Plasma NEFA (mmol/L)	Pre BR	0.53 ± 0.04	0.01 ± 0.002
	Post BR	0.57 ± 0.1	0.01 ± 0.001
	Post Remob	0.38 ± 0.05*	0.01 ± 0.001

Serum TAGs (mmol/L)	Pre BR	0.69 ± 0.1	0.40 ± 0.04
	Post BR	0.76 ± 0.06	0.48 ± 0.03
	Post Remob	0.54 ± 0.05*	0.34 ± 0.03**

4.5 Discussion

The study described in Chapter 3 demonstrated that as little as 3 days of bed rest reduced insulin-stimulated whole-body glucose disposal and muscle glycogen storage in volunteers maintained in energy balance compared with the pre bed rest state. As far as I am aware, simultaneous measurements of both insulin-stimulated whole-body glucose disposal, limb glucose uptake and muscle protein turnover have not been undertaken before in the same participants undergoing short durations of bed rest (<5 days) or post-bed rest remobilisation, with most previous studies predominantly focussed on glucose disposal/insulin sensitivity or muscle protein turnover alone in response to bed rest. Indeed, it is unclear if the restoration in whole-body and limb glucose uptake and MPS with remobilisation is as rapid as their reduction with bed rest.

Principal findings from this study are the simultaneous reductions in whole-body glucose disposal, leg glucose uptake, and insulin-stimulated muscle glycogen storage as well as MPS and whole-body MPB after 3 days of bed rest. In addition, ESR was able to restore the decrease in whole-body

glucose disposal, leg muscle volume and MPS, but not insulin-stimulated leg glucose uptake or muscle-glycogen content. Furthermore, ambulation alone was unable to restore the decrease in leg muscle volume and MPS in the control leg. A key novel finding in this study is the mismatch in the restoration of leg glucose uptake and muscle glycogen storage following ESR after 3 days of bed rest compared with leg muscle volume and MPS.

A primary finding from this study was the failure of 3 days resistance exercise-supplemented remobilisation to restore deficits in insulin-stimulated leg glucose uptake or muscle glycogen storage induced by bed rest. This decrement in leg glucose uptake during the insulin clamp after bed rest appeared to be largely explained by a reduction in leg blood flow. Our findings confirm previous studies which have demonstrated a reduction in limb glucose uptake after 24-hours of unilateral forearm immobilisation which was isolated to the immobilised limb (Burns et al. 2021) and 7 days of bed rest (Mikines et al. 1991). Previous studies have reported vascular dysfunction after bed rest, including a reduction in calf blood flow after 5 days' bed rest, measured using venous occlusion plethysmography (Hamburg et al. 2007). Other studies also report a diminished effect of insulin on the stimulation of skeletal muscle blood flow, both in the forearm (measured with venous occlusion plethysmography) after 10 days' bed rest (Sonne et al. 2010) and in the leg (after 7 days bed rest), with a preserved AV difference across the leg (Mikines et al. 1991). Importantly, the deficits in leg glucose uptake and glycogen storage in this study persisted after exercise-supplemented remobilisation. Evidence suggests that a single bout of resistance exercise improves insulin sensitivity in healthy volunteers,

measured using an intravenous insulin tolerance test (Koopman et al. 2005). However, it is unclear what type, intensity and duration of activity is required to fully restore muscle insulin sensitivity following bed rest, or what duration of free living alone would completely restore it. In a previous 21 day bed rest study in healthy, sedentary young males maintained in energy balance, 4 days of normal ambulation was unable to restore whole-body glucose tolerance (measured using an oral glucose tolerance test), and 5-14 days of normal ambulation was required to restore impaired glucose tolerance (Heer et al. 2014). I am not aware of any study that has examined the effect of exercise-supplemented remobilisation on both insulin-stimulated leg glucose uptake and muscle glycogen storage following short duration disuse, and the present findings are an important addition to the literature.

Alongside the reductions in limb glucose uptake and storage after bed rest there was a decrease in MPS which coincided with a ~2.5% decrease in leg volume. However, there was also a decrease in whole-body MPB over the initial 2 days of bed rest. Early studies utilising intravenous amino acid tracer techniques to estimate acute (~3 to 4 hours) MPS, reported a decline in both fasted and fed MPS following >7 days of immobilisation (de Boer et al. 2007; Glover et al. 2008). However, these studies do not inform upon more chronic MPS responses over time and studies evaluating chronic MPS rates in short-duration immobilisation are lacking. A study utilising 4 days of unilateral leg immobilisation in healthy males demonstrated reductions in chronic MPS with no change in MPB reported (Brook et al. 2022). I observed a decline in MPS between 1 and 3 days of bed rest, but not within the first 24 hours of the onset

of immobilisation. A previous study reported no change in MPS after 2 days of unilateral lower limb suspension (Kilroe, Fulford, Holwerda, et al. 2020) but to my knowledge, this chapter reports the earliest changes in integrated MPS thus far. The discrepancy in our MPB findings with those of Brook et al. may be due to the different models of immobilisation employed, the different approaches in measuring MPB, the timeframe during which MPB was determined (2 days vs 4 days) and/or that volunteers in the current study were maintained in energy balance and therefore daily energy intake was reduced during bed rest which reduced the rate of MPB. Tesch et al. reported an increase in muscle protein breakdown after 72 hours of unilateral leg immobilisation; demonstrated by a 44% increase in interstitial 3-methylhistidine within the *vastus lateralis* measured using microdialysis (Tesch et al. 2008). However the authors in this paper did not measure local blood flow, so the elevated 3-MeH could have been attributed to decreased washout from the tissue as a result of immobilisation (Rennie, Phillips, and Smith 2008). In longer duration immobilisation, a study estimating MPB during a 9.5 day and 15 day duration spaceflight, and a 17-day bed rest experiment, showed no change in urinary 3-MeH excretion in either spaceflight or bed rest (Stein and Schluter 1997). A further study utilising deuterated water, determined MPB to be lower in older individuals during 2 weeks of lower limb immobilisation compared with a 2 week retraining period (Dideriksen et al. 2020). Whilst we found that whole-body myofibrillar protein breakdown was in fact decreased within the first 2 days of bed rest, the data in this chapter do not definitively inform on what was happening beyond 2 days of bed rest or what was occurring at a muscle cellular level.

Three days of resistance ESR, but not ambulation alone, was able to fully restore bed rest-associated decreases in MPS. This was paralleled by a restoration of leg muscle volume in the same limb. Previous studies measuring the restoration MPS *in vivo* in humans after a short period of remobilisation after bed rest are lacking. Rodent studies have found MPS rates to be restored in as little as 6 hours after 7 days of hindlimb immobilisation of the *gastrocnemius* (Tucker, Seider, and Booth 1981). However, the metabolic rates of rodents are substantially higher compared with humans, limiting the generalisation of these findings. Although previous studies in humans have shown restoration of MPS in the leg with remobilisation after 5 days of bed rest, these have been after prolonged high intensity resistance exercise rehabilitation programmes of 8 weeks duration (Tanner et al. 2015). The design of study presented in this chapter allows for the comparison with the control leg to scrutinise the impact of free living versus resistance exercise plus free living on restoration of MPS. These findings have important clinical implications as it indicates that MPS is acutely sensitive to a resumption of muscular contraction via a short period of resistance exercise known to exert an anabolic stimulus, but more modest resumption of muscle contraction in the form of ambulation is insufficient to fully restore MPS rates and muscle mass to baseline after only 3 days. This should be considered when designing countermeasures following short periods of disuse, such as following acute illness or a hospital stay, which is currently not the case in UK clinical care packages.

The changes in muscle mRNA expression of genes related to insulin sensitivity, fuel metabolism and mass regulation in response to acute bed rest

and exercise supplemented remobilisation were very similar in magnitude, as were the IPA predicted cellular events arising from these changes. For example, in the case of 'cellular growth and proliferation', where you might expect differences in the direction of change of mRNAs between the bed rest state and structured remobilisation, IPA-predicted changes in cellular events with high confidence that were very similar, namely 'proliferation of connective cell tissues' and 'proliferation of muscle cells', despite measurable differences in MPS and leg muscle volume after bed rest and resistance exercise-supplemented remobilisation. Given MPS declined after bed rest but restored after structured remobilisation in the ESR leg, this suggests that the regulation of MPS in response to acute bed rest and remobilisation is unlikely to be controlled by gene transcription. This is in contrast to findings from Chapter 3 in which fuel oxidation changes manifested after 56 days of bed rest were reflected by muscle gene changes identified by IPA at this same timepoint. Regulation of MPS on an hourly basis is predominantly regulated at a translational level, with changes in phosphorylation of the Akt-MTOR-p70S6 pathway proteins playing a crucial role (Proud 2007). Our findings are in alignment with the acute responses of MPS seen following feeding and exercise, which do not appear to be regulated by transcription (Drummond et al. 2012; Drummond et al. 2009). Interestingly, there was a disparity in predicted cellular events related to cellular morphology between the bed rest and remobilisation state, with the activation of 'autophagy' in bed rest, but inhibition of 'macroautophagy' predicted after remobilisation. Previous studies have shown that autophagy-related gene and protein expression increase

during 2 weeks of immobilisation which mirror changes in muscle mass and return to baseline after 2 weeks of rehabilitation in humans (Møller et al. 2019). Overall, these findings point to acute mRNA abundance changes as not being central to the regulation of muscle fuel and protein metabolism during acute bed rest and short-term exercise rehabilitation following bed rest.

After 3 days of bed rest there was a decrease in muscle volume in the lower body, which was not mirrored by parallel changes in the upper body and torso (data presented in Appendix 3). This suggests a variability in the degree and location of muscle loss. Previous limb immobilisation models have suggested that certain muscle groups are “atrophy susceptible” whilst others are “atrophy resistant” (Bass et al. 2021). MPS rates were only measured in the *vastus lateralis* in response to immobilisation so I cannot draw conclusions as to the differential mechanisms that may explain this. However, in the bed rest model, participants can turn over in bed with one shoulder in contact with a pillow at all times, eat and work on laptops whilst supine or prone, and thus upper body muscle use is not as severely restricted compared to the lower body. This is in contrast to spaceflight where muscle mass loss in the paraspinal muscles is significant due to the complete unloading of the spinal musculature (Chang et al. 2016). Another perhaps more likely explanation is that lower limb musculature is loaded more frequently in everyday living and thus at the cessation of loading, those muscles with the higher muscle protein turnover rates will experience greater atrophy. A potential confounding factor however is the cephalic fluid shifts with head down tilt bed rest, where there may be apparent change of muscle volume, when in fact net muscle protein loss was

unchanged (Conley et al. 1996). Most bed rest studies have focussed on muscle mass loss in the lower extremity only, with few studies taking measures of upper and lower body concurrently, and none that I am aware of after only 3 days of bed rest. Of the few that have, there appears to be a preferential atrophy and strength loss of muscles in the lower body, and in the extensor rather than flexor muscle groups (Gogia et al. 1988). In this study, 3 days of ESR was able to restore muscle volume and FSR in the quadriceps, but not in the control leg or calf musculature (which were subjected to ambulation alone), indicating that a short duration of free living alone was not sufficient to restore muscle mass losses throughout all of the muscles of the lower leg.

In summary, acute bed rest caused a decline in insulin-stimulated leg glucose uptake and muscle glycogen storage in healthy, young volunteers, as well as reductions in muscle volume, integrated MPS and whole-body MPB in the same individuals. However, 3 days of resistance exercise-supplemented remobilisation after bed rest restored muscle volume and MPS, but leg glucose uptake and muscle glycogen storage remained depressed. This chapter provides novel insight of the mechanistic regulation of leg glucose uptake and muscle mass during immobilisation and subsequent short-term structured remobilisation in humans, which also has implications for maximising effective recovery following short duration immobilisation or bed rest.

Chapter 5

The impact of ankle fracture surgical fixation and subsequent limb immobilisation versus limb immobilisation alone on muscle architecture and protein metabolism in human volunteers.

5.1 Introduction

Muscle atrophy is a phenotypic trait of both immobilisation and inflammation and trauma. The study in Chapter 4 demonstrated that 3 days of bed rest resulted in a reduction in leg muscle volume, leg MPS and whole-body MPB, as well as reductions in whole-body glucose disposal, leg glucose uptake and insulin-simulated muscle glycogen storage. Additionally, these MPS changes in response to 3 days bed rest and subsequent remobilisation appeared not to be associated with changes in muscle mRNA transcript abundance in IPA-predicted cellular functions related to regulation of muscle mass and fuel oxidation. As demonstrated by others and the previous chapter, the suppression of MPS appears to be the primary driver of muscle mass loss in immobilisation in humans (de Boer et al. 2007). Furthermore, muscle anabolic resistance has been reported in response to immobilisation (Glover et al. 2008), whilst uncertainty exists whether changes in MPB contribute to disuse muscle atrophy in human volunteers. Previous research in rodents has suggested increases in MPB may be implicated early in disuse-associated

muscle mass loss (Taillandier et al. 2003; Abadi et al. 2009). However the generalisability of rodent models to humans is problematic due to the inherent differences in metabolic rate between young rodents and humans, and the physiological stress induced by hindlimb immobilisation models (Rennie et al. 2010). Evidence in humans is mixed with some reporting increased mRNA levels of MAFbx and MURF-1 after 3 days of ULLS (Gustafsson, Osterlund, Flanagan, von Waldén, et al. 2010) with others reporting no change in rates of MPB during 4 days ULLS (Brook et al. 2022). The previous chapter demonstrated an increase in whole-body MPB after 2 days of bed rest, contrary to some of the published literature. One of the reasons for this uncertainty is the inherent difficult in measuring MPB *in vivo*. Nevertheless, the mechanistic and molecular causes of these physiological changes remain to be fully elucidated.

A heightened inflammatory state, such as is present during sepsis, trauma, and some chronic non-communicable diseases is associated with a reduction in muscle mass (Puthucheary et al. 2013; Psatha et al. 2012) and insulin sensitivity (Varadhan et al. 2018; Thorell, Nygren, and Ljungqvist 1999). Muscle mass loss has clinical implications such as muscle strength loss, suboptimal wound healing and reduced ambulation and so understanding the key drivers is important to develop clinical countermeasures. A reduction in leg muscle CSA has been reported following ankle fracture, with a loss of 8.7% reported in the medial gastrocnemius and 9.8% in the soleus at day 40 compared to time of casting (Psatha et al. 2012). In addition, there was a 5.9% reduction in medial gastrocnemius and 4.6% reduction in soleus reported in the

contralateral (uninjured side) compared to the time of casting. One drawback to studies in populations with acute injuries is the lack of baseline or study physical activity data, making it difficult to determine if muscle mass loss is driven by a reduction in step count, inflammation associated with the injury or surgery itself, or a combination of both. Furthermore, the relative contribution of MPS and MPB to muscle mass loss and the molecular regulators governing these processes still remain unclear.

Inflammation, mediated by pro-inflammatory cytokines such as IL6, CRP and TNF-α, has been shown to impact muscle protein turnover, in particular MPB, in both rodents and humans and includes the suppression of muscle anabolic signalling (Lang, Frost, and Vary 2007). Short duration (4-hour) endotoxin administration, used as a model for the initial phase of sepsis, in healthy volunteers under postabsorptive conditions has demonstrated acute decreases in estimates of both muscle protein synthesis and breakdown measured using tracer balance techniques to an equal extent, thereby resulting in an unaffected protein balance (Vesali et al. 2009). However, the generalisability of this 4 hour acute model to clinical populations may be limited, in part as they are taken in the postabsorptive state when one would expect dampened MPS, as well as its inability to ascertain what is happening to protein turnover chronically over days to weeks. In patients with critical illness, muscle wasting occurs within days. One study evaluating leg muscle mass loss and muscle protein turnover using stable isotope tracer methodologies in patients with critical illness reported a 12.5% loss of *rectus femoris* CSA measured using ultrasound at day 7 compared to the day of admission, and decreased further

to -17.7% by day 10 (Puthucheary et al. 2013). Measures of MPS and MPB in this study however were equivocal due to the impact of confounding variables such as nasogastric feeding, insulin infusion and short time periods to measure muscle protein turnover in ICU. Other studies report early elevation of muscle cytokine mRNA and inactivation of proteins regulating protein translation initiation and protein synthesis as well as increased muscle-ubiquitin ligase (MAFBx and MURF1) mRNA and protein expression in patients 6-8 hours after admission to ICU compared with healthy matched controls (Constantin et al. 2011). However, it is unclear whether these changes persist over longer periods of time such as days or weeks and whether they accurately reflect changes in protein turnover. Direct measures of muscle protein turnover over an extended period of time (days to weeks) have, as far as I am aware, never been used in the setting of an acute lower limb injury to determine the major drivers of muscle mass loss.

The stress response to trauma or major surgery is characterised by autonomic, hormonal and metabolic changes which manifest as hypermetabolism, hyperdynamic cardiovascular state and systemic inflammation (Baigrie et al. 1992; Bone, Sprung, and Sibbald 1992) which peak within the first 24-48 hours after surgery and last for several days postoperatively (Thorell et al. 1996). The metabolic response begins as a local response and develops into a systemic one, and evidence suggests that the local cytokine response is greater than the systemic one after musculoskeletal trauma (Bastian et al. 2009, 2008). Limited research however has attempted to differentiate between the effect of local muscle inflammation, such as local to

the site of surgery, versus a systemic inflammatory response on muscle volume and MPS. In one study in patients undergoing major abdominal surgery, mRNA expression levels associated with inflammation, protein breakdown and impaired carbohydrate oxidation increased within 24 hours of surgery in muscle (*rectus abdominus)* local to the site of surgery, with a smaller response seen in muscle remote to the site of surgery (*vastus lateralis*)(Varadhan et al. 2018). Furthermore, these muscle mRNA changes were mirrored by protein level changes at the site local to surgical trauma, but not in muscle remote to the site of surgery. These observations were accompanied by increased systemic inflammation and impaired glucose tolerance. Collectively, these findings suggest muscle level responses local to the site of injury contribute to impairments in muscle mass and insulin sensitivity in the first few days following surgery. It is unclear whether these molecular and physiological changes persist for longer durations after trauma and surgery, or if systemic inflammation can cause similar muscle level changes. The study in this chapter will allow the evaluation of whether any systemic inflammation caused by trauma will impact muscle mass and MPS both locally and remote to the site of surgery.

5.2 Research Question

By employing oral stable-isotope tracers and a unilateral limb immobilisation 'control' group and unilateral ankle fracture patients, whilst investigating both limbs of each volunteer, this study aimed to determine the relative contributions

of immobilisation and inflammation to *medial gastrocnemius* muscle thickness, myofibrillar protein synthesis over 2 weeks and whole-body muscle protein breakdown at the 2-week time point in these two catabolic states. The use of unilateral models also allowed interrogation of the contribution of systemic inflammation to end point measures following ankle fracture.

Research Aims

i) To determine the impact of 2 weeks immobilisation alone (in healthy volunteers) versus trauma plus immobilisation in patients undergoing ankle fracture surgical fixation on muscle thickness, myofibrillar protein synthesis and whole-body muscle protein breakdown and any associated muscle transcriptional responses.

ii) To determine the impact of any systemic inflammatory response on muscle thickness, MPS and muscle mRNA expression on the contralateral uninjured leg in these patients, particularly compared with the local trauma and inflammation in the injured leg.

5.3 Methods

5.3.1 Plan of investigation

Eleven patients (patient group) aged between 18 and 60 years presenting to Queen's Medical Centre, Nottingham, UK with isolated operable ankle fractures were recruited. Of these, 8 patients had an ankle fracture caused by a low velocity injury and 3 due to a high velocity injury sustained whilst playing contact

sports. The average time to surgery after admission was 4.7 ± 1.1 days. In addition, 9 healthy volunteer participants, matched for age and sex, without an ankle fracture (healthy volunteer group) were recruited from the general population to take part in this study. Patients were identified as suitable for the study by the treating team at the daily trauma meeting and during fracture clinics. Following discussion with the patient and verbal agreement they were referred on to the study team for possible recruitment. Patients were approached prior to surgery if they met inclusion criteria (Table 5.1) and were given a written patient information sheet and verbal explanation of the study and a chance to ask questions. Patients were given a minimum of 1 hour to consider the study and enrolled once they gave written informed consent to take part. In total 12 patients were recruited, and 1 dropped out prior to surgery with the reason cited as a significant delay in surgery, thus 11 patients completed the study. Nine healthy volunteers, age-matched to patients, were also recruited from the general population. Recruitment was via posters placed around the University of Nottingham, as well as advertisements placed on popular national (Facebook, Twitter) and local (In Your Area [www.inyourarea.co.uk]) social media platforms. After expressing initial interest in the study, healthy, non-patient volunteers were sent a detailed healthy volunteer participant information sheet and then they were invited to attend the DGHPU for an initial meeting. Healthy volunteers who gave written consent to participate then underwent medical screening (Chapter 2, **Section 2.3**).

Table 5.1. Inclusion and exclusion criteria for the ankle fracture study. Inclusion (patients only) and exclusion criteria (patients and healthy volunteers) for individuals participating in the ankle fracture study.

Inclusion criteria:
1. All participants aged 18-60 years undergoing operative treatment of isolated ankle fractures, or healthy control. 2. Fibular fracture requiring operative fixation, or healthy control.
Exclusion criteria:
1. Inability to provide informed consent 2. Unable to speak or understand English 3. Patients with diabetes or impaired glucose tolerance, 4. Obese participants (BMI 30+) 5. Smokers 6. Diabetic or arterial non-healing leg/foot ulcers 7. Steroid users 8. Sarcopenic (defined as below 20^{th} percentile for gender and age) 9. Pregnancy 10. Previous personal or family history of venous thromboembolism or clotting abnormalities identified on screening bloods (control participants only)

5.3.2 Experimental protocol – ankle fracture patient group

The experimental protocol is shown in

Figure *5.1*. Once the patient was anaesthetised via general anaesthetic or spinal anaesthetic (or both) 3ml of whole blood was collected from an antecubital vein for the measurement of serum pro-inflammatory cytokines. Bilateral muscle biopsies of the *medial gastrocnemius* were performed on the operating table prior to the surgical tourniquet being applied to thigh of the injured limb and the initial skin incision made, with a 12g (10cm) automated disposable Bard ® Monopty ® microbiopsy (Bard Ltd, Crawley, UK) needle. Up to 4 passes were used through the same incision and muscle samples were immediately frozen and stored in liquid nitrogen until further analysis. The incision on the uninjured leg was closed using sterile Steristrips™ ensuring opposition of the wound edges and a Tegaderm™ and Coban™ compression bandage applied over the top. The injured leg was thereafter prepped for surgery by the treating team.

The morning after surgery, when in a fasted state, a repeat venous blood sample was collected for the measurement of serum pro-inflammatory cytokines and plasma body-water deuterium enrichment. Thereafter an ultrasound scan (Toshiba Diagnostic Ultrasound System, Model SSA-77OA) of the *medial gastrocnemius* was performed of both legs to measure muscle thickness, pennation angle and fascicle length. In the injured leg, the backslab or boot was carefully removed temporarily by a doctor without moving the ankle in order to acquire the images, or the scan was performed in the plaster room when the patient had their cast changed before discharge. When medically fit

for discharge (average time from surgery 1.8 ± 0.4 days, range 1-5 days), participants ingested the oral stable isotope tracer deuterated water (D_2O) to quantify cumulative fractional MPS rates. An initial oral bolus of 3mg/kg D_2O was administered (divided into 3 equal doses 30 minutes apart to reduce the risk of side effects) with individualised top-ups to take on day 7 at home calculated based upon the rate of decay of water and total body water of 60% in men (Chapter 2, **Section 2.9.1**). To monitor body water D_2O enrichment throughout the study, saliva samples (1ml) were collected prior to and two hours after D_2O ingestion and on the morning of their 2-week outpatient appointment. They were advised not to drink fluids 30 minutes prior to each saliva sample and any samples done at home were kept refrigerated until handed over to the research team. Samples were cold centrifuged at 16G to remove any debris that may have been present and then aliquoted into 2ml vials and frozen at -80^{o}C until analysis. The habitual activity of participants was objectively measured at home over a period of 14 consecutive days starting from the day they were discharged from hospital using triaxial accelerometry (Actiheart™, CamNtech Ltd., UK). As part of their usual post-fracture care, patients were instructed to use crutches to ambulate and not to weight bear on the injured leg during the two weeks at home. They were also told to elevate their injured leg above the level of their heart for as many hours a day as possible to reduce oedema.

Two weeks after discharge, patients returned to Queen's Medical Centre in a fasted state for outpatient follow-up whereby they were assessed by the treating orthopaedic team. In the instance where patients were given

prophylactic low molecular weight heparin to prevent a deep vein thrombosis (decided on an individual basis according to venous thromboembolism risk calculated using an NHS hospital protocol), this was stopped for 48 hours prior to the biopsy. After their follow-up appointment, patients returned to the DGHPU and were given 10mg (dissolved in 50ml distilled water) of the stable isotope tracer 3-methylhistidine (3-MeH) to drink in order to determine the rate of whole-body MPB (which was measured the following day). Following the ingestion of tracer, a repeat blood sample was collected for serum pro-inflammatory cytokines and patients then, after carefully removing their cast or boot, had a repeat bilateral ultrasound scan of the *medial gastrocnemius*. Following this, bilateral muscle biopsies of the *medial gastrocnemius* were performed with the patient awake under ultrasound guidance and local anaesthesia (~5mls of 1% lidocaine infiltrated down to the fascia) using a Bard® Magnum® reusable biopsy instrument loaded with 12g (10cm) disposable needle as described above. After the final biopsy, firm pressure was applied with a sterile gauze for a further 5 minutes, or longer if there was persistently oozing. The incision was closed using sterile Steristrips™ ensuring opposition of the wound edges. A Tegaderm™ was applied over the top for further protection and a compression bandage e.g. Coban™ used on the uninjured leg for up to 12 hours to apply compression thereafter. Patients were given food in the unit before returning home. The following day, 24 hours after ingestion of 3-MeH, in a fasted state, an anterograde venous cannula was inserted into the arm at the antecubital fossa for sampling of venous blood every hour for a total of 7 hours for the measurement of 3-MeH enrichment. After this, patients were fed and returned

home after which they had completed the study. They received post-operative follow-up with the treating orthopaedic team as per their normal care. One patient did not have an ultrasound scan one day after surgery or a biopsy on the injured leg 2 weeks after surgery due to a traumatic abrasion which occurred at the time of injury and the potential risk of infection. One patient declined a biopsy on the injured leg 2 weeks after surgery due to pain. Two patients declined an ultrasound on the injured leg one day after surgery due to pain.

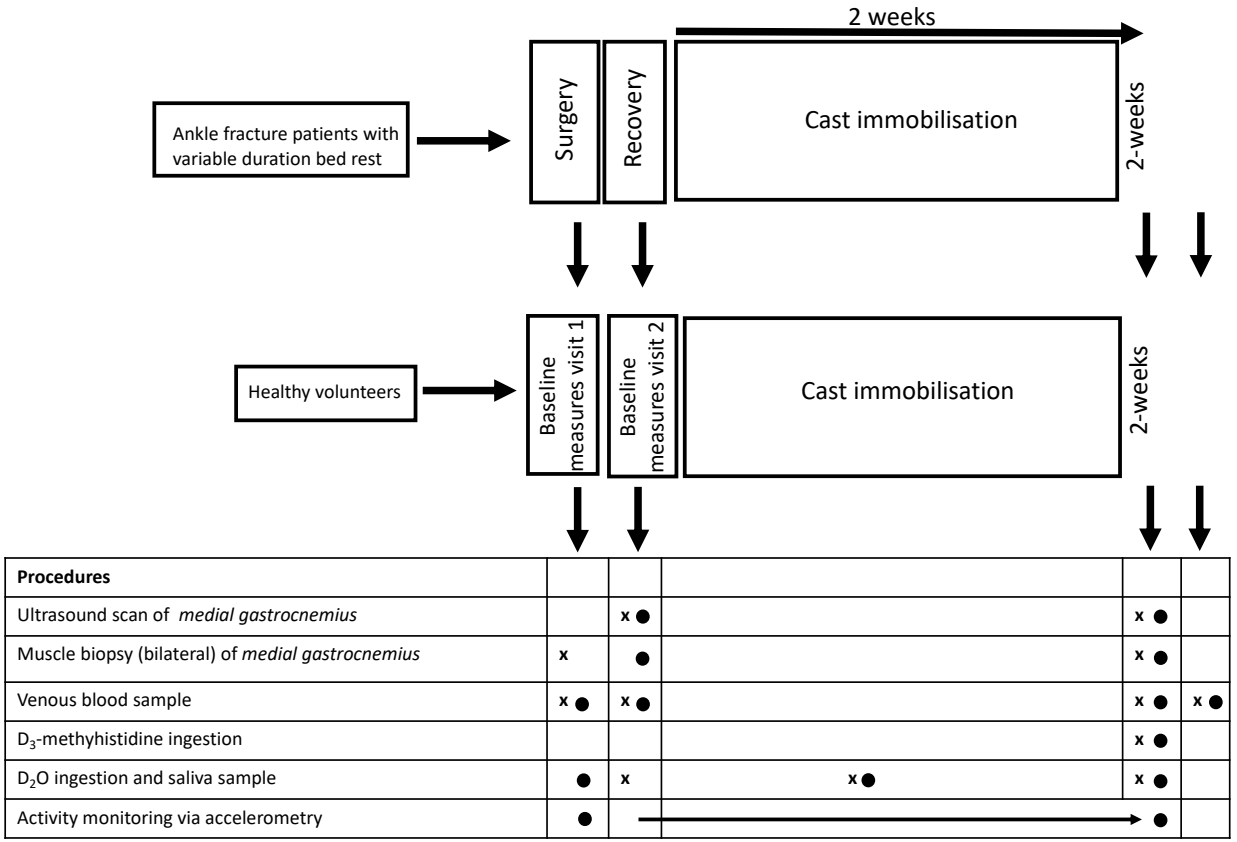

Figure 5.1. Experimental schema for the ankle fracture study. Experimental protocol for the ankle fracture patient group and healthy volunteer group. 'x' indicates measure taken in patient group; solid circle indicates measure taken in healthy volunteer group.

5.3.3 Experimental protocol – non-patient, healthy volunteer group

The experimental protocol in the non-patient, healthy volunteer group is shown in

Figure *5.1*. Healthy volunteers presented to the DGHPU (baseline measures 1) in a fasted state and had venous blood collected from an antecubital vein for serum pro-inflammatory cytokines and basal plasma body-water deuterium enrichment. Following this, participants ingested the oral stable isotope tracer D_2O as described above to quantify cumulative MPS rates. Four days after the first visit (baseline visit 2), participants returned to the DGHPU and had an ultrasound scan of the *medial gastrocnemius* to measure muscle thickness, pennation angle and fascicle length. After this they had bilateral muscle biopsies of the *medial gastrocnemius* performed under ultrasound guidance and local anaesthetic using a Bard® Magnum® reusable biopsy instrument loaded with 12g (10cm) disposable needle as described above. Participants then had a below knee plaster cast applied, randomised to either their right or left leg (using a coin toss) and they were familiarised with how to use crutches and told not to weight bear on their casted leg during the 2 week period before returning home. They were also given a D_2O top up to take 1 week after casting at home with saliva samples taken before and 2 hours after. The habitual activity of participants was objectively measured at home over a period of 14 consecutive days using an Accelerometer from visit 2 (Actiheart™, CamNtech Ltd., UK).

Two weeks following their previous visit, healthy volunteers returned to the DGHPU in a fasted state and were given 10mg (dissolved in 50ml distilled water) of the stable isotope tracer 3-methylhistidine (3-MeH) to drink in order to determine the rate of MPB as described above (which was measured the following day). Following the ingestion of tracer, a repeat blood sample was collected for serum pro-inflammatory cytokines and a D-dimer and after having their cast removed and being instructed not to contract their calf, had a repeat bilateral ultrasound scan of the *medial gastrocnemius*. Following this, bilateral muscle biopsies of the *medial gastrocnemius* were performed, with the volunteer awake, under ultrasound guidance and local anaesthesia as described above. After the final biopsy, firm pressure was applied with a sterile gauze for a further 5 minutes. Volunteers were given food in the unit before returning home. The following day, 24 hours after ingestion of 3-MeH tracer, in a fasted state, an anterograde venous cannula was inserted into the arm at the antecubital fossa for sampling of venous blood every hour for a total of 7-hours for the measurement of 3-MeH enrichment. After this, volunteers were fed and returned home after which they had completed the study. They were provided with verbal and written post-biopsy aftercare advice and a contact number for the unit. One healthy volunteer was removed from the study due to a medical complication prior to the final 3-MeH measures being taken. Two other participants had several 3-MeH sampling timepoints missing and so their data were excluded.

5.3.4. Muscle biopsies of the medial gastrocnemius

Patients had their initial muscle biopsy performed whilst anaesthetised (general anaesthetic or spinal anaesthetic or both) in either the prone or supine position but prior to the tourniquet being applied to the thigh of the injured leg or the first incision being made for fracture fixation and without ultrasound guidance (any bleeding could be controlled locally with compression whilst under anaesthetic). The muscle biopsy taken at the 2 week time point in patients and healthy volunteers had theirs performed whilst awake under ultrasound guidance and with local anaesthetic. This method is described here. To undertake the biopsy, participants were positioned in the prone position with feet slightly off the end of the bed (Figure 5.2a). The participant was exposed from the mid-thigh down and without socks or shoes on. An ultrasound scanner (Toshiba Diagnostic Ultrasound System, Model SSA-77OA) with a musculoskeletal setting was used to locate a region in the medial gastrocnemius with minimal vasculature and of appropriate depth to be within the belly of the muscle. The point of entry was marked for the biopsy with a surgical marker pen. The skin surrounding the mark was cleaned with sterile gauze soaked with betadine solution in an approximately 5-10cm circumference around the mark. The skin and subcutaneous tissues were then infiltrated with 2-5 mls of 1% lidocaine (Figure 5.2b), and a further 3-5 mls was infiltrated down to the muscle using ultrasound guidance up to a maximum of 3mg/kg (Figure 5.2c). In contrast to previously described techniques for microbiopsy (Hayot et al. 2005), an insertion cannula was not used for biopsy needle placement as it was unnecessary to obtain a sufficient sample. Each biopsy pass was performed through the same incision.

Once the superficial skin and tissue down to the muscle was anaesthetised, a small 2-3mm incision with a surgical blade was made in order to introduce the biopsy needle. Under real-time ultrasound guidance, the biopsy needle was inserted through the incision and advanced down obliquely towards the parallel to the muscle fibres, through the superficial fascia (Figure 5.2d). The needle was advanced in the same direction through the muscle until the tip of the biopsy needle was clearly visible within it, while still leaving sufficient depth within the depth of the gastrocnemius to fire the needle and a biopsy of the muscle was performed. The instrument and needle were then removed and the core tissue specimen processed. Up to 4 passes was used in this study. Firm pressure was applied using a sterile gauze to the wound in between passes to reduce bleeding. After the final biopsy, firm pressure was applied with a sterile gauze for a further 5 minutes, or longer if there was persistent oozing. The incision was closed using sterile Steristrips™ ensuring opposition of the wound edges and a Tegaderm™ and Coban™ compression bandage applied over the top for up to 12 hours. Written aftercare advice was given to the participant. All muscle biopsies were immediately frozen and stored in liquid nitrogen until further analysis.

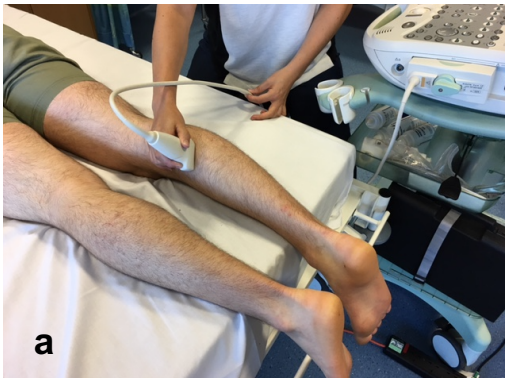

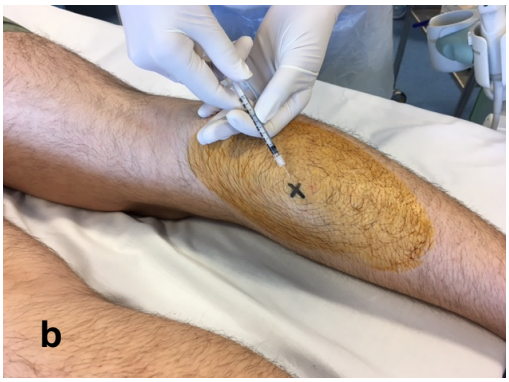

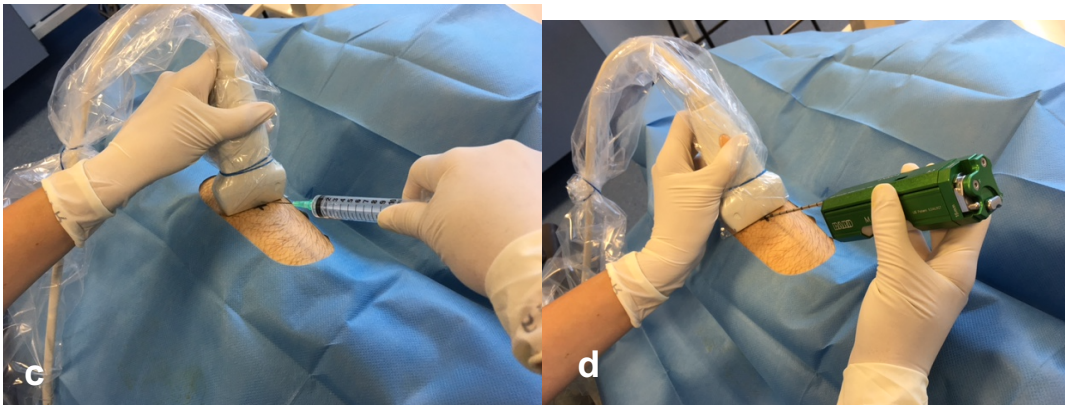

Figure 5.2 Ultrasound-guided medial gastrocnemius muscle biopsy procedure. a) Prone position during ultrasound identification of vessels b) Infiltration of local anaesthetic into subcutaneous tissues c) Ultrasound-guided infiltration of local anaesthetic down to muscle (cranial to caudal direction) d) Ultrasound-guided insertion of biopsy needle into muscle (cranial to caudal direction).

5.3.5. Ethical approval

All participants gave their informed written consent to participate in this study. The study was approved by the NHS Health Research Authority Research Ethics Committee (REC reference: 18/EM/0404).

5.3.6. Analytical methods

Muscle thickness, pennation angle and fascicle length

With the volunteer positioned supine, they were asked to gently externally-rotate their leg to expose the *medial gastrocnemius* muscle (Figure 5.3a). The mid-axial point of the mid-sagittal length (corresponding with the centre of the muscle belly) was located by identifying the proximal and distal myotendinous junctions and the medial and lateral myotendinous junctions and marking half the distance between these points. The probe was orientated sagittally along this line in order to align the muscle fibres within the view and three images were acquired at this point. Image analysis was performed using Image J software (Wayne Rasband, NIH, USA, version 2.0). Each ultrasound image was calibrated using the scale provided in Image J software and a line was drawn along the upper and lower aponeurosis. Three fascicles were measured along their length between the two aponeuroses and pennation angle was also measured (Figure 5.3b). Muscle thickness was measured on the image at 50% by measuring from the upper to deep aponeurosis. The mean of 3 measurements was used for each value.

a

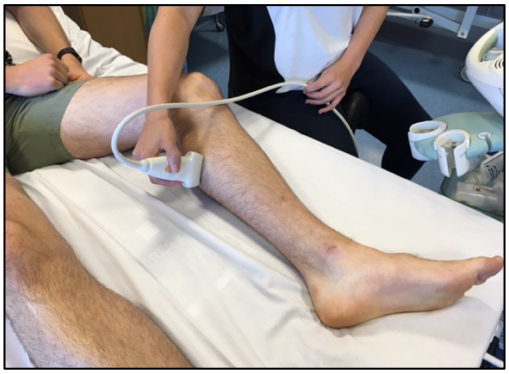

b

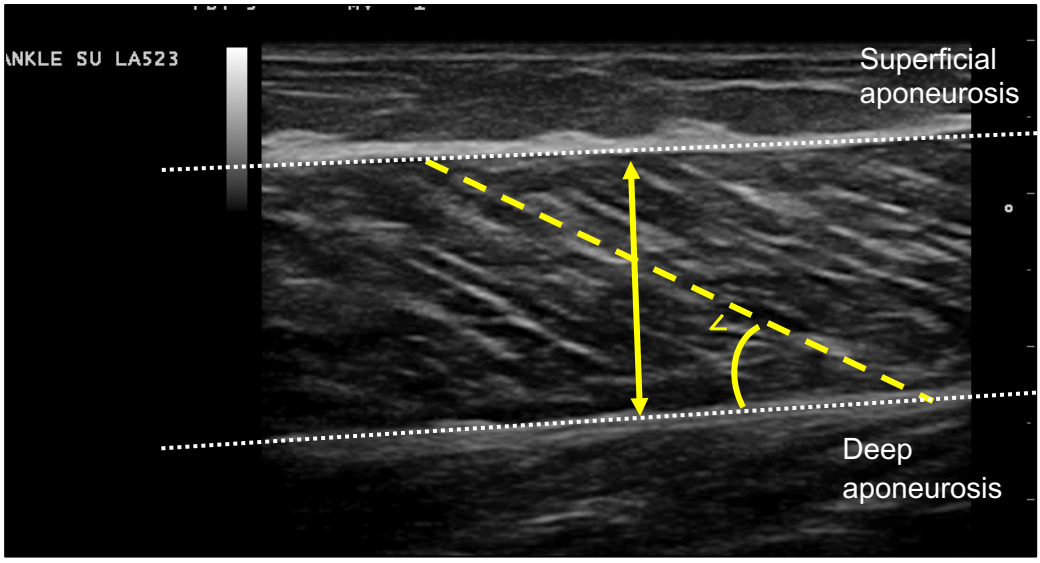

Figure 5.3. Ultrasound of the medial gastrocnemius. a) Ultrasound medial gastrocnemius image acquisition during the ankle fracture study b) Example ultrasound image demonstrating medial gastrocnemius muscle thickness (double headed arrow) between the deep and superficial aponeuroses (white dotted lines), pennation angle (∠) and fascicle length (dashed yellow line).

Blood analyses

Whole blood was collected for analysis of serum CRP, IL6, and plasma D_2O enrichment. Blood for determination of serum variables was collected into a microtube with coagulation activator (Sarstedt, Nümbrecht, Germany) and left to clot for at least 15 minutes before being centrifuged (15G for 2 minutes). Serum was aliquoted into 2 cryovials and frozen at -80°C. Serum CRP and IL6 were analysed at the Metabolic Physiology Analytical Laboratory, University of Nottingham using an Enzyme-Linked ImmunoSorbent Assay (Quantikine ®

ELISA Human CRP and IL6 Immunoassay, USA R&D Systems, Inc, Minneapolis, USA) according to the manufacturer's protocol guidance apart from CRP in which the serum was diluted 1:1000. In brief, monoclonal α Human CRP or IL6 antibodies were pre-bound to a 96-well plate, to which the standards and samples were added. Following incubation, the plate was washed to remove any excess sample prior to addition of a secondary detection antibody and horseradish peroxidase conjugate. The plate was left to incubate, and the plate was washed to remove any unbound antibody before a chromogenic solution, which reacts with horseradish peroxidase was added. The reaction was stopped with sulfuric acid and the optical density read at 450 nm against a reference filter set at 570 nm to generate a standard curve from which the sample values could then be determined. Coefficient of variation for intra-assay precision for CRP and IL6 was 5.5% and 3.0% respectively.

Body water D_2O enrichment in saliva and muscle

Body water and muscle protein D_2O enrichment were measured as previously described (Wilkinson et al. 2014). For plasma D_2O enrichment, 2.5ml whole blood was collected into a lithium heparin microtube (Sarstedt, Nümbrecht, Germany) and immediately cold centrifuged after gentle inversion at 17.5G, with the plasma fraction aliquoted and frozen at -80^{o}C until further analysis. Full description of the method is detailed in the General Methods chapter of this thesis.

Calculation of Myofibrillar Protein Fractional Synthetic Rate (FSR)

The FSR of myofibrillar proteins using the D_2O tracer was determined as described by Wilkinson (Wilkinson et al. 2015). This was achieved using the precursor-product approach, from the incorporation of deuterium labelled alanine into protein, using the enrichment of body water (corrected for the mean number of deuterium moieties incorporated per alanine and the total number of hydrogens within the alanine derivative) as the surrogate precursor labelling between subsequent biopsies. This is described further in the General Methods Section in Chapter 2.

Whole-body muscle protein breakdown

A validated, stable-isotopic methodology was used to quantify the rate of MPB using D_3-MH (Sheffield-Moore et al. 2014), using the same method as described by Gharahdaghi (Gharahdaghi et al. 2019) and in Chapter 4. Enrichment decay (k) of 3-MeH over the 7 hours of sampling in plasma was calculated at the 2 week time point in both patients and healthy volunteers.

Total RNA extraction and targeted muscle mRNA expression measurements

Total RNA was extracted from frozen muscle biopsies according to a method previously described(Constantin et al. 2013). In brief, the RNAs were extracted using TRI Reagent (Ambion, Huntingdon, UK), according to the manufacturers protocol. First strand cDNA was then synthesised from 1 µg RNA using random primers (Promega, Southampton, UK) and Superscript III (InVitrogen Ltd., Paisley, UK). Multiple mRNA expression measurements (191 targets, [Chapter 2, **Section 2.9.5**, Table 2.1]) were made according to the manufacturer's

instructions using 100 ng of cDNA obtained from total mRNA isolated from *medial gastrocnemius* muscle from both legs in ankle fracture patients before surgery and at 2 weeks and from both legs of the healthy volunteers before and 2 weeks after casting using Applied Biosystems 384-well microfluidics TaqMan array cards (Thermo Fisher Scientific Ltd, Loughborough, UK). Procedures for muscle mRNA expression measurements using a microfluidic gene card approach (191 targets) are described in Chapter 2.

5.3.7. Statistical Analysis

The statistics, calculations and Figures presented were completed using SPSS software (version 24; SPSS, Chicago, IL) or GraphPad Prism (version 7; Graphpad Software Inc, USA). Data were first assessed for their suitability for parametric statistical testing using Shapiro-Wilks to assess the distribution of data. A two-way analysis of variance (ANOVA) for repeated measures was performed to detect any main effects of visit (before or 2 weeks after surgery in patients and before or 2 weeks after casting in healthy volunteers) and leg (injured or uninjured leg in patients and casted or uncasted leg in healthy volunteers) on outcome measures. Post-hoc analysis was performed using pairwise comparison t-tests with Bonferroni correction. One-way repeated measures ANOVA was used to measure single variables over time and Student's t test (or non-parametric equivalent) was used when an ANOVA was not appropriate. A one-tailed Spearman correlation was used to assess the relationship between change in muscle thickness versus FSR in the patients

injured leg and the healthy volunteers' casted leg measured over 2 weeks immobilisation. All data are presented as mean ± SEM. Statistical significance was declared at $p<0.05$.

5.4. Results

5.4.4. Participant Demographics

Eleven patients (7 males and 4 females) with ankle fractures completed the study with an average age of 38.1 ± 5.2 years (range 19-58 years) and a BMI of 26.8 ± 01.3 kg/m^2. Eight healthy volunteers (4 males and 4 females) completed the study with an average age of 28.5 ± 4.2 years (range 18-59 years) and a BMI of 23.5 ± 1.8 kg/m^2. Average PAL for the two-week cast immobilisation was 1.23 ± 0.02 for patients and 1.28 ± 0.02 for healthy controls which corresponds to a "sedentary activity level" in both groups being equivalent of <3000 steps per day (Ohkawara et al. 2011). There were no differences in age ($p=0.17$) or BMI ($p=0.14$) at baseline, or PAL during immobilisation ($p=0.13$) between groups. For completeness, in order to characterise the patient group, the remaining injury and patient characteristics are shown in Table 5.2.

Table 5.2. Injury and patient characteristics in the ankle fracture study.

Parameter	**Value**
Mechanism, n (%)	
Low velocity	8 (73%)
High velocity/contact sports	3 (27%)
Weber classification, n (%)	
B	5 (45%)
C	6 (55%)
Fracture dislocation, n (%)	6 (55%)
Malleolar, n (%)	
Unimalleolar	1 (9%)
Bimalleolar	3 (27%)
Trimalleolar	7 (64%)
Average time to present to A&E after injury (hours)	3.3 ± 1.1
Average time to surgery after admission (days)	4.7 ± 1.1
Number of regular medications taken, n(%)	
0	8 (73%)
1	1 (9%)
2	2 (18%)
Number of comorbidities	
0	7 (63%)
1 (Gastro-oesophageal reflux disease [GORD], corrected congenital heart defect, Raynaud's disease)	3 (27%)
2 (Asthma, GORD)	1 (9%)

5.4.5. Medial gastrocnemius muscle thickness, fascicle length and pennation angle

Substantial muscle wasting of the calf was noted in the casted leg of the healthy volunteers and the injured leg of the patients (Fig 5.4a). At baseline (pre casting/1-day post-surgery) there was a difference in muscle thickness between the casted leg of the healthy volunteers and injured leg of the patients (15.3 ± 0.5 vs 17.4 ± 1.0 mm, $p<0.05$). There was a 7.2% decrease in *medial gastrocnemius* muscle thickness from before casting to 2 weeks after casting in the casted leg of the healthy volunteers (15.3 ± 0.5 vs 14.2 ± 0.6mm, $p\leq0.01$) and a 16.7% decrease in muscle thickness from 1 day post-surgery to 2 weeks after surgery in the injured leg of the patients (17.4 ± 1.0 vs 14.5 ± 0.80mm, $p\leq0.01$; Figure 5.4b). There was a difference in absolute muscle thickness change between the healthy volunteers casted leg and the patients injured leg (-1.0 ± 0.4 vs -2.6 ± 0.6 mm, $p<0.05$) but no difference in % change (-14.9 ± 3.2 vs -7.0 ± 2.7, $p=0.07$).

There was a trend for *medial gastrocnemius* muscle thickness to decrease (3.8%) in the non-casted leg of healthy volunteers from before casting to 2 weeks after casting (15.7 ± 0.6mm vs 15.1 ± 0.7mm, $p=0.06$) and no change in the uninjured leg of the patients from 1 day post-surgery to 2 weeks after surgery (16.8 ± 0.9mm vs 16.6 ± 1.0mm, $p=0.59$). However, the muscle thickness in the injured leg was lower than the uninjured leg of the patients at 2 weeks (14.6 ± 0.8 vs 16.6 ± 1.0 mm, $p<0.05$).

There was no change in either fascicle length (36.0 ± 1.4 vs 33.1 ± 1.3mm, $p=0.22$) or pennation angle (27.4 ± 0.5 vs 27.4 ± 1.5 degrees, $p=1.0$)

in the casted leg of the healthy volunteers from before casting to 2 weeks after casting. Similarly, there was no change in fascicle length (34.7 ± 5.5 vs 37.0 ± 4.0mm, p=0.50) but a trend for a decrease in pennation angle (25.4 ± 2.3 vs 23.2 ± 2.5mm, p=0.06) in the injured leg of the patients from 1 day post-surgery to 2 weeks after surgery; (Figure 5.4c and d).

a

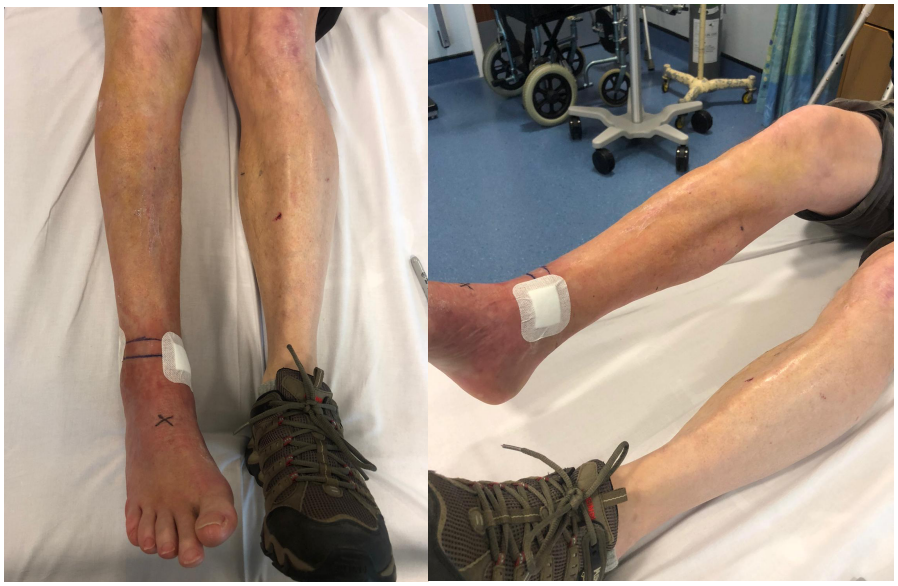

Healthy - casted leg

Patients - injured leg

Healthy - non-casted leg

Patients - uninjured leg

b

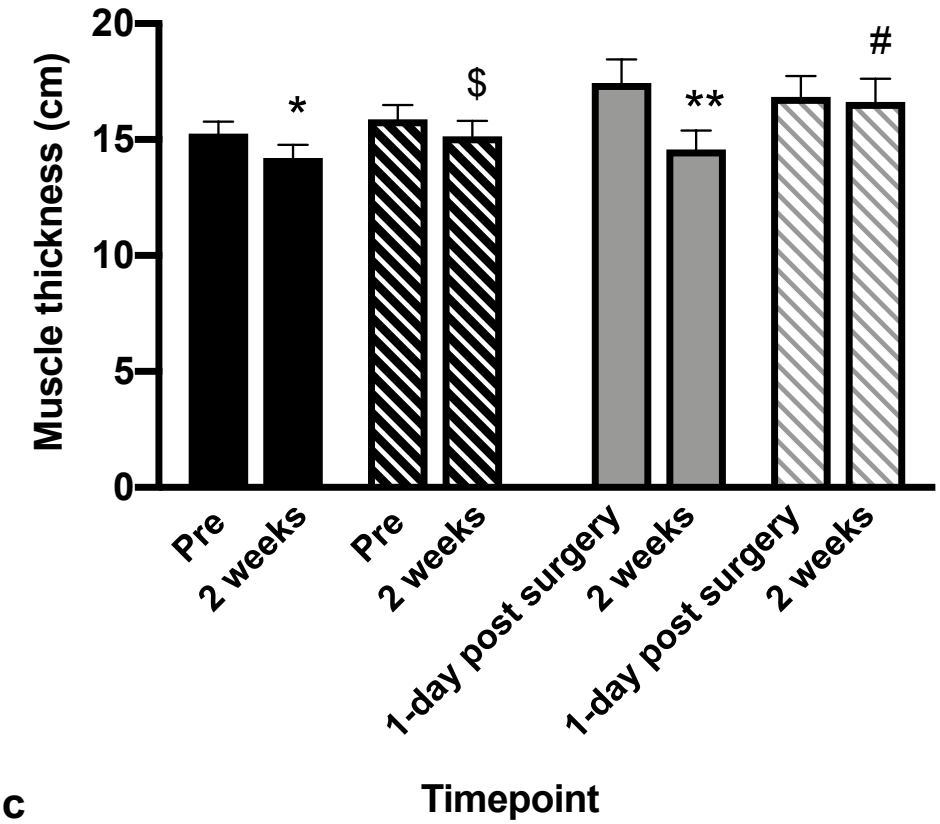
Muscle thickness (cm)
20
15
10
5
0
*
$
**
#
Pre
2 weeks
Pre
2 weeks
1-day post surgery
2 weeks
1-day post surgery
2 weeks
Timepoint

c

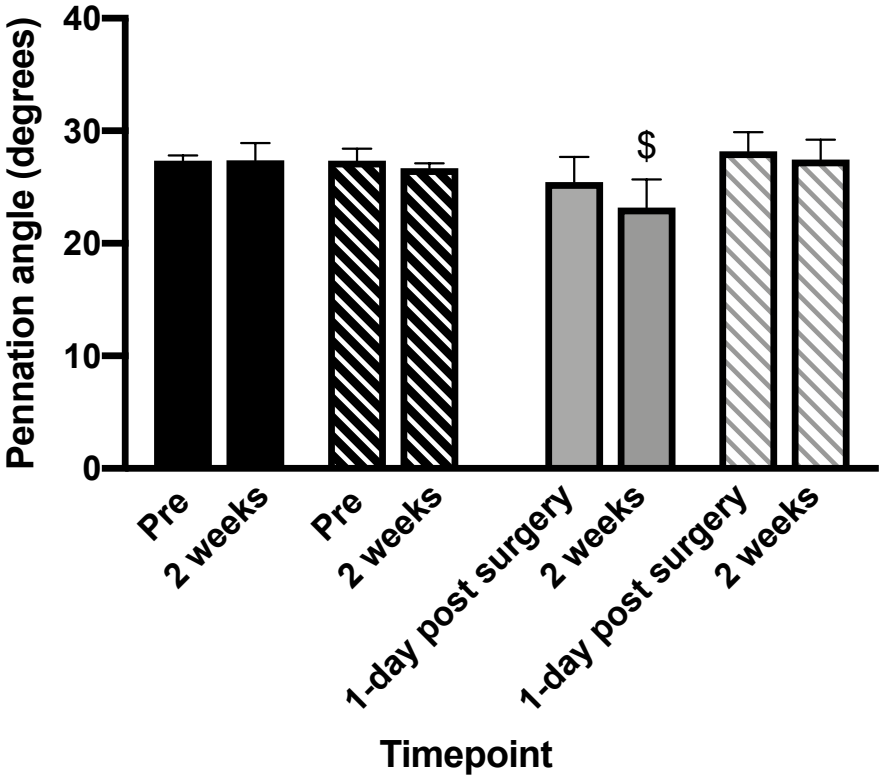
Pennation angle (degrees)
40
30
20
10
0
$
Pre
2 weeks
Pre
2 weeks
1-day post surgery
2 weeks
1-day post surgery
2 weeks
Timepoint

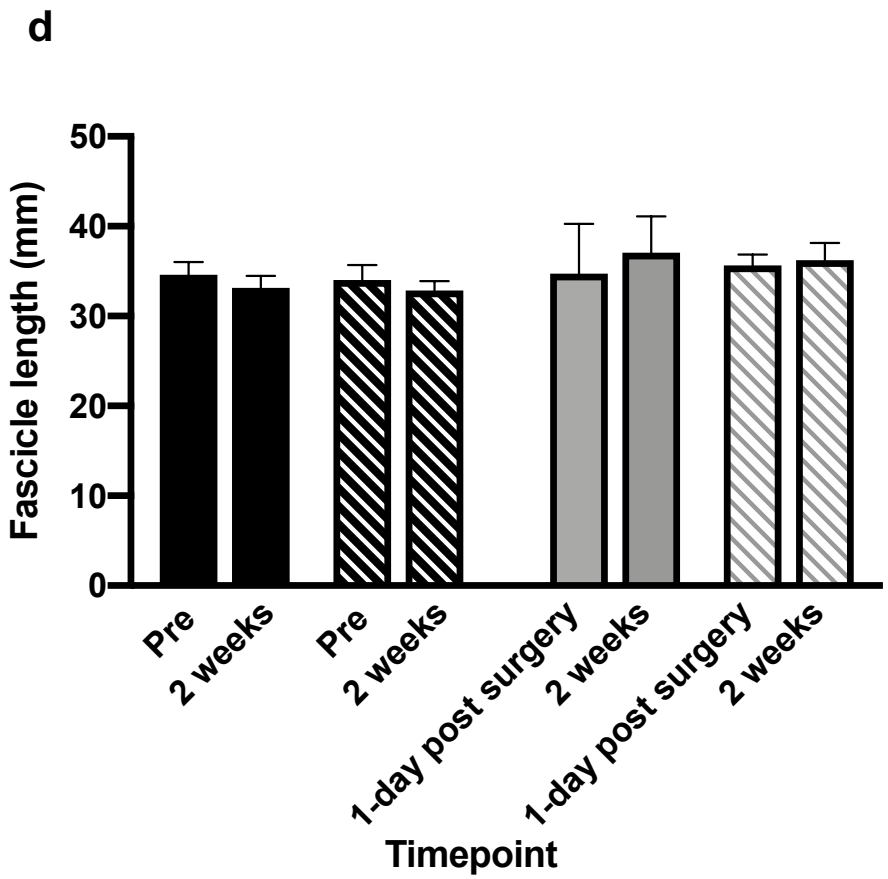

*Figure 5.4. Muscle thickness and architecture data. a) Lower leg of one of the ankle fracture patients 2 weeks after their surgical ankle fixation, demonstrating significant muscle atrophy. Medial gastrocnemius b) muscle thickness (mm) c) fascicle length (mm) and d) pennation angle (degrees) in healthy volunteers and patients. **, p<0.05, p≤ 0.01 vs Pre within each limb, $, p=0.06 vs Pre within each limb, #, p<0.05 vs injured leg at corresponding time point.*

5.4.6. Myofibrillar protein fractional synthetic rate

Compared with FSR (%/day) measured in healthy volunteers before casting (and assuming baseline FSR would be the same for patients), average daily muscle FSR was lower over the 2 weeks of limb immobilisation in healthy

volunteers (1.51 ± 0.04 %/day vs 0.63 ± 0.11 %/day, p≤0.001) and over the 2 weeks of limb immobilisation in the injured leg of the patients (1.51 ± 0.04 %/day vs 0.57 ± 0.12 %/day, p≤0.001; Figure 5.5). Furthermore, there was no difference when comparing healthy volunteers (casted leg) and patients (injured leg) over this 2 week period (p=0.90). Compared with FSR measured in healthy volunteers before casting, average daily muscle FSR was lower in the non-casted leg of the healthy volunteers (1.51 ± 0.04 %/day vs 0.89 ± 0.11, p≤0.001), and there was no difference when comparing casted and non-casted leg over this 2 week period (p=0.12). Compared with FSR measured in healthy volunteers before casting there was no difference in average daily muscle FSR over the 2 weeks following surgery in the uninjured limb of the patients (1.51 ± 0.04 vs 1.09 ± 0.25 %/day, p=0.67) and this was different compared with the injured leg during the 2 weeks (1.09 ± 0.25 vs 0.57 ± 0.12 %/day, p<0.05). Change in muscle thickness (mm) was plotted against FSR (%/day) in the patients injured leg and healthy volunteers casted leg and a Spearman correlation run. There was a moderate correlation (r=0.5, p=0.03) between muscle thickness and FSR with an R^2 of 0.19. This is presented in Figure 5.6.

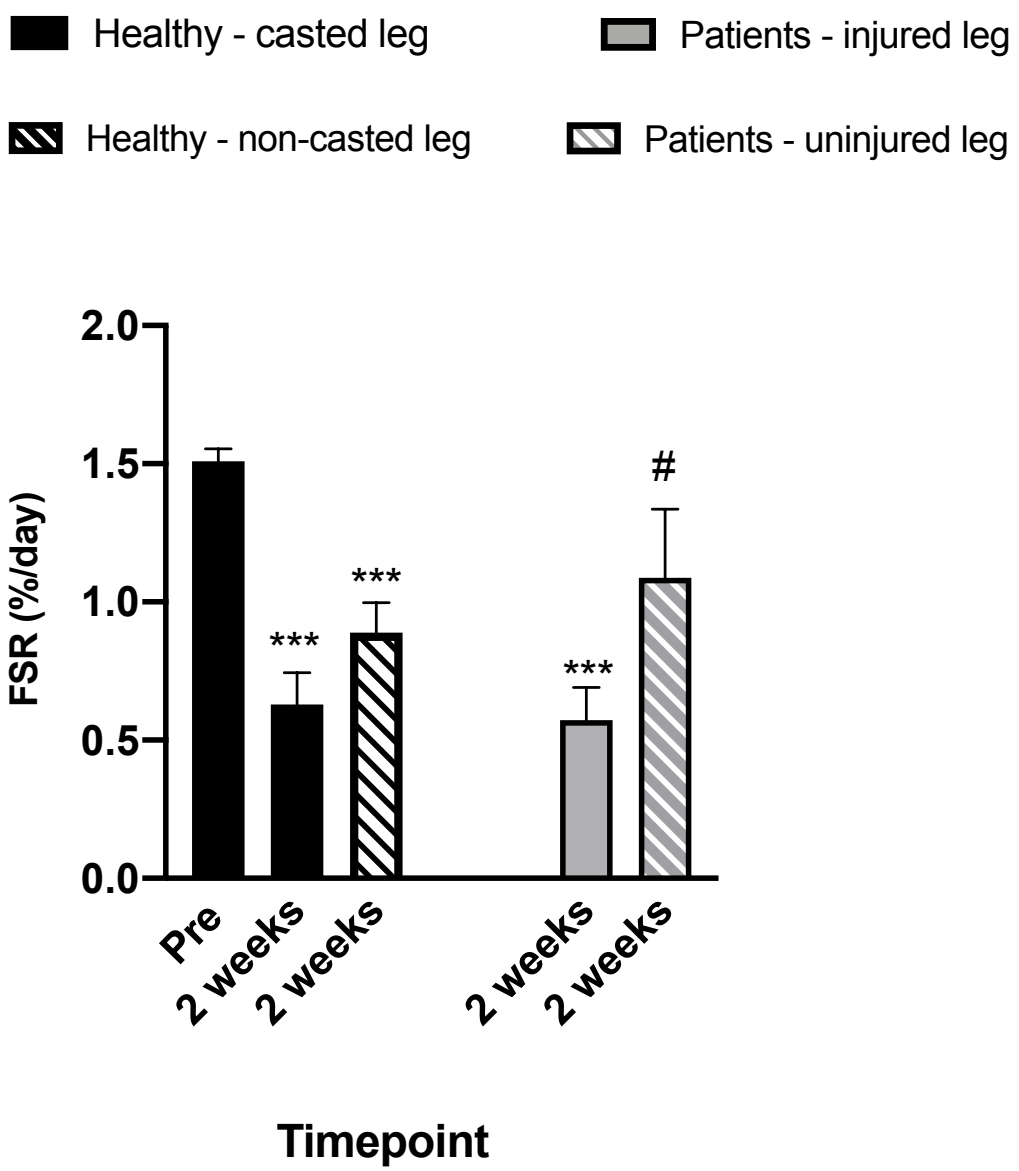

*Figure 5.5. Myofibrillar protein synthesis data. Muscle protein fractional synthetic rate (%/day) in healthy volunteers and patients. ***, p≤0.001 vs healthy volunteer Pre-casted state, #, p<0.05 vs injured leg in patient group. Values are mean ± SEM.*

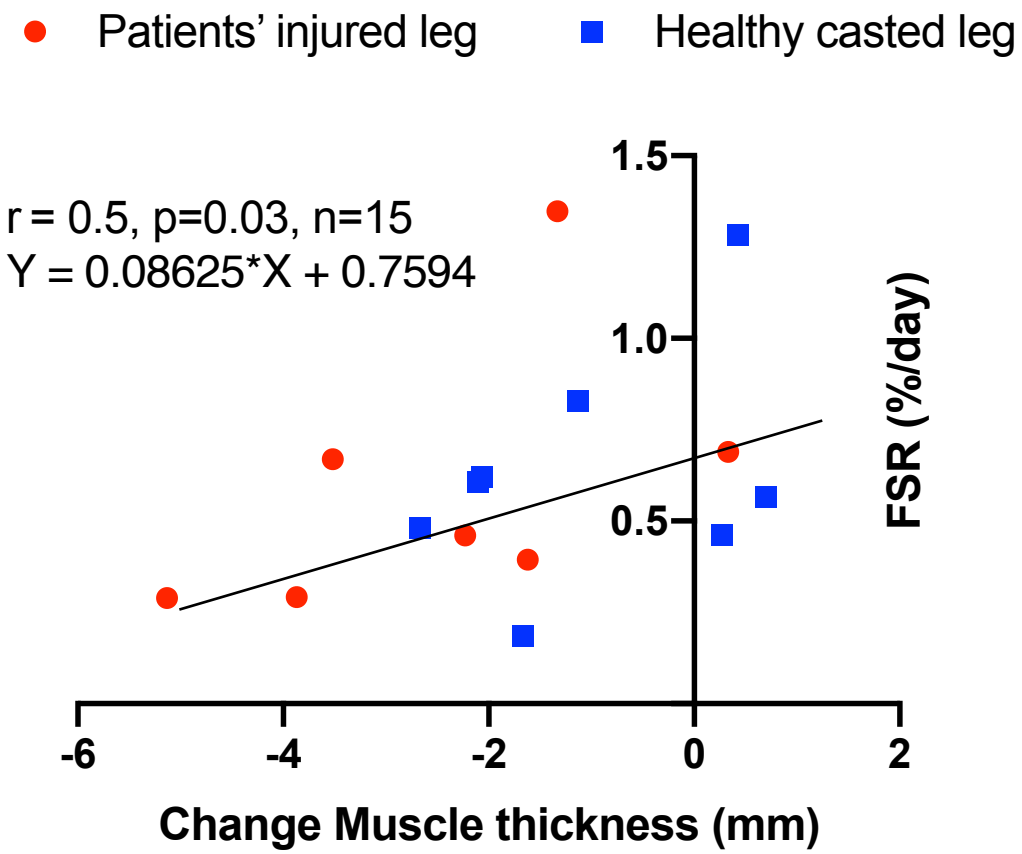

Figure 5.6. Correlation of MPS vs change in muscle thickness. a) One-tailed Spearman correlation for change in muscle thickness (mm) versus FSR (%/day) in the patients injured leg (red dots) and the healthy volunteers' casted leg (blue squares) measured over 2 weeks immobilisation. Line indicates the logistic regression line with an R^2 of 0.19.

5.4.7. Whole-body muscle protein breakdown

Isotopic enrichment of 3-MeH in plasma after 2 weeks of cast immobilisation in healthy volunteers and patients is shown in Figure 5.7a, and from this enrichment decay rate constants (k) were calculated, shown in Figure 5.7b.

Over the 7 hours of sampling plasma 3-MeH k was no different when comparing patients with healthy volunteers (0.034 ± 0.007 vs 0.028 ± 0.008, p=0.56), resulting in no difference in whole-body muscle protein breakdown when comparing groups at this time-point (p=0.42).

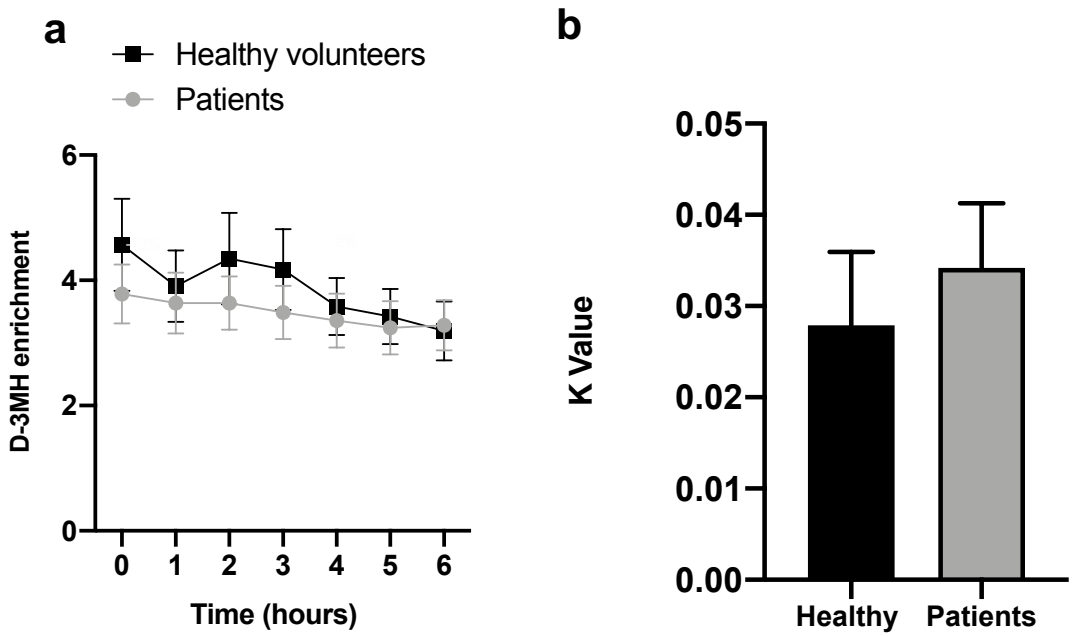

Figure 5.7. Whole-body muscle protein breakdown. a) Decay curves of D_3-methylhistidine in the plasma by endogenous 3-methylhistidine release in patients and healthy volunteers after 2 weeks of cast immobilisation b) Rate of whole-body muscle protein breakdown (k) using D_3-methylhistidine. Values are mean ± SEM (and individual values in Figure 5.4b), for healthy volunteers and n=10 for patients.

5.4.8. Pro-Inflammatory cytokines

Serum CRP (mg/l) and IL6 (pg/ml) concentrations are shown in Table 5.3. Serum CRP concentration was greater in patients pre-surgery (but post-injury)

than in healthy volunteers pre-casting ($p \leq 0.01$). Compared with both pre and 1 day post-surgery, CRP at 2 weeks was lower in patients ($p < 0.05$). Compared with pre-casting, limb immobilisation had no impact on CRP in healthy volunteers ($p = 0.89$). Serum IL6 concentration was greater in patients pre-surgery (but post-injury) than in healthy volunteers before casting ($p < 0.05$). Compared with pre-surgery, IL6 was greater 1-day after surgery in patients ($p < 0.05$) and had declined at 2 weeks in patients compared to before ($p \leq 0.01$) and 1 day post-surgery ($p < 0.05$). Compared with pre-casting, limb immobilisation had no impact on IL6 concentration in healthy volunteers ($p = 0.46$).

*Table 5.3. Pro-inflammatory cytokines. Serum C-reactive protein (CRP) and Interleukin-6 (IL6) concentration measured in healthy volunteers before (pre) and 2 weeks after (2 weeks) lower limb casting and ankle fracture patients before surgery (pre-surgery), 1-day after surgery (1-day post-surgery) and 2 weeks after surgery (2 weeks). *, p<0.05 vs pre surgery, †, p=0.051 vs pre surgery, #, p<0.05, ##, p≤0.01 vs 1-day post-surgery, $, p<0.05, $$, p≤0.01 vs corresponding time point in healthy volunteers. Values are mean ± SEM.*

	Healthy volunteers		Patients		
	Pre-casting	2 weeks	Pre-surgery	1 day post-surgery	2 weeks
CRP (mg/l)	2.7 ± 1.2	2.9 ± 1.6	11.1 ± 2.3$^{\$\$}$	21.5 ± 5.5	6.5 ± 2.8 $^{*\#}$
IL6 (pg/ml)	1.1 ± 0.4	1.4 ± 0.7	6.5 ± 2.4$^{\$}$	22.4 ± 6.5*	2.3 ± 0.8$^{\#\#\dagger}$

5.4.9 Muscle mRNA expression

mRNA expression of 191 targets (the same genes as in Chapter 3 and 4) in muscle was quantified using low-density array cards before surgery and after 2 weeks in patients and before casting and 2 weeks after casting of the healthy volunteers. Cellular functions identified by IPA as being altered 2 weeks post-surgery in the injured leg of patients relative to before surgery, and in the casted leg of healthy control participants compared to before casting, are depicted in Figure 5.8 (note this does not depict the direction of change). The magnitude of change (-log (p value)) for the majority of altered cellular functions was greater in the injured leg of the patients compared with the casted leg of the controls. There were 21 cellular functions that displayed a -log (p value) of ≥10 in the patients compared with 13 in the healthy volunteers. There were 12 cellular functions common to both the injured leg of the patients and casted leg of the healthy volunteers that were altered (Table 5.4), with the most notably affected [-log (*p* value) ≥ 15] in both being 'organismal injury and abnormalities' and 'skeletal and muscular disorders'. There were 9 cellular functions that were altered in the patients injured leg but not the healthy volunteers' casted leg including 'immune cell trafficking' and 'inflammatory response', and 8 cellular functions that were altered in the healthy volunteers' casted leg but not the patients injured leg including 'organismal development' and 'organ morphology' (Table 5.4).

Cellular functions identified by IPA as being altered in the uninjured leg of patients and the non-casted leg of healthy volunteers relative to before

surgery or limb casting (in the contralateral leg) are depicted in Figure 5.9 (note this does not depict the direction of change). The magnitude of change in mRNA expression overall was greater in the uninjured leg of the patients compared with the non-casted leg of the controls. There were 10 cellular functions that had a -log (p value) ≥10 in the patients compared with none in the healthy volunteers of this magnitude. There were 9 cellular functions common to both the uninjured leg of the patients and the non-casted leg of the healthy volunteers that were altered (Table 5.5). There were 10 cellular functions that were altered in the patients uninjured leg but not the healthy volunteers non-casted leg, including ‘immune cell trafficking’, ‘inflammatory response’ and ‘cell-mediated immune response’. There were 11 cellular functions altered in the healthy volunteers non-casted leg but no the patient’s uninjured leg including ‘organismal development’ and ‘tissue morphology’ (Table 5.5).

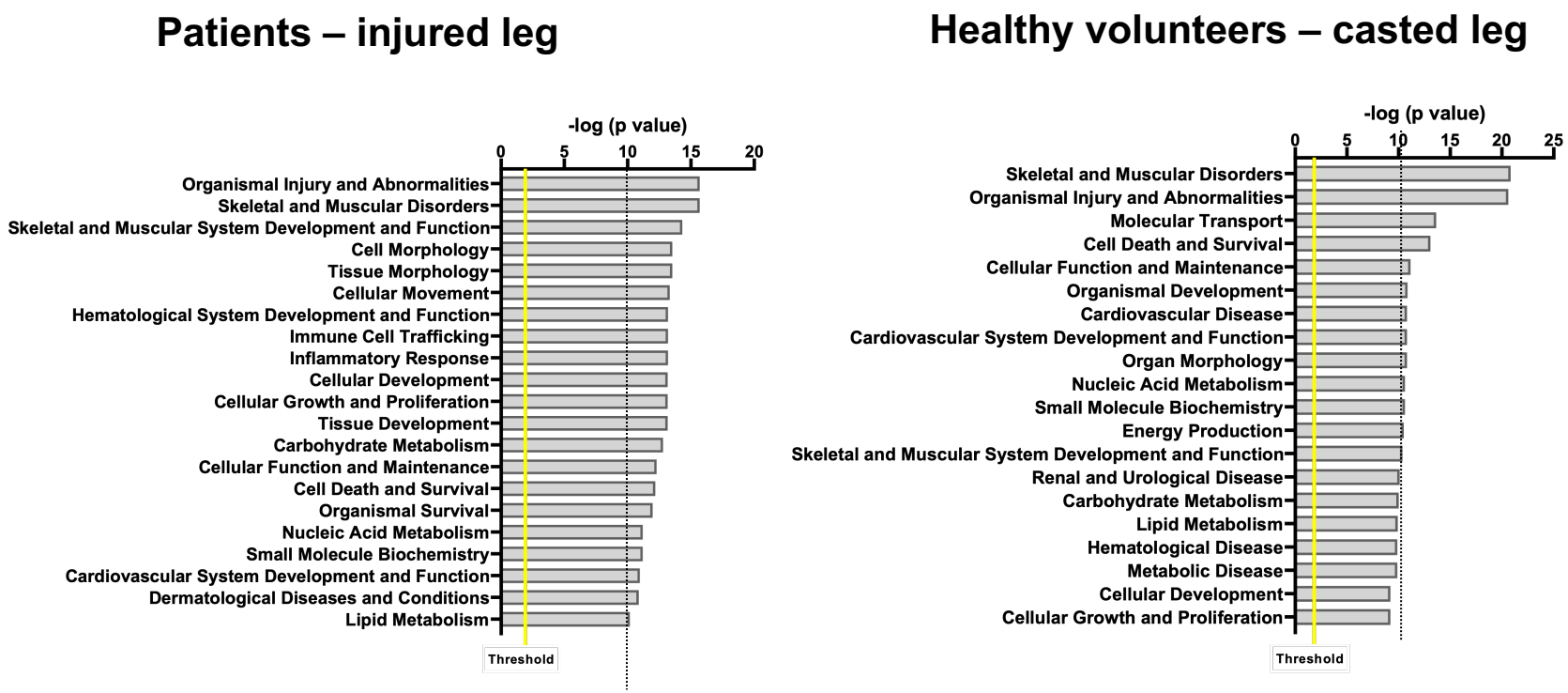

Figure 5.8. Muscle cellular functions in the patient's injured leg and healthy volunteer's casted leg. Cellular functions identified by IPA as being altered in the injured leg of patients and the casted leg of healthy control participants relative to before surgery or casting based on mRNA expression data generated using low-density micro-array cards. The y-axis displays cellular functions and the x-

axis displays -log of the p value. The threshold line (yellow) corresponds to a fold change of 1.5 above baseline with a p value of 0.05, and for ease of comparison the black dotted line represents [-log (p value) ≥10].

Table 5.4. Summary of cellular functions in the patient's injured leg and healthy volunteer's casted leg. Cellular functions identified by IPA as being altered (relative to before surgery in patients and before casting for healthy volunteers) in the injured leg of patients and the casted leg of healthy volunteers.

Common to both patients injured leg & healthy volunteers casted leg	**Patients injured leg only**	**Healthy casted leg only**
• Organismal injury and abnormalities • Skeletal and muscular disorders • Skeletal and muscular system development & function • Cellular development • Cellular growth and proliferation, • Carbohydrate metabolism • Cellular function and maintenance • Cell death and survival • Nucleic acid metabolism • Small molecule biochemistry • Cardiovascular system development and function • Lipid metabolism	• Cell morphology • Tissue morphology • Cellular movement • Haematological system development and function • Immune cell trafficking • Inflammatory response • Tissue development • Organismal survival • Dermatological diseases & conditions	• Molecular transport • Organismal development • Cardiovascular disease • Organ morphology • Energy production • Renal and urological disease • Haematological disease • Metabolic disease

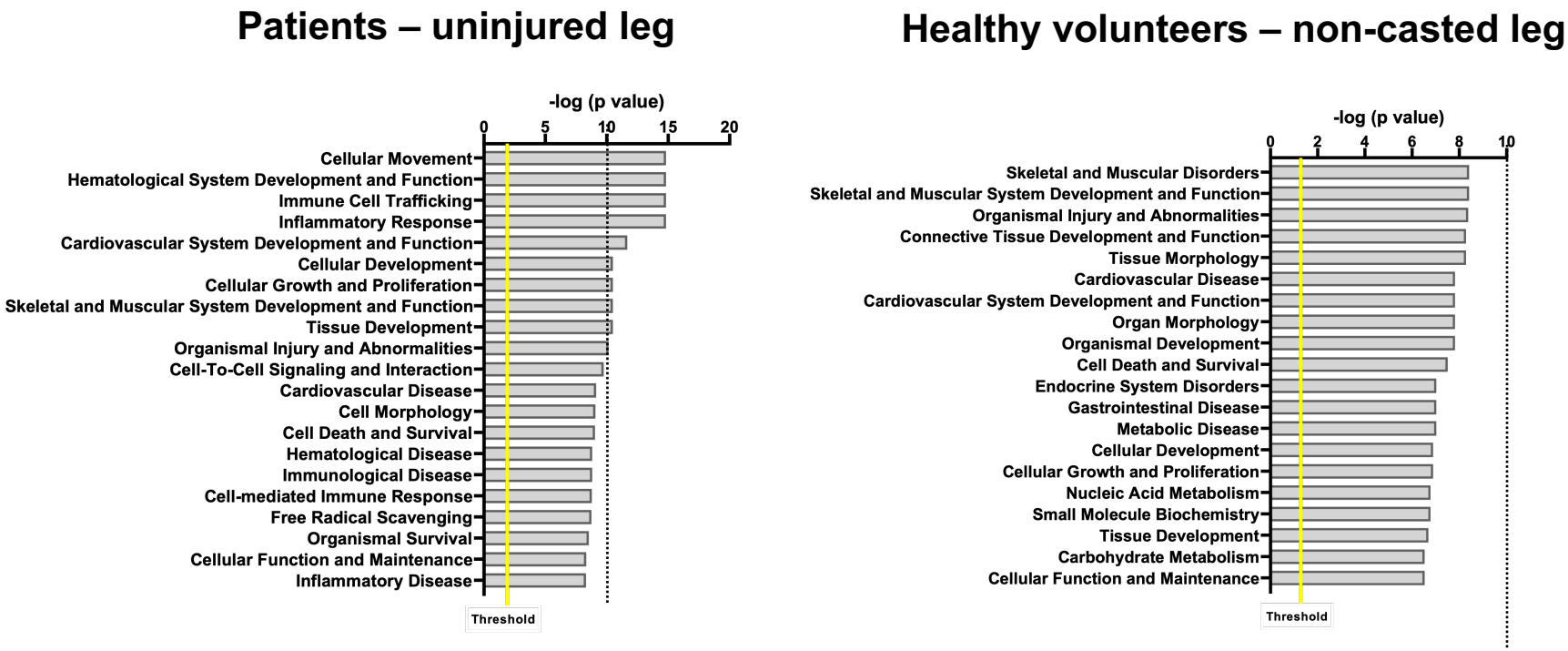

Figure 5.9. Muscle cellular functions in the patient's uninjured leg and healthy volunteer's non-casted leg. Cellular functions identified by IPA as being altered in the uninjured legs of patients and the casted legs of healthy control participants relative to before surgery or casting based on mRNA expression data generated using the low-density micro-array cards. The y-axis displays cellular functions and the x-axis displays -log of the p value. The threshold line corresponds to a fold change of 1.5 above baseline with a p value of 0.05 and, for ease of comparison, the black dotted line represents [-log (p value) ≥10].

Table 5.5. Summary of cellular functions in the patient's uninjured leg and healthy volunteer's non-casted leg. Cellular functions identified by IPA as being altered (relative to before surgery in patients and before casting for healthy volunteers) in the uninjured leg of patients and the non-casted leg of healthy volunteers.

Common to both patients uninjured leg & healthy volunteers non-casted leg	**Patients uninjured leg only**	**Healthy volunteers non-casted leg only**
• Cardiovascular system development and function • Cellular development • Cellular growth and proliferation • Skeletal and muscular system development and function • Tissue development • Organismal injury and abnormalities • Cardiovascular disease • Cell death and survival • Cellular function and maintenance	• Cellular movement • Haematological system development and function • Immune cell trafficking • Inflammatory response • Cell-to-cell signalling and interaction • Cell morphology • Haematological disease • Immunological disease • Cell-mediated immune response • Inflammatory disease	• Skeletal and muscular disorders • Connective tissue development and function • Tissue morphology • Organ morphology • Organismal development • Endocrine system disorders • Gastrointestinal disease • Metabolic disease • Nucleic acid metabolism • Small molecule biochemistry • Carbohydrate metabolism

One of the most altered cellular functions in both the patients injured leg and the healthy volunteers casted leg was ‘organismal injury and abnormalities’. When considering the mRNA networks and predicted cellular events generated by IPA for this cellular function however, distinct differences were evident (Figure 5.10). In the patients injured leg, 21 transcripts were altered in abundance (15 upregulated and 6 downregulated) 2 weeks after surgery compared with before surgery and based on these collective responses IPA strongly predicted (amongst others) an activation of ‘apoptosis of epithelial cells’, ‘apoptosis of endothelial cells’, ‘dyslipidaemia’ and ‘diabetes mellitus’ and an inhibition of ‘oedema’, ‘fibrosis’, ‘hyperinsulinism’ and ‘inflammation of joint’. In the casted leg of the healthy volunteers, there were 18 transcripts altered in abundance (9 upregulated and 9 downregulated) 2 weeks after casting compared with before. Based on these collective differences IPA strongly predicted (amongst others) an activation of ‘insulin resistance’, ‘hyperglycaemia’, ‘wasting’, ‘fibrosis’ and ‘abnormal metabolism’ and an inhibition of ‘rheumatic disease’. In the case of ‘skeletal and muscular disorders’, another notably altered cellular function, the mRNA networks and predicted cellular events generated by IPA were more similar (Figure 5.10). In the patients injured leg, 13 transcripts were altered in abundance (11 upregulated and 2 downregulated) 2 weeks after surgery compared with before surgery and based on these collective responses IPA strongly predicted (amongst others) an activation of ‘apoptosis of muscle cells’, ‘cell death of muscle cells’, ‘abnormality of limb’, ‘and an inhibition of ‘inflammation of joint’. In the casted leg of the control participants, there were 11 transcripts altered in

abundance (4 upregulated and 7 downregulated) 2 weeks after casting compared with before casting and based on these collective differences IPA strongly predicted (amongst others) an activation of ‘apoptosis of muscle cells’, ‘cell death of muscle cells’, ‘atrophy of muscle cells’, ‘fatigue of muscle’ and ‘abnormality of limb’. The cellular functions ‘cellular function and maintenance’ and ‘cell death and survival’ are also shown in Table 5.6 and the IPA schematics of these functions and predicted cellular events are included in Appendix 3. These cellular functions have been included as the magnitude of change (-log(p value) were >10 for both the patients injured leg and the healthy volunteers casted leg.

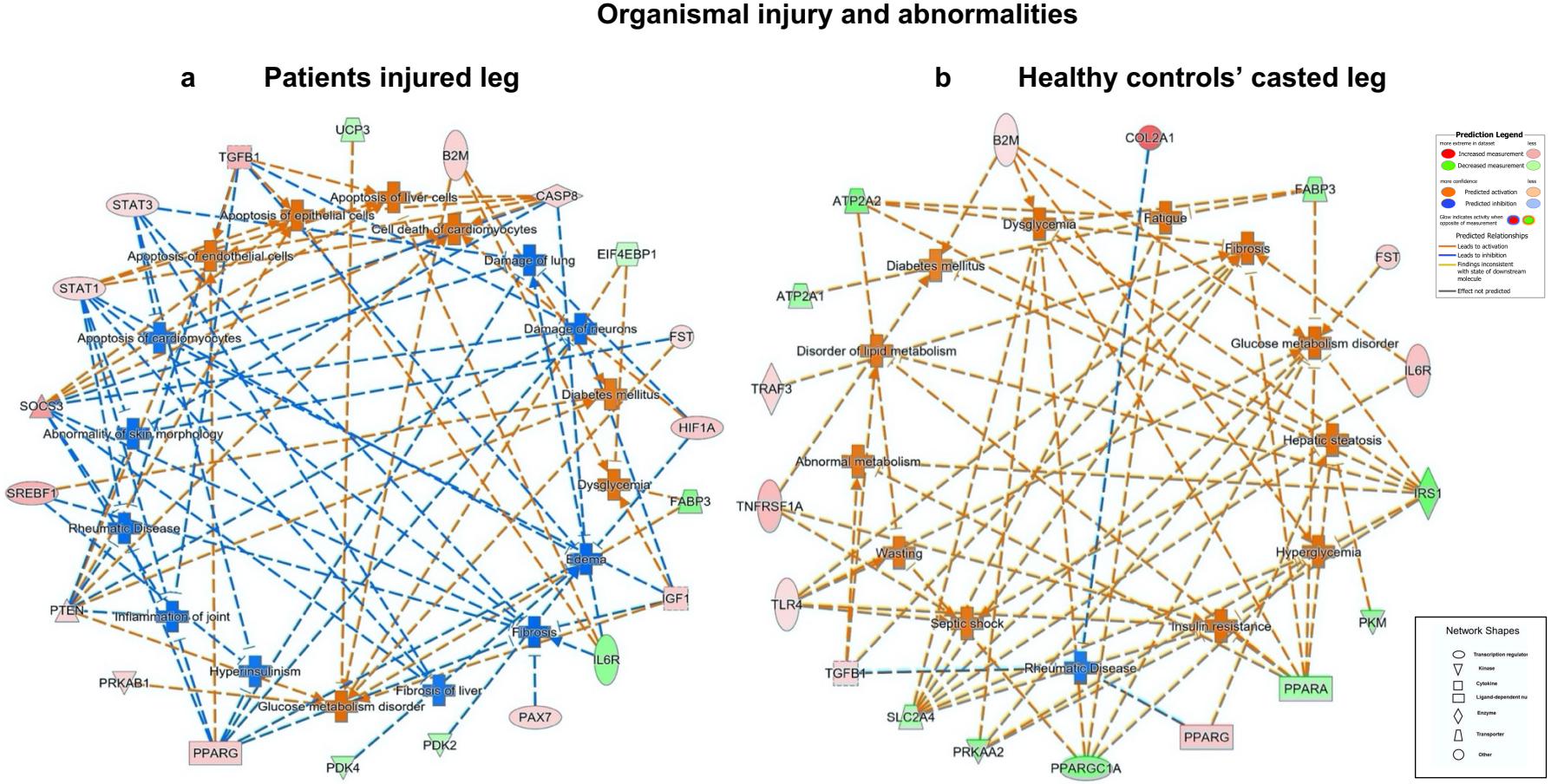

Figure 5.10. Pathway analysis for organismal injuries and abnormalities. Ingenuity Pathway Analysis schematic highlighting mRNAs differentially regulated from baseline in the organismal injury and abnormalities network (outer ring) and the predicted cellular events (inner octagons) associated with these collective changes in the a) injured legs of patients and b) casted leg of controls compared with before surgery and casting.

Skeletal and muscular disorders

a Patients injured leg **b Healthy controls' casted leg**

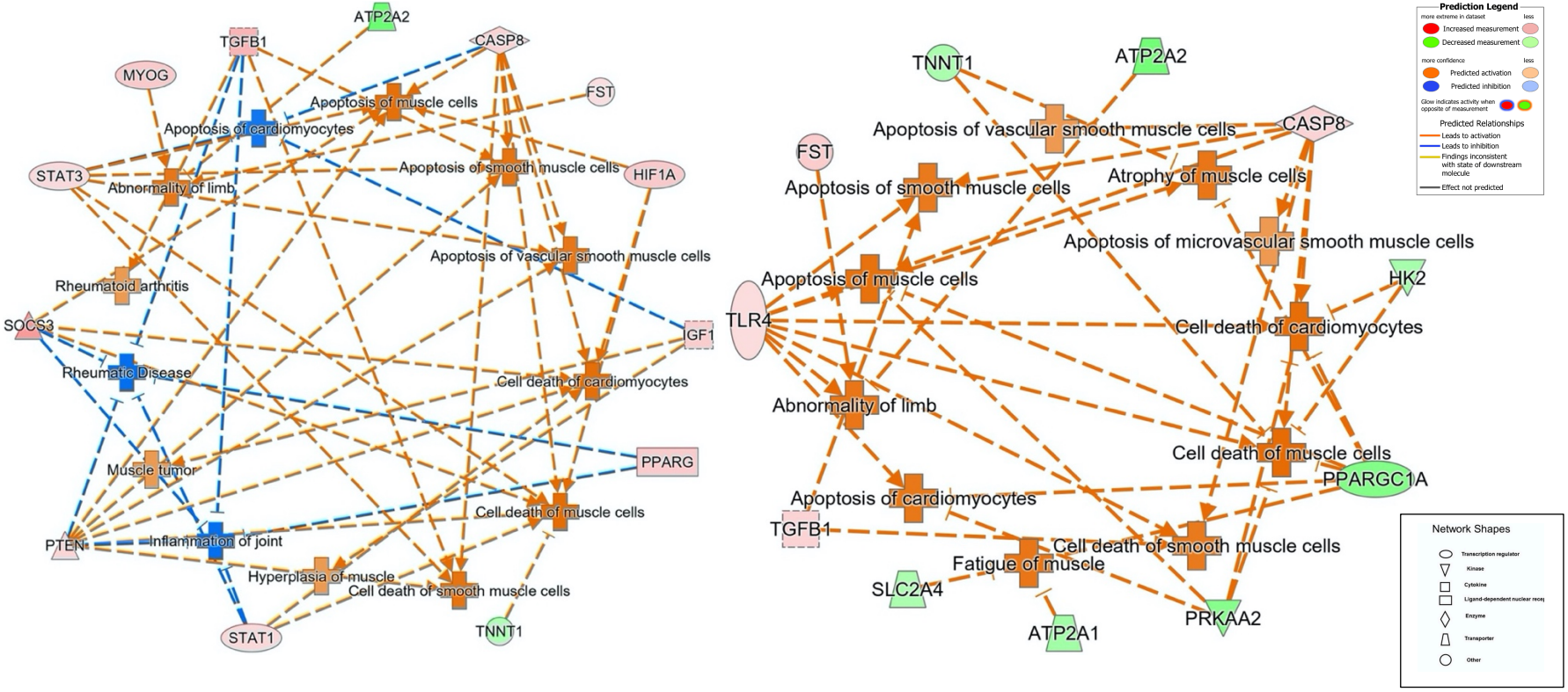

Figure 5.11. Pathway analysis for skeletal and muscular disorders. Ingenuity Pathway Analysis schematic highlighting mRNAs differentially regulated from baseline in the skeletal and muscular disorders network (outer ring) and the predicted cellular events (inner octagons) associated with these collective changes in the a) injured legs of patients and b) casted leg of controls compared with before surgery and casting.

Table 5.6. Summary of cellular functions in the patient's injured leg and healthy volunteer's casted leg. Summary of the cellular functions 'Organismal Injury and Abnormalities', 'Skeletal and Muscular Disorders', 'Cellular function and maintenance' and 'Cell death and survival' and the cellular events predicted by IPA as altered and their number of differentially regulated mRNAs in the injured legs of patients 2 weeks after surgery and cast immobilisation relative to before surgery and in the casted leg of healthy volunteers 2 weeks after cast immobilisation relative to before casting. Cellular predictions not directly related to the aims of this study have not been commented on.

	Injured leg of patients		Casted leg of healthy volunteers	
Cellular functions	**Number of differentially regulated mRNAs**	**IPA prediction of cellular events**	**Number of differentially regulated mRNAs**	**IPA prediction of cellular events**
Organismal Injury and Abnormalities	20 – 14 upregulated, 6 downregulated	• Activation of 'epithelial cells', 'apoptosis of endothelial cells', • Inhibition of 'oedema', 'fibrosis', 'hyperinsulinism', 'inflammation of joint'	18 – 9 upregulated, 9 downregulated	• Activation of 'insulin resistance', 'hyperglycaemia', 'diabetes' mellitus', 'wasting', 'dysglycaemia', 'fibrosis' • Inhibition of 'rheumatic disease',
Skeletal and Muscular Disorders	13 – 12 upregulated and 1 downregulated	• Activation of 'apoptosis of muscle cells', 'abnormality of limb', 'cell death of muscle cells' • Inhibition of 'inflammation of joint'.	11 – 7 downregulated and 4 upregulated	• Activation of 'atrophy of muscle cells', 'apoptosis of muscle cells', 'cell death of muscle cells', 'fatigue of muscle', 'abnormality of limb'.
Cellular function and maintenance	19 – 4 upregulated, 15 downregulated	• Activation of 'autophagy of cells', 'autophagy', 'engulfment of antigen presenting cells', 'engulfment of phagocytes' • Inhibition of 'proliferation of endothelial cells'	19 – 10 upregulated, 9 downregulated	• Activation of 'autophagy', 'autophagy of cells', 'cellular homeostasis', 'influx of calcium', 'ion homeostasis of cells', • Inhibition of 'glycolysis of tumour cell lines' and 'respiration of mitochondria'
Cell death and survival	28 – 7 upregulated and 21 downregulated	• Activation of 'apoptosis of muscle cells', 'cell death of muscle cells', 'cell viability'. • Inhibition of 'apoptosis',	35 – 20 upregulated, 15 downregulated	• Activation of 'apoptosis', 'apoptosis of muscle cells', 'cellular degradation', 'necrosis' • Inhibition of 'cell survival' and 'cell viability'

A noticeable difference in the transcriptional response overall in the patients compared with the healthy volunteers was the observation that the cellular functions ‘immune cell trafficking’ and ‘inflammatory response’ were identified by IPA as being altered relative to before surgery, in both the injured and uninjured legs of the patients [-log (*p* value) ≥ 10], and the magnitude of change (-log(p value)) for each function was similar in both limbs (Table 5.7). However, in distinct contrast to these observations, in the healthy volunteers there was no immune or inflammatory response observed in either the casted or non-casted leg (Figure 5.8 and Figure 5.9), which aligns with the responses in serum pro-inflammatory cytokines shown in Table 5.3. In the case of ‘immune cell trafficking’ in the patients injured leg there were 19 transcripts altered in abundance (15 upregulated and 4 downregulated) and based on these collective changes, IPA predicted amongst a number of things an activation of ‘migration of phagocytes, ‘recruitment of leucocytes’, ‘cell movement of monocytes’ and an inhibition of ‘cell movement of neutrophils’, ‘cell movement of phagocytes’, ‘cellular infiltration of macrophages’ (Figure 5.11 and Table 5.7). In the patients uninjured leg there were 12 transcripts upregulated and based on these collective changes, IPA predicted an activation of ‘recruitment of phagocytes, neutrophils and leucocytes’, ‘cellular movement of macrophages’ and ‘adhesion of immune cells’. In the case of ‘inflammatory response’, in the patients injured leg there were 21 transcripts altered in abundance (17 upregulated and 4 downregulated) compared with before surgery and based on these collective differences IPA predicted an activation of ‘response of macrophages’, ‘recruitment of phagocytes’, ‘quantity

of phagocyctes', 'migration of monocytes' and an inhibition of 'inflammatory response', 'cell movement of neutrophils and phagocytes', 'activation of leucocytes.' (Figure 5.12 and Table 5.7). In the patients uninjured leg there were 14 transcripts altered in abundance (13 upregulated and 1 downregulated) and based on these collective changes IPA predicted an activation of 'inflammatory response', 'migration of neutrophils', 'immune response of cells', 'recruitment of neutrophils and phagocytes' and an inhibition of 'quantity of phagocytes.

Immune cell trafficking

a Patients injured leg

b Patients uninjured leg

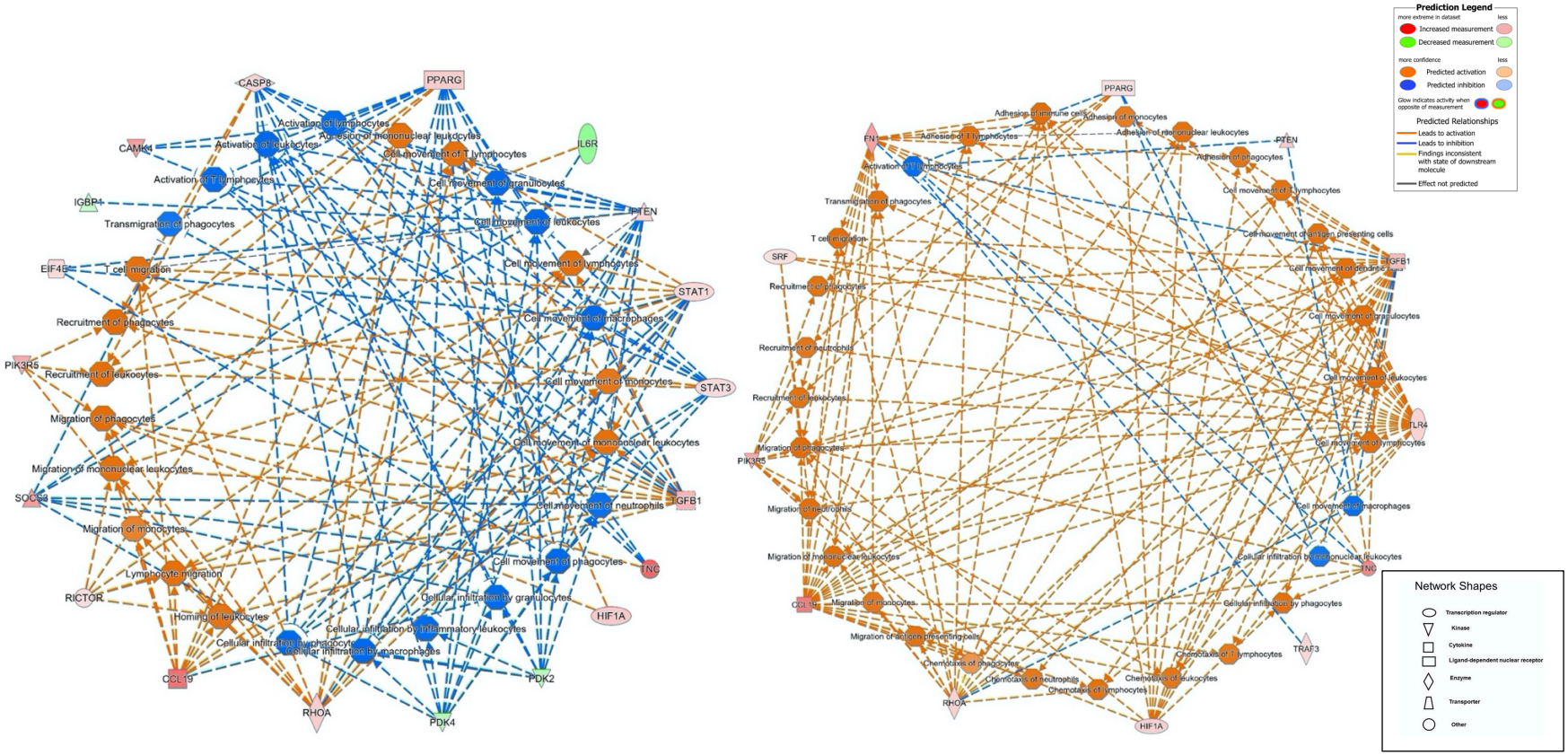

Figure 5.11. Pathway analysis for immune cell trafficking. Ingenuity Pathway Analysis schematic highlighting mRNAs differentially regulated from baseline in the 'Immune cell trafficking' network (outer ring) and predicted cellular events (inner octagons) associated with these collective changes in a) injured legs of patients and b) uninjured compared with before surgery.

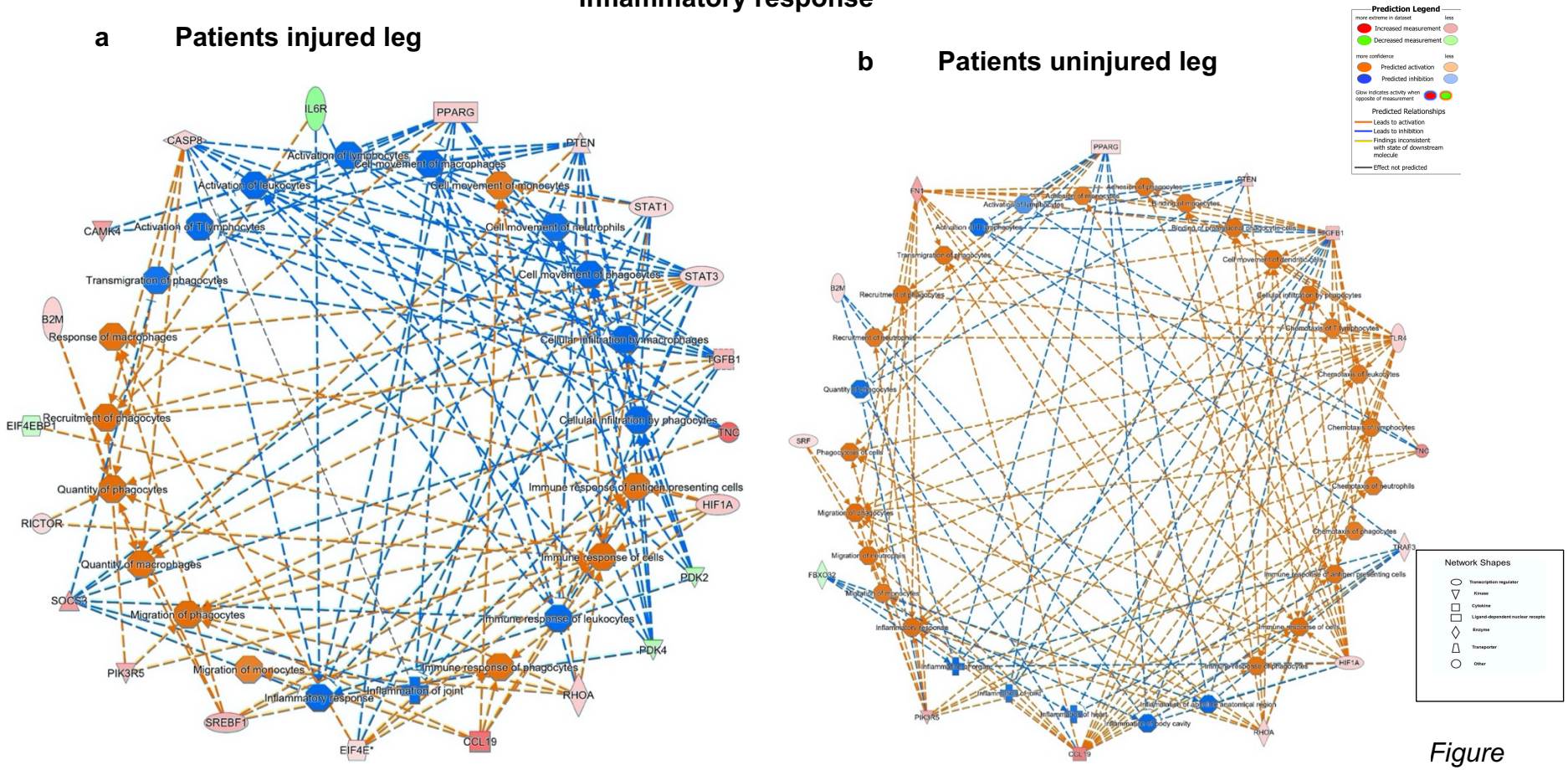

Figure 5.12. Pathway analysis for inflammatory response. Ingenuity Pathway Analysis schematic highlighting mRNAs differentially regulated from baseline in the 'Immune cell trafficking' network (outer ring) and the predicted cellular events (inner octagons) associated with these collective changes in the a) injured legs of patients and b) uninjured compared with before surgery.

Table 5.7. Summary of the cellular functions in the patient's injured and uninjured leg. Summary of the cellular functions 'Immune cell trafficking' and 'Inflammatory response' and the cellular events predicted by IPA as altered and their number of differentially regulated mRNAs in the injured legs of patients 2 weeks after surgery and cast immobilisation relative to before surgery and in the uninjured leg of patients after 2 weeks. Cellular predictions not directly related to the aims of this study have not been commented on.

	Injured leg of patients		**Uninjured leg of patients**	
Cellular functions	**Number of differentially regulated mRNAs**	**IPA prediction of cellular events**	**Number of differentially regulated mRNAs**	**IPA prediction of cellular events**
Immune cell trafficking	19 – 15 upregulated, 4 downregulated	• Activation of 'migration of phagocytes, 'recruitment of leucocytes', 'cell movement of monocytes' • Inhibition of 'cell movement of neutrophils', 'cell movement of phagocytes', 'cellular infiltration of macrophages'	12 –all upregulated	• Activation of 'recruitment of phagocytes, neutrophils and leucocytes', 'cellular movement of macrophages', 'adhesion of immune cells'.
Inflammatory response	21 – 17 upregulated and 4 downregulated	• Activation of 'response of macrophages', 'recruitment of phagocytes', 'quantity of phagocyctes', 'migration of monocytes' • Inhibition of 'inflammatory response', 'cell movement of neutrophils and phagocytes', 'activation of leucocytes.'.	14 – 13 upregulated and 1 downregulated	• Activation of 'inflammatory response', 'migration of neutrophils', 'immune response of cells', 'recruitment of neutrophils and phagocytes', • Inhibition of 'quantity of phagocytes'.

5.5. Discussion

This study aimed to investigate the impact of immobilisation and inflammation on *medial gastrocnemius* muscle thickness and myofibrillar protein synthesis over 2 weeks in patients following ankle fracture fixation, and whole-body muscle protein breakdown at the 2 week time point, in comparison to matched healthy volunteers that underwent unilateral limb immobilisation over the same time period. The major findings are firstly, that *medial gastrocnemius* muscle thickness declined 7.2% in the casted legs of healthy volunteers and 16.7% in the injured leg of ankle fracture patients after 2 weeks immobilisation. This corresponded to a greater absolute muscle thickness change in the patients compared with healthy controls but no difference in % change. Secondly, average daily FSR rates over these 2 weeks declined in the immobilised limb of healthy volunteers from the pre immobilisation state and was no different from the rate measured in the injured limb of patients. Thirdly, the rate of whole-body muscle protein breakdown at the 2 week time point was also comparable between volunteer groups. Finally, patients had a marked inflammatory response reflected in raised serum pro-inflammatory cytokines perioperatively and changes in muscle mRNA abundance at 2 weeks, which were evident in both limbs, but completely absent in serum and muscle in the healthy volunteers.

This study demonstrated a greater absolute change in *medial gastrocnemius* muscle thickness in patients injured legs compared with healthy

controls casted legs, implying that inflammation plus immobilisation causes greater changes in muscle mass than immobilisation alone. This may reflect a greater muscle protein loss in the legs of the patients due to the inflammation caused by the injury and subsequent surgery. Previous studies of simple disuse have reported a ~10% reduction in ankle extensor (gastrocnemius and soleus) muscle volume measured using MRI after 2 weeks of bed rest (LeBlanc et al. 1992). Greater degrees of change have been reported after longer periods, e.g., a 17% reduction in *medial gastrocnemius* volume measured using MRI has been reported after 4 weeks of bed rest (Miokovic et al. 2014). In contrast, in models of lower limb injury, Psatha showed a total muscle volume loss of 16% and *medial gastrocnemius* CSA reduction of ~16% using MRI in the immobilised leg of conservatively managed (no surgical fixation) ankle fracture patients 15 days after casting (Psatha et al. 2012). Other studies have reported a decrease of 14% in posterior calf (gastrocnemius and soleus) volume after 2 weeks casting following ankle fracture (Stevens et al. 2004) and a decrease of 8% in calf CSA after 4 weeks of below knee casting following an fifth metatarsal or fibular fracture measured using MRI (Yoshiko et al. 2018). The greater degree of atrophy in studies where *medial gastrocnemius* only is measured compared with whole calf likely reflects the differential muscle atrophy according to the different muscle compartments e.g., deep vs superficial plantarflexors. The degree of muscle thickness change in this study therefore appear to be in keeping with previous literature. The difference in muscle thickness change may also however partly be explained by a larger baseline muscle volume in the patients, given this was conducted 1 day post-surgery,

and oedema may have falsely caused a larger muscle thickness on US at this first time point. The presence of oedema following injury is difficult to quantify accurately using imaging, particularly ultrasound, and such it is not clear how much this may have contributed to the muscle thickness change. Nevertheless, muscle CSA loss measured using this method has been confirmed in other similar studies in clinical populations, and the protein to DNA ratio was also quantified in order to support protein, rather than fluid loss (Puthucheary et al. 2013).

The present study supports the findings in Chapter 4 and the literature that a reduction in MPS is a primary driver of muscle mass loss in simple disuse in humans and with previous studies that have shown it is an important factor in muscle mass loss under circumstances of inflammation. In situations of simple disuse, studies have reported a 50% decline in postabsorptive myofibrillar protein synthesis after 10 days of limb suspension in healthy volunteers (de Boer et al. 2007) as well as blunting of post-prandial increases in MPS also being implicated (Glover et al. 2008). There are limited studies that directly measure MPS in human models of musculoskeletal trauma. Puthucheary reported an increase in FSR from day 1 to day 7 after admission to ICU measured using acute IV tracer techniques, however this study was confounded by nasogastric feeding in all patients and the use of insulin sliding scales to maintain blood glucose. In the study in this chapter, there was a depression of MPS at 2 weeks in the patients injured leg, which was comparable to the MPS decrease in the healthy volunteer casted leg. There was also a significant but moderate correlation between change in muscle

thickness and FSR over the 2 weeks of immobilisation (in the patients injured leg and healthy volunteers casted leg) with 20% of the variability between the two parameters explained by this relationship, indicating that although a reduction in MPS is an important factor and directly related to muscle mass loss, other influences are implicated. Overall, therefore, an equal blunting of MPS is observed in immobilisation plus inflammation and immobilisation alone.

Turning to the muscle mRNA responses, there were 12 cellular functions altered common to both groups with “organismal injury and abnormalities” and “skeletal and muscular disorders” being the most altered functions. Interestingly, the cellular events predicted by IPA related to ‘organismal injury and abnormalities’ were different between the injured limb of patients and casted limb of healthy volunteers and overall, the magnitude of change (-log(p value)) for the majority of altered cellular functions was greater with trauma and immobilisation compared with immobilisation alone. This indicates that the combination of musculoskeletal injury and immobilisation was a greater cellular insult than disuse alone. There were also 9 altered functions specific to the patients injured leg (largely related to inflammation and cellular and tissue functions) and 8 altered functions specific to the healthy volunteer’s casted leg (for example related to organismal development and metabolic disease). This points to a differential transcriptional response between simple disuse and disuse plus inflammation.

Previous research in rodents has suggested increases in MPB may be apparent early in disuse and contribute to muscle mass loss (Taillandier et al. 2003; Abadi et al. 2009) and has been implicated in inflammatory-related

muscle atrophy (Constantin et al. 2011). The study in Chapter 4 which measured MPB using the same method as the present study demonstrated a reduced, rather than raised, MPB after 2 days of bed rest. In the present study there was no difference in whole-body MPB measured at 2 weeks in patients and healthy volunteers, indicating a similar level of catabolism in both immobilisation plus inflammation and immobilisation at this time point. These results should be interpreted with caution however due to the limitation of a single time point which was 2 weeks after discharge from hospital (due to the logistical difficulty in measuring this immediately perioperatively) or 2 weeks after casting which may not have captured any early changes in MPB, and which also reflects the whole-body and not the muscle. Previous studies in patients with critical illness which have attempted to measure MPB, have been confounded by nasogastric feeding and concomitant insulin infusion to control hyperglycaemia, both of which may depress rates of MPB (Wandrag et al. 2019; Puthucheary et al. 2013) and it is therefore difficult to directly compare the present results with such clinical studies which also used different methods for determining MPB. Acute studies using endotoxin administration found simultaneous increases in MPS and MPB with unaffected protein balance (Vesali et al. 2009), however this was in the postabsorptive state where MPS is normally expected to be depressed. The rate constant (k) reflecting MPB in this study was substantially lower than that measured using the same method previously in older adults under free living conditions where they report a rate constant of approximately 0.08 (Cegielski et al. 2021; Sheffield-Moore et al. 2014), potentially suggesting the rates of MPB measured in this study were not

raised compared to normal free living conditions. However, in the study by Cegielski et al, participants were not fasted during period of sampling, and as insulin suppresses MPB, these results reflect MPB in the fed state. Overall, the results in this chapter suggest there were no difference in rates of whole-body MPB between patients or healthy volunteers at 2 weeks, however the single time point at 2 weeks and whole-body measurement may have missed any transient early changes in limb MPB. We therefore cannot conclude from this study the differential impact of inflammation plus immobilisation and immobilisation alone on limb MPB acutely.

An additional finding of this study was the reduction in rates of MPS in the uncasted leg of the healthy volunteers. A possible explanation for this is the low physical activity levels measured in the healthy volunteers which equated with a “sedentary” physical activity level/ <3000 steps. Although the effect of lower leg casting on healthy individuals’ physical activity behaviour has rarely been explored in the literature, anecdotally healthy volunteers in this study reported that they were significantly more sedentary during the study compared with normal e.g., ordered home food deliveries instead of visiting the supermarket. Overall, however, the magnitude of change (-log(p value) of altered cellular functions was less compared to the patients or the healthy volunteer’s casted leg, with none having a -log (p value) ≥10. Whilst patients were also equally as physically inactive and one would assume the same pattern may have been observed in the uninjured leg, there was a wide variation in the period of bed rest prior to surgery and prior to chronic measures of MPS being taken, and any acute changes in MPS in the uninjured leg that may have

occurred after injury may have been missed, especially in patients whose delay to surgery was substantial.

One of the marked differences overall between patients and healthy volunteers was the inflammatory response, with patients having a profound increase in serum pro-inflammatory cytokines compared with healthy volunteers both pre-surgery (post-injury) and post-surgery, and this was reflected by increases in mRNA expression of genes related to inflammation measured at 2 weeks. This supports previous research in patients undergoing elective surgery for hip osteoarthritis who reported a similar degree of increase in serum IL6 1 day after surgery as the patients in the present study (Reikerås and Borgen 2014). The patients in this study were already in a pro-inflammatory state prior to surgery due to their injury (albeit there was a large range in time between injury and surgery), but the insult of the surgery caused a further increase in serum pro-inflammatory cytokines (e.g., CRP went from 11.1 to 21.5 mg/L). In comparison, the healthy volunteers had pro-inflammatory cytokines within the normal reference range, both at baseline (e.g., CRP 2.7 mg/L) and in response to casting (CRP 2.9 mg/L), and there was an absence of a muscle transcriptional inflammatory signature, challenging the assertion that physical inactivity and immobilisation *per se* may cause a pro-inflammatory state. Cross sectional data in humans has suggested increased sedentary time is independently associated with chronic low-grade systemic inflammation (CRP and IL6)(Yates et al. 2012; Howard et al. 2015; Mora et al. 2006) however, the absolute values of cytokines in these studies remain within the normal reference range (e.g. CRP <5 mg/L), and the results are often attenuated when

adjusting for BMI and sedentary time has tended to be captured using self-report. When looking at mechanistic studies using bed rest models, although some have reported an increase in muscle IL6 mRNA expression (Drummond et al. 2013), this was alongside an increase of only 2 (interferon-γ and macrophage inflammatory protein-1β) out of 17 measured serum proinflammatory cytokines. Similarly, others have found no change in serum CRP, IL6 or TNF-alpha after 5 days bed rest (Hamburg et al. 2007). One study reported an increase in CRP (1.2 to 2.3 mg/L) and IL6 (3.4 to 11.4 pg/ml) after 2 weeks of bed rest, however CRP remained within the standard reference range (Bosutti et al. 2008) questioning the clinical significance despite a statistical increase. Similarly, increases in serum IL6 (approximately 16 to 25 pg/ml) and TNF-α (6 to 8 pg/ml) were demonstrated in older adults, but not young, after 2 weeks of bed rest. However this was associated with an increase in fat free mass (Jurdana et al. 2015) and obesity has been associated with chronic low-grade inflammation via several different mechanisms (Wu and Ballantyne 2017). Taken together with the results from the present study, this demonstrates that the inflammatory response secondary to major trauma both at a systemic level and muscle mRNA abundance is substantively greater than that associated with physical inactivity, ageing and obesity. This supports the notion that the mechanisms behind muscle atrophy associated with inflammation “inflammatory-mediated muscle atrophy” and immobilisation “non-inflammatory mediated muscle atrophy” are distinct.

One of the novel aspects of this study design was the ability to investigate whether systemic inflammation impacted the contralateral uninjured

limb in the patients. There was no change in muscle thickness or FSR in the uninjured leg of the patients, however there was a clear inflammatory transcriptional signature in the muscle. This suggests that systemic inflammation alone was insufficient to cause muscle atrophy and a reduction in MPS. There were differences in the cellular events predicted by IPA between legs based on collective mRNA changes. For example, in the injured legs of the patients, there were more cellular events related to inflammation that were inhibited compared to the uninjured leg where the majority of predicted cellular events were activated. In the injured leg, the gene networks may have already been significantly altered at the time of the first biopsy due to the fracture and delay in surgery. These findings indicate a differential influence of local versus systemic inflammation on mRNA changes at the muscle level and that local injury causing muscle inflammation is key in inducing muscle atrophy in situations of inflammation. Previous research has reported differences in cytokine concentration after elective total hip arthroplasty locally (wound drain samples) and systemically (serum), with local cytokine concentration substantially higher compared with systemically (Bastian et al. 2008). Another previous study in patients undergoing major abdominal surgery reported mRNA expression levels associated with tissue inflammation, protein breakdown and impaired carbohydrate oxidation increased local to the site of surgery in the *rectus abdominus*, with a similar but smaller response seen at an site remote to surgery, the *vastus lateralis,* within 24 hours (Varadhan et al. 2018). This was accompanied by increased systemic inflammation and impaired glucose tolerance. Changes at the muscle protein level mirrored changes at the gene

level at the site local to surgical trauma, but not in muscle remote to the site of surgery, suggesting muscle level responses contribute to impairments in muscle mass and insulin sensitivity in the few days following surgery. The findings of the present study add important insight into the regulation of muscle mass and protein turnover in the context of local and systemic inflammation 2 weeks after injury and suggest that wholesale transcriptional change both local and remote to the site of injury occur in a number of cellular functions including those related to inflammation, however this is only mirrored as a reduction in MPS local to the trauma, with no change in MPS remote to the site of trauma.

In summary, ankle fracture fixation plus casting causes greater reductions in muscle thickness measured using ultrasound compared to casting alone, with comparable reductions in MPS over 2 weeks, and similar rates of whole-body MPB at the 2 week time point. This corresponds with muscle transcriptional responses, of which the magnitude of change is much greater in patients compared with healthy volunteers. Surgical trauma also causes a pro-inflammatory systemic cytokine response which is absent in immobilised healthy volunteers, and the former is reflected in widespread muscle transcriptional change both local and remote to the injury. This provides novel evidence in support of distinct mechanisms governing “inflammatory-mediated” and “non-inflammatory mediated” muscle atrophy in the face of similar detectable endpoints.

Chapter 6 General Discussion

6.1 Thesis aims and major findings

The present thesis examined the effect of immobilisation and inflammation on muscle metabolic health and the underlying mechanisms driving changes in muscle volume, protein turnover and insulin sensitivity. The overarching research questions were as follows:

1. What is the impact of acute (3 days) and chronic (56 days) bed rest on insulin-stimulated whole-body glucose disposal, substrate oxidation, and glycogen storage in healthy men maintained in energy balance and are these the same? Can these responses be associated with changes in leg IMCL content or targeted muscle mRNA expression as a result of bed rest?
2. What is impact of acute bed rest on insulin-stimulated leg glucose uptake, muscle volume and muscle protein turnover in the same individuals and are any responses associated changes in targeted muscle mRNA abundance during bed rest?
3. Can an acute period of structured remobilisation (3 days) restore any deficits in whole-body glucose disposal, leg glucose uptake, muscle glycogen storage and MPS after 3 days of bed rest?
4. What are the individual and combined impacts of immobilisation and trauma/inflammation on *medial gastrocnemius* muscle thickness, pennation angle and fascicle length, cumulative MPS and whole-body MPB in ankle fracture patients and matched healthy volunteers undergoing 2 weeks of unilateral cast immobilisation.

5. Is there a differential impact of systemic versus local inflammation in ankle fracture patients on muscle architecture, MPS and targeted muscle mRNA responses?

Major findings responding to each other the above questions from this research include the following:

1. The decrease in insulin-stimulated whole-body glucose disposal and muscle glycogen storage after acute bed rest was of a similar magnitude to that observed after chronic bed rest, and muscle glycogen storage after acute bed rest was of a similar magnitude to that observed after chronic bed rest. However, chronic bed rest was associated with a shift in fuel oxidation which could not be rationalised by changes in blood lipid concentrations or IMCL content but was reflected by the muscle transcriptional response to chronic bed rest.

2. Demonstration of reductions in insulin-stimulated whole-body glucose disposal, leg glucose uptake, and muscle glycogen storage as well as MPS and whole-body MPB after 3 days of bed rest. The decrement in leg glucose uptake during the insulin clamp after bed rest appeared to be largely explained by a reduction in leg blood flow.

3. Structured remobilisation restored reductions in leg muscle volume and MPS, but not insulin-stimulated leg glucose uptake or muscle glycogen storage after bed rest. Furthermore, leg muscle volume and MPS did not restore after 3 days of ambulation alone.

4. Trauma plus immobilisation caused greater declines in *medial gastrocnemius* muscle thickness compared with immobilisation alone, but similar declines in cumulative MPS over 2 weeks and no difference in whole-body MPB measured at 2 weeks.

5. Trauma was associated with a profound systemic (pro-inflammatory cytokines) and muscle (mRNA) inflammatory response which was completely absent in the healthy volunteers. However, a reduction in chronic MPS and muscle thickness was evident in the injured leg, but not the uninjured leg, suggesting a differential impact on muscle of local vs systemic inflammation.

6.2 Strengths of this thesis

The studies in this thesis have been able to lend new insight into the time course of changes secondary to immobilisation and inflammation due to their design. Previous bed rest studies have tended to focus on pre and post changes after long duration (>2 weeks) bed rest, with little understanding as to the temporal onset of these changes and the underlying mechanisms. Chapter 3 utilised the same study design across both acute and chronic bed rest experiments in order to uncover some of the early whole-body and muscle adaptations to bed rest. In addition, one of the strengths of Chapter 4 was that leg glucose uptake and measures of muscle volume and protein turnover were obtained concurrently in the same individuals, whereas previously investigators have tended to focus on the effect of immobilisation and recovery on one or the other outcome measures. Furthermore, in Chapter 4, the acute bed rest study utilised a within subject control design to examine the effect of structured remobilisation,

incorporating a unilateral resistance exercise protocol after bed rest. This allowed a comparison of the differential response in MPS in the rehabilitated leg and non-rehabilitated leg. Further insight may have been gained from a control group who had a prolonged period of remobilisation >3 days to determine the exact timeframe for full recovery of leg glucose uptake and muscle glycogen storage following bed rest. This particular acute bed rest model would also allow additional interventions, for example nutritional such as overfeeding, to be combined with immobilisation to examine the summative effect of energy surplus and physical inactivity. The ankle fracture study in Chapter 5 utilised both a between-subjects design (patients and healthy volunteers) as well as a within-subject control, with both patients and healthy volunteers having an immobilised and non-immobilised limb. As well as the impact of local (injured limb) and systemic (uninjured limb) inflammation in the patients, this unique design allowed for the first time for the impact of immobilisation and inflammation to be separated. The studies in Chapters 4 and 5 also provided novel data describing the cumulative change in MPS over 3 days in bed rest, and over 2 weeks in leg casting. Previous studies, particularly in clinical populations, examining the impact of inflammation on muscle atrophy e.g., in intensive care, have only been able to provide a snap-shot of changes in MPS over hours. I have shown that the use of orally ingested deuterium oxide in clinical populations with acute trauma is safe, feasible and acceptable, and could be implemented in similar clinical situations to provide unique mechanistic data on muscle protein turnover.

Another strength is the commonality in targeted mRNAs measured across all 3 experimental chapters of this thesis. These were deemed to be representative of insulin sensitivity, carbohydrate and fat metabolism, inflammation, and protein turnover according to research findings in muscle from human volunteer studies that included unbiased gene analysis (Murton et al. 2014; Murton et al. 2015; Stephens et al. 2013; Porter et al. 2017), and from an *in vivo* animal study (Murton et al. 2015). The benefit of this approach was to assess changes in abundance of these genes across several different circumstances; chronic bed rest, acute bed rest, remobilisation following acute bed rest, 2 weeks of leg casting (immobilised and non-immobilised leg) and 2 weeks of leg casting following ankle fracture fixation (injured and uninjured leg). Overall, I found that 3 days of bed rest and 3 days remobilisation led to a wholesale change in multiple cellular functions in reaction to the acute insult of immobilisation and subsequent remobilisation, which were nonspecific and did not reflect changes at a whole-body and muscle physiology level. Similarly, 2 weeks of leg casting resulted in a large transcriptional response in genes related to, for example, organismal development, but these did not necessarily directly relate to physiological measures. In contrast, a much more prolonged period of immobilisation of 56 days bed rest resulted in a much smaller mRNA network size change, but the cellular events specified by IPA were robustly predicted, and reflected whole-body physiological change e.g., in fuel oxidation. This would suggest mechanisms underlying changes in insulin sensitivity and muscle mass in response to acute immobilisation of hours to only a few days are governed by other processes e.g., alterations in insulin-stimulated leg blood

flow related to leg glucose uptake. Although, if the insult of immobilisation persists over several weeks, transcriptional level change may be important as a causative mechanism in maintaining metabolic dysregulation or leading to more persistent changes. Finally, the combination of trauma plus immobilisation caused a larger magnitude of change in muscle mRNA in the targets measured compared to immobilisation alone, and there were distinct cellular functions altered between the two states, particularly related to inflammation and immune cell turnover, which was completely absent in the healthy volunteers. These findings demonstrate the differential impact of inflammation and disuse on muscle transcription, despite a similar physiological endpoint of muscle atrophy.

6.3 Future directions emerging from the research in this thesis

6.3.1 Intervention during chronic bed rest to mitigate decreased glucose disposal and altered fuel oxidation.

The study in Chapter 3 demonstrated that 56 days of bed rest caused a reduction in insulin-stimulated glucose disposal and muscle glycogen storage, associated with a shift in fuel oxidation. Strategies to counter these changes during long duration immobilisation are required. Downs et al., utilised a combination of resistance (3 days per week) and aerobic (6 days per week) exercise during 70 days of HDT bed rest in men in energy balance (Downs et al. 2020). Although exercise was protective against increases in OGTT-induced glucose and insulin responses compared with controls, they found that exercise

alone was not able to completely prevent gains in fat mass and decreases in lean mass, without the addition of intermittent, low-dose testosterone. Currently, the dose of exercise (intensity, frequency, volume) required to offset reductions in glucose disposal and changes in fuel oxidation is unknown. Other countermeasures which have been explored include neuromuscular electrical stimulation, which has been shown to enhance energy expenditure and carbohydrate oxidation and reduce postprandial insulinaemia compared with inactive controls (Chen et al. 2021). Surprisingly few studies using a dietary intervention to prevent bed rest-associated reductions in glucose disposal have been conducted. One study evaluated the impact of a low-glycaemic index (thought to reduce postprandial blood glucose and insulin responses) pulse-based diet vs a typical hospital diet on insulin sensitivity during 4 days of bed rest (Gao et al. 2019). They found that compared to the hospital diet, a low-glycaemic index diet increased insulin sensitivity, assessed by the Matsuda index. The results from Chapter 3 showed that a daily antioxidant and anti-inflammatory cocktail failed to mitigate against reductions in whole-body glucose disposal or a shift in fuel oxidation after chronic bed rest. Other authors found similar ineffectiveness of the antioxidant cocktail on preventing muscle mass loss (Arc-Chagnaud et al. 2020) or increases in glycaemia (Trim et al. 2023). Thus far, there is no single countermeasure shown to completely prevent reductions in whole-body insulin-stimulated glucose disposal and changes in fuel oxidation associated with chronic physical inactivity, even when maintained in energy balance.

6.3.2 The combined effect of chronic bed rest plus energy excess on insulin sensitivity and IMCL content.

The work in this thesis demonstrated that an accumulation of IMCL under conditions of energy balance was not the primary driver of changes to whole-body glucose disposal under insulin-stimulated conditions. Future work could investigate the combination of bed rest and overfeeding on whole-body insulin sensitivity and whether underlying mechanisms differ from immobilisation alone e.g., impact on IMCL content or fuel selection. The few studies that have examined energy excess plus physical inactivity have found no impact of overfeeding on muscle insulin sensitivity after 24 hours of bed rest (Dirks et al. 2018). A study of longer duration found that reduced step count (<1500 steps) of 2 weeks' duration in addition to overfeeding caused reductions in insulin sensitivity which preceded subsequent increases in visceral and whole-body adiposity, however, no measures of IMCL were made in this study (Knudsen et al. 2012). Future work could also probe the influence of macronutrient content during overfeeding and bed rest. A previous study by Stettler showed 60 hours of bed rest plus a overfeeding with a high-fat (~45%), but not a high-carbohydrate (~75%) diet caused a reduction in insulin-mediated glucose disposal, whilst both increased IMCL content measured using ^{1}H-MRS (Stettler et al. 2005). Work building on this to determine fibre-type specific changes in IMCL content in response to bed rest plus overfeeding would provide useful further insight into the relationship and temporal onset of insulin resistance and increased IMCL content with physical inactivity, particularly given type I fibres have a greater ability for glucose uptake compared with other fibre types.

Understanding the precise mechanisms underpinning IMCL accumulation and its association with insulin sensitivity would allow for the development of potential pharmaceutical, nutritional or exercise countermeasures.

6.3.3 Restoration of insulin sensitivity and MPS after bed rest

The work presented in Chapter 4 identified that 3 days of structured remobilisation after acute bed rest restored insulin-stimulated whole-body insulin sensitivity and MPS, but not insulin-stimulated leg glucose uptake or muscle glycogen storage. It would be useful to determine the exercise dose (volume, type and frequency) required to restore insulin-stimulated leg glucose uptake and muscle glycogen content. Whilst there is plentiful research exploring the impact of disuse on glucose disposal, relatively fewer have explored the reversal with a return to ambulation or specific rehabilitation, particularly over short periods of time of only a few days. Again, this is especially relevant to clinical populations having a period of disuse due to injury or illness. A previous study showed it took >4 days' of normal ambulation to fully restore glucose tolerance in healthy males following 21 days of bed rest (Heer et al. 2014). Another study measuring whole-body and muscle insulin sensitivity, as well as adiposity after 14 days step reduction followed by 14 days resumption of normal activity, found incomplete restoration of muscle insulin sensitivity (Bowden Davies et al. 2018). A similar study in older, pre-diabetic individuals found that both insulin sensitivity measured using HOMA-IR index and integrated MPS did not return to baseline after 14 days of a return to free living (McGlory et al. 2018). It is unknown if deficits in whole-body glucose disposal and MPS after

shorter durations of bed rest are more readily restored than immobilisation of longer duration e.g., >7 days. Information on time to recover insulin sensitivity and muscle mass following shorter duration immobilisation would be useful to guide advice to patients who may have undergone immobilisation in hospital of only a few days. It is also unclear if there are multiple short periods of disuse in quick succession, whether the intervals between them are sufficient to fully restore deficits in insulin sensitivity or muscle mass, or if incomplete restoration before subsequent immobilisation causes longer lasting effects. Furthermore, recovery in young versus older participants after short duration bed rest would provide useful insight into the rapidity of restoration and true plasticity of insulin sensitivity and MPS in the aged state.

6.3.4 Countermeasures after musculoskeletal trauma

The work in Chapter 5 showed that reductions in muscle thickness and FSR seen in the injured leg were not present in the uninjured leg of the patients. This suggests that muscle inflammation local to the musculoskeletal injury, but not systemic or in the contralateral uninjured limb, influences muscle level responses which contribute to impairments in muscle mass following surgery. It is also plausible that loading of the uninjured leg may have countered any systemic inflammatory burden, lending support to isometric muscle contractions or percutaneous electrical stimulation as a potential countermeasure after musculoskeletal trauma. Work by Gibson et al. showed that low-voltage percutaneous electrical stimulation could reduce quadriceps atrophy in the injured leg of individuals with fracture of the tibia and leg

immobilisation, secondary to preventing a reduction in MPS (Gibson, Smith, and Rennie 1988). The potential role of immunomodulation such as cytokine blockade or ant-inflammatory therapy has been suggested to have a potential role to optimise recovery after musculoskeletal injury, both to reduce muscle atrophy and promote fracture healing. IL6 blockade in preclinical models have shown attenuation of muscle atrophy and inhibition of autophagy with a decrease in expression in MuRF1 and MAFbx (Huang et al. 2020). Activation of autophagy was identified by IPA in the injured leg of patients and thus may be a potential target for future research. The role of anti-TNF therapies in the context of acute illness and musculoskeletal trauma is far from clear. Therapeutic anti-TNF failed to show any convincing benefit in prospective clinical trials (Abraham et al. 1998), although subsequent pooling of several clinical trial results showed a small (3.6%) benefit in decreasing mortality in patients with sepsis (Reinhart and Karzai 2001). Conversely, local but not systemic recombinant human TNF given during the early phase (within 24-hours) of repair in a murine model of tibial fracture improved fracture healing (Chan et al. 2015). Whether early posttraumatic TNF therapy or indeed anti-TNF therapy would help bony healing and prevent muscle mass loss is still unclear.

6.4 Considerations

One consideration that should be acknowledged is that muscle volume measured using MRI in Chapter 4, and muscle thickness, measured using ultrasound in Chapter 5 may have been confounded by fluid shifts. It is

recognised that in head-down tilt bed rest, there is a cephalic shift of fluid as well as fluid redistribution from the intravascular to extravascular space reflected by a reduction in plasma volume (Hargens and Vico 2016). There may therefore be an apparent change of muscle volume, in particular an increase in the upper body, when in fact net muscle protein loss was unchanged, and these effects have previously been reported after 2 (Berg, Tedner, and Tesch 1993) and 24-hours of HDT bed rest (Conley et al. 1996). Despite this, changes in muscle volume of the lower limb mirrored changes seen in MPS, suggesting that it was unlikely a significant issue in these two studies. It was not possible to accurately quantify interstitial fluid content in the bed rest studies using MRI. Similarly, posttraumatic oedema of the limb in the ankle fracture patients was significant in all individuals and, from clinical experience, generally tends to peak 3-5 days after injury and be greater in the evenings. This may have confounded muscle thickness measurements particularly at the perioperative time-point and may have overestimated muscle thickness and therefore overall muscle thickness change. Additional measures such as determining the protein to DNA ratio in muscle biopsy samples would have been useful to assess for muscle protein loss in the leg, however a lack of muscle tissue meant that it was not possible to undertake this after the primary outcome measures were determined. The changes in muscle volume and thickness in this thesis therefore should be considered in the context of possible acute and posttraumatic fluid shifts.

In the remobilisation period in Chapter 4, it is not possible to determine whether whole-body glucose disposal would have restored in 3 days with

ambulation alone. The use of a control group which did not undergo unilateral resistance exercise following bed rest would have helped to determine this. As discussed in Chapter 4, the exact duration to restore both whole-body and limb insulin sensitivity, as well as MPS following acute bed rest with ambulation alone is unclear. Further studies determining the acute restoration of insulin sensitivity following acute bed rest should be explored, particularly given this is a similar duration of immobilisation seen in patients admitted to hospital.

Both bed rest studies in this thesis did not include older individuals or females as participants. The chronic bed rest study run by the European Space Agency only recruited young, healthy males which was predetermined by the ESA team. This may limit the generalisability of the findings, particularly as there is growing evidence of sex dimorphism in various factors known to influence to skeletal muscle metabolism and atrophy (Rosa-Caldwell and Greene 2019; Della Peruta et al. 2023) as well as differences between males and females in response to disuse (Black et al. 2021; Mekjavic et al. 2021). Special considerations are required to account for the impact of the menstrual cycle on experimental measures, particularly when bone metabolism or training measures are part of a study design. To my knowledge no study has directly compared the effect of bed rest and remobilisation on whole-body and limb insulin-sensitivity in males and females. Previous studies have also found age-related differences in muscle atrophy during 5 days of bed rest between older and younger adults, with no difference in insulin sensitivity (Reidy et al. 2017), thus there are limitations in extrapolating our findings to the older adult.

The study in Chapter 5 aimed to examine the impact of local (injured limb) versus systemic (uninjured) inflammation on muscle thickness and MPS in patients with an acute ankle fracture undergoing surgical fixation. One could argue, however, that the model is complicated by the reduced physical activity level of patients post-injury, and thus the uninjured limb does not solely represent systemic inflammation. Another potential model, which has been successfully used in disuse muscle atrophy research, is the unilateral forearm immobilisation model (Burns et al., 2021), in which reduced step count is not directly implicated in muscle mass reduction. Similarly, a forearm immobilisation model after acute upper limb trauma could be considered. However, it should be noted that the majority of forearm fractures occur in frail, older populations, or paediatric populations, so this should be considered. The endotoxin model as described in **Section 1.8.2** causes a reproducible acute increased concentration of plasma cytokines such as IL6 and IL10 and a systemic response of fever. However, findings are limited in their generalisability due to the acute nature of the measures and time period. Finally, if local inflammation is a driver of muscle atrophy in trauma, another approach could be to pharmacologically reduce inflammation in lower limb fracture patients and compare this with a placebo group. There are several approaches which are plausible, including preconditioned mesenchymal stromal cells or using anti-inflammatory cytokines. However, concerns around supressing the initial acute inflammatory phase, which is essential for robust fracture healing exist.

6.5 Conclusion

Overall, this thesis has provided important scientific understanding into the impact of immobilisation and inflammation on muscle volume, protein turnover and insulin sensitivity. The studies in this thesis have shown that reductions in insulin-stimulated glucose disposal during acute and chronic bed rest are similar and substantial and could not be explained by changes in IMCL content. However chronic bed rest was associated with a shift in fuel oxidation, underpinned by the muscle transcriptional response to chronic bed rest. Furthermore, acute bed rest causes concurrent reductions in leg glucose uptake, and muscle glycogen storage as well as cumulative MPS rates and whole-body MPB. However, structured remobilisation (but not ambulation alone) restored reductions in leg muscle volume and MPS, but not insulin-stimulated leg glucose uptake or muscle glycogen storage after bed rest. The implications of this are directly relevant to clinical populations, with the average length of stay in hospital in the UK a similar duration to the acute bed rest study in this thesis. Further research would be helpful to determine the dose of physical activity required to restore leg glucose uptake, in order to restore declines in insulin sensitivity in populations undergoing short periods of immobilisation.

This body of work has also helped to elucidate some key information differentiating the mechanisms underlying muscle atrophy relating to immobilisation vs immobilisation plus trauma. Trauma plus immobilisation caused a greater reduction of *medial gastrocnemius* muscle thickness compared with immobilisation alone but similar declines in cumulative MPS

over 2 weeks. However, only trauma was associated with a profound systemic and muscle inflammatory response, which manifested as a reduction in cumulative MPS and muscle thickness in injured leg, but not the uninjured leg. This lends evidence that local trauma is the primary driver of muscle atrophy in this situation. This information could form the basis of potential future countermeasures in musculoskeletal trauma to aid recovery following injury.

Chapter 7 Appendices

Appendix 1 – Study files

Appendix 2 – Supplementary information

Appendix 3 – Supplementary data

Appendix 1 STUDY FILES

7.1 Chronic bed rest study ethics approval

COMITÉ de PROTECTION des PERSONNES
SUD-OUEST ET OUTRE-MER I
Secrétariat : Mme CHÉRON - Mme DUNY
AGENCE RÉGIONALE de SANTÉ MIDI PYRÉNÉES – Bureau 1028
10 chemin du raisin - 31050 TOULOUSE CEDEX 9
Tél : 05 34 30 27 55 / 05 34 30 27 56 - Fax 05 34 30 27 38 - Mail : cppsoom1-2@ars.sante.fr

REÇU
Le 10 JUIN 2016
16A00303

MEDES IMPS
Mme BAREILLE
Bp 74404
31405 TOULOUSE cedex 4

Toulouse, le 24 Mai 2016

Madame,

Dans sa séance du 23 mai 2016, le comité de protection des personnes (C.P.P.) Sud-Ouest et Outre-Mer I a examiné vos réponses à l'avis du 11 avril 2016 concernant le projet de recherche intitulé :

Evaluation des effets d'une association de compléments alimentaires anti-oxydants et anti-inflammatoires pour prévenir le déconditionnement induit par 60 jours d'alitement anti-orthostatique. Une étude monocentrique, ouverte, randomisée et contrôlée chez 20 hommes volontaires sains - Medes LTBR Cocktail – protocole 14-981 v2 du 10 mai 2016 - n° IDRCB 2016-A00401-50 – **(dossier 1-16-12)**

que vous lui avez soumis en qualité de représentant du promoteur CNES et dont l'investigateur-coordonnateur est le Dr BECK.

Etaient présents en qualité de titulaires : Mrs SENARD et CONIL personnes qualifiées en matière de recherche biomédicale ; Dr ANÉ médecin généraliste, Mme BARLA pharmacien hospitalier, Mr CAZOTTES infirmier (1er collège) ; Me BENAYOUN personne compétente en matière juridique, Mr DIVERNET et Mme SFEDJ représentants des associations de malades et usagers de la santé (2ème collège).

Assistaient aussi à la séance, en qualité de suppléants : Mmes NASR et DI DONATO, Mrs SAVY et MOESCH personnes qualifiées en matière de recherche biomédicale, Mr RIVIERE médecin généraliste (1er collège) ; Mme BIMES-ARBUS personne compétente en matière d'éthique, Mme HENDERSON psychologue, Mme CHARRAS personne compétente en matière juridique, M. SERVILLE représentant des associations de malades et usagers de la santé (2ème collège).

Le comité a examiné les documents de réponse suivants:
- Courrier de réponse (daté et signé signé du 10 mai 2016)
- Protocole de recherche (MedesCOCKTAIL bed rest study version 2 du 10/05/2016)
- Résumé du protocole (MedesCOCKTAIL bed rest study version 3 du 10/05/2016)
- Notice d'information et recueil du consentement (Version 2 du 10/05/2016)

Après avoir entendu les rapporteurs et délibéré, le comité fait de votre dossier l'analyse suivante :

La justification de l'étude est pertinente, précise et bien référencée, le rapport des bénéfices et des risques est toutefois élevé pour le volontaire sain.

Les moyens mis en œuvre pour atteindre ces objectifs sont décrits avec précision et semblent bien adaptés à la solution du problème abordé.

La méthodologie est décrite et adaptée aux objectifs

La notice d'information et formulaires de consentements - version 3 du 10 mai 2016 sont clairement rédigés et contiennent toutes les mentions nécessaires.

En conséquence, il émet un

AVIS FAVORABLE

à la mise en œuvre de cette étude.

Je vous prie d'agréer, Madame, l'assurance de ma considération distinguée.

Le Président
Me D. BENAYOUN

7.2 Acute bed rest study ethics approval

The University of Nottingham

E-mail: FMHS-ResearchEthics@nottingham.ac.uk

Faculty of Medicine and Health Sciences

Research Ethics Committee
C/o Faculty PVC Office
School of Medicine Education Centre
B Floor, Medical School
Queen's Medical Centre Campus
Nottingham University Hospitals
Nottingham
NG7 2UH

30th May 2017

Dr Natalie Shur
Academic Clinical Fellow
School of Life Sciences
D Floor, Medical School
QMC Campus
Nottingham University Hospitals
NG7 2UH

Dear Dr Shur

Ethics Reference No: 6-1704 – **please always quote**	
Study Title: Determination of the time-course of development of insulin resistance, and associated molecular and muscular adaptations, during inactivity in 3 days of bed-rest.	
Chief Investigator/Supervisor: Professor Ian Macdonald, Metabolic Physiology, Life Sciences	
Lead Investigators/student: Natalie Shur, Academic Clinical Fellow, School of Life Sciences	
Other Key Investigators: Dr EJ Simpson, Senior Research Fellow, Professor PL Greenhaff, Life Sciences, Dr Kenny Smith, Principal Research Fellow, Dr Phil Atherton, Associate Professor, Division of Medical Sciences and Graduate Entry Medicine.	
Type of Study: research, physiology, insulin monitoring, muscle biopsy.	
Proposed Start Date: 1.4.17	**Proposed End Date:** 30.4.18 12mths
No of Subjects: 10	**Age:** 18+years
School: Life Sciences and Medicine	

Thank you for your letter dated 10 May 2017 responding to the comments made by the Committee and the following documents were received:

- Nottingham bed rest protocol v1.3 10.05.17
- DEXA leaflet
- SPMIC MRI safety screening form
- Muscle Biopsy (thigh) leaflet v1.1 8.11.16
- MHS REC application and supporting documents dated 10th April 2017
- Dexa Scan sign off by IRMER practitioner Aline Nixon dated 5th April 2017

These have been reviewed and are satisfactory and the study has been given a favourable opinion.

A favourable opinion is given on the understanding that the conditions set out below are followed:

1. You should follow the protocol agreed and inform the Committee of any changes using a notification of amendment form (please request a form).

2. You must notify the Chair of any serious or unexpected event.

3. This study is approved for the period of active recruitment requested. The Committee also provides a further 5 year approval for any necessary work to be performed on the study which may arise in the process of publication and peer review.

4. An End of Project Progress Report is completed and returned when the study has finished (Please request a form).

Yours sincerely

Professor Ravi Mahajan
Chair, Faculty of Medicine & Health Sciences Research Ethics Committee

7.3 Ankle fracture study HRA approval

Ymchwil Iechyd a Gofal Cymru
Health and Care Research Wales

NHS
Health Research Authority

Mr Ben Ollivere
Clinical Associate Professor, Honorary Consultant
Trauma and Orthopaedics
C Floor, West Block
Queen's Medical Centre
NG7 2UH

Email: hra.approval@nhs.net
Research-permissions@wales.nhs.uk

01 March 2019

Dear Mr. Ollivere,

HRA and Health and Care Research Wales (HCRW) Approval Letter

Study title:	**The application and clinical validation of novel approaches to quantify the effect of early versus delayed ankle fracture fixation on muscle mass and metabolic health status**
IRAS project ID:	**235196**
Protocol number:	**18078**
REC reference:	**18/EM/0404**
Sponsor	**The University of Nottingham**

I am pleased to confirm that **HRA and Health and Care Research Wales (HCRW) Approval** has been given for the above referenced study, on the basis described in the application form, protocol, supporting documentation and any clarifications received. You should not expect to receive anything further relating to this application.

How should I continue to work with participating NHS organisations in England and Wales?
You should now provide a copy of this letter to all participating NHS organisations in England and Wales, as well as any documentation that has been updated as a result of the assessment.

Following the arranging of capacity and capability, participating NHS organisations should **formally confirm** their capacity and capability to undertake the study. How this will be confirmed is detailed in the "*summary of assessment*" section towards the end of this letter.

You should provide, if you have not already done so, detailed instructions to each organisation as to how you will notify them that research activities may commence at site following their confirmation of capacity and capability (e.g. provision by you of a 'green light' email, formal notification following a site initiation visit, activities may commence immediately following confirmation by participating organisation, etc.).

It is important that you involve both the research management function (e.g. R&D office) supporting each organisation and the local research team (where there is one) in setting up your study. Contact details of the research management function for each organisation can be accessed here.

How should I work with participating NHS/HSC organisations in Northern Ireland and Scotland?
HRA and HCRW Approval does not apply to NHS/HSC organisations within the devolved administrations of Northern Ireland and Scotland.

If you indicated in your IRAS form that you do have participating organisations in either of these devolved administrations, the final document set and the study wide governance report (including this letter) has been sent to the coordinating centre of each participating nation. You should work with the relevant national coordinating functions to ensure any nation specific checks are complete, and with each site so that they are able to give management permission for the study to begin.

Please see IRAS Help for information on working with NHS/HSC organisations in Northern Ireland and Scotland.

How should I work with participating non-NHS organisations?
HRA and HCRW Approval does not apply to non-NHS organisations. You should work with your non-NHS organisations to obtain local agreement in accordance with their procedures.

What are my notification responsibilities during the study?
The document "*After Ethical Review – guidance for sponsors and investigators*", issued with your REC favourable opinion, gives detailed guidance on reporting expectations for studies, including:

- Registration of research
- Notifying amendments
- Notifying the end of the study

The HRA website also provides guidance on these topics, and is updated in the light of changes in reporting expectations or procedures.

I am a participating NHS organisation in England or Wales. What should I do once I receive this letter?
You should work with the applicant and sponsor to complete any outstanding arrangements so you are able to confirm capacity and capability in line with the information provided in this letter.

The sponsor contact for this application is as follows:

Name: Ms Angela Shone
Tel: 01157486731
Email: sponsor@nottingham.ac.uk

Who should I contact for further information?
Please do not hesitate to contact me for assistance with this application. My contact details are below.

Your IRAS project ID is **235196**. Please quote this on all correspondence.

Yours sincerely

Laura Greenfield
Assessor

Email: hra.approval@nhs.net

Copy to: *Ms Angela Shone [Sponsor Contact on behalf of the University of Nottingham]*
Dr Maria Koufali [Lead NHS R&D Office Contact on behalf of Nottingham University Hospitals NHS Trust]

7.4 DEXA leaflet (This is folded and then handed to the participant)

DEXA Scan information leaflet

What is a DEXA scan and what does it measure?
DEXA stands for 'Dual Energy X-ray Absorptiometry' and it is a test used in hospitals to measure the density of bone. Density means how much of something there is in a certain amount of space and this test is usually used to help diagnose those who have brittle bones (osteoporosis). In Physiology and Nutrition research, we use the DEXA machine to measure the amount of fat and lean tissue you have in your body, as well as the density of your bones.

How does a DEXA scan work?
A DEXA scan sends X-rays of two different strengths through the body. Bone blocks a certain amount of the X-rays, whereas muscle and fat block the X-rays to a lesser extent. The denser the tissue is, the fewer X-rays get through to the detector.

What does the scan involve?
This is a simple and painless procedure, and requires very little preparation.

However metal and other objects, such as zips, buckles, bra clips / under wires and body piercing, can affect the result of the DEXA Scan. It is advisable to wear loose clothing which has no zips, metal buttons etc. If you attend wearing clothing that is not suitable, you will be asked to change into surgical tops and/or trousers prior to the scan. Lockers are provided. If you wear any kind of metal jewellery, you will need to remove it before the test. If you are unable to remove any items, please inform the DEXA operator.

On the day of the study you will be asked to have nothing to eat or drink, other than water from midnight the night before

You will also:

- Have your height and weight measured
- Complete a safety questionnaire; this questionnaire will ask you about any procedures or treatments that you have had in the past year which involved X-rays and any metal that you might have in your body.
- Go to the toilet to empty your bladder before the scan

The scan itself involves you lying on your back on a table whilst an X-ray arm passes over you. The X-ray arm does not touch you and you will not be in a "tunnel" (see picture).

You will need to remain completely still and not talk while the scan is being carried out.

If you have any hip, back or neck injury, please tell the DEXA operator before the scan.

The actual scanning time is about 10 minutes but you should allow 30 minutes for the entire procedure.

What are the risks?
The DEXA scan involves you receiving a low dose X-ray, which is a form of radiation.

We're constantly being exposed to natural radiation from the environment around us - from the earth, through rays from outer

space, even from the food we eat. The radiation dose that you receive is less than 1μSv per scan. This is equivalent to the amount of radiation that you would be exposed to if you spent 15min on a transatlantic flight or the amount of radiation contained in 10 brazil nuts.

As a part of this study you will be exposed to a very small amount of X-rays (ionising radiation) during your DEXA scan. X-rays can induce harmful effects such as the development of cancer. However, the amount used in this study is very tiny and you experience a similar risk from 2.5hours of natural background radiation (to which we are all exposed) in the UK. A similar risk of harm would also be experienced by smoking less than one cigarette.

Is there anyone who should not have this test?
It is not advisable for you to have this scan if you are pregnant. Pregnancy test kits (requiring a urine sample) are available in the toilets. You will be asked to empty your bladder before having the DEXA scan. Please feel free to use the pregnancy test at this time if you think there might be a chance that you are pregnant. You do not need to tell anyone that you are doing so, but you can talk to the DEXA operator in confidence if you wish to.

If you have had another X-ray, or if you have had a nuclear scan (such as a bone or thyroid scan) in the last 7 days, you should not have this test

If for any reason you do not wish to proceed with the scan, please let the DEXA operator know, but you do not need to disclose the reason why.

What are the benefits?
A DEXA scan is the most accurate way of measuring your total body composition and it is a quick and simple measurement to make.

Osteoporosis, is a serious medical problem which can affect both men and women as they get older. However, we often don't know that our bones are getting weaker until we break a bone. Although the researchers are interested in your body composition, the scan will estimate the bone density of your skeleton. If the results show that the density of your bones is too low, then you will be informed and the study doctor will discuss the results with you. Therefore, having the DEXA scan could identify a problem with your bones and allow you to receive treatment at an earlier stage.

For more information please contact:

Aline Nixon: tel- 0115 8230248
Aline.Nixon@nottingham.ac.uk

The University of Nottingham

David Greenfield Human Physiology Laboratories

Having a DEXA Scan

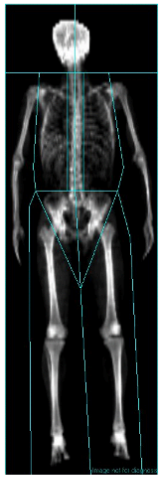

7.5 General Health Questionnaire

GENERAL HEALTH QUESTIONAIRE

1. In general would you say your health is; Please tick one response

a. …… *Much better than a year ago*
b. …… *Somewhat better than a year ago*
c. …… *About the same*
d. …… *Somewhat worse than a year ago*
e. …… *Much worse than a year age*

2. The following questions are concerned with any medical conditions you might have. Please tick one box on each line

Condition	No	Yes	Don't Know
Diabetes			
Epilepsy			
Depression or mental health problem			
Hayfever			
Asthma			
Migraines			
High blood pressure			
Heart problems			
Breathing problems			
Indigestion / heartburn			
Irritable bowel			
Thyroid problems			
Kidney problems			
Orthopaedic/musculoskeletal problems			
Blood clots e.g. DVT			
Vestibular problems, claustrophobia or orthostatic intolerance			
Any other medical condition not listed above (please detail below)			

Please detail any other medical condition/s:

……

3. Do you have a family history of coagulation/blood clotting disorders or a deep vein thrombosis (DVT) or pulmonary embolus (PE)?

Yes…….. No……..

If yes please give details

……
……

4. Do you take any regular medication? Yes…….. No……..

If yes please provide further information: (drug, dose, frequency, duration)

……
……

5. Do you have a tendency to faint in certain situations?

Yes…….. No…….. Don't Know……..

eg. on standing, in a warm room or after fasting

6. On average, how many cigarettes do you smoke a day? ……
Did you ever smoke in the past? ……
If so, how when did you quit? ……

6. Have you had any previous injuries* which affected any of your lower limbs?

* An injury which limited your walking ability for more than 2 days in the last year.

7. Do you drink alcohol:

Yes…….. No……..

If yes please provide further information: (units per average week)

……
……

7.6 Hyperinsulinaemic euglycaemic data collection form

3 day Bed Rest Study

Clamp Sheet

Subject Name :……

Date : ……../……./…….. **Visit No:** **1 2 3**

Height: …… cm **Weight:** …… kg **Surface area:** ……m^2

Calculations:

_____ m^2 x 60 = …….. x 7.52 = …….. mls/hr
0.5 40 x 3.28 = …….. mls/hr
x 2.99 = …….. mls/hr
x 2.82 = …….. mls/hr
x 2.57 = …….. mls/hr
x 2.40 = …….. mls/hr

Glucose @ 2mg / kg / min @ 4 min

2 x kg x 60 = ……..ml/hr
200mg

Glucose @ 2.5mg / kg / min @ 10 min

2.5 x kg x 60 = ……..ml/hr
200mg

Infusion start time: …….

Time	Ins Inf^{n}	Blood G	G Inf^{n}	Blood sample	Calorimetry	Commen
-20						
-10						
-5						
0						
2						
4						Open tap
5						
6						
8						
10						
15						
20						
25						
30						
35						
40						
45						
50						
55						
60						

Time	Ins Inf^{n}	Blood G	G Inf^{n}	Blood sample	Calorimetry	Comments
65						
70						
75						
80						
85						
90						
95						
100						
105						
110						
115						
120				120		
125						
130						
135				135		
140						
145						
150				150		
155						
160						
165				165		
170						
175						
180				180		
	Subject	fed and	insulin	discontinued		
190						
200						
210						
220						
230						
240						
250						
260						
270						
280						
290						
300						

Comments:
Saline used:
Glucose used:
Food given:
Leg length:

7.7 MRI questionnaire

Sir Peter Mansfield Imaging Centre

MR Volunteer Safety Screening Questionnaire:

NAME	Date of Scan	Date of Birth
ADDRESS	Volunteer Number	
	Ethics Code	
Phone number	Weight	Height if applicable

MR scanning uses strong magnetic fields. For your own safety and the safety of others it is **very important** that you do not go into the magnet halls with any metal in or on your body or clothing. Please answer the following questions carefully and ask if anything is not clear. All information is held in the strictest confidence.

1. Do you have any implants in your body? e.g. replacement joints, drug pumps
   Y/N
2. Do you have aneurysm clips (clips put around blood vessels during surgery)?
   Y/N
3. Do you have a pacemaker or artificial heart valve? *(These stop working near MR Scanners)*
   Y/N
4. Have you ever had any surgery? Please give brief details over.
   Y/N

(We do not need to know about uncomplicated caesarean delivery, vasectomy or termination of pregnancy)

5. Do you have any foreign bodies in your body (e.g. shrapnel)?
   Y/N
6. Have you ever worked in a machine tool shop without eye protection?
   Y/N
7. Do you wear a hearing aid or cochlear implant?
   Y/N
8. Could you be pregnant? (Pregnancy tests are available in the female toilets)
   Y/N
9. Have you ever suffered from tinnitus?
   Y/N
10. Do you wear dentures, a dental plate or a brace?
    Y/N
11. Are you susceptible to claustrophobia?
    Y/N
12. Do you suffer from blackouts, epilepsy or fits?
    Y/N
13. Do you have any tattoos? (If yes, you may be asked to read and sign another form) Y/N
14. Do you have any body piercing jewellery that cannot be removed?
    Y/N
15. Do you have any skin patches (trans-dermal patches)?
    Y/N
16. Do you have a coil in place (IUD) for contraception? Do you know what type?
    Y/N
17. Do you have any condition that may affect your ability to control your temperature ?
    (e.g. Do you have a fever, cardiovascular disease, hypertension, diabetes or cerebrovascular disease?) Y/N
18. Will you remove all metal including coins, body-piercing jewellery, false-teeth, hearing aids
    etc. before entering the magnet hall? *(lockers available by the changing rooms)*
    Y/N

19. Is there anything else you think we should know?
    Y/N

I have read and understood all the questions **Signature:**	 **Date:**
Verified by: **Scanner Operator/MR Assistant Signature :**	 **Date**

Appendix 2 SUPPLEMENTARY INFORMATION

7.8 M value calculation

The M value represents the milligrams of glucose per kilogram of body weight (mg/ kg/ min) disposed into tissues per minute during the steady state period of the hyperinsulinaemic euglycaemic clamp for the specific fixed insulin infusion rate at which the clamp is performed.

To calculate the M value, whole blood glucose concentration is measured at 5-minute intervals. The difference in blood glucose concentration between each successive interval and the glucose infusion rate (*GIR*; the variable rate at which exogeneous glucose is infused), are also recorded at these 5-minute intervals. The volume of glucose solution infused (*GSI*) during each 5-minute interval is then calculated as follows:

$$GSI\ (ml) = \frac{GIR\ (ml/hr)}{60}\ X\ 5$$

(Equation 2-1)

Glucose has a molecular weight of 180.156 g/mol and in the protocols described here 20% w/v solutions were used. To calculate the moles of glucose (*GI*) in the volume of glucose solution infused during the 5-minute interval:

$$GI\ (mol) = \frac{GSI\ x\ 0.2}{180}$$

$$GI\ (mmol) = GI\ (mol)\ x\ 1000$$

(Equation 2-2, 2-3)

To calculate the amount of glucose disposed (GD) during a 5-minute interval:

$$GD\ (mmol/min)\ = GI\ (mmol)\ x\ (BG1 - BG0)$$

(Equation 2-4)

Where (*BG1 – BG0*) is the difference in the blood glucose concentration measured at the end of the 5-minute interval (*BG1*) and the beginning of the 5-minute interval (*BG0*). These 5-minute interval glucose disposal values are then used to calculate 15-minute averages ($\bar{x}GD$) which are standardised to body weight:

$$\bar{x}GD\ (mmol/min/kg) = \frac{\bar{x}GD(mmol/min)}{Bodyweight\ (kg)}$$

(Equation 2-5)

The final M value is then calculated by multiplying the *x̄GD* by the molecular weight of glucose as shown in ***Equation 2-5***:

$$M\ value\ (mg/min/kg) = \bar{x}GD\ (mmol/min/kg)\ x\ 180$$

(Equation 2-6)

7.9 Details of antioxidant cocktail composition

The composition of consists of a mix of natural polyphenol extracts from food plants: Plant families; Liliaceae, Vernenaceae, Lamiaceae, Vitaceae, Rubiaceae, Theaceae. Rutaceae Genres; Allium cepa, Liipia citriodora, Ajuga reptans, Vitis vinifera, Coffea robusta, Camellia sinensis, Citrus aurantium.

Dosage:

- Flavonols: 323.4mg
- Phenylpropanoides: 45.6mg
- Oligostilbenes: 78.0mg
- Acide hydroxycinnamiques: 50.4mg
- Flavanols: 135.6mg
- Flavanones: 108.0mg

Vitamin E/Selenium

The Vitamin E/Selenium component was composed of commercially available pills and manufactured by Solgar. The pill contains 168mg of Vitamin E associated with 80µg of Selenium. The daily proposed doses are 6 and 5 times respectively lower than the maximum allowed doses according to the US National academy of sciences (ref).

Omega-3

Omega-3 fatty acids capsules (Omacor®, Pierra Fabre) comprises eicosapentaenoic acid (EPA) ethyl ester [EPA:46%] and docosahexaenoic acid ethyl ester [DHA:38%] 840mg/caps. Thus the daily dose of EPA will be 1.1g and the dose of DHA will be 1g. This dose was chosen because it is close to the dose approved by the Food and Drug Administration (USA) for lowering plasma TAG concentrations in hypertriglyceridaemic subjects and thus has previously been shown to the physiologically relevant in human subjects.

Appendix 3 SUPPLEMENTARY DATA

7.10 Antioxidant supplement effect on insulin-stimulated whole-body glucose disposal

a.

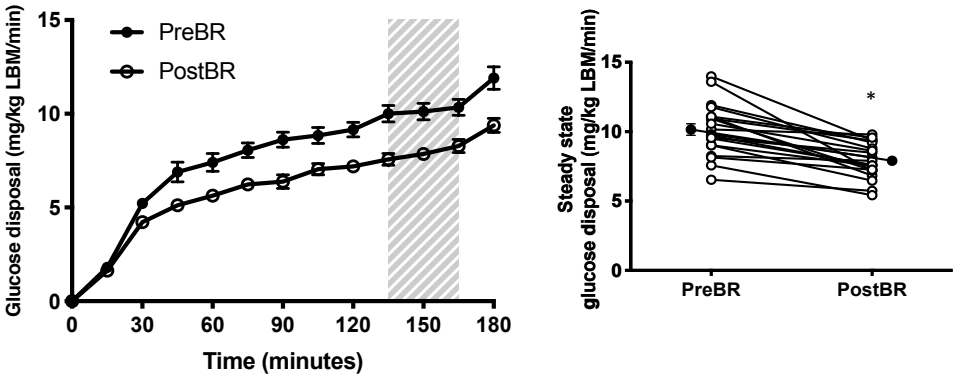

b.

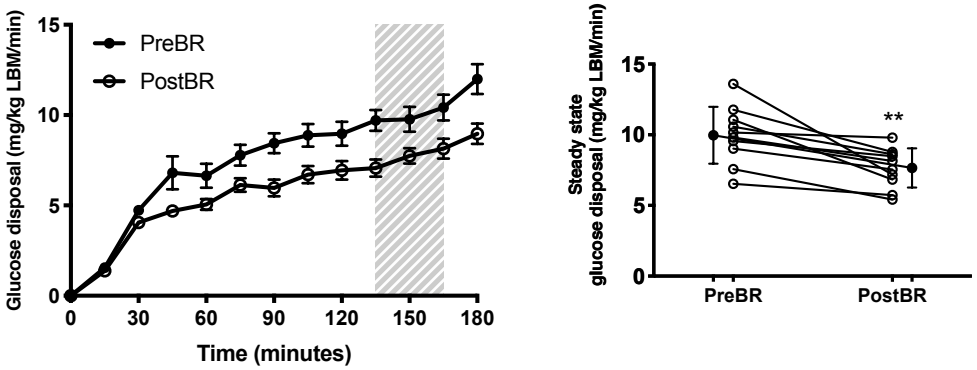

Supplementary Figure 7.1. Whole-body glucose disposal data in all and placebo-supplemented participants during chronic bed rest. Whole-body glucose disposal under insulin clamp conditions in a) all volunteers and b) volunteers who received placebo in the chronic bed rest study.

*7.11 Supplementary Table 7.1. IMCL fibre type data. Lipid droplet (LD) Count (Droplets/μm2) per fibre type, mean LD size (μm2) and % IMCL per fibre type in acute and chronic bed rest. * p<0.05, vs Pre Bed Rest. Values are mean ± SEM.*

		Acute Bed Rest		
		Pre Bed Rest	Post Bed Best	P Value
Type I	LD Count	0.06 ± 0.01	0.07 ± 0.01	0.82
	LD Size	0.73 ± 0.08	0.88 ± 0.13	0.76
	%IMCL	6.11 ± 0.68	8.97 ± 1.52	0.32
Type IIA	LD Count	0.05 ± 0.01	0.05 ± 0.00	1.00
	LD Size	0.52 ± 0.03	0.68 ± 0.11	0.50
	%IMCL	3.44 ± 0.29	4.34 ± 0.75	0.64
Type IIX	LD Count	0.04 ± 0.00	0.04 ± 0.01	1.00
	LD Size	0.43 ± 0.03	0.68 ± 0.12	0.34
	%IMCL	2.56 ± 0.39	4.05 ± 0.81	0.39
		Chronic Bed rest		
		Pre Bed Rest	Post Bed Rest	P Value
Type I	LD Count	0.08 ± 0.00	0.06 ± 0.00	0.02*
	LD Size	1.00 ± 0.06	1.14 ± 0.10	0.56
	%IMCL	15.26 ± 2.18	12.96 ± 2.30	0.86
Type IIA	LD Count	0.05 ± 0.00	0.06 ± 0.00	0.76
	LD Size	0.86 ± 0.06	0.89 ± 0.09	0.87
	%IMCL	7.63 ± 1.30	7.38 ± 1.28	0.96

Type IIX	LD Count	0.04 ± 0.00	0.05 ± 0.01	0.31
	LD Size	0.60 ± 0.05	0.65 ± 0.05	0.64
	%IMCL	5.15 ± 0.94	6.08 ± 1.05	0.75

*7.12 Supplementary Table 7.2. Muscle volume data. Muscle volume change in % for the arm, torso and calf after bed rest (Post Bed Rest) and after remobilisation (Post Remob). * is significant on one-way repeated measures ANOVA.*

	Time point	Right (ESR side for leg)	Left (remobilised side for leg)
Arm % change	Post Bed rest	1.2 ± 0.4%*	0.5 ± 0.2%
	Post Remob	1.1 ± 0.8%*	0.1 ± 0.6%
Torso % change	Post Bed rest	1.0 ± 0.4%	n/a
	Post Remob	0.01 ± -0.6%	n/a
Calf % change	Post Bed rest	-2.2 ± 0.5%**	-2.1 ± 0.4%**
	Post Remob	-2.1 ± 0.6%*	-2.1 ± 0.7%*

7.13 Supplementary IPA schematics related to Chapter 3

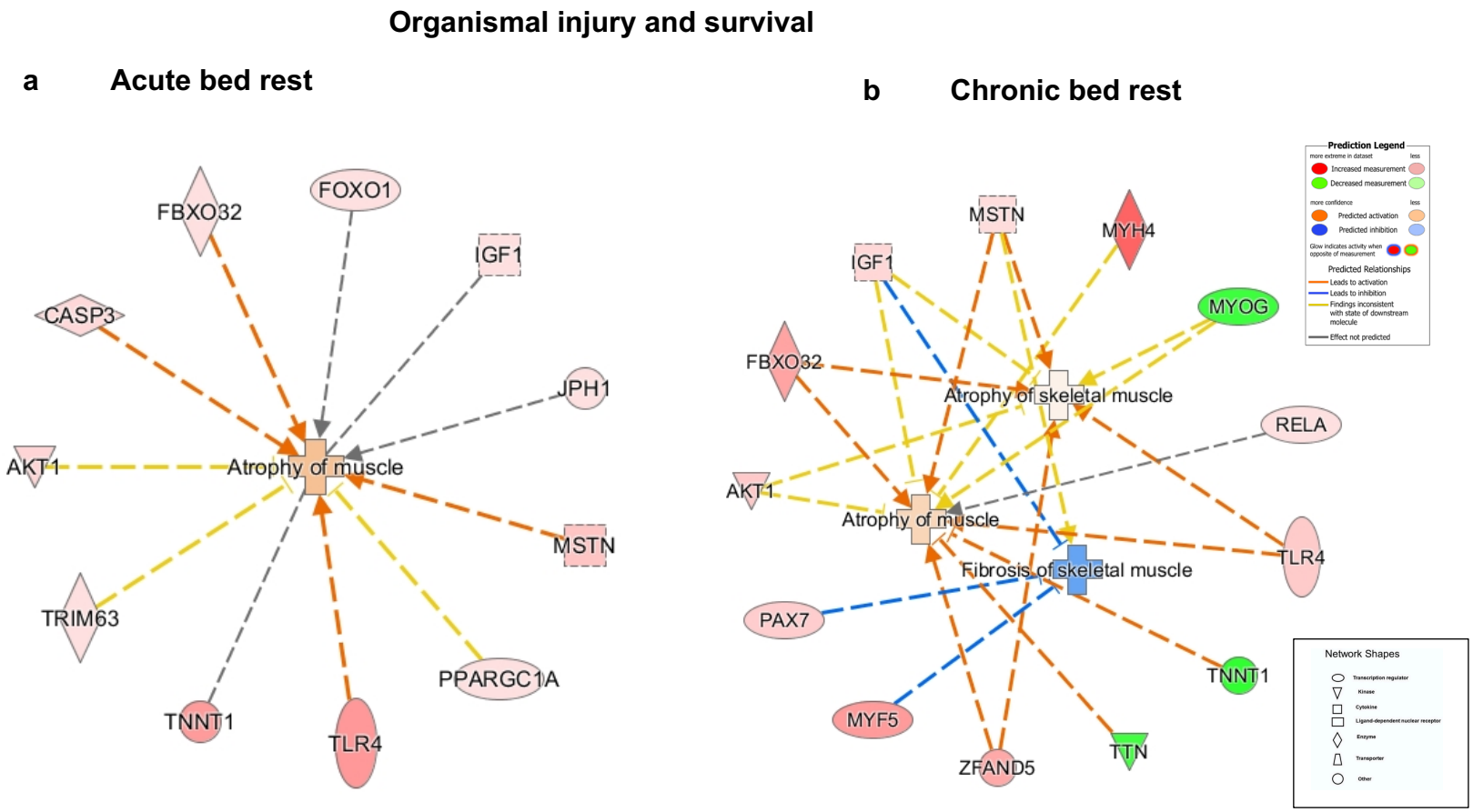

Supplementary Figure 7.2. Pathway analysis for organismal injury and survival. Schematic highlighting the most differentially regulated muscle gene expression (outer ring) & the cellular events predicted by Ingenuity Pathway Analysis to result from the collective changes in mRNA abundance (inner circles) associated with "Organismal injury and survival" after bed rest compared with pre bed rest in a) acute bed rest and b) chronic bed rest.

Skeletal and muscular disorders

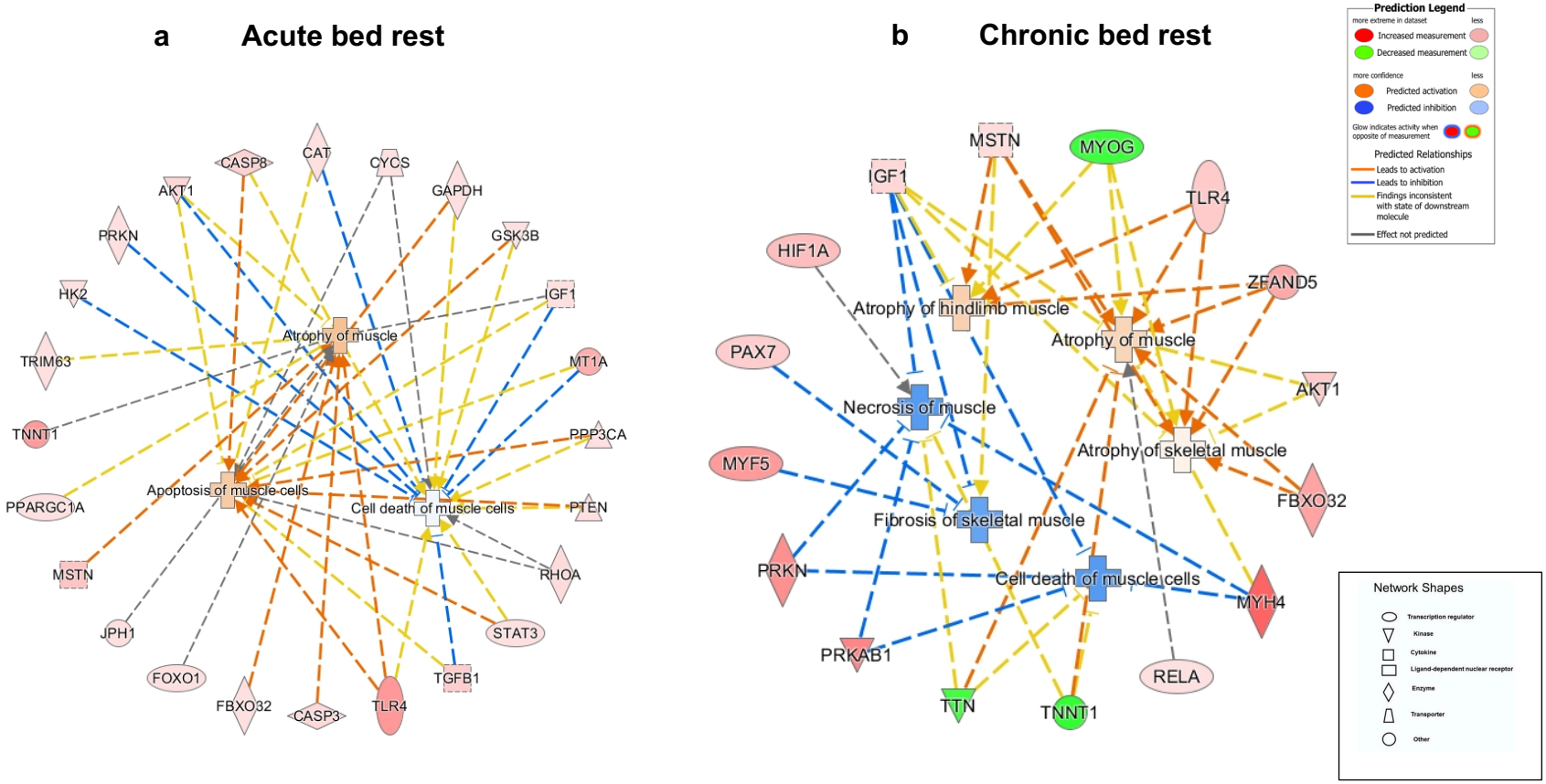

Supplementary Figure 7.3. Pathway analysis for skeletal and muscular disorders. Schematic highlighting the most differentially regulated muscle gene expression (outer ring) and the cellular events predicted by Ingenuity Pathway Analysis to result from the collective changes in mRNA abundance (inner circles) associated with "Skeletal and muscular disorders" after bed rest compared with pre bed rest in a) acute bed rest and b) chronic bed rest. The associated prediction legend indicates the degree of confidence which is depicted by colour intensity.

Skeletal and muscular system development and function

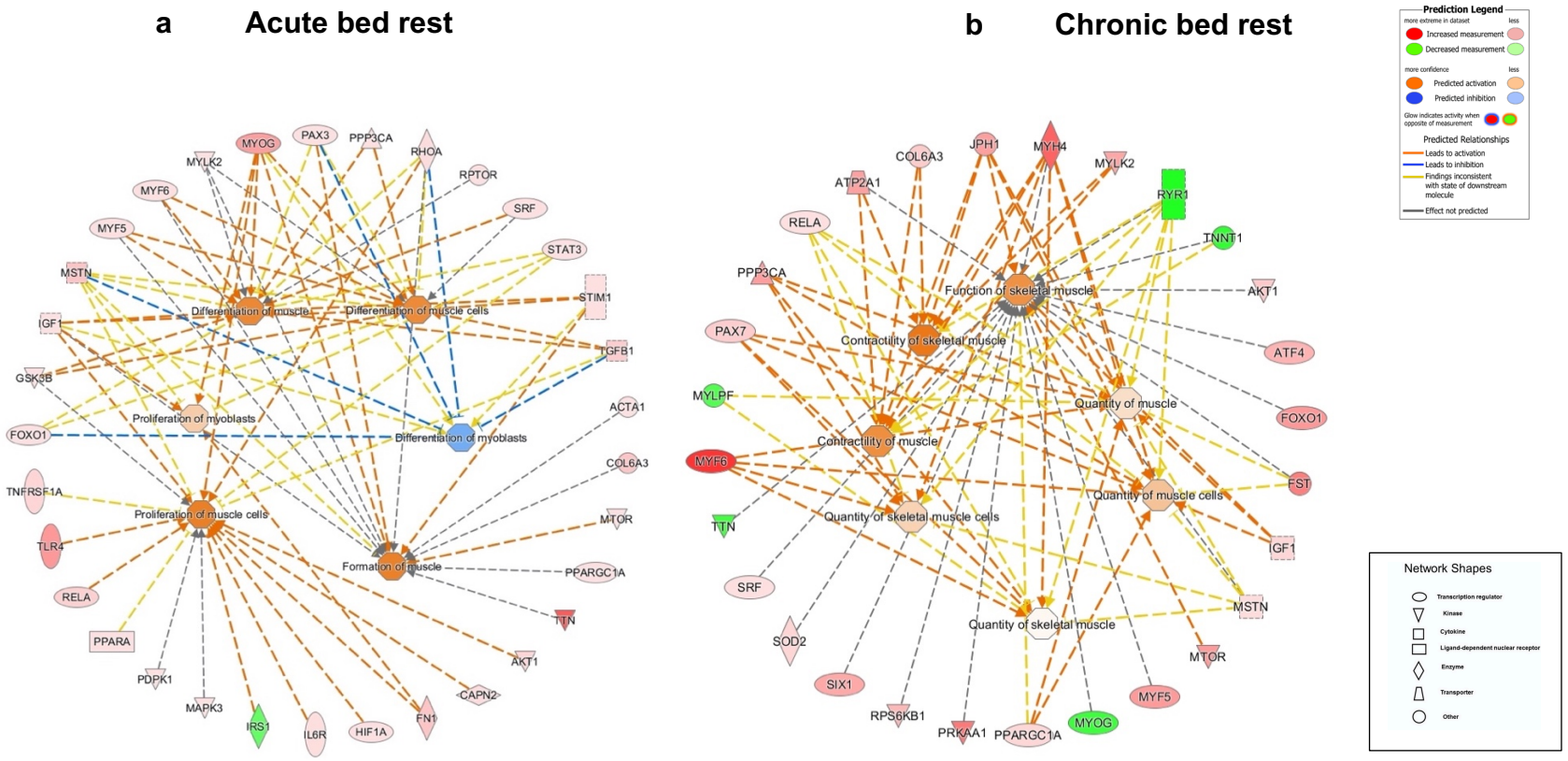

Supplementary Figure 7.4. Pathway analysis for skeletal and muscular system development and function. Schematic highlighting the most differentially regulated muscle gene expression (outer ring) and the cellular events predicted by Ingenuity Pathway Analysis to result from the collective changes in mRNA abundance (inner circles) associated with "Skeletal and muscular system development and function" after bed rest compared with pre bed rest in a) acute bed rest and b) chronic bed rest.

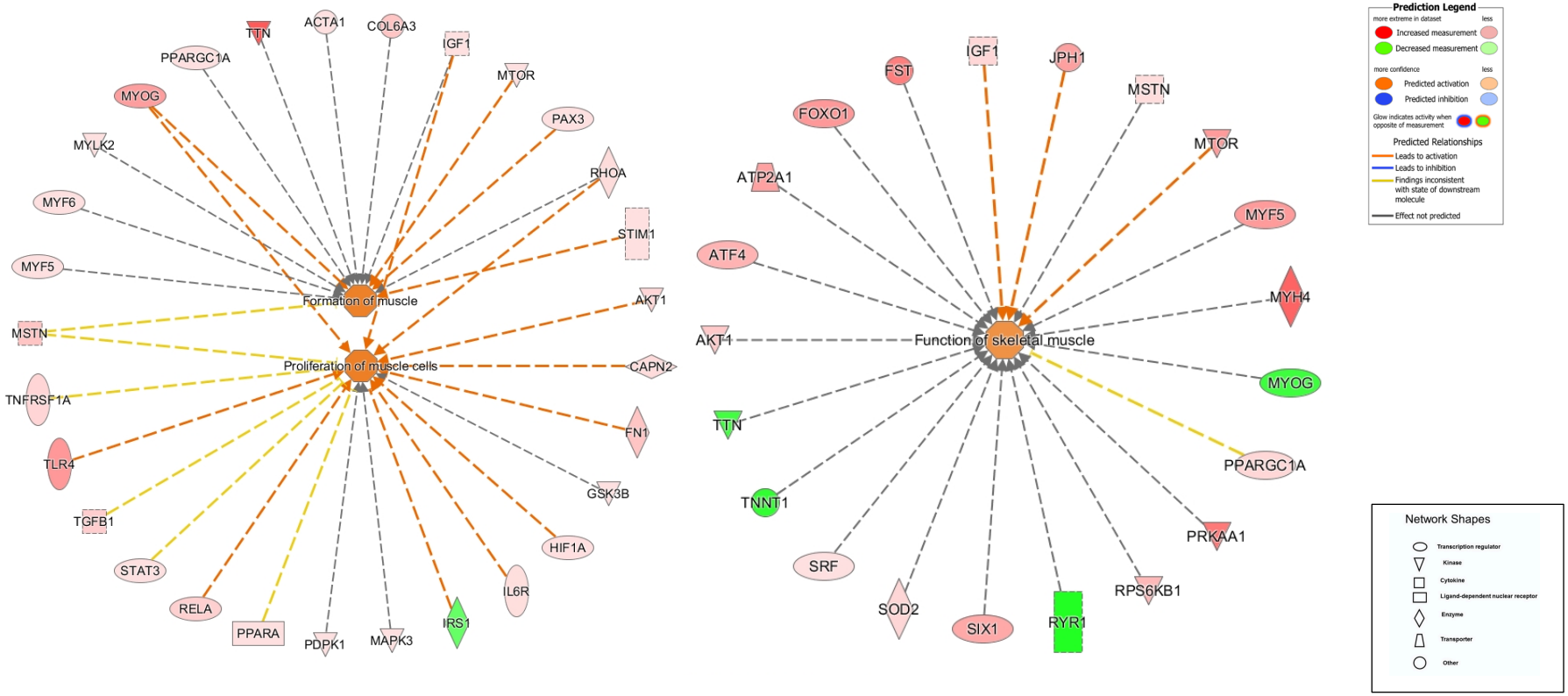

Supplementary Figure 7.5. Pathway analysis for organ development. Schematic highlighting the most differentially regulated muscle gene expression (outer ring) and the cellular events predicted by Ingenuity Pathway Analysis to result from the collective changes in mRNA abundance (inner circles) associated with "Organ development" after bed rest compared with pre bed rest in a) acute bed rest and b) chronic bed rest. The associated prediction legend indicates the degree of confidence which is depicted by colour intensity.

7.14 Supplementary IPA schematics related to Chapter 5

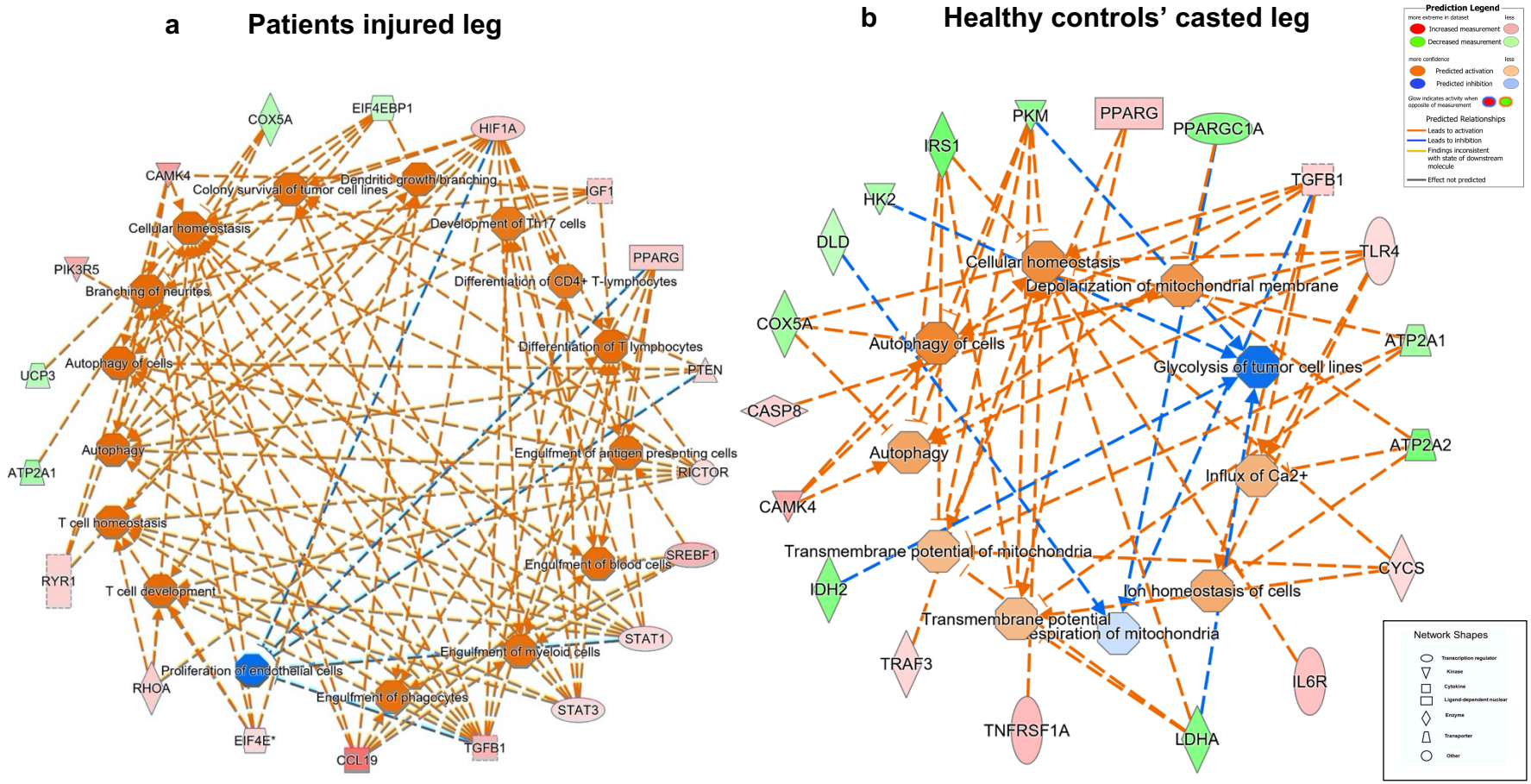

Supplementary Figure 7.6. Ingenuity Pathway Analysis schematic highlighting mRNAs differentially regulated from baseline in the "cellular function and maintenance" network (outer ring) and the predicted cellular events (inner octagons) associated with these collective changes in the a) injured legs of patients and b) casted leg of controls compared with before surgery and casting.

Cell death and Survival

a Patients injured leg

b Healthy controls' casted leg

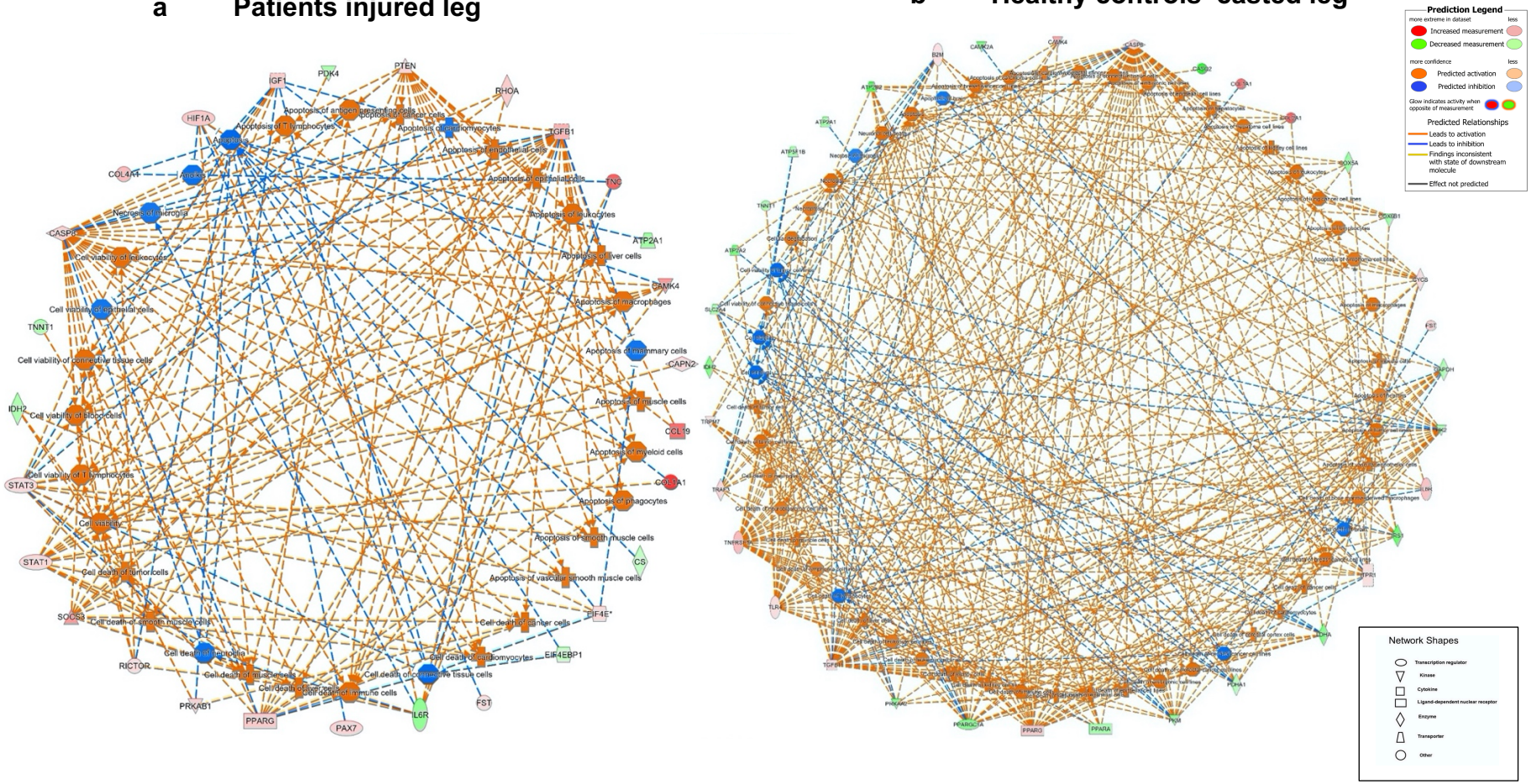

Supplementary Figure 7.7. Ingenuity Pathway Analysis schematic highlighting mRNAs differentially regulated from baseline in the "Cell death and survival" network (outer ring) and the predicted cellular events (inner octagons) associated with these collective changes in the a) injured legs of patients and b) casted leg of controls compared with before surgery and casting.

References

Abadi A., Glover EI, Isfort RJ, Raha S, Safdar A, Yasuda N, Kaczor JJ, Melov S , Hubbard H., Qu X, Phillips SM, and Tarnopolsky M. (2009). Limb immobilization induces a coordinate down-regulation of mitochondrial and other metabolic pathways in men and women, *PLoS One*, 4: e6518.

Abraham E, Anzueto A, Gutierrez G, Tessler S, San Pedro G, Wunderink R, Dal Nogare A, Nasraway S, Berman S, Cooney R, Levy H, Baughman R, Rumbak M, Light RB, Poole L, Allred R, Constant J, Pennington J, Porter S. (1998) Double-blind randomised controlled trial of monoclonal antibody to human tumour necrosis factor in treatment of septic shock. NORASEPT II Study Group. *Lancet*. 1998 Mar 28;351(9107):929-33.

Acheson KJ, Décombaz J, Piguet-Welsch C, Montigon F, Decarli B, Bartholdi I, Fern EB. (1995) Energy, protein, and substrate metabolism in simulated microgravity. *Am J Physiol.* 269(2 Pt 2):R252-60.

Adams GR, Caiozzo VJ, and Baldwin KM. (2003). Skeletal muscle unweighting: spaceflight and ground-based models, *J Appl Physiol (1985)*, 95: 2185-201.

Agrawal A, Suryakumar G, and Rathor R. (2018). Role of defective Ca(2+) signaling in skeletal muscle weakness: Pharmacological implications, *J Cell Commun Signal*, 12: 645-59.

Aguer C, Mercier J, Man CY, Metz L, Bordenave S, Lambert K, Jean E, Lantier L, Bounoua L, Brun JF, Raynaud de Mauverger E, Andreelli F, Foretz M, Kitzmann M. (2010) Intramyocellular lipid accumulation is associated with permanent relocation ex vivo and in vitro of fatty acid translocase (FAT)/CD36 in obese patients. *Diabetologia*. 53(6):1151-63.

Akima H, Kuno S, Suzuki Y, Gunji A, Fukunaga T. (1997) Effects of 20 days of bed rest on physiological cross-sectional area of human thigh and leg muscles evaluated by magnetic resonance imaging. *J Gravit Physiol*. 4(1):S15-21. PMID: 11541171.

Akima H, Ushiyama J, Kubo J, Tonosaki S, Itoh M, Kawakami Y, Fukuoka H, Kanehisa H, Fukunaga T. (2003) Resistance training during unweighting maintains muscle size and function in human calf. *Med Sci Sports Exerc*. 35(4):655-62.

Alibegovic AC, Sonne MP, Højbjerre L, Bork-Jensen J, Jacobsen S, Nilsson E, Faerch K, Hiscock N, Mortensen B, Friedrichsen M, Stallknecht B, Dela F, Vaag A. (2010). Insulin resistance induced by physical inactivity is

associated with multiple transcriptional changes in skeletal muscle in young men. *Am J Physiol Endocrinol Metab.* 299(5):E752-63.

Alkner BA, and Tesch PA. (2004). Knee extensor and plantar flexor muscle size and function following 90 days of bed rest with or without resistance exercise, *Eur J Appl Physiol*, 93: 294-305.

Allison SP, Hinton P, and Chamberlain MJ, (1968).'Intravenous glucose-tolerance, insulin, and free-fatty-acid levels in burned patients. *Lancet.* 23;2(7578):1113-6.

Andersen P, and Saltin B. (1985). Maximal perfusion of skeletal muscle in man, *J Physiol*, 366: 233-49.

Arc-Chagnaud C, Py G, Fovet T, Roumanille R, Demangel R, Pagano AF, Delobel P, Blanc S, Jasmin BJ, Blottner D, Salanova M, Gomez-Cabrera MC, Viña J, Brioche T, Chopard A. (2020). Evaluation of an Antioxidant and Anti-inflammatory Cocktail Against Human Hypoactivity-Induced Skeletal Muscle Deconditioning. *Front Physiol.* 12;11:71.

Atkins R, Constantin-Teodosiu D, Varadhan KK, Constantin D, Lobo DN, Greenhaff PL. (2021). Major elective abdominal surgery acutely impairs lower limb muscle pyruvate dehydrogenase complex activity and mitochondrial function. *Clin Nutr.* 40(3):1046-1051.

Aune D, Norat T, Leitzmann M, Tonstad S, Vatten LJ. (2015). Physical activity and the risk of type 2 diabetes: a systematic review and dose-response meta-analysis. *Eur J Epidemiol*. 30(7):529-42.

Baehr LM, West DW, Marcotte G, Marshall AG, De Sousa LG, Baar K, Bodine SC. (2016). Age-related deficits in skeletal muscle recovery following disuse are associated with neuromuscular junction instability and ER stress, not impaired protein synthesis. *Aging*. 8(1):127-46.

Bahador M., and Cross AS. (2007). From therapy to experimental model: a hundred years of endotoxin administration to human subjects, *J Endotoxin Res*, 13: 251-79.

Baigrie RJ, Lamont PM, Kwiatkowski D, Dallman MJ, Morris PJ. (1992). Systemic cytokine response after major surgery. *Br J Surg*. 79(8):757-60.

Baldwin C , van Kessel G , Phillips A and Johnston K. (2017). Accelerometry Shows Inpatients With Acute Medical or Surgical Conditions Spend Little Time Upright and Are Highly Sedentary: Systematic Review. *Phys Ther*, 97: 1044-65.

Bamman MM, Clarke MS, Feeback DL, Talmadge RJ, Stevens BR, Lieberman SA, Greenisen MC. (1998). Impact of resistance exercise during bed rest

on skeletal muscle sarcopenia and myosin isoform distribution. *J Appl Physiol.* 84(1):157-63.

Baron AD, Laakso M, Brechtel G, Edelman SV. (1991). Mechanism of insulin resistance in insulin-dependent diabetes mellitus: a major role for reduced skeletal muscle blood flow. *J Clin Endocrinol Metab.* 73(3):637-43. d

Bass JJ, Hardy EJO, Inns TB, Wilkinson DJ, Piasecki M, Morris RH, Spicer A, Sale C, Smith K, Atherton PJ, Phillips BE. (2021). Atrophy Resistant vs. Atrophy Susceptible Skeletal Muscles: "aRaS" as a Novel Experimental Paradigm to Study the Mechanisms of Human Disuse Atrophy. *Front Physiol.* 12:653060.

Bastian D, Tamburstuen MV, Lyngstadaas SP, Reikerås O. S. (2008). Systemic and local cytokine kinetics after total hip replacement surgery. *Eur Surg Res.* 41(4):334-40.

Bastian D, Tamburstuen MV, Lyngstadaas SP, Reikerås O. (2009). Local and systemic chemokine patterns in a human musculoskeletal trauma model. *Inflamm Res.* 58(8):483-9.

Battaglia GM, Zheng D, Hickner RC, Houmard JA. (2012). Effect of exercise training on metabolic flexibility in response to a high-fat diet in obese individuals. *Am J Physiol Endocrinol Metab.* 2012 Dec 15;303(12):E1440-5.

Berg HE, Tedner B, and Tesch PA. (1993). Changes in lower limb muscle cross-sectional area and tissue fluid volume after transition from standing to supine, *Acta Physiol Scand*, 148: 379-85.

Bergouignan A, Antoun E, Momken I, Schoeller DA, Gauquelin-Koch G, Simon C, Blanc S. (2012). Effect of contrasted levels of habitual physical activity on metabolic flexibility. *J Appl Physiol.* 114(3):371-9.

Bergouignan A, Rudwill F, Simon C, Blanc S. Physical inactivity as the culprit of metabolic inflexibility: evidence from bed rest studies. J Appl Physiol (1985). 2011 Oct;111(4):1201-10. doi: 10.1152/japplphysiol.00698.2011. Epub 2011 Aug 11. PMID: 21836047.

Bergstrom, J. (1975). Percutaneous needle biopsy of skeletal muscle in physiological and clinical research, *Scand J Clin Lab Invest*, 35: 609-16.

Biensø RS, Ringholm S, Kiilerich K, Aachmann-Andersen NJ, Krogh-Madsen R, Guerra B, Plomgaard P, van Hall G, Treebak JT, Saltin B, Lundby C, Calbet JA, Pilegaard H, Wojtaszewski JF. (2012). GLUT4 and glycogen synthase are key players in bed rest-induced insulin resistance. *Diabetes*. 61(5):1090-9. d

Bierbrauer J, Koch S, Olbricht C, Hamati J, Lodka D, Schneider J, Luther-Schröder A, Kleber C, Faust K, Wiesener S, Spies CD, Spranger J, Spuler S, Fielitz J, Weber-Carstens S. (2012). Early type II fiber atrophy in intensive care unit patients with nonexcitable muscle membrane. *Crit Care Med.* 40(2):647-50.

Birnbaum MJ. (1989). Identification of a novel gene encoding an insulin-responsive glucose transporter protein. *Cell*. 21;57(2):305-15.

Biswas A, Oh PI, Faulkner GE, Bajaj RR, Silver MA, Mitchell MS, Alter DA. (2015). Sedentary time and its association with risk for disease incidence, mortality, and hospitalization in adults: a systematic review and meta-analysis. *Ann Intern Med.* 162(2):123-32.

Black MN, Wilkinson JA, Webb EK, Kamal M, Bahniwal R, McGlory C, Phillips SM, Devries MC. (2021). Two weeks of single-leg immobilization alters intramyocellular lipid storage characteristics in healthy, young women. *J Appl Physiol.* 1;130(4):1247-1258.

Bodine SC, Latres E, Baumhueter S, Lai VK, Nunez L, Clarke BA, Poueymirou WT, Panaro FJ, Na E, Dharmarajan K, Pan ZQ, Valenzuela DM, DeChiara TM, Stitt TN, Yancopoulos GD, Glass DJ. (2001). Identification of ubiquitin ligases required for skeletal muscle atrophy. *Science*. 294(5547):1704-8. d

Bodine, S. C., T. N. Stitt, M. Gonzalez, W. O. Kline, G. L. Stover, R. Bauerlein, E. Zlotchenko, A. Scrimgeour, J. C. Lawrence, D. J. Glass, and G. D. Yancopoulos. (2001). Akt/mTOR pathway is a crucial regulator of skeletal muscle hypertrophy and can prevent muscle atrophy in vivo. *Nat Cell Biol*, 3: 1014-9.

Bonadonna, R. C., L. Groop, N. Kraemer, E. Ferrannini, S. Del Prato, and R. A. DeFronzo. (1990). Obesity and insulin resistance in humans: a dose-response study, *Metabolism*, 39: 452-9.

Bone, R. C., C. L. Sprung, and W. J. Sibbald. (1992).'Definitions for sepsis and organ failure, *Crit Care Med*, 20: 724-6.

Bonora, E., P. Moghetti, C. Zancanaro, M. Cigolini, M. Querena, V. Cacciatori, A. Corgnati, and M. Muggeo. (1989). Estimates of in vivo insulin action in man: comparison of insulin tolerance tests with euglycemic and hyperglycemic glucose clamp studies, *J Clin Endocrinol Metab*, 68: 374-8.

Bosutti, A., G. Malaponte, M. Zanetti, P. Castellino, M. Heer, G. Guarnieri, and G. Biolo. (2008). Calorie restriction modulates inactivity-induced changes in the inflammatory markers C-reactive protein and pentraxin-3. *J Clin Endocrinol Metab*. 93(8):3226-9.

Bowden Davies, K. A., V. S. Sprung, J. A. Norman, A. Thompson, K. L. Mitchell, J. C. G. Halford, J. A. Harrold, J. P. H. Wilding, G. J. Kemp, and D. J. Cuthbertson. (2018). Short-term decreased physical activity with increased sedentary behaviour causes metabolic derangements and altered body composition: effects in individuals with and without a first-degree relative with type 2 diabetes, *Diabetologia*, 61: 1282-94.

Bowker-Kinley, M. M., W. I. Davis, P. Wu, R. A. Harris, and K. M. Popov. (1998). Evidence for existence of tissue-specific regulation of the mammalian pyruvate dehydrogenase complex, *Biochem J*. 329 (Pt 1): 191-6.

Bratanova-Tochkova, T. K., H. Cheng, S. Daniel, S. Gunawardana, Y. J. Liu, J. Mulvaney-Musa, T. Schermerhorn, S. G. Straub, H. Yajima, and G. W. Sharp. (2002). Triggering and augmentation mechanisms, granule pools, and biphasic insulin secretion, *Diabetes*, 51 Suppl 1: S83-90.

Brocca, L., J. Cannavino, L. Coletto, G. Biolo, M. Sandri, R. Bottinelli, and M. A. Pellegrino. (2012). The time course of the adaptations of human muscle proteome to bed rest and the underlying mechanisms. *J Physiol*. 590: 5211-30.

Brook, M. S., T. Stokes, S. H. M. Gorissen, J. J. Bass, C. McGlory, J. Cegielski, D. J. Wilkinson, B. E. Phillips, K. Smith, S. M. Phillips, and P. J. Atherton. (2022). Declines in muscle protein synthesis account for short-term muscle disuse atrophy in humans in the absence of increased muscle protein breakdown. *J Cachexia Sarcopenia Muscle*. 13(4):2005-2016.

Brook, M. S., D. J. Wilkinson, W. K. Mitchell, J. N. Lund, B. E. Phillips, N. J. Szewczyk, P. L. Greenhaff, K. Smith, and P. J. Atherton. (2016). Synchronous deficits in cumulative muscle protein synthesis and ribosomal biogenesis underlie age-related anabolic resistance to exercise in humans. *J Physiol*. 594: 7399-417.

Brook, M. S., D. J. Wilkinson, W. K. Mitchell, J. N. Lund, N. J. Szewczyk, P. L. Greenhaff, K. Smith, and P. J. Atherton. (2015). Skeletal muscle hypertrophy adaptations predominate in the early stages of resistance exercise training, matching deuterium oxide-derived measures of muscle protein synthesis and mechanistic target of rapamycin complex 1 signaling. *Faseb j*. 29(11):4485-96.

Bruss, M. D., E. B. Arias, G. E. Lienhard, and G. D. Cartee. (2005). Increased phosphorylation of Akt substrate of 160 kDa (AS160) in rat skeletal muscle in response to insulin or contractile activity. *Diabetes*. 54(1):41-50.

Bryant, N. J., R. Govers, and D. E. James. (2002). Regulated transport of the glucose transporter GLUT4. *Nat Rev Mol Cell Biol*. 3(4):267-77.

Burns, A. M., A. Nixon, J. Mallinson, S. M. Cordon, F. B. Stephens, and P. L. Greenhaff. (2021). Immobilisation induces sizeable and sustained reductions in forearm glucose uptake in just 24 hours but does not change lipid uptake in healthy men. *J Physiol*. 599(8):2197-2210.

Campbell, P. J., L. J. Mandarino, and J. E. Gerich. (1988). Quantification of the relative impairment in actions of insulin on hepatic glucose production and peripheral glucose uptake in non-insulin-dependent diabetes mellitus. *Metabolism*. 37(1):15-21.

Campbell, R. M., and D. P. Cuthbertson. (1967). Effect of environmental temperature on the metabolic response to injury. *Q J Exp Physiol Cogn Med Sci*, 52: 114-29.

Cederblad, G., J. I. Carlin, D. Constantin-Teodosiu, P. Harper, and E. Hultman. (1990). Radioisotopic assays of CoASH and carnitine and their acetylated forms in human skeletal muscle. *Anal Biochem*. 185(2):274-8.

Cegielski, J., D. J. Wilkinson, M. S. Brook, C. Boereboom, B. E. Phillips, J. F. R. Gladman, K. Smith, and P. J. Atherton. (2021). Combined in vivo muscle mass, muscle protein synthesis and muscle protein breakdown measurement: a 'Combined Oral Stable Isotope Assessment of Muscle (COSIAM)' approach. *Geroscience*, 43: 2653-65.

Chambrier, C., M. Laville, K. Rhzioual Berrada, M. Odeon, P. Bouletreau, and M. Beylot. (2000). Insulin sensitivity of glucose and fat metabolism in severe sepsis. *Clin Sci.* 99: 321-8.

Chan, J. K., G. E. Glass, A. Ersek, A. Freidin, G. A. Williams, K. Gowers, A. I. Espirito Santo, R. Jeffery, W. R. Otto, R. Poulsom, M. Feldmann, S. M. Rankin, N. J. Horwood, and J. Nanchahal. (2015). Low-dose TNF augments fracture healing in normal and osteoporotic bone by up-regulating the innate immune response. *EMBO Mol Med*, 7: 547-61.

Chang, D. G., R. M. Healey, A. J. Snyder, J. V. Sayson, B. R. Macias, D. G. Coughlin, J. F. Bailey, S. E. Parazynski, J. C. Lotz, and A. R. Hargens. (2016). Lumbar Spine Paraspinal Muscle and Intervertebral Disc Height Changes in Astronauts After Long-Duration Spaceflight on the International Space Station. *Spine*. 41: 1917-24.

Chau, J. Y., A. C. Grunseit, T. Chey, E. Stamatakis, W. J. Brown, C. E. Matthews, A. E. Bauman, and H. P. van der Ploeg. (2013). Daily sitting time and all-cause mortality: a meta-analysis. *PLoS One*, 8: e80000.

Chen, Y. C., R. G. Davies, A. Hengist, H. A. Carroll, O. J. Perkin, J. A. Betts, and D. Thompson. 2(021). Effects of neuromuscular electrical stimulation on energy expenditure and postprandial metabolism in healthy men. *Appl Physiol Nutr Metab*: 1-7.

Chen, Z. P., G. K. McConell, B. J. Michell, R. J. Snow, B. J. Canny, and B. E. Kemp. (2000). AMPK signaling in contracting human skeletal muscle: acetyl-CoA carboxylase and NO synthase phosphorylation. *Am J Physiol Endocrinol Metab*, 279: E1202-6.

Chokkalingam, K., K. Tsintzas, L. Norton, K. Jewell, I. A. Macdonald, and P. I. Mansell. (2007). Exercise under hyperinsulinaemic conditions increases whole-body glucose disposal without affecting muscle glycogen utilisation in type 1 diabetes. *Diabetologia*, 50: 414-21.

Conley, M. S., J. M. Foley, L. L. Ploutz-Snyder, R. A. Meyer, and G. A. Dudley. (1996). Effect of acute head-down tilt on skeletal muscle cross-sectional area and proton transverse relaxation time. *J Appl Physiol.* 81: 1572-7.

Constantin, D., D. Constantin-Teodosiu, R. Layfield, K. Tsintzas, A. J. Bennett, and P. L. Greenhaff. (2007). PPARdelta agonism induces a change in fuel metabolism and activation of an atrophy programme, but does not impair mitochondrial function in rat skeletal muscle. *J Physiol*, 583: 381-90.

Constantin, D., J. McCullough, R. P. Mahajan, and P. L. Greenhaff. (2011). Novel events in the molecular regulation of muscle mass in critically ill patients. *J Physiol*, 589: 3883-95.

Constantin, D., M. K. Menon, L. Houchen-Wolloff, M. D. Morgan, S. J. Singh, P. Greenhaff, and M. C. Steiner. (2013). Skeletal muscle molecular responses to resistance training and dietary supplementation in COPD. *Thorax*. 68(7):625-33

Constantin-Teodosiu, D., G. Cederblad, M. Bergström, and P. L. Greenhaff. (2019). Maximal-intensity exercise does not fully restore muscle pyruvate dehydrogenase complex activation after 3 days of high-fat dietary intake. *Clin Nutr.* 38(2):948-953.

Conte, C., E. Fabbrini, M. Kars, B. Mittendorfer, B. W. Patterson, and S. Klein. (2012). Multiorgan insulin sensitivity in lean and obese subjects. *Diabetes Care*, 35: 1316-21.

Cree, M. G., B. R. Newcomer, D. N. Herndon, T. Qian, D. Sun, B. Morio, J. J. Zwetsloot, G. L. Dohm, R. Y. Fram, R. P. Mlcak, A. Aarsland, and R. R. Wolfe. (2007). PPAR-alpha agonism improves whole-body and muscle mitochondrial fat oxidation, but does not alter intracellular fat concentrations in burn trauma children in a randomized controlled trial. *Nutr Metab (Lond)*, 4: 9.

Cree, M. G., D. Paddon-Jones, B. R. Newcomer, O. Ronsen, A. Aarsland, R. R. Wolfe, and A. Ferrando. (2010). Twenty-eight-day bed rest with hypercortisolemia induces peripheral insulin resistance and increases intramuscular triglycerides. *Metabolism*, 59: 703-10.

Crossland, H., D. Constantin-Teodosiu, S. M. Gardiner, D. Constantin, and P. L. Greenhaff. (2008). A potential role for Akt/FOXO signalling in both protein loss and the impairment of muscle carbohydrate oxidation during sepsis in rodent skeletal muscle. *J Physiol*, 586: 5589-600.

Cuthbertson, D. P. (1929). The influence of prolonged muscular rest on metabolism. *Biochem J*, 23: 1328-45.

Cuthbertson, D., K. Smith, J. Babraj, G. Leese, T. Waddell, P. Atherton, H. Wackerhage, P. M. Taylor, and M. J. Rennie. (2005). Anabolic signaling deficits underlie amino acid resistance of wasting, aging muscle. *Faseb j*. 19(3):422-4.

de Boer, M. D., A. Selby, P. Atherton, K. Smith, O. R. Seynnes, C. N. Maganaris, N. Maffulli, T. Movin, M. V. Narici, and M. J. Rennie. (2007). The temporal responses of protein synthesis, gene expression and cell signalling in human quadriceps muscle and patellar tendon to disuse. *J Physiol*, 585: 241-51.

DeFronzo, R. A., E. Ferrannini, Y. Sato, P. Felig, and J. Wahren. (1981). Synergistic interaction between exercise and insulin on peripheral glucose uptake. *J Clin Invest*, 68: 1468-74.

DeFronzo, R. A., J. D. Tobin, and R. Andres. (1979). Glucose clamp technique: a method for quantifying insulin secretion and resistance. *Am J Physiol*, 237: E214-23.

Deitrick, J. E., G. D. Whedon, and E. Shorr. (1948). Effects of immobilization upon various metabolic and physiologic functions of normal men. *Am J Med*, 4: 3-36.

Della Peruta, C., B. Lozanoska-Ochser, A. Renzini, V. Moresi, C. Sanchez Riera, M. Bouché, and D. Coletti. (2023). Sex Differences in Inflammation and Muscle Wasting in Aging and Disease. *Int J Mol Sci*. 24(5):4651.

Demangel, R., L. Treffel, G. Py, T. Brioche, A. F. Pagano, M. P. Bareille, A. Beck, L. Pessemesse, R. Candau, C. Gharib, A. Chopard, and C. Millet. (2017). Early structural and functional signature of 3-day human skeletal muscle disuse using the dry immersion model. *J Physiol*, 595: 4301-15.

Dideriksen, K., S. Reitelseder, J. Agergaard, A. P. Boesen, S. N. Aas, T. Raastad, and L. Holm. (2020). Muscle protein breakdown is impaired during immobilization compared to during a subsequent retraining period in older men: no effect of anti-inflammatory medication. *Pflugers Arch*, 472: 281-92.

Dirks, M. L., F. B. Stephens, S. R. Jackman, J. Galera Gordo, D. J. Machin, R. M. Pulsford, L. J. C. van Loon, and B. T. Wall. (2018). A single day of

bed rest, irrespective of energy balance, does not affect skeletal muscle gene expression or insulin sensitivity. *Exp Physiol*, 103: 860-75.

Dirks, M. L., B. T. Wall, T. Snijders, C. L. Ottenbros, L. B. Verdijk, and L. J. van Loon. (2014). 'Neuromuscular electrical stimulation prevents muscle disuse atrophy during leg immobilization in humans', *Acta Physiol.* 210: 628-41.

Dirks, M. L., B. T. Wall, and F. B. Stephens. (2020). CrossTalk opposing view: Intramuscular lipid accumulation does not cause insulin resistance. *J Physiol*, 598: 3807-10.

Dirks, M. L., B. T. Wall, B. van de Valk, T. M. Holloway, G. P. Holloway, A. Chabowski, G. H. Goossens, and L. J. van Loon. (2016). One week of bed rest leads to substantial muscle atrophy and induces whole-body insulin resistance in the absence of skeletal muscle lipid accumulation. *Diabetes*. 65(10):2862-75.

Downs, M. E., J. M. Scott, L. L. Ploutz-Snyder, R. Ploutz-Snyder, E. Goetchius, R. E. Buxton, C. P. Danesi, K. M. Randolph, R. J. Urban, M. Sheffield-Moore, and E. L. Dillon. (2020). Exercise and Testosterone Countermeasures to Mitigate Metabolic Changes during Bed Rest. *Life Sci Space Res*. 26: 97-104.

Drummond, M. J., J. M. Dickinson, C. S. Fry, D. K. Walker, D. M. Gundermann, P. T. Reidy, K. L. Timmerman, M. M. Markofski, D. Paddon-Jones, B. B. Rasmussen, and E. Volpi. (2012). Bed rest impairs skeletal muscle amino acid transporter expression, mTORC1 signaling, and protein synthesis in response to essential amino acids in older adults. *Am J Physiol Endocrinol Metab*, 302: E1113-22.

Drummond, M. J., C. S. Fry, E. L. Glynn, H. C. Dreyer, S. Dhanani, K. L. Timmerman, E. Volpi, and B. B. Rasmussen. (2009). Rapamycin administration in humans blocks the contraction-induced increase in skeletal muscle protein synthesis, *J Physiol*, 587: 1535-46.

Drummond, M. J., K. L. Timmerman, M. M. Markofski, D. K. Walker, J. M. Dickinson, M. Jamaluddin, A. R. Brasier, B. B. Rasmussen, and E. Volpi. (2013). Short-term bed rest increases TLR4 and IL-6 expression in skeletal muscle of older adults. *Am J Physiol Regul Integr Comp Physiol*, 305: R216-23.

Duchateau, J. (1995). Bed rest induces neural and contractile adaptations in triceps surae, *Med Sci Sports Exerc*, 27: 1581-9.

Ekelund, U., J. Steene-Johannessen, W. J. Brown, M. W. Fagerland, N. Owen, K. E. Powell, A. Bauman, and I. M. Lee. (2016). Does physical activity attenuate, or even eliminate, the detrimental association of sitting time

with mortality? A harmonised meta-analysis of data from more than 1 million men and women. *Lancet.* 24;388(10051):1302-10.

Ekelund, U., J. Tarp, J. Steene-Johannessen, B. H. Hansen, B. Jefferis, M. W. Fagerland, P. Whincup, K. M. Diaz, S. P. Hooker, A. Chernofsky, M. G. Larson, N. Spartano, R. S. Vasan, I. M. Dohrn, M. Hagstromer, C. Edwardson, T. Yates, E. Shiroma, S. A. Anderssen, and I. M. Lee. (2019). Dose-response associations between accelerometry measured physical activity and sedentary time and all cause mortality: systematic review and harmonised meta-analysis. *BMJ*, 366: l4570.

Fedorov, A., R. Beichel, J. Kalpathy-Cramer, J. Finet, J. C. Fillion-Robin, S. Pujol, C. Bauer, D. Jennings, F. Fennessy, M. Sonka, J. Buatti, S. Aylward, J. V. Miller, S. Pieper, and R. Kikinis. (2012). 3D Slicer as an image computing platform for the Quantitative Imaging Network, *Magn Reson Imaging*, 30: 1323-41.

Felber, J. P., E. Ferrannini, A. Golay, H. U. Meyer, D. Theibaud, B. Curchod, E. Maeder, E. Jequier, and R. A. DeFronzo. (1987). Role of lipid oxidation in pathogenesis of insulin resistance of obesity and type II diabetes. *Diabetes*, 36: 1341-50.

Ferrando, A. A., H. W. Lane, C. A. Stuart, J. Davis-Street, and R. R. Wolfe. (1996). Prolonged bed rest decreases skeletal muscle and whole-body protein synthesis. *Am J Physiol*, 270: E627-33.

Ferrando, A. A., C. A. Stuart, D. G. Brunder, and G. R. Hillman. (1995). Magnetic resonance imaging quantitation of changes in muscle volume during 7 days of strict bed rest. *Aviat Space Environ Med*, 66: 976-81.

Ferrucci, L., and E. Fabbri. (2018). Inflammageing: chronic inflammation in ageing, cardiovascular disease, and frailty. *Nat Rev Cardiol*, 15: 505-22.

Fitts, R. H., J. G. Romatowski, J. R. Peters, D. Paddon-Jones, R. R. Wolfe, and A. A. Ferrando. (2007). The deleterious effects of bed rest on human skeletal muscle fibers are exacerbated by hypercortisolemia and ameliorated by dietary supplementation. *Am J Physiol Cell Physiol*, 293: C313-20.

Fitts, R. H., S. W. Trappe, D. L. Costill, P. M. Gallagher, A. C. Creer, P. A. Colloton, J. R. Peters, J. G. Romatowski, J. L. Bain, and D. A. Riley. (2010). Prolonged space flight-induced alterations in the structure and function of human skeletal muscle fibres. *J Physiol*, 588: 3567-92.

Frayn, K. N. (1986). Hormonal control of metabolism in trauma and sepsis. *Clin Endocrinol (Oxf)*, 24: 577-99.

Frayn, K. N., R. A. Little, P. F. Maycock, and H. B. Stoner. (1985). The relationship of plasma catecholamines to acute metabolic and hormonal responses to injury in man. *Circ Shock*, 16: 229-40.

Fritz, I. B., and B. McEwen. (1959). Effects of carnitine on fatty-acid oxidation by muscle, *Science*, 129: 334-5.

Fukuda, M. (2008). Regulation of secretory vesicle traffic by Rab small GTPases. *Cell Mol Life Sci*, 65: 2801-13.

Gallen, I. W., and I. A. Macdonald. (1990). Effects of blood glucose concentration on thermogenesis and glucose disposal during hyperinsulinaemia. *Clin Sci (Lond)*, 79: 279-85.

Gao, R., W. Duff, D. Chizen, G. A. Zello, and P. D. Chilibeck. (2019). The Effect of a Low Glycemic Index Pulse-Based Diet on Insulin Sensitivity, Insulin Resistance, Bone Resorption and Cardiovascular Risk Factors during Bed Rest. *Nutrients* (Switzerland). 27;11(9):2012.

Gemmink, A., B. H. Goodpaster, P. Schrauwen, and M. K. C. Hesselink. (2017). Intramyocellular lipid droplets and insulin sensitivity, the human perspective. *Biochim Biophys Acta Mol Cell Biol Lipids*. 1862(10 Pt B):1242-1249.

Gharahdaghi, N., S. Rudrappa, M. S. Brook, I. Idris, H. Crossland, C. Hamrock, M. H. Abdul Aziz, F. Kadi, J. Tarum, P. L. Greenhaff, D. Constantin-Teodosiu, J. Cegielski, B. E. Phillips, D. J. Wilkinson, N. J. Szewczyk, K. Smith, and P. J. Atherton. (2019). Testosterone therapy induces molecular programming augmenting physiological adaptations to resistance exercise in older men. *J Cachexia Sarcopenia Muscle*. 10(6):1276-1294.

Gibson, J. N., D. Halliday, W. L. Morrison, P. J. Stoward, G. A. Hornsby, P. W. Watt, G. Murdoch, and M. J. Rennie. (1987). Decrease in human quadriceps muscle protein turnover consequent upon leg immobilization. *Clin Sci (Lond)*, 72: 503-9.

Gibson, J. N., K. Smith, and M. J. Rennie. (1988). Prevention of disuse muscle atrophy by means of electrical stimulation: maintenance of protein synthesis. *Lancet*, 2: 767-70.

Gingras, A. C., S. P. Gygi, B. Raught, R. D. Polakiewicz, R. T. Abraham, M. F. Hoekstra, R. Aebersold, and N. Sonenberg. (1999). Regulation of 4E-BP1 phosphorylation: a novel two-step mechanism. *Genes Dev*, 13: 1422-37.

Glover, E. I., S. M. Phillips, B. R. Oates, J. E. Tang, M. A. Tarnopolsky, A. Selby, K. Smith, and M. J. Rennie. (2008). Immobilization induces anabolic

resistance in human myofibrillar protein synthesis with low and high dose amino acid infusion. *J Physiol*, 586: 6049-61.

Gogia, P., V. S. Schneider, A. D. LeBlanc, J. Krebs, C. Kasson, and C. Pientok. (1988). Bed rest effect on extremity muscle torque in healthy men. *Arch Phys Med Rehabil*, 69: 1030-2.

Goodpaster, B. H., R. Theriault, S. C. Watkins, and D. E. Kelley. (2000). Intramuscular lipid content is increased in obesity and decreased by weight loss. *Metabolism* 49(4):467-72.

Gordon, B. A., S. F. Fraser, S. R. Bird, and A. C. Benson. (2012). Insulin sensitivity in response to a single resistance exercise session in apparently healthy individuals. *J Endocrinol Invest*. 35(7):665-9.

Greenhaff, P. L., L. G. Karagounis, N. Peirce, E. J. Simpson, M. Hazell, R. Layfield, H. Wackerhage, K. Smith, P. Atherton, A. Selby, and M. J. Rennie. (2008). Disassociation between the effects of amino acids and insulin on signaling, ubiquitin ligases, and protein turnover in human muscle. *Am J Physiol Endocrinol Metab*, 295: E595-604.

Gustafsson, T., T. Osterlund, J. N. Flanagan, F. von Walden, T. A. Trappe, R. M. Linnehan, and P. A. Tesch. (2010). Effects of 3 days unloading on molecular regulators of muscle size in humans. *J Appl Physiol.* 109(3):721-7.

Guthold, R., G. A. Stevens, L. M. Riley, and F. C. Bull. (2018). Worldwide trends in insufficient physical activity from 2001 to 2016: a pooled analysis of 358 population-based surveys with 1·9 million participants. *Lancet Glob Health*, 6: e1077-e86.

Haddad, F., F. Zaldivar, D. M. Cooper, and G. R. Adams. (2005). IL-6-induced skeletal muscle atrophy. *J Appl Physiol.* 98(3):911-7.

Halter, J. B., A. E. Pflug, and D. Porte, Jr. (1977). Mechanism of plasma catecholamine increases during surgical stress in man. *J Clin Endocrinol Metab*, 45: 936-44.

Hamburg, N. M., C. J. McMackin, A. L. Huang, S. M. Shenouda, M. E. Widlansky, E. Schulz, N. Gokce, N. B. Ruderman, J. F. Keaney, Jr., and J. A. Vita. (2007). Physical inactivity rapidly induces insulin resistance and microvascular dysfunction in healthy volunteers. *Arterioscler Thromb Vasc Biol*, 27: 2650-6.

Hargens, A. R., and L. Vico. (2016). Long-duration bed rest as an analog to microgravity. *J Appl Physiol (1985)*, 120: 891-903.

Harris, R. C., E. Hultman, and L. O. Nordesjo. (1974). Glycogen, glycolytic intermediates and high-energy phosphates determined in biopsy

samples of musculus quadriceps femoris of man at rest. Methods and variance of values. *Scand J Clin Lab Invest*, 33: 109-20.

Heer, M., N. Baecker, S. Wnendt, A. Fischer, G. Biolo, and P. Frings-Meuthen. (2014). How fast is recovery of impaired glucose tolerance after 21-day bed rest (NUC study) in healthy adults? *ScientificWorldJournal*, 11;2014:803083.

Hennessey, J. V., J. A. Chromiak, S. Della Ventura, J. Guertin, and D. B. MacLean. (1997). Increase in percutaneous muscle biopsy yield with a suction-enhancement technique. *J Appl Physiol.* 82: 1739-42.

Herridge, M. S., A. M. Cheung, C. M. Tansey, A. Matte-Martyn, N. Diaz-Granados, F. Al-Saidi, A. B. Cooper, C. B. Guest, C. D. Mazer, S. Mehta, T. E. Stewart, A. Barr, D. Cook, and A. S. Slutsky. (2003). One-year outcomes in survivors of the acute respiratory distress syndrome. *N Engl J Med.* 20;348(8):683-93.

Hodges, P. W., L. H. Pengel, R. D. Herbert, and S. C. Gandevia. (2003). Measurement of muscle contraction with ultrasound imaging. *Muscle Nerve*, 27: 682-92.

Howard, B. J., B. Balkau, A. A. Thorp, D. J. Magliano, J. E. Shaw, N. Owen, and D. W. Dunstan. (2015). Associations of overall sitting time and TV viewing time with fibrinogen and C reactive protein: the AusDiab study. *Br J Sports Med* 49(4):255-8.

Huang, Z., L. Zhong, J. Zhu, H. Xu, W. Ma, L. Zhang, Y. Shen, B. Y. Law, F. Ding, X. Gu, and H. Sun. (2020). Inhibition of IL-6/JAK/STAT3 pathway rescues denervation-induced skeletal muscle atrophy'.*Ann Transl Med*, 8: 1681.

Hvid, L., P. Aagaard, L. Justesen, M. L. Bayer, J. L. Andersen, N. Ortenblad, M. Kjaer, and C. Suetta. (2010). Effects of aging on muscle mechanical function and muscle fiber morphology during short-term immobilization and subsequent retraining. *J Appl Physiol (1985)*, 109: 1628-34.

Inns, T. B., J. J. Bass, E. J. O. Hardy, D. J. Wilkinson, D. W. Stashuk, P. J. Atherton, B. E. Phillips, and M. Piasecki. (2022). Motor unit dysregulation following 15 days of unilateral lower limb immobilisation. *J Physiol*, 600: 4753-69.

Isokuortti, E., Y. Zhou, M. Peltonen, E. Bugianesi, K. Clement, D. Bonnefont-Rousselot, J. M. Lacorte, A. Gastaldelli, D. Schuppan, J. M. Schattenberg, A. Hakkarainen, N. Lundbom, P. Jousilahti, S. Männistö, S. Keinänen-Kiukaanniemi, J. Saltevo, Q. M. Anstee, and H. Yki-Järvinen. (2017). Use of HOMA-IR to diagnose non-alcoholic fatty liver disease: a population-based and inter-laboratory study. *Diabetologia*, 60: 1873-82.

Jaconelli, M., P. L. Greenhaff, P. J. Atherton, D. N. Lobo, and M. S. Brook. (2022). The effects of elective abdominal surgery on protein turnover: A meta-analysis of stable isotope techniques to investigate postoperative catabolism. *Clin Nutr*, 41: 709-22.

Jessen, N., and L. J. Goodyear. (2005). Contraction signaling to glucose transport in skeletal muscle. *J Appl Physiol (1985)*, 99: 330-7.

Jones, S. W., R. J. Hill, P. A. Krasney, B. O'Conner, N. Peirce, and P. L. Greenhaff. (2004). Disuse atrophy and exercise rehabilitation in humans profoundly affects the expression of genes associated with the regulation of skeletal muscle mass. *Faseb j*, 18: 1025-7.

Jurdana, M., Z. Jenko-Pražnikar, N. Mohorko, A. Petelin, T. Jakus, B. Šimunič, and R. Pišot. (2015). Impact of 14-day bed rest on serum adipokines and low-grade inflammation in younger and older adults. *Age (Dordr)*, 37: 116.

Kahn, C. R. (1978). Insulin resistance, insulin insensitivity, and insulin unresponsiveness: a necessary distinction. *Metabolism* (United States). 27(12 Suppl 2):1893-902.

Katz, A., S. S. Nambi, K. Mather, A. D. Baron, D. A. Follmann, G. Sullivan, and M. J. Quon. (2000). Quantitative insulin sensitivity check index: a simple, accurate method for assessing insulin sensitivity in humans. *J Clin Endocrinol Metab*, 85: 2402-10.

Kelley, D. E., and L. J. Mandarino. (1990). Hyperglycemia normalizes insulin-stimulated skeletal muscle glucose oxidation and storage in noninsulin-dependent diabetes mellitus. *J Clin Invest*, 86: 1999-2007.

Kelley, D. E., M. A. Mintun, S. C. Watkins, J. A. Simoneau, F. Jadali, A. Fredrickson, J. Beattie, and R. Theriault. (1996). The effect of non-insulin-dependent diabetes mellitus and obesity on glucose transport and phosphorylation in skeletal muscle. *J Clin Invest*, 97: 2705-13.

Kelley, D. E., M. Mokan, J. A. Simoneau, and L. J. Mandarino. (1993). Interaction between glucose and free fatty acid metabolism in human skeletal muscle. *J Clin Invest*, 92: 91-8.

Kelley, D. E., J. P. Reilly, T. Veneman, and L. J. Mandarino. (1990). Effects of insulin on skeletal muscle glucose storage, oxidation, and glycolysis in humans. *Am J Physiol*, 258: E923-9.

Kenny, H. C., F. Rudwill, L. Breen, M. Salanova, D. Blottner, T. Heise, M. Heer, S. Blanc, and D. J. O'Gorman. (2017). Bed rest and resistive vibration exercise unveil novel links between skeletal muscle mitochondrial function and insulin resistance.' in, *Diabetologia*. 60(8):1491-1501.

Kilroe, S. P., J. Fulford, A. M. Holwerda, S. R. Jackman, B. P. Lee, A. P. Gijsen, L. J. C. van Loon, and B. T. Wall. (2020). Short-term muscle disuse induces a rapid and sustained decline in daily myofibrillar protein synthesis rates. *Am J Physiol Endocrinol Metab*, 318: E117-E30.

Kilroe, S. P., J. Fulford, S. R. Jackman, V. A. N. Loon LJC, and B. T. Wall. (2020). Temporal Muscle-specific Disuse Atrophy during One Week of Leg Immobilization. *Med Sci Sports Exerc*, 52: 944-54.

King, D. S., P. J. Baldus, R. L. Sharp, L. D. Kesl, T. L. Feltmeyer, and M. S. Riddle. (1995). Time course for exercise-induced alterations in insulin action and glucose tolerance in middle-aged people. *J Appl Physiol (1985)*, 78: 17-22.

Knudsen, S. H., L. S. Hansen, M. Pedersen, T. Dejgaard, J. Hansen, G. V. Hall, C. Thomsen, T. P. Solomon, B. K. Pedersen, and R. Krogh-Madsen. (2012). Changes in insulin sensitivity precede changes in body composition during 14 days of step reduction combined with overfeeding in healthy young men. *J Appl Physiol (1985)* 113(1):7-15.

Koopman, R., R. J. Manders, A. H. Zorenc, G. B. Hul, H. Kuipers, H. A. Keizer, and L. J. van Loon. (2005). A single session of resistance exercise enhances insulin sensitivity for at least 24 h in healthy men. *Eur J Appl Physiol*, 94: 180-7.

Kortebein, P., A. Ferrando, J. Lombeida, R. Wolfe, and W. J. Evans. (2007). Effect of 10 days of bed rest on skeletal muscle in healthy older adults. *JAMA*. 25;297(16):1772-4.

Krawiec, B. J., R. A. Frost, T. C. Vary, L. S. Jefferson, and C. H. Lang. (2005). Hindlimb casting decreases muscle mass in part by proteasome-dependent proteolysis but independent of protein synthesis. *Am J Physiol Endocrinol Metab*, 289: E969-80.

Kristensen, M. D., S. M. Petersen, K. E. Møller, M. T. Lund, M. Hansen, C. N. Hansen, J. Courraud, J. W. Helge, F. Dela, and C. Prats. (2018). Obesity leads to impairments in the morphology and organization of human skeletal muscle lipid droplets and mitochondrial networks, which are resolved with gastric bypass surgery-induced improvements in insulin sensitivity. *Acta Physiol (Oxf)*, 224: e13100.

Krogh-Madsen, R., J. P. Thyfault, C. Broholm, O. H. Mortensen, R. H. Olsen, R. Mounier, P. Plomgaard, G. van Hall, F. W. Booth, and B. K. Pedersen. 2010. A 2-wk reduction of ambulatory activity attenuates peripheral insulin sensitivity. *J Appl Physiol.* 108(5):1034-40.

Kumar, V., P. Atherton, K. Smith, and M. J. Rennie. (2009). Human muscle protein synthesis and breakdown during and after exercise. *J Appl Physiol.* 106: 2026-39.

Kumar, V., A. Selby, D. Rankin, R. Patel, P. Atherton, W. Hildebrandt, J. Williams, K. Smith, O. Seynnes, N. Hiscock, and M. J. Rennie. (2009). Age-related differences in the dose-response relationship of muscle protein synthesis to resistance exercise in young and old men. *J Physiol*, 587: 211-7.

Laakso, M., S. V. Edelman, G. Brechtel, and A. D. Baron. (1990). Decreased effect of insulin to stimulate skeletal muscle blood flow in obese man. A novel mechanism for insulin resistance. *J Clin Invest*, 85: 1844-52.

Lamboley, C. R., V. L. Wyckelsma, B. D. Perry, M. J. McKenna, and G. D. Lamb. (2016). Effect of 23-day muscle disuse on sarcoplasmic reticulum Ca2+ properties and contractility in human type I and type II skeletal muscle fibers. in, *J Appl Physiol (1985)* 1;121(2):483-92.

Lang, C. H., R. A. Frost, and T. C. Vary. (2007). Regulation of muscle protein synthesis during sepsis and inflammation. *Am J Physiol Endocrinol Metab*. 293(2):E453-9.

LeBlanc, A. D., V. S. Schneider, H. J. Evans, C. Pientok, R. Rowe, and E. Spector. (1992). Regional changes in muscle mass following 17 weeks of bed rest. *J Appl Physiol (1985)*, 73: 2172-8.

Lebovitz, H. E. (2001). Insulin resistance: definition and consequences. *Exp Clin Endocrinol Diabetes*, 109 Suppl 2: S135-48.

Lecker, S. H., R. T. Jagoe, A. Gilbert, M. Gomes, V. Baracos, J. Bailey, S. R. Price, W. E. Mitch, and A. L. Goldberg. (2004). Multiple types of skeletal muscle atrophy involve a common program of changes in gene expression. *Faseb j*. 18(1):39-51.

Lee, I. M., E. J. Shiroma, F. Lobelo, P. Puska, S. N. Blair, and P. T. Katzmarzyk.(2012). Effect of physical inactivity on major non-communicable diseases worldwide: an analysis of burden of disease and life expectancy. *Lancet*, 380: 219-29.

Liu, D., E. Moberg, M. Kollind, P. E. Lins, U. Adamson, and I. A. Macdonald. (1992). Arterial, arterialized venous, venous and capillary blood glucose measurements in normal man during hyperinsulinaemic euglycaemia and hypoglycaemia. *Diabetologia*, 35: 287-90.

Longo, N., C. Amat di San Filippo, and M. Pasquali. (2006). Disorders of carnitine transport and the carnitine cycle. *Am J Med Genet C Semin Med Genet*, 142c: 77-85.

Loscalzo, J., and J. A. Vita. (1994). Ischemia, hyperemia, exercise, and nitric oxide. Complex physiology and complex molecular adaptations. *Circulation*, 90: 2556-9.

Manini, T. M., B. C. Clark, M. A. Nalls, B. H. Goodpaster, L. L. Ploutz-Snyder, and T. B. Harris. (2007). Reduced physical activity increases intermuscular adipose tissue in healthy young adults. *Am J Clin Nutr*. 85(2):377-84.

Mather, K. J., A. E. Hunt, H. O. Steinberg, G. Paradisi, G. Hook, A. Katz, M. J. Quon, and A. D. Baron. (2001). Repeatability characteristics of simple indices of insulin resistance: implications for research applications. *J Clin Endocrinol Metab*, 86: 5457-64.

Matthews, D. R., J. P. Hosker, A. S. Rudenski, B. A. Naylor, D. F. Treacher, and R. C. Turner. (1985). Homeostasis model assessment: insulin resistance and beta-cell function from fasting plasma glucose and insulin concentrations in man. *Diabetologia*, 28: 412-9.

McGlory, C., M. T. von Allmen, T. Stokes, R. W. Morton, A. J. Hector, B. A. Lago, A. R. Raphenya, B. K. Smith, A. G. McArthur, G. R. Steinberg, S. K. Baker, and S. M. Phillips. (2018). Failed Recovery of Glycemic Control and Myofibrillar Protein Synthesis With 2 wk of Physical Inactivity in Overweight, Prediabetic Older Adults. *J Gerontol A Biol Sci Med Sci*, 73: 1070-77.

Mekjavic, I. B., O. Eiken, P. J. Mekjavic, and A. C. McDonnell. (2021). Do females and males exhibit a similar sarcopenic response as a consequence of normoxic and hypoxic bed rest? *Exp Physiol*, 106: 37-51.

Mikines, K. J., E. A. Richter, F. Dela, and H. Galbo. (1991). Seven days of bed rest decrease insulin action on glucose uptake in leg and whole-body. *J Appl Physiol.* 70: 1245-54.

Miokovic, T., G. Armbrecht, U. Gast, R. Rawer, H. J. Roth, M. Runge, D. Felsenberg, and D. L. Belavý. (2014). Muscle atrophy, pain, and damage in bed rest reduced by resistive (vibration) exercise. *Med Sci Sports Exerc*, 46: 1506-16.

Miró, O., A. Barrientos, J. R. Alonso, J. Casademont, D. Jarreta, A. Urbano-Márquez, and F. Cardellach. (1999). Effects of general anaesthetic procedures on mitochondrial function of human skeletal muscle. *Eur J Clin Pharmacol*, 55: 35-41.

Møller, A. B., M. H. Vendelbo, P. Schjerling, C. Couppé, N. Møller, M. Kjær, M. Hansen, and N. Jessen. (2019). Immobilization Decreases FOXO3a Phosphorylation and Increases Autophagy-Related Gene and Protein Expression in Human Skeletal Muscle. *Front Physiol*, 10: 736.

Montero, D., L. Oberholzer, T. Haider, A. Breenfeldt-Andersen, S. Dandanell, A. K. Meinild-Lundby, H. Maconochie, and C. Lundby. (2018). Increased capillary density in skeletal muscle is not associated with impaired insulin

sensitivity induced by bed rest in healthy young men. *Appl Physiol Nutr Metab*, 43: 1334-40.

Monti, E., C. Reggiani, M. V. Franchi, L. Toniolo, M. Sandri, A. Armani, S. Zampieri, E. Giacomello, F. Sarto, G. Sirago, M. Murgia, L. Nogara, L. Marcucci, S. Ciciliot, B. Šimunic, R. Pišot, and M. V. Narici. (2021). Neuromuscular junction instability and altered intracellular calcium handling as early determinants of force loss during unloading in humans. *J Physiol*. 599(12):3037-3061.

Mora, S., I. M. Lee, J. E. Buring, and P. M. Ridker. (2006). Association of physical activity and body mass index with novel and traditional cardiovascular biomarkers in women. *JAMA*. 22;295(12):1412-9.

Morris, A. D., S. Ueda, J. R. Petrie, J. M. Connell, H. L. Elliott, and R. Donnelly. (1997). The euglycaemic hyperinsulinaemic clamp: an evaluation of current methodology. *Clin Exp Pharmacol Physiol*, 24: 513-8.

Mortensen, B., M. Friedrichsen, N. R. Andersen, A. C. Alibegovic, L. Hojbjerre, M. P. Sonne, B. Stallknecht, F. Dela, J. F. Wojtaszewski, and A. Vaag. (2014). Physical inactivity affects skeletal muscle insulin signaling in a birth weight-dependent manner. *J Diabetes Complications*. 28(1):71-8.

Muniyappa, R., S. Lee, H. Chen, and M. J. Quon. (2008). Current approaches for assessing insulin sensitivity and resistance in vivo: advantages, limitations, and appropriate usage. in, *Am J Physiol Endocrinol Metab*. 294(1):E15-26.

Murton, A. J., R. Billeter, F. B. Stephens, S. G. Des Etages, F. Graber, R. J. Hill, K. Marimuthu, and P. L. Greenhaff. (2014). Transient transcriptional events in human skeletal muscle at the outset of concentric resistance exercise training. *J Appl Physiol (1985)* 116(1):113-25.

Murton, A. J., K. Marimuthu, J. E. Mallinson, A. L. Selby, K. Smith, M. J. Rennie, and P. L. Greenhaff. (2015). Obesity Appears to Be Associated With Altered Muscle Protein Synthetic and Breakdown Responses to Increased Nutrient Delivery in Older Men, but Not Reduced Muscle Mass or Contractile Function. *Diabetes*. 64(9):3160-71.

Navasiolava, N. M., F. Dignat-George, F. Sabatier, I. M. Larina, C. Demiot, J. O. Fortrat, G. Gauquelin-Koch, I. B. Kozlovskaya, and M. A. Custaud. (2010). Enforced physical inactivity increases endothelial microparticle levels in healthy volunteers. *Am J Physiol Heart Circ Physiol*. 299(2):H248-56.

NHS Digital. (2019). Hospital Admitted Patient Care and Adult Critical Care Activity. Health and Social Care Information Centre. Government Statistical Service.

NHS Digital. (2022). Hospital Admitted Patient Care Activity 2021-2022. Health and Social Care Information Centre. Government Statistical Service.

Nielsen, J., M. Mogensen, B. F. Vind, K. Sahlin, K. Hojlund, H. D. Schroder, and N. Ortenblad. (2010). Increased subsarcolemmal lipids in type 2 diabetes: effect of training on localization of lipids, mitochondria, and glycogen in sedentary human skeletal muscle. in, *Am J Physiol Endocrinol Metab*. 298(3):E706-13.

Nuutila, P., M. Raitakari, H. Laine, O. Kirvelä, T. Takala, T. Utriainen, S. Mäkimattila, O. P. Pitkänen, U. Ruotsalainen, H. Iida, J. Knuuti, and H. Yki-Järvinen. (1996). Role of blood flow in regulating insulin-stimulated glucose uptake in humans. Studies using bradykinin, [15O]water, and [18F]fluoro-deoxy-glucose and positron emission tomography. *J Clin Invest*, 97: 1741-7.

Ochala, J., and L. Larsson. (2008). Effects of a preferential myosin loss on Ca2+ activation of force generation in single human skeletal muscle fibres. *Exp Physiol*, 93: 486-95.

OECD (2023), Length of hospital stay (indicator). doi: 10.1787/8dda6b7a-en (Accessed on 16 July 2023)

Ofei, F., S. Hurel, J. Newkirk, M. Sopwith, and R. Taylor. (1996). Effects of an engineered human anti-TNF-alpha antibody (CDP571) on insulin sensitivity and glycemic control in patients with NIDDM. *Diabetes*, 45: 881-5.

Ohkawara, K., K. Ishikawa-Takata, J. H. Park, I. Tabata, and S. Tanaka. (2011). How much locomotive activity is needed for an active physical activity level: analysis of total step counts. *BMC Res Notes*, 4: 512.

Olsen, R. H., R. Krogh-Madsen, C. Thomsen, F. W. Booth, and B. K. Pedersen. (2008). Metabolic responses to reduced daily steps in healthy nonexercising men. *Jama* 299(11):1261-3.

Pagano, A. F., T. Brioche, C. Arc-Chagnaud, R. Demangel, A. Chopard, and G. Py. (2018). Short-term disuse promotes fatty acid infiltration into skeletal muscle. *J Cachexia Sarcopenia Muscle*, 9: 335-47.

Pan, D. A., S. Lillioja, A. D. Kriketos, M. R. Milner, L. A. Baur, C. Bogardus, A. B. Jenkins, and L. H. Storlien. (1997). Skeletal muscle triglyceride levels are inversely related to insulin action. *Diabetes*, 46: 983-8.

Parry, S. M., and Z. A. Puthucheary. (2015). The impact of extended bed rest on the musculoskeletal system in the critical care environment. *Extrem Physiol Med*, 4: 16.

Pearson, S. J., A. Young, A. Macaluso, G. Devito, M. A. Nimmo, M. Cobbold, and S. D. Harridge. (2002). Muscle function in elite master weightlifters. *Med Sci Sports Exerc*, 34: 1199-206.

Peppler, W. W., and R. B. Mazess. (1981). Total body bone mineral and lean body mass by dual-photon absorptiometry. I. Theory and measurement procedure. *Calcif Tissue Int*, 33: 353-9.

Peronnet, F., and D. Massicotte. (1991). Table of nonprotein respiratory quotient: an update. *Can J Sport Sci*, 16: 23-9.

Phillips, S. M., E. I. Glover, and M. J. Rennie. (2009). Alterations of protein turnover underlying disuse atrophy in human skeletal muscle. *J Appl Physiol.* 107(3):645-54.

Porter, C., D. Constantin-Teodosiu, D. Constantin, B. Leighton, S. M. Poucher, and P. L. Greenhaff. (2017). Muscle carnitine availability plays a central role in regulating fuel metabolism in the rodent. *J Physiol*, 595: 5765-80.

Powell, C., M. P. Herring, K. P. Dowd, A. E. Donnelly, and B. P. Carson. (2018). The cross-sectional associations between objectively measured sedentary time and cardiometabolic health markers in adults - a systematic review with meta-analysis component. *Obes Rev*, 19: 381-95.

Pozefsky, T., R. G. Tancredi, R. T. Moxley, J. Dupre, and J. D. Tobin. (1976). Effects of brief starvation on muscle amino acid metabolism in nonobese man. *J Clin Invest*, 57: 444-9.

Prats, C., A. Gomez-Cabello, P. Nordby, J. L. Andersen, J. W. Helge, F. Dela, O. Baba, and T. Ploug. (2013). An optimized histochemical method to assess skeletal muscle glycogen and lipid stores reveals two metabolically distinct populations of type I muscle fibers. *PLoS One*, 8: e77774.

Proud, C. G. (2007). Signalling to translation: how signal transduction pathways control the protein synthetic machinery. *Biochem J* . 15;403(2):217-34.

Psatha, M., Z. Wu, F. M. Gammie, A. Ratkevicius, H. Wackerhage, J. H. Lee, T. W. Redpath, F. J. Gilbert, G. P. Ashcroft, J. R. Meakin, and R. M. Aspden. (2012). A longitudinal MRI study of muscle atrophy during lower leg immobilization following ankle fracture. *J Magn Reson Imaging*, 35: 686-95.

Puthucheary, Z. A., J. Rawal, M. McPhail, B. Connolly, G. Ratnayake, P. Chan, N. S. Hopkinson, R. Phadke, T. Dew, P. S. Sidhu, C. Velloso, J. Seymour, C. C. Agley, A. Selby, M. Limb, L. M. Edwards, K. Smith, A. Rowlerson, M. J. Rennie, J. Moxham, S. D. Harridge, N. Hart, and H. E.

Montgomery. (2013). Acute skeletal muscle wasting in critical illness. *JAMA*. 16;310(15):1591-600.

Randle, P. J. (1998). Regulatory interactions between lipids and carbohydrates: the glucose fatty acid cycle after 35 years. *Diabetes Metab Rev.* 14(4):263-83.

Randle, P. J., P. B. Garland, C. N. Hales, and E. A. Newsholme. (1963). The glucose fatty-acid cycle. Its role in insulin sensitivity and the metabolic disturbances of diabetes mellitus. *Lancet*. 3;1(7285):785-9

Reidy, P. T., C. C. Lindsay, A. I. McKenzie, C. S. Fry, M. A. Supiano, R. L. Marcus, P. C. LaStayo, and M. J. Drummond. (2017). Aging-related effects of bed rest followed by eccentric exercise rehabilitation on skeletal muscle macrophages and insulin sensitivity. *Exp Gerontol*. 1;107:37-49.

Reikerås, O., and P. Borgen. (2014). Activation of markers of inflammation, coagulation and fibrinolysis in musculoskeletal trauma. *PLoS One*, 9: e107881.

Reinhart, K., and W. Karzai. (2001). Anti-tumor necrosis factor therapy in sepsis: update on clinical trials and lessons learned. *Crit Care Med*, 29: S121-5.

Rennie, M. J. (2005). Body maintenance and repair: how food and exercise keep the musculoskeletal system in good shape. *Exp Physiol*, 90: 427-36.

Rennie, M. J., S. Phillips, and K. Smith. (2008). Reliability of results and interpretation of measures of 3-methylhistidine in muscle interstitium as marker of muscle proteolysis. *J Appl Physiol (1985)*. 105(4):1380-1.

Rennie, M. J., A. Selby, P. Atherton, K. Smith, V. Kumar, E. L. Glover, and S. M. Philips. (2010). Facts, noise and wishful thinking: muscle protein turnover in aging and human disuse atrophy. *Scand J Med Sci Sports*. 20(1):5-9.

Richter, E. A., B. Kiens, M. Mizuno, and S. Strange. (1989). Insulin action in human thighs after one-legged immobilization. *J Appl Physiol (1985)*, 67: 19-23.

Richter, E. A., and N. B. Ruderman. (2009). AMPK and the biochemistry of exercise: implications for human health and disease. *Biochem J*, 418: 261-75.

Ringholm, S., R. S. Bienso, K. Kiilerich, A. Guadalupe-Grau, N. J. Aachmann-Andersen, B. Saltin, P. Plomgaard, C. Lundby, J. F. Wojtaszewski, J. A. Calbet, and H. Pilegaard. (2011). Bed rest reduces metabolic protein

content and abolishes exercise-induced mRNA responses in human skeletal muscle. *Am J Physiol Endocrinol Metab.* 301(4):E649-58.

Roberts, D. J., and S. Miyamoto. (2015). Hexokinase II integrates energy metabolism and cellular protection: Akting on mitochondria and TORCing to autophagy. *Cell Death Differ*, 22: 248-57.

Roberts, I., D. Yates, P. Sandercock, B. Farrell, J. Wasserberg, G. Lomas, R. Cottingham, P. Svoboda, N. Brayley, G. Mazairac, V. Laloë, A. Muñoz-Sánchez, M. Arango, B. Hartzenberg, H. Khamis, S. Yutthakasemsunt, E. Komolafe, F. Olldashi, Y. Yadav, F. Murillo-Cabezas, H. Shakur, and P. Edwards. (2004). Effect of intravenous corticosteroids on death within 14 days in 10008 adults with clinically significant head injury (MRC CRASH trial): randomised placebo-controlled trial. *Lancet*, 364: 1321-8.

Roden, M. (2007). *Clinical Diabetes Research : Methods and Techniques* (Wiley).

Rosa-Caldwell, M. E., and N. P. Greene. (2019). Muscle metabolism and atrophy: let's talk about sex. *Biol Sex Differ*, 10: 43.

Roza, A. M., and H. M. Shizgal. (1984). The Harris Benedict equation reevaluated: resting energy requirements and the body cell mass. *Am J Clin Nutr*, 40: 168-82.

Rudrappa, S. S., D. J. Wilkinson, P. L. Greenhaff, K. Smith, I. Idris, and P. J. Atherton. (2016). Human Skeletal Muscle Disuse Atrophy: Effects on Muscle Protein Synthesis, Breakdown, and Insulin Resistance-A Qualitative Review. *Front Physiol*, 7: 361.

Rudwill, F., D. O'Gorman, E. Lefai, I. Chery, A. Zahariev, S. Normand, A. F. Pagano, A. Chopard, A. Damiot, C. Laurens, L. Hodson, E. Canet-Soulas, M. Heer, P. F. Meuthen, J. Buehlmeier, N. Baecker, L. Meiller, G. Gauquelin-Koch, S. Blanc, C. Simon, and A. Bergouignan. (2018). Metabolic Inflexibility Is an Early Marker of Bed rest-Induced Glucose Intolerance Even When Fat Mass Is Stable. *J Clin Endocrinol Metab*. 1;103(5):1910-1920.

Rytter, N., P. Piil, H. Carter, M. Nyberg, Y. Hellsten, and L. Gliemann. (2020). Microvascular Function Is Impaired after Short-Term Immobilization in Healthy Men. *Med Sci Sports Exerc*, 52: 2107-16.

Saggini R, Carmignano SM, Cosenza L, et al. (2017) Sarcopenia in Chronic Illness and Rehabilitative Approaches. Frailty and Sarcopenia - Onset, Development and Clinical Challenges. InTech. London.

Santoleri, D., and P. M. Titchenell. (2019). Resolving the Paradox of Hepatic Insulin Resistance. *Cell Mol Gastroenterol Hepatol*, 7: 447-56.

Sarto, F., R. Bottinelli, M. V. Franchi, S. Porcelli, B. Simunič, R. Pišot, and M. V. Narici. (2023). Pathophysiological mechanisms of reduced physical activity: Insights from the human step reduction model and animal analogues. *Acta Physiol (Oxf)*: e13986.

Schiaffino, S., L. Gorza, S. Sartore, L. Saggin, S. Ausoni, M. Vianello, K. Gundersen, and T. Lomo. (1989). Three myosin heavy chain isoforms in type 2 skeletal muscle fibres. *J Muscle Res Cell Motil*, 10: 197-205.

Schindelin, J., I. Arganda-Carreras, E. Frise, V. Kaynig, M. Longair, T. Pietzsch, S. Preibisch, C. Rueden, S. Saalfeld, B. Schmid, J. Y. Tinevez, D. J. White, V. Hartenstein, K. Eliceiri, P. Tomancak, and A. Cardona. (2012). Fiji: an open-source platform for biological-image analysis. *Nat Methods*, 9: 676-82.

Sheffield-Moore, M., E. L. Dillon, K. M. Randolph, S. L. Casperson, G. R. White, K. Jennings, J. Rathmacher, S. Schuette, M. Janghorbani, R. J. Urban, V. Hoang, M. Willis, and W. J. Durham. (2014). Isotopic decay of urinary or plasma 3-methylhistidine as a potential biomarker of pathologic skeletal muscle loss. *J Cachexia Sarcopenia Muscle*, 5: 19-25.

Shenkman, B. S., I. B. Kozlovskaya, T. L. Nemirovskaya, and I. A. Tcheglova. (1997). Human muscle atrophy in supportlessness: effects of short-term exposure to dry immersion. *J Gravit Physiol*, 4: P137-8.

Shur, N. F., L. Creedon, S. Skirrow, P. J. Atherton, I. A. MacDonald, J. Lund, and P. L. Greenhaff. (2021). Age-related changes in muscle architecture and metabolism in humans: The likely contribution of physical inactivity to age-related functional decline. *Ageing Res Rev*, 68: 101344.

Smorawinski, J., H. Kaciuba-Uscilko, K. Nazar, P. Kubala, E. Kaminska, A. W. Ziemba, J. Adrian, and J. E. Greenleaf. (2000). Effects of three-day bed rest on metabolic, hormonal and circulatory responses to an oral glucose load in endurance or strength trained athletes and untrained subjects. *J Physiol Pharmacol*, 51: 279-89.

Sonne, M. P., A. C. Alibegovic, L. Højbjerre, A. Vaag, B. Stallknecht, and F. Dela. (2010). Effect of 10 days of bedrest on metabolic and vascular insulin action: a study in individuals at risk for type 2 diabetes. *J Appl Physiol (1985)*, 108: 830-7.

Spriet, L. L. (2014). New insights into the interaction of carbohydrate and fat metabolism during exercise. *Sports Med*, 44 Suppl 1: S87-96.

Stahel, P. F., W. R. Smith, and E. E. Moore. (2007). Role of biological modifiers regulating the immune response after trauma. *Injury*, 38: 1409-22.

Stein, T. P., and M. D. Schluter. (1997). Human skeletal muscle protein breakdown during spaceflight. *Am J Physiol*, 272: E688-95.

Steinberg, H. O., G. Brechtel, A. Johnson, N. Fineberg, and A. D. Baron. (1994). Insulin-mediated skeletal muscle vasodilation is nitric oxide dependent. A novel action of insulin to increase nitric oxide release. *J Clin Invest*, 94: 1172-9.

Steinberg, K. P., L. D. Hudson, R. B. Goodman, C. L. Hough, P. N. Lanken, R. Hyzy, B. T. Thompson, and M. Ancukiewicz. (2006). Efficacy and safety of corticosteroids for persistent acute respiratory distress syndrome. *N Engl J Med*, 354: 1671-84.

Stephens, F. B., D. Constantin-Teodosiu, and P. L. Greenhaff. (2007). New insights concerning the role of carnitine in the regulation of fuel metabolism in skeletal muscle. *J Physiol*, 581: 431-44.

Stephens, F. B., D. Constantin-Teodosiu, D. Laithwaite, E. J. Simpson, and P. L. Greenhaff. (2006). An acute increase in skeletal muscle carnitine content alters fuel metabolism in resting human skeletal muscle. *J Clin Endocrinol Metab*. 91(12):5013-8.

Stephens, F. B., B. T. Wall, K. Marimuthu, C. E. Shannon, D. Constantin-Teodosiu, I. A. Macdonald, and P. L. Greenhaff. (2013). Skeletal muscle carnitine loading increases energy expenditure, modulates fuel metabolism gene networks and prevents body fat accumulation in humans. *J Physiol*, 591: 4655-66.

Stettler, R., M. Ith, K. J. Acheson, J. Decombaz, C. Boesch, L. Tappy, and C. Binnert. (2005). Interaction between dietary lipids and physical inactivity on insulin sensitivity and on intramyocellular lipids in healthy men. *Diabetes Care* (United States). 28(6):1404-9.

Stevens, J. E., G. A. Walter, E. Okereke, M. T. Scarborough, J. L. Esterhai, S. Z. George, M. J. Kelley, S. M. Tillman, J. D. Gibbs, M. A. Elliott, T. N. Frimel, C. P. Gibbs, and K. Vandenborne. (2004). Muscle adaptations with immobilization and rehabilitation after ankle fracture. *Med Sci Sports Exerc*, 36: 1695-701.

Stuart, C. A., R. E. Shangraw, M. J. Prince, E. J. Peters, and R. R. Wolfe. (1988). Bed rest-induced insulin resistance occurs primarily in muscle. in, *Metabolism*. 37: 802-6.

Suetta, C., U. Frandsen, L. Jensen, M. M. Jensen, J. G. Jespersen, L. G. Hvid, M. Bayer, S. J. Petersson, H. D. Schroder, J. L. Andersen, K. M. Heinemeier, P. Aagaard, P. Schjerling, and M. Kjaer. (2012). Aging affects the transcriptional regulation of human skeletal muscle disuse atrophy. *PLoS One*, 7: e51238.

Symons, T. B., M. Sheffield-Moore, D. L. Chinkes, A. A. Ferrando, and D. Paddon-Jones. (2009). Artificial gravity maintains skeletal muscle

protein synthesis during 21 days of simulated microgravity. *J Appl Physiol (1985)*, 107: 34-8.

Taillandier, D., E. Aurousseau, L. Combaret, C. Y. Guezennec, and D. Attaix. (2003). Regulation of proteolysis during reloading of the unweighted soleus muscle. *Int J Biochem Cell Biol*. 35(5):665-75.

Tanner, R. E., L. B. Brunker, J. Agergaard, K. M. Barrows, R. A. Briggs, O. S. Kwon, L. M. Young, P. N. Hopkins, E. Volpi, R. L. Marcus, P. C. LaStayo, and M. J. Drummond. (2015). Age-related differences in lean mass, protein synthesis and skeletal muscle markers of proteolysis after bed rest and exercise rehabilitation. *J Physiol*, 593: 4259-73.

Tesch, P. A., F. von Walden, T. Gustafsson, R. M. Linnehan, and T. A. Trappe. (2008). Skeletal muscle proteolysis in response to short-term unloading in humans. *J Appl Physiol (1985)*, 105: 902-6.

Thom, J. M., M. W. Thompson, P. A. Ruell, G. J. Bryant, J. S. Fonda, A. R. Harmer, X. A. Janse de Jonge, and S. K. Hunter. (2001). Effect of 10-day cast immobilization on sarcoplasmic reticulum calcium regulation in humans. *Acta Physiol Scand.* 172(2):141-7.

Thomas, A. C., and J. E. Stevens-Lapsley. (2012). Importance of attenuating quadriceps activation deficits after total knee arthroplasty. *Exerc Sport Sci Rev*, 40: 95-101.

Thomason, D. B., and F. W. Booth. (1990). Atrophy of the soleus muscle by hindlimb unweighting. *J Appl Physiol (1985)*, 68: 1-12.

Thompson, D. G., D. L. Wingate, M. Thomas, and D. Harrison. (1982). Gastric emptying as a determinant of the oral glucose tolerance test. *Gastroenterology*. 82(1):51-5.

Thomsen, T. K., V. J. Jensen, and M. G. Henriksen. (1998). In vivo measurement of human body composition by dual-energy X-ray absorptiometry (DXA). *Eur J Surg*, 164: 133-7.

Thorell, A., A. Loftenius, B. Andersson, and O. Ljungqvist. (1996). Postoperative insulin resistance and circulating concentrations of stress hormones and cytokines. *Clin Nutr*. 15(2):75-9.

Thorell, A., J. Nygren, and O. Ljungqvist. (1999). Insulin resistance: a marker of surgical stress. *Curr Opin Clin Nutr Metab Care*, 2: 69-78.

Trappe, S., T. Trappe, P. Gallagher, M. Harber, B. Alkner, and P. Tesch. (2004). Human single muscle fibre function with 84 day bed rest and resistance exercise. *J Physiol*, 557: 501-13.

Trim, W. V., J. P. Walhin, F. Koumanov, J. E. Turner, N. F. Shur, E. J. Simpson, I. A. Macdonald, P. L. Greenhaff, and D. Thompson. (2023). The impact

of physical inactivity on glucose homeostasis when diet is adjusted to maintain energy balance in healthy, young males. *Clin Nutr*, 42: 532-40.

Tucker, K. R., M. J. Seider, and F. W. Booth. (1981). Protein synthesis rates in atrophied gastrocnemius muscles after limb immobilization. *J Appl Physiol Respir Environ Exerc Physiol*, 51: 73-7.

Tudor-Locke, C., and D. R. Bassett, Jr. (2004). How many steps/day are enough? Preliminary pedometer indices for public health. *Sports Med*. 34(1):1-8.

Van Obberghen, E., V. Baron, L. Delahaye, B. Emanuelli, N. Filippa, S. Giorgetti-Peraldi, P. Lebrun, I. Mothe-Satney, P. Peraldi, S. Rocchi, D. Sawka-Verhelle, S. Tartare-Deckert, and J. Giudicelli. (2001). Surfing the insulin signaling web. *Eur J Clin Invest*. 31(11):966-77.

Varadhan, K. K., D. Constantin-Teodosiu, D. Constantin, P. L. Greenhaff, and D. N. Lobo. (2018). Inflammation-mediated muscle metabolic dysregulation local and remote to the site of major abdominal surgery. *Clin Nutr*, 37: 2178-85.

Vesali, R. F., N. Cibicek, T. Jakobsson, M. Klaude, J. Wernerman, and O. Rooyackers. (2009). Protein metabolism in leg muscle following an endotoxin injection in healthy volunteers. *Clin Sci.* 14;118(6):421-7.

Vincent, M. A., E. J. Barrett, J. R. Lindner, M. G. Clark, and S. Rattigan. (2003). Inhibiting NOS blocks microvascular recruitment and blunts muscle glucose uptake in response to insulin. *Am J Physiol Endocrinol Metab*, 285: E123-9.

Vincent, M. A., L. H. Clerk, J. R. Lindner, A. L. Klibanov, M. G. Clark, S. Rattigan, and E. J. Barrett. 2004. 'Microvascular recruitment is an early insulin effect that regulates skeletal muscle glucose uptake in vivo', *Diabetes*, 53: 1418-23.

Vincent, M. A., D. Dawson, A. D. Clark, J. R. Lindner, S. Rattigan, M. G. Clark, and E. J. Barrett. (2002). Skeletal muscle microvascular recruitment by physiological hyperinsulinemia precedes increases in total blood flow. *Diabetes*, 51: 42-8.

Wahlin-Larsson, B., D. J. Wilkinson, E. Strandberg, A. Hosford-Donovan, P. J. Atherton, and F. Kadi. (2017). Mechanistic Links Underlying the Impact of C-Reactive Protein on Muscle Mass in Elderly. *Cell Physiol Biochem*. 44(1):267-278.

Wall, B. T., M. L. Dirks, T. Snijders, J. M. Senden, J. Dolmans, and L. J. van Loon. (2014). Substantial skeletal muscle loss occurs during only 5 days of disuse. *Acta Physiol (Oxf)*, 210: 600-11.

Wall, B. T., M. L. Dirks, T. Snijders, J. W. van Dijk, M. Fritsch, L. B. Verdijk, and L. J. van Loon. (2016). Short-term muscle disuse lowers myofibrillar protein synthesis rates and induces anabolic resistance to protein ingestion. *Am J Physiol Endocrinol Metab.* 15;310(2):E137-47.

Wall, B. T., M. L. Dirks, and L. J. van Loon. (2013). Skeletal muscle atrophy during short-term disuse: implications for age-related sarcopenia. *Ageing Res Rev*. 12(4):898-906.

Wall, B. T., T. Snijders, J. M. Senden, C. L. Ottenbros, A. P. Gijsen, L. B. Verdijk, and L. J. van Loon. (2013). Disuse impairs the muscle protein synthetic response to protein ingestion in healthy men. *J Clin Endocrinol Metab*, 98: 4872-81.

Wandrag, L., S. J. Brett, G. S. Frost, V. Bountziouka, and M. Hickson. (2019). Exploration of muscle loss and metabolic state during prolonged critical illness: Implications for intervention? *PLoS One*, 14: e0224565.

Wellen, K. E., and G. S. Hotamisligil. (2003). Obesity-induced inflammatory changes in adipose tissue. *J Clin Invest*, 112: 1785-8.

WHO. (2010). Global recommendation on physical activity for health. World Health Organization, 23–32. Geneva, Switzerland.

WHO. (2018). Global Action Plan on Physical Activity 2018-2030: More active people for a healthier world. World Health Organization. Geneva, Switzerland.

WHO. (2022). Global status report on physical activity 2022. World Health Organization. Geneva, Switzerland.

Wieland, O. H. (1983). The mammalian pyruvate dehydrogenase complex: structure and regulation. *Rev Physiol Biochem Pharmacol*, 96: 123-70.

Wilkinson, D. J., M. S. Brook, K. Smith, and P. J. Atherton. (2017). Stable isotope tracers and exercise physiology: past, present and future. *J Physiol*, 595: 2873-82.

Wilkinson, D. J., J. Cegielski, B. E. Phillips, C. Boereboom, J. N. Lund, P. J. Atherton, and K. Smith. (2015). Internal comparison between deuterium oxide (D2O) and L-[ring-13C6] phenylalanine for acute measurement of muscle protein synthesis in humans. *Physiol Rep*. 3(7):e12433.

Wilkinson, D. J., M. V. Franchi, M. S. Brook, M. V. Narici, J. P. Williams, W. K. Mitchell, N. J. Szewczyk, P. L. Greenhaff, P. J. Atherton, and K. Smith. (2014). A validation of the application of D(2)O stable isotope tracer techniques for monitoring day-to-day changes in muscle protein subfraction synthesis in humans. *Am J Physiol Endocrinol Metab*, 306: E571-9.

Willis, C. R. G., I. J. Gallagher, D. J. Wilkinson, M. S. Brook, J. J. Bass, B. E. Phillips, K. Smith, T. Etheridge, T. Stokes, C. McGlory, S. H. M. Gorissen, N. J. Szewczyk, S. M. Phillips, and P. J. Atherton. (2021). Transcriptomic links to muscle mass loss and declines in cumulative muscle protein synthesis during short-term disuse in healthy younger humans. *Faseb j*, 35: e21830.

Wojtaszewski, J. F., P. Nielsen, B. F. Hansen, E. A. Richter, and B. Kiens. (2000). Isoform-specific and exercise intensity-dependent activation of 5'-AMP-activated protein kinase in human skeletal muscle. *J Physiol*, 528 Pt 1: 221-6.

Wolfe, R. R., J. R. Allsop, and J. F. Burke. (1977). Experimental sepsis and glucose metabolism: time course of response. *Surg Forum*, 28: 42-3.

Wu, H., and C. M. Ballantyne. (2017). Skeletal muscle inflammation and insulin resistance in obesity. *J Clin Invest*, 127: 43-54.

Yanagibori, R., Y. Suzuki, K. Kawakubo, Y. Makita, and A. Gunji. (1994). Carbohydrate and lipid metabolism after 20 days of bed rest. *Acta Physiol Scand Suppl*, 616: 51-7.

Yates, T., K. Khunti, E. G. Wilmot, E. Brady, D. Webb, B. Srinivasan, J. Henson, D. Talbot, and M. J. Davies. (2012). Self-reported sitting time and markers of inflammation, insulin resistance, and adiposity. *Am J Prev Med*. 42(1):1-7.

Yoshiko, A., K. Yamauchi, T. Kato, K. Ishida, T. Koike, Y. Oshida, and H. Akima. (2018). Effects of post-fracture non-weight-bearing immobilization on muscle atrophy, intramuscular and intermuscular adipose tissues in the thigh and calf. *Skeletal Radiol*. 47(11):1541-1549.

Yellow Springs International (2009). User's Manual YSI 2300 STAT Plus Glucose and Lactate Analyzer. Retrieved from https://www.ysi.com/file%20library/documents/manuals%20for%20discontinued%20products/ysi-2300-stat-plus-manual-j.pdf